



The
University
Of
Sheffield.

Neural noise in Autism Spectrum Conditions (ASC)

Aikaterini Giannadou

A thesis submitted for the degree of
Doctor of Philosophy

The University of Sheffield
Department of Psychology

Student ID: 160110676

Acknowledgements

I am forever grateful to my beloved mother and father, who instilled values of lifelong learning to me, financially supported my education and emotionally nurtured me, through all the “ups” and the “downs” along this very long journey. Mum you taught me to work hard, persevere through difficulties, keep learning until the end. Dad you taught me to be a good problem-solver and resilient, no matter what happens I know I have your back. I am who I am because of you. This thesis was possible because of you.

Liz I am honoured to have had you as a PhD supervisor. You are something more than a mentor and a teacher to me- throughout the years you have become a friend and a different kind of “mother” figure, a person that really helped me develop my scientific thinking and research identity. I remember all the times that came running to you with problems, coding issues and all sorts of questions. Thank you for always being there for me. The greatest role model I could have ever asked for.

Myles thank you for always being the voice of logic and explaining complex concepts to me in a way that is less intimidating. It was June 2019 when I came up to you really upset and asked you to explain to me the physics of $1/f$ noise. Our conversations at times of crisis, helped me pull through and keep my cool. Thank you for everything.

Megan thank you for the feedback throughout those years and for bringing a completely different perspective into the work. It has been invaluable and helped me see my work from a very different lens and viewpoint, that of clinical psychology.

Andrea massive thank you to you too for all the scientific discussions, research opportunities and for always being there for me- always an ally. I still remember trying to polish off Chapter 2 during our writing week in France. Our discussions helped my thinking and your feedback and direction were integral to the direction of the work.

Dan, you have been instrumental for the success of the mobile EEG data collection. I owe you a massive thank you for helping me set up the Lab Streaming Layer and for problem solving with me

when I needed it the most. Similarly, I would like to thank James Henshaw for giving me the initial directions on how to get started.

During those 5 years at the University of Sheffield, I met some exceptional human beings, people that deeply care about innovation, constantly pushing the boundaries of science. Amber and Anton our discussions during lunch breaks (and not only) kept me sane. Thank you for being such good listeners and for your good advice during all those years.

I would also like to thank my fellow PhD students Mate, Laura and Stan, who, not only did I share desk space with for so many years at UoS, but also research ideas and conversations about different topics. Mate I want to personally thank you for being so patient with me when I was bombarding you with all sorts of questions about statistics and coding in Matlab. Stan and Laura thank you for always being there through thick and thin (breakups, research successes, etc). You have been a fantastic lot. I am very lucky to have met you.

I also owe a BIG thank you to Tom Stafford for opening up my eyes and introducing me to the open science framework. Tom, thank you for helping me learn to work more efficiently and make my work more reproducible. You have been an exceptional role model for me. Our conversations have been a real treasure, stimulating my thinking at every level.

I am also thankful to all the adults with ADHD that took part in this work. Some of you travelled all the way from Leeds, Manchester, Hampshire, London and other parts of the UK. Some of you refused to accept money/vouchers for your time and insisted that the cause is more important than money. Some of you found more participants to take part in my study by talking to friends and family. You showed kindness, graciousness, courtesy to a complete stranger. I feel extremely lucky to have met you all.

I would also like to express my deepest gratitude to the children with autism and their families, who generously gave their time in order to help me collect EEG data in their own homes. In 2019, I was travelling up and down the country on the train with a bag full of equipment for more than a year-sometimes I was in Sheffield at 9am for testing, in Derbyshire at 12, in Manchester at 5pm. It was tough. Sometimes I would not get any data. But I did it. Well, we did it. I would have achieved nothing without the parents and children that opened up their own homes to me. Thank you to each and every one of you, my biggest advocates.

Lastly but most importantly, Jandro you have been a ray of sunshine in my life since I met you. You provided me with the emotional stability I needed to be able to complete this piece of work. You did not mind when I was working weekends and when I was coming home tired after testing and I still had to wash EEG caps! I am thankful to you for teaching me to always pose the “So what?” question and stay true to our values for real-world impact. For the endless conversations on statistics, modelling and maths. For helping me become a critical thinker. You have been a true inspiration for me. Thank you for everything that you have done all those years, everything that made this thesis possible.

Contents

List of figures	10
List of tables	Error! Bookmark not defined.
Abstract	18
Chapter 1:	19
Introduction	19
1.1 Autism Spectrum Condition (ASC)	20
1.2 Identification of biomarkers in ASC	23
1.3 Scope of the present thesis	25
1.4 Definitions	25
1.4.1 Neural communication	25
1.4.2 Neural oscillations	26
1.4.3 Neural noise	28
1.4.4 Inter-trial Phase Coherence (ITPC)	29
1.4.5 1/f noise of Power Spectral Density (PSD)	32
1.5 Increased neural noise in the autistic brain	34
1.5.1 The theoretical framework	34
1.5.2 A computational modelling perspective	37
1.5.3 Methodological challenges	38
1.5.4 Measuring neural noise using Electroencephalography (EEG)	40
1.5.4.1 Advantages of EEG	40
1.5.4.2 EEG metrics used to quantify neural noise	40
1.5.4.3 Trial averaging vs single-trial analysis	41
1.5.5 Experimental studies investigating neural noise in ASC	43
1.6 Inter-trial Phase Coherence (ITPC)	45
1.6.1 Inter-trial Phase Coherence in disorders of the brain	45
1.7 1/f noise of Power Spectral Density (PSD)	51
1.7.1 1/f noise of Power Spectral Density (PSD) in disorders of the brain	51
1.7.2 What can Phase/Amplitude Coupling (PAC) tell us about the pathological undercoupling hypothesis in ASC?	52
1.7.3 Parameterisation of Power Spectral Density (PSD)	54
1.8 Overlap of Autism Spectrum Conditions (ASC) and Attention Deficit Hyperactivity Disorder (ADHD)	55
1.9 Experimental approach followed in the present thesis	58
1.10 Aims of the present thesis	60
1.10.1 General aims	60

1.10.2 Aim 1	61
1.10.3 Aim 2	62
1.10.4 Aim 3	63
1.10.5 Aim 4	64
Chapter 2:	65
Neural noise in adults with Autism Spectrum Conditions (ASC) and Attention Deficit Hyperactivity Disorder (ADHD)	65
2.1 Introduction	66
2.1.1 Genetic overlap	66
2.1.2 Neurocognitive overlap	67
2.1.3 Neural variability	70
2.1.4 Neural variability in ASC and ADHD	72
2.1.5 Aims of the current study	76
2.2 Materials and Methods	78
2.2.1 Participants	78
2.2.2 Psychometric assessments	80
2.2.3 Procedure	81
2.2.3.1 Apparatus	81
2.2.3.2 EEG experiment	81
2.2.3.3 Data acquisition	81
2.2.3.4 Task- based EEG	82
2.2.3.5 Resting- state EEG	82
2.2.4 General data preprocessing	83
2.2.5 Data integrity	85
2.2.6 EEG data preparation for Inter- Trial Phase Coherence analysis	88
2.2.6.1 Data preprocessing	88
2.2.6.2 Data selection	88
2.2.7 Data analysis	91
2.2.8 EEG data preparation for 1/f noise analysis	91
2.2.8.1 Data preprocessing	91
2.2.8.2 Data selection	92
2.2.9 Data analysis	94
2.2.10 Statistical analysis	94
2.3 Results	97
2.3.1 Group comparisons: Inter- Trial Phase Coherence	97
2.3.2 Group comparisons: 1/f noise of Power Spectral Density	103
2.3.2.1 Method 1	103

2.3.2.2 Method 2	105
2.3.3 Association between age and ITPC	107
2.3.4 Association between age and 1/f slope of PSD	108
2.3.5 Association between ITPC and 1/f noise	109
2.4 Discussion	111
Chapter 3:	118
Investigating neural dynamics in Autism Spectrum Conditions (ASC) outside of the laboratory using mobile EEG	118
3.1. Introduction	119
3.2 Materials and Methods	121
3.2.1 Participants	121
3.2.2 Psychometric assessments	124
3.2.3 Procedure	125
3.2.3.1 Apparatus	125
3.2.3.2 Visual task	126
3.2.3.3 User experience measures	126
3.2.3.4 Standardisation of study parameters	128
3.2.3.5 Adaptation of procedures	129
3.2.4 Data analysis	130
3.2.4.1 Temporal accuracy of LSL triggers	130
3.2.4.2 Evaluation of EEG data quality	130
3.2.4.3 Statistical analysis of user experience measures	132
3.3 Results	133
3.3.1 Temporal accuracy of LSL triggers	133
3.3.2 EEG data quality assessment	133
3.3.3 User experience	138
3.4 Discussion	142
3.5 Conclusions	147
Chapter 4:	148
Neural noise in children with Autism Spectrum Conditions (ASC)	148
4.1 Introduction	149
4.1.2 Aims of the current study	150
4.2 Materials and Methods	150
4.2.1 Participants	150
4.2.2 Psychometric assessments	154
4.2.3 Procedure	155
4.2.3.1 Apparatus	155

4.2.3.2 EEG experiment	155
4.2.3.3 Data acquisition	155
4.2.3.4 EEG task	155
4.2.4 General data preprocessing	157
4.2.5 Data integrity	159
4.2.6 EEG data preparation for Inter- Trial Phase Coherence analysis	163
4.2.6.1 Data preprocessing	163
4.2.6.2 Data selection	163
4.2.7 Data analysis	166
4.2.8 EEG data preparation for 1/f noise analysis	166
4.2.8.1 Data preprocessing	166
4.2.8.2 Data selection	167
4.2.9 Data analysis	169
4.2.10 Statistical analysis	169
4.3 Results	172
4.3.1 Group comparisons: Inter-Trial Phase Coherence	172
4.3.2 Group comparisons: 1/f noise of Power Spectral Density	179
4.4 Discussion	184
Chapter 5:	188
The relationship between neural noise and the Autism Spectrum Conditions (ASC) phenotype	188
5.1 Introduction	189
5.1.1 Neural variability as a marker of ASC	189
5.1.2 Neural variability and the ASC phenotype	191
5.1.3 Aims of the current study	195
5.2 Materials and Methods	196
5.2.1 Participants	196
5.2.2 Psychometric measures	201
5.2.3 Procedure	204
5.2.4 EEG experiment	204
5.2.5 Data preprocessing	205
5.2.6 Data integrity	205
5.2.7 EEG data preparation for Inter- Trial Phase Coherence analysis	205
5.2.7.1 Data preprocessing	205
5.2.7.2 Data selection	206
5.2.7.3 Data analysis	209
5.2.8 EEG data preparation for 1/f noise analysis	210

5.2.8.1 Data preprocessing	210
5.2.8.2 Data selection	210
5.2.8.3 Data analysis	212
5.2.9 Regression analysis	213
5.3 Results	214
5.3.1 Descriptive statistics	214
5.3.2 Regression Analysis	216
5.4 Discussion	224
Chapter 6:	230
Discussion	230
6.1 Summary of key findings	231
6.2 Implications	236
6.4 Future directions	244
6.5 Conclusion	245
Appendix 1	246
Annex 1	247
Annex 2	253
Annex 3	254
Annex 4	255
Annex 5	256
Annex 6	257
Annex 7	258
Annex 8	263
Annex 9	264
Annex 10	265
References	267

List of figures

Chapter 1

Figure 1.1	Power Spectral Density of signal coming from a single electrode presented as a function of frequencies (f) ranging from 0-250Hz (A) and its corresponding 1/f noise slope for frequencies ranging from 2-24 Hz (B).....	33
-------------------	---	----

Chapter 2

Figure 2.1	Schematic representation of the EEG experiment.....	82
Figure 2.2	Schematic representation of the resting state condition.....	83
Figure 2.3	Summary of A) the general and B) analysis specific preprocessing steps followed.....	84
Figure 2.4	ERPs of the selected Independent Components (ICs) included in the group analysis, presented for the ASC group(n=28).....	86
Figure 2.5	ERPs of the selected channels included in the group analysis, presented for the ASC group(n=28).....	87
Figure 2.6	Scalp maps of the Independent Component with maximum ITPC selected for each participant (n=28) in the ASC group	90
Figure 2.7	Log- transformed Power Spectral Density (log ₁₀ Power) of signal coming from a single electrode F8, is presented here as a function of frequencies (f) ranging from A) 0-250Hz, B) 2-24 Hz including alpha band and C) 2-24 Hz excluding alpha band. A regression line with a negative slope $a = -0.056175$ is fitted to the data in graphs B and C.....	93
Figure 2.8	Method 1 involved a) computing the mean slope of all 64 electrodes for every participant, b) calculating the grand mean slope for each group and c) comparing the grand mean slopes. Here we present the comparison between the ADHD and the TD group.....	95
Figure 2.9	Method 2 involved a) computing the mean slope for each electrode in one group and b) comparing it to the mean slope of the same electrode in the other group. Here we present the comparison between the ADHD and the TD group.....	96
Figure 2.10	Boxplots of maximum ITPC for the three groups, TD, ADHD and ASC (range of values= 0-1), showing differences in central tendency between groups.....	98
Figure 2.11	Average maximum ITPC maps computed for the TD, ADHD and ASC group.....	99
Figure 2.12	Frequency (Hz) where maximum ITPC was observed for each group, TD, ADHD, ASC....	99
Figure 2.13	Boxplots of maximum ITPC for the three groups, TD, ADHD and ASC (range of values= 0-1), showing differences in central tendency between groups.....	101
Figure 2.14	Electrode where maximum ITPC was captured for each group, TD, ADHD, ASC.....	102
Figure 2.15	Frequency (Hz) where maximum ITPC was observed for each group, TD, ADHD, ASC....	102

Figure 2.16	Boxplots of 1/f slopes for the three groups, TD, ADHD and ASC, showing central tendency group differences in the task-based (A) and resting-state condition (B).....	104
Figure 2.17	Scalp maps representing the mean slope computed from different electrode locations for the TD (A), ASC (B) and ADHD (C) group in the task- based condition and for the TD (D), ASC (E) and ADHD (F) group in the resting-state condition.....	105
Figure 2.18	Scalp maps representing uncorrected p-values produced from the comparison of individual electrode slopes in the ADHD vs TD group (A), ASD vs TD group (B), ASD vs ADHD group (C) in the task- based condition and the ADHD vs TD group (D), ASD vs TD group (E), ASD vs ADHD group (F) in the resting- state condition.....	106
Figure 2.19	Scatterplot of age and maximum ITPC computed from the task-based data and plotted for the TD, ADHD and ASC group.	107
Figure 2.20	Scatterplots of age and average 1/f slope of PSD computed from the task-based (A) and resting state data (B) and plotted for the TD, ASC and ADHD groups.....	108
Figure 2.21	Scatterplot of ITPC and 1/f mean slope of PSD computed from individual channels for all participants (n=94)	109
Figure 2.22	Scatterplot of ITPC and 1/f mean slope of PSD computed from Independent Components for all participants (n=94)	110
 Chapter 3		
Figure 3.1	Schematic representation of the Lab Streaming Layer (LSL) protocol.....	125
Figure 3.2	User experience questionnaire.....	127
Figure 3.3	Schematic representation of the EEG experiment.....	128
Figure 3.4	Histogram of jitter time (x axis), presented in seconds (s) for all triggers (y axis).....	133
Figure 3.5	Example Independent Component (IC) scalp maps.....	135
Figure 3.6	a) Grand-average ERPs computed from electrodes P3, P4, Pz, POz, O1, Oz, O2 for all participants and b) ERP traces plotted for the example electrode O2, as extracted for all participants.....	138
Figure 3.7	Proportion of children that responded positively (“Excellent”, “Very good”), neutrally (“Good”, “Okay”) and negatively (“Poor”, “Very poor”) to Questions 1-3.....	139
 Chapter 4		
Figure 4.1	Schematic representation of the EEG experiment.....	156
Figure 4.2	Summary of A) the general and B) analysis specific preprocessing steps followed.....	158

Figure 4.3	ERPs of the selected Independent Components (ICs) included in the group analysis ($n=65$), presented for the ASC group. Participants with a less clear VEP, excluded from the group analysis, are marked in red ($n=2$).	160
Figure 4.4	ERPs of the selected channels included in the group analysis ($n=67$), presented for the ASC group.....	162
Figure 4.5	Scalp maps of the Independent Component with maximum ITPC for participants 1-67 in the ASC group. Data of two participants outlined in red were excluded from further analysis.	164
Figure 4.6	Scalp maps of the Independent Component with maximum ITPC selected for participants 1-25 in the TD group.....	165
Figure 4.7	Log-transformed Power Spectral Density (\log_{10} Power) of signal coming from a single electrode CP5 from a participant in the ASC group, is presented here as a function of frequencies (f) ranging from A) 0-250Hz, B) 2-24 Hz including alpha band and C) 2-24 Hz excluding alpha band. A regression line with a negative slope $a = -0.063614$ is fitted to the data in graphs B and C.....	168
Figure 4.8	Method 1 involved a) computing the mean slope of all 32 electrodes for every participant in the ASC and TD group, b) calculating the grand mean slope for each group and c) comparing the grand mean slopes.....	171
Figure 4.9	Scatterplot of age and maximum ITPC computed from the task-based data and plotted for the ASC and TD group.....	172
Figure 4.10	Scatterplot of Performance IQ and maximum ITPC computed from the task-based data and plotted for the ASC and TD group.....	173
Figure 4.11	Boxplots of maximum ITPC for the ASC and TD group, showing differences in central tendency between groups.....	174
Figure 4.12	Average maximum ITPC maps computed for the ASC and TD group.....	175
Figure 4.13	Frequency (Hz) where maximum ITPC was observed for the TD and ASC group.....	176
Figure 4.14	Boxplots of maximum ITPC for the TD and ASC (range of values= 0-1), showing differences in central tendency between groups.....	177
Figure 4.15	Electrode where maximum ITPC was captured for each group, TD and ASC.....	178
Figure 4.16	Frequency (Hz) where maximum ITPC was observed for each group, TD and ASC.....	179
Figure 4.17	Scatterplots of age and average $1/f$ slope of PSD computed from the task-based (A) and resting state data (B) plotted for the ASC and TD group.....	180
Figure 4.18	Scatterplots of Performance IQ and average $1/f$ slope of PSD computed from the task-based (A) and resting state data (B) plotted for the ASC and TD group.	181
Figure 4.19	Boxplots of $1/f$ slopes for the two groups, ASC and TD, in the task-based (A) and resting-state condition (B).	182

Figure 4.20	Scalp maps representing the mean slope computed from different electrode locations for the ASC (A) and TD group (B) in the task- based condition and for the ASC (C) and TD group (D) in the resting-state condition.	183
 Chapter 5		
Figure 5.1	A striped pattern with high spatial frequency and high contrast. Reproduced with the kind permission of Prof Arnold Wilkins and Prof Bruce Evans.....	194
Figure 5.2	“Natural” (A) vs “Unnatural” (B) patterns in the environment.....	194
Figure 5.3	Number of participants included in the study after exclusion criteria was applied.....	200
Figure 5.4	The Pattern Glare Test. Reproduced with the kind permission of Prof Arnold Wilkins....	203
Figure 5.5	Scalp maps of the Independent Component with maximum ITPC selected for participants 1-35 in the ASC group.....	207
Figure 5.6	Scalp maps of the Independent Component with maximum ITPC selected for participants 36-67 in the ASC group.....	208
Figure 5.7	Log-transformed PSD (log10 Power) of signal coming from a single electrode CP5, is presented here as a function of frequencies (f) ranging from A) 0-250Hz, B) 2-24 Hz including alpha band and C) 2-24 Hz excluding alpha band. A regression line with a negative slope $a = -0.063614$ is fitted to the data in graphs B and C.....	211
Figure 5.8	The mean slope of all 32 electrodes was computed for every participant.....	212
Figure 5.9	Frequency (Hz) where maximum ITPC was observed.....	215
Figure 5.10	Average maximum ITPC maps computed for all participants ($n=65$).....	215
Figure 5.11	Scalp maps representing the mean slope computed for the task-based condition ($n=67$) and the resting-state condition ($n=62$).....	216
Figure 5.12	Scatterplot showing the relationship between maximum ITPC and Visual Distortions.....	220
Figure 5.13	Scatterplot showing the relationship between 1/f slope of PSD as computed from resting state data and Visual Symptoms.....	224
 Appendix 1		
Figure 1.1	Scatterplot of ITPC and 1/f slope of PSD grouped by the number of additional diagnoses and the type of diagnoses for the ASC group (A, B) and the TD group (C).....	246
 Annex 1		
Figure 1.1	ERPs of the selected Independent Components (ICs) included in the group analysis, presented for the TD group ($n=34$)	247
Figure 1.2	ERPs of the selected Independent Components (ICs) included in the group analysis, presented for the ADHD group ($n=32$)	248

Figure 1.3	ERPs of the selected Independent Components (ICs) included in the group analysis, presented for the ASC group (<i>n</i> =28)	249
Figure 1.4	ERPs of the selected channels included in the group analysis, presented for the TD group (<i>n</i> =34).	250
Figure 1.5	ERPs of the selected channels included in the group analysis, presented for the ADHD group (<i>n</i> =32).	251
Figure 1.6	ERPs of the selected channels included in the group analysis, presented for the ASC group (<i>n</i> =28).	252
 Annex 2		
Figure 2.1	Independent Components with maximum ITPC for the TD, ADHD and ASC group	253
 Annex 3		
Figure 3.1	1/ <i>f</i> slope of all electrodes computed from Participant 6 in the ASC group	254
 Annex 4		
Figure 4.1	Maximum ITPC heat maps for the TD, ADHD and ASC group.....	255
 Annex 5		
Figure 5.1	Communication cards used during the mobile EEG session.....	256
 Annex 6		
Figure 6.1	Participant and experimenter interactions during the mobile EEG testing session.....	257
 Annex 7		
Figure 7.1	ERPs of the selected Independent Components (ICs) included in the group analysis, presented for the TD group (<i>n</i> =25)	258
Figure 7.2	ERPs of the selected Independent Components (ICs) included in the group analysis, presented for the ASC group (<i>n</i> =65)	259
Figure 7.3	ERPs of the selected channels included in the group analysis, presented for the TD group (<i>n</i> =25).	260
Figure 7.4	ERPs of the selected channels included in the group analysis, presented for the ASC group (<i>n</i> =67).	261
 Annex 8		
Figure 8.1	1/ <i>f</i> slope of all electrodes computed from Participant 26 in the ASC group.....	263
 Annex 9		
Figure 9.1	Maximum ITPC heat maps for the TD and ASC group.....	264

List of tables

Chapter 1

Table 1.1	Studies measuring ITPC in individuals with a clinical diagnosis of ASC.....	48
Table 1.2	Studies measuring ITPC in other clinical populations.....	49

Chapter 2

Table 2.1	Studies measuring neural variability in individuals with a clinical diagnosis of ADHD.....	75
Table 2.2	Participant demographics.....	79
Table 2.3	Number of participants in each group with formal diagnosis of a co-morbid condition.....	79
Table 2.4	Drug intake of participants recorded up to 16 hours prior to the EEG experiment.....	80
Table 2.5	Mean values (M) and Standard Deviations (SD) of the max ITPC extracted from the Independent Components presented for the three groups ADHD, ASC and TD.....	97
Table 2.6	Mean values (M) and Standard Deviations (SD) of the max ITPC extracted from the occipital electrode cluster, presented for the three groups TD, ADHD and ASC.....	100
Table 2.7	Mean values (M) and Standard Deviations (SD) of the 1/f slope of PSD, computed for the three groups TD, ADHD and ASC.....	103

Chapter 3

Table 3.1	Participant demographics.....	122
Table 3.2	Number of participants with a diagnosed comorbid condition.....	123
Table 3.3	Drug intake of participants recorded up to 24 hours prior to the EEG experiment.....	124
Table 3.4	Mean (M), Standard Deviation (SD), Minimum (Min) and Maximum (Max) number of EEG channels and epochs retained, as computed from data acquired using the 32-channel Eego Sports mobile system.....	134
Table 3.5	P1 and N1 Amplitude (uV) and Latency (ms) computed from electrodes P3, P4, Pz, POz, O1, Oz, O2 from all participants (Mean, Minimum, Maximum) and the reliability values (R) given for the peak P1 and N1 Amplitude and Latency.....	136
Table 3.6	Number and percentage of participants in the group showing P1 and N1 deflections at each of the electrodes P3, P4, Pz, POz, O1, Oz, O2.....	137
Table 3.7	Key themes and subthemes, as emerged from children's responses to Question 4 and 5.....	141
Table 3.8	Available mobile EEG systems and their technical specifications.....	145

Chapter 4

Table 4.1	Participant demographics.....	151
Table 4.2	Number of participants with a diagnosed comorbid condition.....	152
Table 4.3	Regular drug intake of participants in the ASC and TD group.....	153
Table 4.4	Severity of social communication impairments in the ASC and TD group as indicated by the SRS-2.....	154
Table 4.5	Mean (M), Standard Deviation (SD, Range of artefact-free EEG channels and experimental trials and the t-statistic presented for the comparison of the means in the ASC and TD group..	162
Table 4.6	Mean values (M) and Standard Deviations (SD) of the max ITPC extracted from the Independent Components presented for the ASC and TD groups.....	172
Table 4.7	Mean values (M), Standard Deviations (SD), Minimum (Min) and Maximum (Max) of the frequency, where maximum ITPC occurred at, presented for the ASC and TD groups.....	175
Table 4.8	Mean values (M) and Standard Deviations (SD) of the max ITPC extracted from the occipital electrode cluster, presented for the ASC and TD groups.....	176
Table 4.9	Mean values (M), Standard Deviations (SD), Minimum (Min) and Maximum (Max) of the 1/f slope of PSD computed for the task-based and resting-state condition, for the ASC and TD group.....	179

Chapter 5

Table 5.1	Participant demographics.....	197
Table 5.2	Regular drug intake of participants.....	198
Table 5.3	Number of participants with a diagnosed comorbid condition.....	199
Table 5.4	Reliability statistics for the items used for further analysis.....	204
Table 5.5	Mean (M), Standard Deviation (SD, Range of artefact-free EEG channels and experimental trials retained for further analysis.....	205
Table 5.6	Mean (M), Standard Deviation (SD), Minimum (Min) and Maximum (Max) value of maximum ITPC and the average Frequency (Hz) it occurs at, as computed from a) linearly and b) logarithmically spaced frequencies.....	209
Table 5.7	Number of participants (N), Mean values (M), Standard Deviations (SD), Minimum (Min) and Maximum (Max) values of the variables used in the regression analysis.....	214
Table 5.8	Pearson's correlation coefficients, Tolerance and Variation Inflation Factors (VIF), for the independent variables included in Model 1, Model 2 and Model 5.....	217
Table 5.9	Regression analysis summary of core diagnostic symptoms of ASC predicting maximum ITPC (Model 1).....	217

Table 5.10	Regression analysis summary of core diagnostic symptoms of ASC predicting 1/f slope of PSD as extracted from the task-based data (Model 2).....	218
Table 5.11	Pearson's correlation coefficients, Tolerance and Variation Inflation Factors (VIF), for the independent variables included in Model 3, Model 4 and Model 6.....	219
Table 5.12	Regression analysis summary of sensory symptoms specific to the visual modality predicting maximum ITPC (Model 3).....	220
Table 5.13	Regression analysis summary of sensory symptoms specific to the visual modality predicting 1/f slope of PSD as extracted from the task-based state data (Model 4).....	221
Table 5.14	Regression analysis summary of core diagnostic symptoms of ASC predicting 1/f slope of PSD as extracted from the resting-state data (Model 5).....	222
Table 5.15	Regression analysis summary of sensory symptoms specific to the visual modality predicting 1/f slope of PSD as extracted from the resting-state data (Model 6).....	223
Annex 10		
Table 10.1	Psychometric tools assessing Sensory Symptoms.....	265

Abstract

Increased neural noise is proposed to be a potential endophenotype of Autism Spectrum Conditions (ASC) (Simmons, 2009; David et al, 2016; Haigh, 2018), capturing disrupted neural synchrony dynamics inherent to the condition (Rubenstein & Merzenich, 2003). Nevertheless, the neural noise hypothesis of ASC has not been previously examined systematically. Using Electroencephalography (EEG), the present thesis investigates neural noise by measuring the degree of phase angle alignment of neural oscillations between experimental trials through the Inter-trial Phase Coherence (ITPC) metric and the steepness of 1/f noise slope of Power Spectral Density (PSD), a variable quantifying broadband changes in power spectra as a function of temporal frequency (Gao et al., 2017; Donoghue et al., 2020) in a visual task-based and a resting state condition. The present thesis comprises of four studies: a) an investigation of neural noise in clinical samples of adults with ASC and ADHD b) the presentation of a new accessible method of studying brain activity of autistic individuals at home, using mobile EEG technology, c) a study of neural noise in a large sample of children with ASC ($n=67$) and d) an investigation of the relationship between neural noise and behavioural symptoms associated with the ASC phenotype. In the present thesis it was established that increased neural variability in the form of low ITPC occurs only in a group of children with ASC. Although levels of ITPC differed significantly between children with and without ASC at a group level, low ITPC could not differentiate participants with ASC from participants without ASC with adequately high accuracy to be considered a biomarker of ASC, as proposed in the literature (David et al., 2016). In addition, it was demonstrated that ITPC, as measured in response to visual stimulation, is not linked to primary phenotypic expressions of ASC but is associated with anomalous visual experiences and visual distortions, a group of visuoperceptual symptoms shown to manifest with varying prevalence in individuals with ASC and other people in the general population. Finally, it was established that 1/f noise power spectral dynamics, measured during processing of simple visual stimuli and during rest, were intact in the ASC and ADHD samples tested, providing evidence against the pathological undercoupling hypothesis proposed by Voytek & Knight (2015).

Chapter 1:
Introduction

1.1 Autism Spectrum Condition (ASC)

Autism Spectrum Condition (ASC) is a heterogeneous disorder with a complex underlying genetic etiology (Bill & Geschwind, 2009). Formal diagnosis of ASC is provided on the basis of the presence of two core clusters of symptoms, a) social communication difficulties and b) repetitive and restricted patterns of behaviour (American Psychiatric Association, 2013). Growing evidence suggests that atypical sensory processing, manifesting as “*hyper- or hypo- reactivity to sensory input or unusual interest in the sensory environment*” (American Psychiatric Association, 2013) also lies at the core of ASC, captured within the restricted and repetitive behaviour diagnostic symptom domain (Simmons et al., 2009; Haigh, 2018). ASC symptom severity varies, ranging from mild to severe (American Psychiatric Association, 2013). Behavioural expressions of ASC are shown to change as the individual transitions from childhood to adulthood (Shattuck et al., 2007; Esbensen et al., 2009; Bal et al., 2019) and are shown to differ in females compared to males (Lai et al., 2012; Frazier & Hardan, 2017; Parish-Morris et al., 2017). Such factors contribute to greater behavioural heterogeneity within the condition (see Jeste & Geschwind, 2014 for a review). Behavioural heterogeneity is also amplified by the high prevalence of comorbid psychiatric (e.g. anxiety disorders, depressive disorders, bipolar and mood disorders, attention-deficit/hyperactivity disorder, see Rosen et al., 2018; Hossain et al., 2020) and other medical conditions in ASC (e.g. epilepsy, motor impairment and sleep disturbances, see Croen et al., 2015; Lukmanji et al., 2019), revealing a complex, multidimensional aspect of ASC not accounted for in the current diagnostic framework. In addition, Intellectual Disability (ID) is one of the most frequently co-occurring conditions, with prevalence rates varying from 16.7% (de Bildt et al., 2005) to 28% (Bryson et al., 2008; Van Naarden Braun et al., 2015). This means that the current diagnostic schema, which classifies individuals as autistic based on whether they exhibit behaviours in both symptom clusters above or below an artificial threshold of severity, is inherently flawed and fails to capture important clinical nuances resulting in diagnostic instability and a difficulty to uncover etiological factors linked to ASC (Dagleish et al., 2020).

Early studies treated autism as a unitary disorder, attributed to a single cause, an idea heavily promoted by the categorical structure of the diagnostic process. In that context, a number of single deficit cognitive theories have been proposed to explain ASC. The Theory of Mind hypothesis (Baron-Cohen et al., 1985; Frith, 2003), Weak Central Coherence (Frith, 2003), Executive Dysfunction (Pennington & Ozonoff, 1996) and the theory of Hypo-Priors (Pellicano & Burr, 2012) are some examples of such single deficit theories. These cognitive theories provide a basis for

exploring very complex aspects of ASC symptomatology and indeed they validly describe many facets of the condition (Belmonte et al., 2004). However, recent advances in autism research suggest that a single cognitive deficit is unlikely to be the main cause of the wide range of behavioural features observed across the autism spectrum (Happé et al., 2006; Happé & Frith, 2020). For example, social deficit theories provide a framework to explain aspects of social communication difficulties but fail to provide sufficient evidence of how these lead to the manifestation of rigid and repetitive patterns of behaviours, particularly sensory perceptual differences in autistic individuals. In addition, the ASC profile is shown to be associated with cognitive peaks and troughs, i.e strengths in visual perception, language, abstract reasoning but weaknesses in cognitive speed and language comprehension, a cognitive profile that varies greatly from one individual to the other (Mandy et al., 2015). On that note, as Happé et al. (2006) eloquently point out, maybe it's "*time to give up on a single explanation for autism*".

Emerging evidence suggests that behavioural symptoms of ASC are in fact "*fractionable*", meaning that core ASC symptom domains are independent from each other at a genetic and cognitive level (Happé et al., 2006; Brunsdon & Happé, 2014; Happé & Frith, 2020). Growing support for this hypothesis stems from large population-based studies such as the one by Ronald et al. (2006) who found that ASC core symptom domains correlate moderately or very little. Social communication difficulties and repetitive and restricted patterns of behaviour are very weakly related both in the general population and in children with high ASC traits (Ronald et al., 2006). Dworzynski et al. (2009) report similar results in clinical ASC samples i.e. in autistic twins. The development of genetic data repositories (e.g. Simons simplex collection) allowed for large-scale molecular genetic studies such as the one conducted by Warrier et al. (2019), which used polygenic score analysis to further demonstrate that social and non-social ASC symptom domains are genetically dissociable. The above studies suggest that separate genes contribute to social, communicative and repetitive/restricted behaviours, reinforcing the message that autism does not exist on a single dimension.

Does this mean that ASC as a condition does not exist? On the contrary, despite the fact that ASC behavioural features are independent from each other, the probability of them co-occurring is at above-chance levels (Happé et al., 2006). Although ASC shares behavioural features and genetic influences with other disorders, the two symptom clusters of ASC interact in a complex way and give rise to a distinct condition (Happé & Frith, 2020). The "*fractionable*" nature of ASC

nevertheless has shaped the thinking of newly emerging research work in a number of different ways. First, ASC symptom domains begin to be studied separately (Bal et al., 2019; Uljarevic et al., 2020). In addition, if the genetic and cognitive causes of ASC symptoms are distinct, this implies that a single, unique neural feature that gives rise to the range of phenotypic expressions may not exist. For that reason, ASC symptom expressions are also studied in the context of specific neural correlates (Lo et al., 2019; McKinnon et al., 2019; Jasmin et al., 2019). Second, a growing number of studies acknowledge that heterogeneity in ASC is the outcome of large variability within two (or more) independent clusters of symptoms, each one with distinct neural underpinnings and with a distinct genetic basis (Happé & Frith, 2020). In an effort to uncover the etiology behind ASC, more and more studies are using cluster analysis to study phenotypically homogeneous subgroups (Kim et al., 2016; Zheng et al., 2020). Others are reversing the problem and are investigating ASC traits in genetically homogeneous samples such as 22q13 deletion syndrome (see hypothesis for hyper-expression of SHANK3 at Harony et al., 2013), Fragile X or other single-gene neurodevelopmental disorders, conditions shown to share synaptic plasticity defects with ASC (Baudouin et al., 2012). Third, considering that ASC behavioural symptoms exist on a continuous dimension, measured both in the general population and in other clinical groups (Constantino et al., 2004; Ruzich et al., 2015; Bralten et al., 2018), the transdiagnostic approach of studying ASC traits across multiple neurodevelopmental disorders is proving to be a useful method of disentangling the genetic influences on behavioural expressions (see Bruining et al., 2010). Taken together, we see a shift in direction towards the study of specific behavioural symptoms in relation to their underlying neural mechanisms and their specific genetic basis (see recent work by Warrier et al., 2019 which links polygenic scores with specific symptoms).

1.2 Identification of biomarkers in ASC

ASC is primarily caused by genetic factors (Tick et al., 2016; Bai et al., 2019; Thapar & Rutter, 2020). Genetic studies suggest that the environmental effect is not strong enough to explain the biggest portion of the variance of ASC phenotypic expressions (Mandy & Lai, 2016). Thirty decades of research in the field has revealed that ASC is a highly heritable disorder. It is characterized not only by great behavioural heterogeneity but also a great genetic heterogeneity and a complex genetic architecture (Shaaf et al., 2020; Thapar & Rutter, 2020). The majority of evidence supporting the genetic risk of ASC has come from twin and family studies. Monozygotic twins- that is twins who share all of their genes- demonstrate 36-96% concordance rate depending on whether the diagnosis is narrowly or strictly defined (Folstein & Rutter, 1977; Rosenberg et al., 2009; Hallmayer et al., 2011; Gaugler et al., 2014; Tick et al., 2016) and dizygotic twins from 0% to 40% (Folstein & Rutter, 1977; Colvert et al., 2015). The estimated probability of a second sibling being diagnosed with ASC is 2 to 14% (Rutter, 2000) compared to only 0.6% in the typically developing population (Wing & Potter, 2002).

Despite the advances in interdisciplinary research of ASC, it has proven extremely difficult to locate autism risk genes and delineate their impact on phenotypic expressions (Schaaf et al., 2020). In the cases where susceptibility loci have been reported in more than one study- mainly on chromosomes 2, 7, 15 and 16 (Benayed et al., 2005; Campell et al., 2006; Sanders et al., 2011)- significance levels are low and lack of replicability remains an important burden (Viding & Blakemore, 2007). Efforts to identify genes leading to the ASC phenotype or else the “*gene-phenotype*” pathways, have not been fruitful for two main reasons; a) genetic studies have been striving to identify specific genes linked to autism as a single entity encompassing both social communication difficulties and rigid/repetitive patterns of behaviour (Happé et al., 2006) and b) ASC is characterised by great behavioural heterogeneity i.e great diversity in the levels of cognitive functioning, symptom severity and the high number of comorbidities manifesting in the condition (Bill & Geschwind, 2009). Even when research efforts are made to link genes to specific behavioural expressions, causal routes leading to the same behavioural symptom can vary (Morton, 2008) and although reliable tools are used to measure clusters of behavioural symptoms in ASC, it has proven challenging to identify etiologically homogeneous groups solely based on clinical symptoms (Rutter, 2011; Loth & Evans, 2019 for a first effort to identify behavioural markers). In other words, there is a large number of biological processes that occur between the one endpoint- the specific *gene*- and the other endpoint- the specific *behaviour* (Betancur, 2011). Therefore, associating intermediate phenotypes or

biomarkers with specific behavioural expressions may be more useful for shedding light on the gene-phenotype pathways as these carry meaningful information about gene expression and act as a “middle stop”, directly bridging the gap between gene and behaviour.

A biomarker is a quantifiable feature that indicates “*a normal biological or a pathological process*” or is objectively used to measure “*the biological responses to a therapeutic intervention*” (Biomarkers Definitions Working Group, 2001). Importantly, it is considered as an inherent part of the causal chain by which psychiatric disorders arise (Viding & Blakemore, 2007). The discovery of disorder-specific biomarkers in psychiatric disorders allows for further investigation of the genetic influences on specific symptoms (Abrahams & Geschwind, 2008; Geschwind, 2008). They can be anatomical, electrophysiological, metabolic, developmental or cognitive (Flint & Munafò, 2007). Certain criteria have to be met for a marker to be characterized as an endophenotype of a psychiatric disorder; it should represent a reliable and consistent characteristic of the phenotype, it should be heritable, explained by shared genes and it should highly correlate with a particular symptom of the diagnostic category (DeGeus & Boomsma, 2001). In ASC, it is likely that these quantifiable features do *not* take the strict form of a biomarker or an endophenotype but rather, they are neural features linked to some aspect of the ASC phenotype, indicative of one of the many pathophysiological routes to disorder expression (Scarr et al.; 2015; Carroll et al., 2021).

The identification of clinically relevant markers in psychiatric conditions ultimately allows for the identification of cohesive subgroups within a highly heterogeneous psychiatric group, thereby allowing for personalised interventions and care (Bridgemohan et al., 2019). While acknowledging that a single genetic or neurocognitive cause of autism as a whole is unlikely to exist, this is a very promising avenue for studying ASC in particular as it also recognizes that a single “treatment” is unlikely to work for every person with ASC (Happé et al., 2006). Unlike other conditions, in ASC there is a lack of pharmacological interventions, therefore early diagnosis and individualised intervention practices currently remain the two most effective approaches to care for individuals with ASC. The shift towards the use of neural signatures to identify homogeneous subgroups of individuals with similar neurocognitive profiles (Viding & Blakemore, 2007), has the potential to lead to improved diagnostic processes (i.e early diagnosis), more accurately defined intervention recommendations and more precisely determined prognostic outcomes (Geschwind & State, 2015; Bridgemohan et al., 2019).

1.3 Scope of the present thesis

A plethora of research studies propose that increased neural noise may be a potential endophenotype of ASC (see Simmons, 2009; David et al., 2016 and Haigh, 2018 for a review), capturing disrupted neural communication dynamics inherent to the condition. This proposal is based on a growing number of experimental findings indicating that levels of neural noise in the form of intra-individual neural variability are increased in samples of individuals with ASC as compared to their typically developing counterparts (see Section 1.5.5 for a detailed discussion). Nevertheless, the neural noise hypothesis of ASC has not been previously examined systematically. Using Electroencephalography (EEG), the present thesis investigates neural noise by measuring the degree of phase angle alignment of neural oscillations between experimental trials through the Inter-trial Phase Coherence (ITPC) metric and the steepness of 1/f noise slope of Power Spectral Density (PSD), a variable quantifying broadband changes in power spectra as a function of temporal frequency (Gao et al., 2017; Donoghue et al., 2020). As discussed in more detail in Section 1.4.3 and 1.4.4, the two metrics provide unique insights into both periodic and aperiodic neural dynamics, allowing to study neural noise locally and globally in the brain of individuals with ASC.

1.4 Definitions

1.4.1 Neural communication

In his *Communication through Coherence* theory, Fries (2016) defines *neural communication* as the signal transmission from a presynaptic group of neurons to a postsynaptic group, mechanistically facilitated by *neural synchrony*. *Neural synchrony* refers to rhythmic synchronization of pre- and postsynaptic groups of neurons in response to an event, such that the output sent by the presynaptic group arrives at phases of maximal excitability of the postsynaptic group, a mechanism allowing for greater effective connectivity (Fries, 2005; Fries, 2015). A set of postsynaptic group of neurons receiving synaptic input from multiple presynaptic groups will selectively respond to the group of cells whose phase is most coherent with theirs, in other words, inputs arriving at random phases of excitation are largely ignored (Fries, 2015; Perez-Cervera et al., 2020). This mechanism places the notion of *phase-locking* and *phase coherence* at the core of neural communication (Sauseng & Klimesch, 2008).

1.4.2 Neural oscillations

Neural oscillations refer to rhythmic patterns of electrical activity, of varying frequency, amplitude and phase, generated naturally in the brain. Depending on the number of wave cycles occurring in a second, they are classified in frequency bands. Slow rhythms include delta (0.5-3Hz), theta (4-8Hz) and alpha band oscillations (8-12Hz), whereas fast(er) rhythms include beta (12-30Hz) and gamma band oscillations (40-70Hz).

How does such a vast number of neural cells, transmitting and re-transmitting signals, coordinate their rhythms to give rise to higher-order cognitive processes? Neural oscillations and their interactions are the building blocks of effective communication in the human brain (Fries, 2015). Low and high frequency oscillations do not exist independently but interact in a complex way to give rise to higher-order cognitive processes; their interplay is integral for the synthesis of information and for the orchestration of multisensory integration (Engel, Senkowski & Schneider in Murray & Wallace, 2011).

Theta oscillations (4-8Hz) play a fundamental role in working memory processes (Wang et al., 2018; Quirk et al., 2021) and in top-down adaptive control (Cavanagh & Frank, 2014). They emerge across the various levels of cortical hierarchy and are particularly prominent in the medial temporal lobe i.e the hippocampus and the parahippocampal cortices (Quirk et al., 2021; Barbeau et al., 2005), the visual cortex (Kienitz et al., 2021) as well as distal areas that are part of the hippocampal memory circuit such as the prefrontal cortex (Simons & Spiers, 2003). Theta oscillations are integral to the formation of episodic memory associations and the effective “binding” of different sensory and cognitive representations in memory (Herweg et al., 2020). Numerous studies in humans have showed that a) power increases of theta oscillations in the hippocampus and the neocortex predict successful episodic memory retrieval (Klimesch, 1996; Klimesch, 1997; Khader et al., 2010; Herweg et al., 2016), b) the strength of theta phase-locking in the visual and auditory cortices predicts memory performance (Wang et al., 2018) and c) phase-locking increases during the P1 and N1 time window, particularly at occipital electrodes, during episodic memory encoding and retrieval (Klimesch et al., 2004). Other lines of work have shown that rhythmic activity in the theta range is enhanced in frontal midline areas during tasks that require increased cognitive control- for example during the processing of novel information, conflict, punishing feedback and error (Hanslmayr et al., 2008; Cavanagh et al., 2009; Nigbur et al, 2012; Anguera et al., 2013). It is therefore proposed

that frontal midline theta facilitates goal-specific information transfer to other task-relevant neural regions i.e sensory or motor cortices oscillating at a similar frequency (McLoughlin et al., 2021).

Alpha band oscillations (8-12Hz) are the dominant rhythms in the brain of humans (Klimesch, 1999). For a long time they were considered to reflect “cortical idling” as they were shown to be more prominent when participants are in an awake state but not engaged in any cognitive task (Pfurtscheller, Stancak & Nueper, 1996). More recent experimental work has demonstrated that alpha oscillations are linked to alertness and are responsible for the inhibition of activity in task-irrelevant regions by suppressing distracting information (Klimesch, Sauseng & Hanslmayr, 2007; Jensen & Mazaheri, 2010). The power of alpha oscillations is shown to increase in disengaged cortical areas but decrease in engaged regions (Thut, 2006; Klimesch et al., 1999; van Diepen et al., 2015). Groups of neurons oscillating in the alpha rhythm are shown to propagate activity from higher to lower-order assemblies- for the visual stream for example from anterosuperior regions to the occipital pole (Halgren et al., 2019).

Beta oscillations (12-20Hz) have been traditionally linked to sensorimotor processing. In the sensorimotor cortex, a well-replicated finding is the tendency of beta oscillations to decrease their power in preparation of movement, but increase their power post-movement, further interpreted as desynchronization and synchronization of local neurons in the area respectively (Kilavik et al., 2013). However, newly emerging evidence has shown that beta oscillations play an important functional role in other cognitive processes such as visual perception (Kloosterman et al., 2015), working memory (Siegel, Warden & Miller, 2009), episodic memory formation and retrieval (Griffiths et al., 2021) and decision-making (Wong et al., 2016). Growing evidence also postulates that beta oscillatory networks facilitate the contextual gating of information (Limanowski, Litvak & Friston, 2020). They are proposed to maintain the current “status-quo” state of the brain (Engel & Fries, 2010) and project information from higher to early sensory systems about the behavioural context of a cognitive task (Foxy & Snyder, 2011). Experimental work has shown that low beta oscillations behave similarly to alpha oscillations (i.e increased power in task-irrelevant cortical areas and decreased power in task-relevant regions), whereas high beta oscillations (20-30 Hz) display similar behaviour to gamma oscillations and therefore increase in power in task-engaged areas (Tallon-Baudry et al., 1998).

Gamma band oscillations (>40Hz) have received considerable scientific attention. They are proposed to play a fundamental role in the perceptual binding process. Multiple lines of work

indicate that gamma oscillations facilitate bottom-up feature binding and information flow from primary sensory areas to higher areas of the brain to create a unified perceptual representation of an event (Fries, 2015). Experimental evidence has showed that fast-oscillating gamma rhythms generate bursts of excitation very rapidly, followed by bursts of inhibition, with a 3ms lag (Atallah & Scanziani, 2009). It is proposed that these fluctuations take place quickly enough to allow network excitation to escape the neural assembly and reach remote projection targets in higher cortical regions, subsequently activating postsynaptic neural cells in those areas (Fries, 2015). Cannon et al. (2014) and Lowet et al. (2015) also demonstrated that assemblies oscillating at a faster frequency are more likely to entrain slower-oscillating groups, when competing against each other to reach higher areas (e.g from V1 to V4 in the visual cortex). In addition, selective attention is shown to strengthen gamma-mediated synchrony in multiple experiments (Fell et al., 2003; Tallon-Baudry, 2009), allowing for task-relevant information to be prioritized over task-irrelevant information (Doesburg, Roggeveen, Kitajo & Ward, 2008). Taken together, when neural assemblies are oscillating at the gamma rhythm, they are able to entrain post-synaptic neurons in distant structures through a bottom-up process.

This feedforward influence of gamma oscillations on the activity of higher-order neural assemblies is suggested to be attenuated by alpha and beta band top-down cortical influences (Fries, 2015). In support of this notion, Van Kerkoerle et al. (2014) showed that electrical stimulation of V1 trigger increases in gamma power in V4, whereas stimulation of V4 trigger subsequent increases in alpha power in V1, in line with the idea of bottom-up influence of gamma and top-down influence of alpha oscillations. Similarly, top-down signalling from V4 is carried over to V1/V2 through beta oscillations prior to the presentation of the expected stimulus and becomes more phase-synchronised with increasing task-demands (Brovelli et al., 2004; Richter, Coppola & Bressler, 2018).

1.4.3 Neural noise

In the neurodevelopmental literature, neural noise is conceptualised in the context of neural variability. Neural variability is defined in terms of reliability and precision of neuronal responses; for example the neural response of the neural assembly is reliable when similar number of nerve impulses is observed from one trial to the other and precise when the impulses are observed at similar time points from one trial to the other (Faisal et al., 2008). Neural noise in the form of neural variability characterises both single neuron and neural ensemble/neural circuit behaviour (Faisal et al., 2008). Although individual neurons' states are highly variable, neural ensembles, which consist

of millions of neurons, demonstrate a reliable, precise, highly consistent response to stimuli, which is shown to vary minimally from trial-to-trial in the neurotypical brain (Faisal et al., 2008).

Both intrinsic and extrinsic parameters may contribute to increased levels of neural variability (Renart & Machens, 2014). Intrinsic sources of neural variability involve the study of small structural components of neural cells such as ion channels and pumps, where noise is related to the ion flow fluctuations on the cell membrane (White et al., 1998) and synapses, where noise is generated during synaptic transmission (Brunel et al., 2001). Synaptic noise is the dominant intrinsic source of variability that influences information transmission. It occurs predominantly due to large amounts of incoming spikes changing the cell's membrane potential, a phenomenon known as synaptic bombardment (Shu et al., 2003). Extrinsic sources of neural variability on the other hand include differing tuning properties of neurons at the time when a stimulus is presented and random top-down signals affecting neuronal firing rates (Masquelier, 2013).

1.4.4 Inter-trial Phase Coherence (ITPC)

Inter-trial phase coherence, also known as inter-trial phase clustering, indicates the degree of alignment of the phase angles of a frequency-specific oscillating sine wave at a given time point across a number of epochs (Delorme & Makeig, 2003; Garrett et al., 2013). Specifically, ITPC is calculated from the average vector length of the phase angles captured at each time-point over experimental trials and is extracted through time-frequency analysis. The application of a sliding window of Fast Fourier Transform (FFT) for a given time-frequency point returns complex numbers with a real and an imaginary part, describing the position vector in the two-dimensional plane of time and frequency, values representing the power and phase of the signal. Because Fourier coefficients are measured on a unit circle around the origin, if phase angles are close to being perfectly aligned, they will approach the maximum value of 1, whereas if they are misaligned from one trial to the other, with a distribution approaching uniformity, they will be characterised by values closer to 0 (with 0 being the minimum value). In that respect, a reliable, precise, highly consistent evoked response across epochs will exhibit high ITPC, whereas a highly variable, noisier evoked response will be characterized by low ITPC (David et al., 2016).

Why does phase coherence matter? Ongoing oscillations are shown to become phase-locked to the onset of an external stimulus or experimental event (Makeig et al., 2002). The degree of precision with which phase angles reach a specific reference point in the oscillatory cycle tells us something

integral about the biology of the neural system under scrutiny and the ability of neuronal oscillations to phase-reset effectively in response to external stimulation. From that perspective, ITPC indicates whether a stimulus triggers trial-to-trial changes in phase synchrony of ongoing oscillatory activity across a wide range of frequencies and- depending on the electrode site it is computed from- in distinct regions. It is important however to note that the ITPC metric is different from other connectivity and phase coherence metrics, as it specifically quantifies the degree of phase consistency over successive trials at a single electrode or a specific electrode cluster of interest rather than phase relationships between regions (i.e phase differences). For that reason, the literature review below focuses on studies that have primarily measured ITPC.

ITPC has been primarily studied in low frequency oscillations in response to a wide range of stimuli. High ITPC in the alpha range is proposed to facilitate stimulus encoding and information transfer through the prioritization of task-relevant information and the suppression of task-irrelevant information (Van Diepen et al., 2015). In animal studies, the phase of low-frequency oscillations is shown to adjust so that it reaches an optimal point within the excitatory cycle during stimulus presentation (Lakatos et al., 2008). Behzad et al. (2020) demonstrated that alpha band ITPC increases in the visual cortex of macaque monkeys when spatial cues are presented signalling the arrival of the visual stimulus. In human studies, top-down attention and temporal expectation of sensory stimuli are suggested to modulate the phase of alpha oscillations in some studies (Tallon-Baudry et al., 1996; Samaha et al., 2015) but not in others (Van Diepen et al., 2015).

Stimulus-induced phase-alignment of theta oscillations in frontal cortices is proposed to provide a mechanism of exerting adaptive control over behaviour (Cavanagh & Frank, 2014). It is particularly prominent at electrode clusters covering the medial prefrontal cortex but is also reported in regions connected to the medial prefrontal cortex during conflict (Cohen & Cavanagh, 2011), error processing (Zavala et al., 2016) and performance feedback (Crowley et al., 2014). Cooper et al. (2017) showed that high ITPC at the frontal and parietal electrode clusters during proactive cognitive control (i.e the anticipation of conflict) is associated with lower behavioural variability and Papenberg et al. (2013) reported a link between levels of ITPC and reaction time variability during performance monitoring. Taken together, a growing body of experimental work in humans has demonstrated that the strength of theta ITPC in the frontal midline electrode site is associated with behavioural performance (Klimesch et al., 2004; Papenberg et al., 2013; Cooper et al., 2017) and is subjected to developmental changes across the lifespan (Papenberg et al., 2013).

Regions in the hippocampal-prefrontal memory circuit and the sensory systems are previously shown to become strongly phase-locked to the theta rhythm during various memory tasks (Buzsaki, 2002; Siapas et al., 2005). Theta oscillations are known to promote long-range communication and temporally influence the rate code of the hippocampus by facilitating the translation of segmented units of sensory inputs into memory representations (Ravassard et al., 2013; Bosch et al., 2014; Grion et al., 2016). A recent study by Guntekin et al. (2020) found that high ITPC in the theta range occurs at the parietal and occipital electrode locations and is associated with successful short-term auditory and visual memory encoding in children. In addition, Hickey et al. (2020) showed that low-frequency auditory cues presented during the processing of visual objects enhance levels of ITPC at electrode Cz and bias memory retrieval of visual information, as shown in a subsequent memory retrieval task. Although research measuring theta ITPC during the investigation of memory functions is sparse, the small number of studies presented above can be interpreted in the context of the literature pointing towards the role of the hippocampus as the “switchboard” between memory and sensory perception (Treder et al., 2021).

A larger body of literature has explored ITPC in response to auditory stimuli. During the processing of speech sounds, Koerner & Zhang (2015) report ITPC reductions of low frequency oscillations (delta/theta/alpha) at electrode Cz at time windows corresponding to the N1 and P2 auditory ERPs with the introduction of distracting background noise. Ponjavic-Conte et al. (2013) report grand averaged theta/alpha ITPC reductions at electrode Cz around the N1 latency in the high distraction condition of a selective-listening pitch discrimination task. A more recent study by Sorati & Behne (2019) found reduced alpha ITPC in a group of participants with greater musical experience during the processing of a syllable presented using audio-visual methods, as compared to audio or video alone. The above evidence indicate that alpha oscillations modulate selective attention to the visual cue presented, leading to the prediction of the anticipated sound in participants with more plastic brains (i.e musicians) and overall, the introduction of distraction modulates the gain of the auditory ERP and disrupts ITPC of low frequencies locally at Cz.

In summary, available evidence suggests that high ITPC is linked to improved cognitive performance in human participants, including improved visual discrimination (Hanslmayr et al., 2005), visual attention (Ding et al., 2006) and memory encoding (Fell et al., 2008; Guntekin et al., 2020), whereas low ITPC is reported in pathophysiological processes in ASC (Milne, 2011), schizophrenia (Light et al., 2006; Koh et al., 2011), ADHD (Groom et al., 2010; Saville et al., 2015), dyslexia (Soltesz et al., 2013), and sleep disorders (Eidelman-Rothman et al., 2019).

1.4.5 1/f noise of Power Spectral Density (PSD)

1/f noise of Power Spectral Density (PSD), also known as “1/f neural electrophysiological noise”, is suggested to capture broadband changes in power spectra as a function of temporal frequency, reflecting dendritic activity in response to an experimental event (Gao, 2016; Lombardi et al., 2017; Haller et al., 2018; Donoghue et al., 2020). It refers to fluctuations of PSD such that the dissipated energy per frequency interval is inversely proportional to the frequency of the signal, with a scaling exponent of one, also known as “noise exponent”, “fractal” or “1/f slope” (Gao, 2015; Voytek et al., 2015; Donoghue et al., 2020). White noise is represented in a spectrogram as a flat line with a scaling exponent of zero. In that context, the closer the exponent is to zero, the flatter the line of the slope will be, indicating a more variable, less synchronized neural response (Voytek et al., 2015). On the other hand, a more negative noise exponent indicates that the system produces a less variable, highly synchronized neural response (Voytek et al., 2015). As proposed in the relevant literature (Voytek et al., 2015; Voytek & Knight, 2015; Donoghue et al., 2020), there is an optimal balance between the two and extreme deviations from the mode- steeper or flatter slope- are strong evidence for disruptions in neural communication across the cortex. *Figure 1.1* shows an example of how power recorded from a single electrode is distributed in the frequency domain and its corresponding 1/f noise slope.

The origin of 1/f noise is a heavily debated topic in theoretical physics and the exact nature of the underlying processes that give rise to power law behaviour is yet to be precisely determined. Neural networks perform exceptionally complex computations, very efficiently and with great precision. Like many other complex systems in nature, neural circuits are shown to achieve optimal information processing capabilities when they are in a state of ‘criticality’ allowing for increased information storage capacity (Beggs & Plenz, 2003; Beggs, 2008), computational power (Bertschinger & Natschlager, 2004) and sensitivity to inputs (Kinouchi & Copelli, 2006). 1/f noise, suggested to be a signature of criticality in the brain, is regularly observed in the statistical properties of observables computed from electrophysiological data (Miller et al., 2009; Markovic & Gros, 2014). From a theoretical physics standpoint, computational modelling efforts link 1/f noise of spectral power to a fine balance of synaptic excitation and inhibition in neuronal avalanche formations operating at a critical point (Poil et al., 2012; Lombardi et al., 2017; Gao et al., 2017). On the other hand, irregularities in 1/f properties of power spectral density suggest deviations from

criticality, impacting the efficiency of neural communications within and between regions (Voytek et al., 2015; Peterson et al., 2017).

Even though both $1/f$ slope of PSD and ITPC have been proposed to quantify the degree of neural variability in the cortex, very little is known about the precise neurobiological mechanisms behind the two metrics and their link. Thus far, the two metrics have not yet been investigated in tandem; the $1/f$ noise literature in particular is at its infancy. Existing work points out that EEG is a mixture of periodic signal (i.e neural oscillations) and aperiodic signal (i.e the $1/f$ slope and offset) (Donoghue et al., 2020). In that context, a fundamental difference between the two metrics seems to be the fact that ITPC is extracted from oscillatory activity defined within canonical frequency bands, whereas the $1/f$ slope component is extracted from aperiodic activity, operating in the background. From that perspective, it is likely that they are capturing distinct neural processes.

Figure 1.1

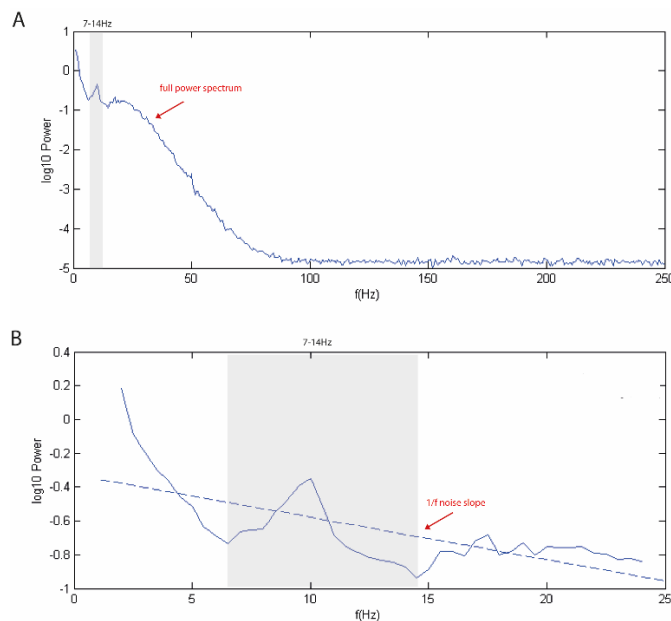


Figure 1.1: Power Spectral Density of signal coming from a single electrode presented as a function of frequencies (f) ranging from 0-250Hz (A) and its corresponding $1/f$ noise slope for frequencies ranging from 2-24 Hz (B).

1.5 Increased neural noise in the autistic brain

1.5.1 The theoretical framework

Converging evidence supports the notion that ASC is a disorder of neural communication. Multiple theoretical frameworks have been developed to explain how atypical neural network behaviour gives rise to ASC phenotypic expressions. An influential study by Just et al. (2004) was one of the first to suggest that cognitive deficits in ASC manifest as a result of the difficulty to coordinate neuronal activity between brain regions. In an effort to refine this idea, Belmonte et al. (2004) proposed that increased functional connectivity locally leads to a computational structure where signal is not adequately differentiated from noise, ultimately causing reductions in long-distance connectivity and affecting the efficiency of overall information transmission in the cortex. Given that many of these cortical regions are implicated in higher order processing, this has been suggested to be a plausible mechanism according to which some of ASC phenotypic expressions emerge (Brock et al., 2002; Belmonte et al., 2004; Rippon et al., 2007). A surge of research investigating how patterns of neural communication arise in the autistic brain was seen in the following 15 years after the two papers were published and multiple reviews on functional connectivity have been published since (MEG/EEG: Schwartz et al., 2017; O'Reilly et al., 2017, fMRI: Monk et al., 2009; Muller et al., 2011; Rane et al., 2015).

Other theoretical models of ASC such as the one proposed Rubenstein & Merzenich, (2003)-recently revisited in Sohal & Rubenstein (2019)- suggests that some subtypes of ASC are associated with reductions in signal-to-noise ratios (SNRs) in key neural circuits underlying sensory and social behaviour, likely to be caused by an increased ratio of excitation and inhibition (E/I) in those key networks. Disproportionally high excitation or weak inhibition impedes functional differentiation of processing systems. If excitation swamps the neural circuit and is greater than the level of inhibition, activity in the neural circuit will increase until it reaches the threshold of maximum activity capacity or until sufficient inhibition from neighbouring neurons is recruited to achieve a balanced state. In this circuit, we would observe a reduction in SNRs; balance is achieved at a higher activity point, therefore the excessive noise generated will lead to poorer neuronal gain and poor responsiveness to true signal. On the other hand, if levels of inhibition are greater than levels of excitation, neural activity will decrease until the system enters a quiescent state or until a phase transition causes greater reductions in inhibition, ultimately reaching a balanced state. Reduction in

SNRs follows a different causal mechanism here; balance is achieved at a lower activity point, which decreases the strength of the signal.

In support of this hypothesis, experimental studies report greater occurrence of epileptic seizures and sharp spike activity in ASC (Gillberg & Billstedt, 2000; Wheless et al., 2002) indicative of noisy, unstable neural circuitry and symptom improvement following pharmacological intervention (i.e bumetadine) targeting GABA receptors (Zhang et al., 2020). Genetic studies demonstrate that altered expression of GABA receptors is linked to ASC symptomatology (Fatemi et al., 2009; Coghlan et al., 2012), whereas computational and animal models manipulating GABA/glutamate concentrations have shown an imbalance in key circuits associated with ASC (Horder et al., 2018). It is important to note that this theoretical model is not necessarily contradictory to the one proposed by Belmonte et al. (2004) and Just et al. (2004) but rather complimentary, providing a biological explanation on how the atypical patterns of functional connectivity may arise in ASC.

Hyperexcitability in the autistic brain has been suggested to result from sparser, less “sharp” neural representations, further affecting behavioural sensitivity to incoming information (i.e poor discrimination of stimuli) (Uzunova et al., 2016; Ward, 2018). In the sensory cortices for example, an increased GABA/glutamate ratio implies a larger neural response to the sensory input and worse behavioral discrimination of sensory stimuli. During stimulus presentation, GABA-ergic and glutamatergic neurons are selectively activated within the cortical space of minicolumns in the neocortex. An important role of GABA-ergic neurons is to increase the contrast or else “sharpen” the receptive field by mediating activity *between* neighbouring minicolumns through lateral inhibition (Cree, 2014). In the neurotypical brain, this is an important mechanism through which global noise in the circuit decreases and activation of higher order neurons takes place only when a strong and consistent signal is transmitted (Cree, 2014). In the autistic brain, a breakdown of this “cross-talk” on a synaptic transmission level, occurring early in development and continuing through developmental phases as “chronic noise” (Simmons et al., 2008), is implicated in cognitive deficits at a behavioural level (Uzunova et al., 2016). To demonstrate that “sharpness” matters, Hibbard & O’Hare (2015) modeled neural responses of the primary visual cortex to images of different spatial frequencies and demonstrated that low spatial frequency images activate a sparser neural response, whereas aversive, mid- and low-frequency images trigger a larger, less sparse response. Therefore, sparser, less “sharp” neural representations is therefore likely to be a mechanism that gives rise to some of the behavioural symptoms observed in ASC (Casanova, 2006; Uzunova et al., 2016).

In extension to the theory developed by Rubenstein & Merzenich, (2003), Simmons and colleagues (2009) propose that increased endogenous neural noise underlies sensory perceptual symptoms in ASC, manifesting both as hypo- and hyper-sensitivity to sensory stimuli, a core phenotypic expression of ASC (Simmons et al., 2009). Although fairly loosely defined (i.e authors do not distinguish between additive or multiplicative noise), they attribute increased neural noise to failures in synaptic transmission or neuronal cross-talk, resulting in increased neural variability at large-scale neural circuits. Adding noise to the neural system leads to reduced SNRs and difficulties to detect signal, therefore reduced sensory sensitivity to incoming sensory stimuli (i.e hyposensitivity). They also propose that the phenomenon of stochastic resonance (McDonnell & Abbott, 2009) can increase SNRs by raising the sensory signal above the threshold, leading to increased sensory sensitivity to sensory input (i.e hypersensitivity). Support for this theory comes from studies using transcranial random noise stimulation (tRNS) to add noise to the neural circuit and transcranial magnetic stimulation (TMS) to manipulate excitation. Van der Groen & Wenderoth (2016) found that by adding an optimal amount of random noise to the visual system, detection performance improves significantly. Another study by Terhune et al. (2015) showed that lower TMS phosphine thresholds, indicative of greater cortical excitability and therefore greater neural noise, are associated with increased levels of glutamate but not GABA in the primary visual cortex. These studies demonstrate that it is plausible that increased neural noise can lead to suboptimal cognitive performance.

Theoretical accounts of *reduced* neural noise in the autistic brain have also been presented (Davis & Plaisted-Grant, 2014). The current debate on whether neural circuits in ASC are characterized by high or low levels of noise highlights the importance of spatial scale in the theoretical framework outlined above. Simmons & Milne (2015) propose that neural circuits are characterized by increased neural noise but as they suggest in a commentary, this is a feature of large-scale neural networks in ASC. In contrast, Davis & Plaisted-Grant (2014) argue that sensory perceptual abnormalities in ASC arise as a result of reduced neural noise. At first these two perspectives look contradictory, however Davis & Plaisted-Grant (2014) suggest that low noise is a feature of small-scale neural networks, giving rise to less stable neural responses and greater inter-trial variability. An explanation by Sohal & Rubenstein (2019) encompasses both possibilities; although large-scale networks establish and maintain a constant E/I ratio at a global level (He & Cline, 2019), local networks within a large circuit (i.e small-scale circuits) experience continuous changes in the levels of excitation and inhibition at very fast time scales, therefore some of them will have reduced E/I

ratio and some increased. As they point out, excitation and inhibition are not unidimensional concepts. Excitation and inhibition are generated in different sites of the circuit and have an effect on multiple projection targets (Sohal & Rubenstein, 2019). In that respect, an E/I balance at a global level can be achieved through numerous configurations of neuronal activations (Sohal & Rubenstein, 2019). Thus, an E/I imbalance of a large-scale circuit involves a change in the relative activity of different types of excitatory or inhibitory neurons within small-scale circuits, such that the threshold at which global balance is achieved shifts (Sohal & Rubenstein, 2019).

1.5.2 A computational modelling perspective

Let's try now to understand mathematically how increased neural noise in a neural circuit may be giving rise to atypical behaviour in ASC and demonstrate this in the context of visual stimulation. One assumption driving the majority of research is that a hypersensitive behavioural response to a sensory stimulus is directly linked to an increase in neural activation in sensory cortices in response to a sensory stimulus. However, it is crucial to understand whether this manifests as increased signal, a scenario where an excess of neural sensitivity is associated with greater behavioural sensitivity or increased noise, in which case increased neural sensitivity comes hand-in-hand with reduced behavioural sensitivity.

Zhaoping (2006)- adopted in O'Hare and Hibbard (2016) and Ward (2018)- modeled this relationship from a simple signal processing perspective. In an additive model, during visual stimulation, the output activity of a group of visual cells is the sum of two types of information; the behaviour of neurons, which are firing in response to the visual stimulus presented and the background spontaneous neuronal activity that is irrelevant to the input signal. This process can be modeled in the following way:

$$O=K(S)+N_a \quad (1)$$

Where O is the output activity, given a specific visual stimulus S, K() is the encoding rate or activity gain and N_a is the spontaneous background noise term. N_a is stimulus independent; it refers to neuronal firing that is not triggered by the visual stimulus. Neural noise in this form is constant across stimulus magnitudes and therefore additive in nature. An increase in neural activation O can take place either if the encoding rate K() to the input is greater, taking the form of hypersensitivity to the visual stimulus or if levels of spontaneous noise N_a increase, in which case the output activity will be increased but the SNR in the system will be decreased. Essentially, the group of neurons has to modify its activity gain i.e encoding function K() to account for the strength of the stimulus. A

high SNR implies that the strength of activity gain or responsiveness to the visual stimulus is low, whereas a low signal-to noise ratio implies greater encoding rate to process the stimulus.

Neural noise can also be multiplicative, proportional to the magnitude of a response to a stimulus (Zhaoping, 2006; Davis & Plaisted-Grant, 2014). If multiplicative noise N_m is added to the system, the above equation will take this form:

$$O=K(S) (1+ N_m)+N_a \quad (2)$$

This means that the output response can vary randomly depending on the magnitude of the visual input. Visual stimulation may lead to an increase in output activity, however, unlike equation 1, no information can be extracted about the strength of the visual stimulus in case of equation 2. In ASC, an increase in N_m could manifest as a result of atypical propagation of signal from pre- to postsynaptic neurons within the sensory region i.e breakdown in neural communication taking multiple forms, affecting signal flow in higher order cortical areas and further resulting in increased neural variability at large-scale neural circuits. It is important to note that if an increase in output response O is observed in an experiment, we have no means of distinguishing whether this increase is due to an increase in multiplicative noise N_m in the network or an increase in encoding rate $K()$ and additive noise N_a . For that reason, increased activation or hyperexcitability in a neural network can describe both possibilities of neural noise arising in the system (O'Hare & Hibbard, 2016).

1.5.3 Methodological challenges

As demonstrated above, aspects of the ASC symptomatology (i.e sensory sensitivities) could be interpreted in the context of increased neural noise or increased inter-trial neural variability (Simmons et al., 2007; Simmons et al., 2009; Milne, 2011). Considering the theoretical framework presented in Section 1.5.1, the focus of the present thesis is to understand atypical patterns of neural communication by studying how increased neural noise manifests in ASC. In order to do that, it is important to identify robust variables to quantify neural noise in ASC and appropriate analytical methods to effectively capture differences between ASC and TD groups. This requires careful examination of the literature to identify variables that are less volatile and are repeatedly shown to be different in ASC as compared to the typically developing population and thereafter in ASC compared to other psychiatric conditions. If ASC is characterised by disrupted neural communication, researchers need to be able to address which particular pattern of atypical neural network behaviour is linked to the disorder and why this pattern leads to one specific disorder and

not another. This brings to light the need to examine definitions and key metrics utilised in study designs with a critical eye and identify more stable variables of discriminant neural features in ASC.

Episodes of synchronous firing takes place within a very short time window of tens of milliseconds, therefore it has been suggested that changes in neural network interactions are unlikely to be detectable using traditional fMRI cross-correlation techniques (Uhlhaas & Singer, 2007). As pointed out, fMRI does not allow for these changes to be sufficiently captured due to its poor temporal resolution and as a result fMRI findings provide only indirect evidence for disrupted neural communication in ASC (Uhlhaas & Singer, 2007). In contrast to this view, there is discussion that long-range interactions cannot be reliably detected using EEG due to volume conduction/leakage and the field-spread effect (Winter et al., 2007; Palva et al., 2018), which induces spurious correlations between electrodes, making it hard to separate signal coming from closely-spaced channels (Picci et al., 2016). For that reason, the focus of this thesis will not be the synchronization or functional connectivity of neural assemblies within the network at a given time point in the experimental trial but will look at neural communication from a different perspective, the degree of phase angle alignment of neural oscillations *between* experimental trials as measured by EEG. It can be argued that in order to understand how neural networks behave and interact in ASC and identify clinically relevant neural features, it is important to explore neural communication in ASC through the lens of neural oscillations and captured by EEG at the source level. As it will be demonstrated in the following sections, recent methodological advances in the EEG field, including more advanced analytical techniques of signal processing, allow for greater confidence in the research findings, making it a good avenue for experimentation in ASC (see McLoughlin et al., 2014 for a review on EEG-based biomarkers in psychiatry). For that reason, the literature review presented in the subsequent sections focuses primarily on EEG/MEG studies.

With that in mind, Section 1.5.5 brings forward evidence supporting the idea of disrupted neural communication in ASC, from the perspective of neural noise. This section is not intended to provide a comprehensive assessment of the validity of the different theoretical models of ASC outlined above, but rather aims to identify variables likely to be capturing pathophysiological processes that may be distinct in ASC compared to other psychiatric conditions and typical development. Following a review of the literature, it is demonstrated that Inter-trial Phase Coherence (ITPC), a variable indexing the amount of trial-to-trial neural variability in the cortex, is a promising metric that could inform current thinking about how neural noise arises in ASC.

1.5.4 Measuring neural noise using Electroencephalography (EEG)

1.5.4.1 Advantages of EEG

First, it is important to discuss what EEG *can* and *cannot* do as a method of experimentation in order to facilitate interpretation of findings in the subsequent experimental chapters. EEG measures voltage fluctuations coming from a large population of neurons (Kirschstein & Kohling, 2009). The source of this electrical activity is not action potentials but rather the dendritic activity of cells and their excitatory and inhibitory postsynaptic potentials (Kirschstein & Kohling, 2009). Although it is characterized by poor spatial resolution of 5-9cm (Nunez et al., 1994), its temporal resolution of millisecond precision is an advantage for studying neural network behaviour in particular. Due to its millisecond precision, it directly captures interactions between large groups of neurons in real time (Sauseng & Klimesch, 2008). EEG can provide useful insights on the behaviour of groups of neurons at a macroscopic scale, which are shown to operate in a near-equilibrium state and be linear in nature, however small scale network dynamics cannot be captured sufficiently as they are chaotic and non-linear in nature (Pritchard, 1996; Wright & Liley, 1996).

1.5.4.2 EEG metrics used to quantify neural noise

Given the wide range of concepts, an equally large number of metrics has been developed and utilised across studies to quantify neural noise. EEG/MEG studies have previously measured SNRs by calculating the power of the signal at a peak latency of interest divided by the mean power of spontaneous activity (Weinger et al., 2014; Butler et al., 2017). However, as it will be discussed in Section 1.5.4.3, using trial averaging to calculate the amplitude of the signal may not reveal existing atypicalities in evoked responses in ASC, therefore more refined analytical techniques need to be deployed to study neural noise in the autistic brain. Other studies have measured the degree of phase angle alignment of neural oscillations between experimental trials through the Inter-trial Phase Coherence (ITPC) metric (Milne, 2011; van Noordt et al., 2017; Yu et al., 2018; Milne et al., 2019). This is a well-established method of quantifying the degree of phase-locking at a specific location (i.e electrode) or signal source of interest (ICA component). In that respect, it is a very effective method of measuring the functional integrity of the neural circuit or signal source activated in response to a stimulus locally.

Newly emerging work also quantifies neural noise from the perspective of 1/f noise of Power Spectral Density (PSD), a global variable capturing broadband changes in power spectra as a function of temporal frequency (Gao et al., 2017; Donoghue et al., 2020). In contrast to traditional approaches computing and comparing oscillatory power between canonical frequency bands in the form of band ratios, 1/f slope of PSD captures *aperiodic* properties of the neural signal. It indicates how power spectra change in relation to its underlying temporal frequency across the full spectrum (Haller et al., 2018), taking the form of greater power at low frequencies and a decrease of power at higher frequencies (Voytek et al., 2015; Dave et al., 2018). The 1/f noise exponent is proposed to capture random background electrical fluctuations of neuronal spiking activity (Voytek et al., 2015). A flatter 1/f slope of power spectra indicates that spiking activity is decoupled from synchronised oscillatory dynamics, whereas a steeper 1/f slope of PSD indicates that fewer temporally uncorrelated spikes occur and population-based neural oscillations are more strongly synchronised. In that context, 1/f slope is a measure of variability of temporal correlations of background population spiking activity. Original work by Voytek et al. (2015) demonstrated that the PSD of older adults is characterised by flatter 1/f slopes compared to younger adults, suggesting that noise exponents provide valuable information about the amount of neural noise in the system and the strength of neural synchrony patterns. Following this research effort, a growing number of studies have been conducted measuring 1/f slopes in disorders of the brain, further discussed in Section 1.7.1.

1.5.4.3 Trial averaging vs single-trial analysis

Levels of neural variability of sensory-evoked responses in ASC are consistently reported as high when single-trial analysis is performed, even when trial averaging does not reveal differences in the average amplitude of the neural responses (Milne, 2011). ERP averaging is a common method of reducing noise in electrophysiological data, however it appears to be problematic when used in pathophysiology as it ignores the rich trial-to-trial variability, which has been shown to be highly informative in neurodevelopmental disorders (David et al., 2016). Conventional ways of ERP analysis aim to extract ERP averages of trial datasets or ERP epochs, time-locked to a specific stimulus. ERP epochs are a mixture of event-related activity but also activity that is not contributing to the evoked response and is “event- unrelated”. ERP averaging removes signal properties that are not phase- locked to the experimental event of interest at all frequencies and latencies (Onton & Makeig, 2009). Therefore, using trial averaging to analyse ERPs does not allow us to study the full dynamics of evoked responses because it only retains activity that influences the phase distribution

of a signal (Onton & Makeig, 2009). This is particularly relevant in ASC research, where the shape of the ERP waveforms has been shown to differ in ASC samples compared to neurotypical groups, consequently reducing the amplitude artificially may not reveal existing atypicalities in evoked responses (David et al, 2016).

ERP averaging is the most prominent method of analyzing ERP data and is often preferred to single-trial analysis. Considering the limitations of the former, it is important to discuss methodological techniques that facilitate single-trial analysis. Bandpass filtering (Salajegheh et al., 2004), maximum likelihood estimation (Jaskowski & Verleger, 1999; De Munck et al., 2004), stochastic modeling (Von Spreckelsen & Bromm, 1988), multivariate version of the matching pursuit algorithm (Mallat & Zhang, 1993; Durka et al., 2005; Sieluzycki et al., 2009), application of wavelet networks (Heinrich et al., 1999), hierarchical general linear model analysis (Pernet et al., 2011) and Independent Component Analysis (ICA) (Makeig et al., 1996; Jung et al., 2001; Delorme & Makeig, 2004) are some of the techniques that have been applied successfully in previous studies.

Taking into account the advantages of single-trial analysis, ICA decomposition was performed to extract neural signal in the experimental studies of the present thesis measuring ITPC. Multiple authors have highlighted the significance of decomposing EEG data into independent components to tackle the problem of trial averaging, amongst other limitations that arise as a result of analyzing the “mixed” EEG signal recorded at the scalp. The EEG signal recorded at the scalp is the sum of signals originating from multiple independent neural and artifact related sources. ICA is a way of “blindly” separating those distinct sources of signal, without any prior knowledge of the nature of the source (Jutten & Herault, 1991). This is based on the assumption that two neural time series are temporally separated and therefore independent from one another, as the value of one at a specific time point does not inform us about the value of the other at the same time point (Onton & Makeig, 2009). ICA ultimately leads to the construction of component scalp maps consisting of spatially independent components of source signal (Stone, 2004; Onton & Makeig, 2009). Going back to neural variability, ICA is a valuable analytical step as it provides a way of separating the signal of interest (i.e. from a specific neural source) from the noise (artifacts and signals from other sources in the EEG). This facilitates single trial analysis and allows to look at variability across trials. Its efficacy as a single-trial analysis step has been pointed out in a number of studies including the one by De Vos et al. (2012) who found that compared to regression-based estimation and bandpass filtering, ICA is the most effective single-trial analysis tool.

1.5.5 Experimental studies investigating neural noise in ASC

Shifting away from the idea of a deficit or surfeit of connectivity in specific networks, studies indicate that neural networks are characterized by sub-optimal properties in line with the idea of a disconnected brain (Peters et al., 2013). Emerging evidence speaks for greater homogeneity and more uniform neural network structure in the brain of individuals with ASC. Using graph theory analysis, Zeng et al. (2017) found disrupted network topology, manifesting as longer path length, reduced clustering, and a decline in global efficiency. The brain consists of multiple segregated, highly specialised groups of neurons working together as an integrated functional network. Longer path length in ASC is indicative of difficulties with regional integration, whereas reduced clustering suggests reductions in local specialization. Peters et al. (2013) also report decreased ratio of long-over short-range coherence and greater resilience of complex networks to targeted attacks when nodes were removed from the network, an indicator of greater randomness and decreased efficiency and specialization in the ASC brain, likely to be the outcome of redundant connectivity in the cortex. In addition, examples of EEG signal complexity reductions in the temporo-parietal and occipital regions are widespread in the literature, providing further evidence for the degradation of small-world architecture in ASC (Catarino et al., 2011; Milne et al., 2019).

Sub-optimal network properties may also be presented as increased neural noise swamping the neural system (Rubenstein & Merzenich, 2003). Indeed, multiple lines of work have shown that ASC is associated with increased neural noise in the form of increased neural variability. In the EEG/MEG literature, neural variability is primarily studied from the perspective of ITPC, a measure of phase consistency over experimental trials. Converging evidence suggests that low ITPC, i.e. reduced phase-consistency / increased phase-inconsistency across trials, occurs in ASC at a group level in response to a variety of stimuli, irrespective of the developmental stage of the participants (see *Table 1.1* for a summary of studies). For example, Milne (2011) found lower ITPC in response to Gabor patches in children with ASC as compared to typically developing children. A larger study by Milne et al. (2019) concludes that low ITPC is capturing atypical neural features prominent in the brain of some individuals with ASC but not all, indicating that reduced ITPC is likely to be one of many neurological features that is associated with ASC. This may also explain the contradictory results brought forward by Butler et al. (2017), who employed a similar methodology but did not find differences in levels of ITPC between groups. In the auditory modality, Edgar et al. (2015) report reduced ITPC in the superior temporal gyrus in response to sinusoidal tones. Yu and

colleagues (2018) report an increase in ITPC of the theta band computed for the P1 time window- a positive ERP component occurring ~100ms after stimulus onset- followed by a reduction in ITPC for the N2 time window- a negative ERP component occurring ~200ms post-stimulus presentation- during processing of pure tones and words. Reductions in ITPC of theta oscillations are also observed in the frontal electrode site during feedback processing of rewards and errors (van Noordt et al., 2017). Taken together, ITPC is consistently reported as low in a wide range of studies aiming to quantify the degree of neural noise in ASC, indicating that the metric may be capturing pathophysiological processes that are distinct in the autistic brain as compared to typical development. This is also reflected in a research review suggesting that low ITPC may be an endophenotype of ASC (David et al., 2016).

In support of the increased neural noise hypothesis, other lines of enquiry report poorer SNRs in groups of children with ASC. Using EEG but a different metric to the above studies, Weinger et al. (2014) showed weaker SNRs in electrophysiological responses of children with ASC, computed from steady state visual evoked potentials. A few studies utilised fMRI paradigms to investigate intra-individual trial-to-trial variability in metabolic responses across a number of sensory modalities. Dinstein et al. (2009) demonstrated that ASC participants show significantly larger standard deviations of BOLD response from one trial to the other during the observation and execution of hand movements. In subsequent studies, Dinstein et al. (2012) conducted three independent fMRI experiments and measured neural variability in key regions in a group of children with ASC during processing of simple visual (moving dots), somatosensory (air puffs) and auditory stimuli (pure tones). The results showed larger trial-by-trial standard deviations and smaller SNRs in the ASC group compared to the typically developing group. In line with Dinstein et al. (2012), Haigh et al. (2015) replicated and extended these results in adults with ASC. Of note, in a follow-up study Haigh et al. (2016b) offer further insights and clarify that this pattern of reduced SNRs in key sensory cortices is a characteristic of ASC in specific and does not characterise the brain of patients with schizophrenia, despite the genetic and phenotypic overlap of the two conditions.

An important hypothesis to establish is whether increased neural noise is linked to a specific aspect of the ASC phenotype. Theoretical accounts propose that increased neural noise in the sensory systems explain individual differences in sensory sensitivities (Simmons et al., 2007). However, none of the studies investigating neural noise have provided adequate mechanistic insight on this process. Current studies on neural noise do not provide clarity on the relationship, potentially due

to methodological pitfalls, as it will be demonstrated. In non-clinical populations, Vilidaite et al., (2017) showed that the global internal noise factor computed from EEG signal in response to three types of sensory stimuli positively correlated with autistic traits as measured by AQ. This is in line with Orchard & vanBoxtel (2019) and computational models by Park et al. (2017). In clinical populations on the other hand, Dinstein et al. (2012) did not find a significant relationship between ASC symptom severity, as assessed by the ADOS, and SNRs extracted from BOLD signal in response to visual, auditory and somatosensory stimuli. Overall ADOS symptom severity scores are unlikely to be capturing the degree of behavioural sensitivity to visual, auditory and somatosensory stimuli; therefore greater specificity in the behavioural measures used is necessary (see Happe et al., 2006 for a discussion on the use of global measures to quantify autism severity). Similarly, Milne et al. (2019) demonstrated that although increased neural noise, measured in the form of low ITPC and reduced multi-scale entropy is observed in the cortex in response to visual stimulation, these variables are not associated with core diagnostic domains of ASC as assessed by the Social Responsiveness Scale (SRS-2, Constantino & Gruber, 2011) and the Adult Repetitive-Behaviors Questionnaire (RBQ-2A, Barrett et al., 2015). Despite the fact that the study was designed to evoke neural responses in the sensory cortices, Milne et al. (2019) did not investigate the relationship between neural noise and sensory sensitivity, an integral aspect of the ASC phenotype. It is still unknown how neural noise manifests in relation to the subjective sensory experience and/or behavioural sensitivity to the sensory stimuli presented. Understanding autism symptoms in the context of neural noise has the potential to be a scientific “*breakthrough*” (Davis & Plaisted-Grant, 2014). Particularly with regards to ITPC, more evidence is needed to understand whether low ITPC in response to sensory stimuli is associated with sensory sensitivities in ASC. This issue is investigated in great detail at Chapter 5 of the present thesis.

1.6 Inter-trial Phase Coherence (ITPC)

1.6.1 Inter-trial Phase Coherence in disorders of the brain

Increased levels of neural variability in the form of low ITPC are reported not only in ASC but also in other psychiatric disorders such as ADHD and psychosis as well as neurogenerative conditions such as Parkinson’s disease (see *Table 1.1* for an overview of studies investigating ITPC in ASC and *Table 1.2* for an overview of studies measuring ITPC in other clinical groups). In the visual domain, groups of adults and children with ASC demonstrate ITPC reductions in the electrode cluster covering the visual cortex in response to low-level visual stimulation (i.e Gabor patches, checkerboard stimuli, see Milne, 2011). A similar pattern of phase-alignment difficulties is observed

in ADHD and psychotic disorders, conditions known to be characterized by neural circuitry abnormalities (Mazaheri et al.; 2014; Lenartowicz & Loo, 2014; Janssen et al., 2017; Hager et al., 2017; Murphy et al., 2020) and previously shown to share genetic and phenotypic features with ASC (McCarthy et al., 2014; Satterstrom et al., 2019). In a similar study design to the one by Milne et al. (2019), Gonen-Yaacovi et al. (2016) demonstrated that adults with ADHD show reductions in theta and alpha band ITPC as extracted from selected electrodes and Independent Components capturing participant's early sensory response to black and white checkerboard stimuli. Adults with psychosis also show reductions in ITPC at the occipital regions during visual processing of black and white checkerboards, although it is still unclear whether these reductions characterize lower or higher frequencies (Basar-Eroglu et al., 2008; Grent-t-Jong et al., 2020). Although Parkinson's disease and ASC seem to be unrelated at surface, recent evidence has shown that neural circuitry structures in both conditions are characterized by increased neural noise (Milne, 2011; Yeener et al., 2019). However, in Parkinson's disease ITPC reductions in response to visual stimulation are evident not just at the occipital electrode site but at all electrode sites, indicating more widespread phase alignment difficulties (Yeener et al., 2019).

In the auditory domain, the picture is more blurry. Depending on the timing and stage of information processing, children with ASC have previously shown ITPC increases within the P1 window and ITPC reductions within the N2 window of theta oscillations (Yu et al., 2018). On the other hand, Edgar et al. (2015) report reduced ITPC at all frequencies during processing of sinusoidal tones in the superior temporal gyrus of children with ASC. ITPC reductions in response to simple tones is also reported in adults with ADHD (Gonen-Yaacovi et al., 2016) and to a wide range of auditory stimuli in adults with psychosis (Koh et al., 2011; Shin et al., 2015). In these studies however it is evident that the stimulus type (clicks, tone pips, binaural tones etc.), spatial cluster (superior temporal gyrus, electrode Fz, electrode with maximum ITPC, etc.) and the developmental stage of participants (children vs adults) differ enormously from one study to the other, therefore findings cannot be directly comparable.

Studies utilizing more complex task designs to target executive functioning processes have shown similar results. Reduced phase clustering in the frontal electrode site is reported in both ASC and ADHD. In ASC, van Noordt et al. (2017) report reduced theta band ITPC in the frontal cortices of adolescents with ASC in response to a reward prediction task, consisting of "win" or "lose"

feedback trials. In ADHD, Groom et al. (2010) report a reduction in early and late theta band ITPC, computed from fronto-central electrodes, in response to visual go/no-go trials.

Taken together, the ability of neuronal oscillations to phase-reset effectively in response to a wide range of external stimuli- simple and more complex- is shown to be diminished not only in ASC but also in other conditions, some of which share genetic influences with ASC (i.e ADHD and schizophrenia). Different patient groups show different patterns of ITPC reductions, with some overlaps between ASC, ADHD and psychosis, particularly in the visual domain. It is important however to note that the wide range of task designs and methodological approaches employed for the measurement of ITPC impedes direct comparisons across disorders. No studies have previously compared levels of neural noise in individuals with different conditions, for example ASC and ADHD. Task characteristics such as type of stimuli, duration of stimulus presentation and targeting modality as well as methods of computing ITPC vary widely from one study to the other. In addition, samples with different characteristics (i.e age, developmental stage, IQ) are recruited in each study. For that reason and although phase clustering abnormalities are evident in all the aforementioned conditions, the wide range of tasks and data analysis techniques used in these studies do not allow to draw firm conclusions regarding neural processes that differ or may be common in these groups.

Table 1.1

Studies measuring ITPC in individuals with a clinical diagnosis of ASC

	Author	Year	Participants*	Modality	Stimulus	Method	Location	Frequency band	Result**
EEG studies	Milne	2011	Adolescents ($n=13$)	Visual	Gabor patches	ITPC ¹	Electrode with the highest P1 amplitude ICA component that best captures the early visual evoked response	Alpha	Reduced ITPC
	van Noordt et al.	2017	Adolescents ($n=27$)	Visual	Coloured balloon images, win feedback image, lose feedback image	ITPC	Frontal midline electrode cluster (5, 6 (Fz), 11, 12)	Theta	Reduced ITPC
	Butler et al.	2017	Children ($n=20$)	Visual, somatosensory	Black and white checkerboard, somatosensory stimuli	ITPC	Not mentioned.	Theta, Alpha, Beta	No difference between the ASC vs control group
	Yu et al.	2018	Children ($n=15$)	Auditory	Pure tones and words	ITPC	Maximum ITPC within the two designated time windows 70-140ms (P1) and 150-250ms (N2)	Theta	Increased theta ITPC during the early time window Reduced theta ITPC during the late time window
	Milne et al.	2019	Adults ($n= 22$)	Visual	Black and white checkerboard	ITPC	ICA component with maximum ITPC	4-9 Hz	Reduced ITPC in the diagnosed group vs undiagnosed group
MEG studies	Edgar et al.	2015	Children and adolescents ($n=17$)	Auditory	Sinusoidal tones	ITPC	Superior temporal gyrus	4-80 Hz	Reduced gamma ITPC

*Sample size given for the ASC group

**The result is reported for the ASC group relative to the control group

¹ Inter-trial Phase Coherence

Table 1.2

Studies measuring ITPC¹ in other clinical groups

Condition	Year	Author	Method	Sample*	Modality	Stimulus	Location	Freq	Result**
ADHD	2010	Groom et al.	EEG	Adolescents (n=23)	Visual	Go/no-go letters 'X', 'K'	Electrode FCz	Theta	Reduced ITPC
	2016	Gonen-Yaacovi et al.	EEG	Young adults (n=17)	Visual, auditory	Black triangles/circles Pure tones	Electrode with the highest P1/N1 amplitude PO8 and FCz electrodes ICA component that best captured the early sensory response	Theta, Alpha	Reduced ITPC in all conditions
Schizophrenia	2008	Basar-Eroglu et al.	EEG	Adults (n=10)	Visual	Black and white checkerboards with target-non-target fixation dot (visual oddball task)	Frontal, central, parietal, occipital electrodes	Theta, Alpha	Reduced theta ITPC at all locations for target stimuli Reduced alpha ITPC at the occipital locations for all stimuli but increased ITPC in the frontal, central, parietal locations
	2020	Grent-t-Jong et al.	MEG	Adults with first episode of psychosis (n=26)	Visual	Circular sine wave gratings	Medial superior frontal gyrus Occipital cortex (i.e primary visual cortex, dorsal-stream area, ventral-stream area)	Delta, Theta, Alpha, Beta, Gamma	Reduced ITPC for beta and gamma bands but not for lower frequencies at the occipital cortex
	2011	Koh et al.	MEG	Adults (n=10)	Auditory	Tone pips (auditory oddball task)	Average ITPC computed from 8 regions: left and right frontal, temporal, parietal, occipital, frontal clusters of electrodes	Alpha	Reduced ITPC
	2012	Kirihara et al.	EEG	Adults (n=234)	Auditory	Clicks	Electrode Fz	Theta, Gamma	Reduced gamma ITPC No difference in theta ITPC
	2015	Shin et al.	MEG	Adults (n=21)	Auditory	Binaural tones	Left and right frontal and temporal clusters of electrodes	Theta, Alpha	Reduced ITPC in both bands
2018	Kim et al.	EEG	Adults (n=45)	Auditory	Clicks (auditory oddball task)	Electrode with maximum ITPC in the parietal electrode site (Pz)	Delta, Theta	Reduced ITPC	

Dyslexia	2013	Soltezs et al.	EEG	Adults (<i>n</i> =16)	Auditory	Continuous rhythmic streams	Electrode with maximum ITPC (FCz)	Delta	Reduced ITPC
	2020	Meyer & Schaadt	EEG	Children (<i>n</i> =28)	Auditory	Syllables /pa/ and /ga/, video of standard mouth movements (audio-visual oddball task)	Electrode with maximum ITPC	Alpha	Increased prestimulus ITPC
Parkinson's disease	2019	Yeener et al.	EEG	Elderly adults (<i>n</i> =25)	Visual	Target and standard visual stimuli (visual oddball task)	Frontal (F3, Fz, F4), central (C3, Cz, C4), parietal (P3, Pz, P4), and occipital (O1, Oz, O2) electrode clusters	Theta, Alpha	Reduced theta and alpha ITPC in all locations
Alzheimer's disease	2019	Guntekin et al.	EEG	Elderly adults (<i>n</i> =30)	Visual	Photos of three basic facial expressions (angry, happy, neutral) of three different female faces	Maximum ITPC in a given frequency band at the specific time window (0–500 ms for theta and 0–350 ms for alpha)	Theta, Alpha	No difference in ITPC

*Sample size given for the clinical group

**The result is reported for the clinical group relative to the control group

¹ Inter-trial Phase Coherence

1.7 1/f noise of Power Spectral Density (PSD)

1.7.1 1/f noise of Power Spectral Density (PSD) in disorders of the brain

One of the recently emerging questions concerns the relevance of 1/f noise for the medical discipline and for psychiatric disorders specifically. Recent work from Voytek and Knight (2015) provides a framework to study disorders of neural synchrony such as ASC in the context of 1/f noise- although it is also important to note that no data currently exists that investigates this aspect of neural functioning in ASC. Network communication disruptions in the brain can take two forms, both equally detrimental for information transmission. They can manifest a) either as a result of ‘overcoupling’ or ‘hypersynchronisation’, meaning that two clusters of neurons are too strongly synchronized or b) ‘undercoupling’, involving difficulties to establish communication (Voytek & Knight, 2015). Noise, in the form of noisy, serially uncorrelated spikes arriving at a moment of low excitability, is introduced in the healthy brain as a corrective mechanism to smooth the threshold of action potentials and prevent overcoupling (Fries, 2005). However, excessive noise works to the expense of the system, resulting in weakened interregional oscillatory coherence and pathological undercoupling (Voytek & Knight, 2015).

Changes in 1/f slope of PSD are suggested to reflect this process. In the first occasion, we expect to observe a steeper 1/f slope of spectral power, as stronger extracellular fields result in stronger dendritic outputs, a larger number of simultaneously triggered spikes and therefore reduced temporal variability in spike timings. In the second scenario, the 1/f slope of PSD will be flatter as weaker oscillatory coupling results in weaker dendritic activity and increased variability of spike timings. It is therefore evident that 1/f slope captures rich information about the underlying synaptic activity of neural ensembles (Gao, 2015), which can be utilized to understand the nature of neural synchronization patterns in disorders of neural connectivity. In extension, 1/f signal opens up new avenues for the development of interventions, aiming to optimise network communications (Voytek & Knight, 2015).

Steeper or flatter 1/f spectral power slope- revealing disruptions in dynamic network communication in the brain- may be a core symptom or a causal mechanism of a number of neurological conditions, particularly those characterized by widespread neural synchrony abnormalities. Although plausible, this hypothesis has only been tested in a very limited number of clinical groups. Five published papers have examined power law scaling in clinical data and only three have computed 1/f properties of PSD. Meisel et al. (2012) demonstrated

that during epileptic attacks, the distribution of phase-locking intervals (PLI) deviate from the characteristic power law $1/f$ shape. In ASC, Tinker and Velazquez (2014) found that power law scaling in the distributions of phase synchrony indices captured by MEG during an auditory and a Stroop task, does occur but not frequently and vanishes as a result of increased task complexity. More recently, using data from a selective attention EEG task, Peterson et al. (2017) computed $1/f$ slopes of PSD in patients with schizophrenia and healthy participants from three distinct electrode sites (central, posterior and midline). $1/f$ noise slope was significantly steeper in the schizophrenia group compared to the control, reliably predicting clinical status. The authors concluded that $1/f$ slope, together with band-limited power, may serve as a valid biomarker of schizophrenia. In contrast to schizophrenia, where $1/f$ slope is shown to be steeper, subsequent work in ADHD, has shown that $1/f$ slope of PSD becomes more negative, less flat, when methylphenidate is administered, a drug known to be restoring SNRs by increasing dopaminergic neurotransmission (Pertermann et al., 2019). This is in line with Ostlund et al. (2021) who demonstrated that adolescents with ADHD show smaller aperiodic exponents in their ongoing oscillatory activity, indicative of a flatter $1/f$ slope of PSD, compared to their typically developing counterparts. It is important to note that no studies have previously computed $1/f$ properties of PSD in ASC. In summary, recent evidence demonstrates that $1/f$ slope of spectral power may be clinically relevant, capturing complex underlying neural dynamics that differ in psychiatric conditions.

1.7.2 What can Phase/Amplitude Coupling (PAC) tell us about the pathological undercoupling hypothesis in ASC?

Voytek & Knight (2015) hypothesized that ASC is likely to be characterized by noise-induced pathological undercoupling, which would in turn be reflected in flatter $1/f$ slopes of PSD. $1/f$ neural electrophysiological noise has not been previously examined in clinical samples of ASC. Nevertheless, support for the pathological undercoupling hypothesis is currently coming from studies that have previously investigated Phase/Amplitude Coupling (PAC) in ASC. PAC is the most common method of quantifying cross-frequency relationships between oscillations and describes the statistical dependence between the phase of low-frequency oscillations and the amplitude of high-frequency oscillations in response to a stimulus (Canolty et al., 2006; Canolty & Knight, 2010). A well-established PAC relationship is that of gamma and alpha oscillations. The amplitude of gamma oscillations ($>40\text{Hz}$), suggested to be emerging from local neuronal interactions (Singer & Gray, 1995), is shown to modulate the phase of alpha

frequency oscillations (8-12Hz), responsible for establishing neural synchrony across multiple populations of neurons at a systems level, thereby facilitating interregional neural communication (Jensen & Mazaheri, 2010). This push and pull relationship is suggested to be highly sensitive to noise i.e temporally decorrelated spikes occurring at random time points in the oscillatory phase cycle (Voytek & Knight, 2015). Computational models have indicated that even when temporal correlations between spike trains change minimally, the impact on PAC is large (Deco et al., 2009). If noisy spikes decoupled from oscillatory dynamics occur in a network, it is expected that these will degrade the strength of PAC. From that perspective, it has been proposed that reduced PAC can serve as an indirect indicator of excessive neural noise in the system.

In the ASC literature, experimental findings on PAC vary greatly and can be contradictory depending on the nature of the task, the network it is targeting and the developmental stage of participants. Patterns of reduced alpha-to-gamma PAC are reported in functional networks of executive functioning (Velazquez et al., 2009), the social brain (Khan et al., 2013) and the sensory system (Seymour et al., 2019). Studies examining intra-regional connectivity, have shown reduced alpha-to-gamma PAC in adolescents with ASC at V1 in response to visual stimulation (Seymour et al., 2019) and at the Face Fusiform Area (FFA) in response to active viewing of emotional faces (Khan et al., 2013). Port et al. (2019) report region-specific alterations in alpha-to-gamma PAC; increased at central midline regions and decreased at lateral regions. In contrast, greater alpha-to-gamma PAC has been observed in children with ASD as computed from resting-state data (Berman et al., 2015 but see Murias et al., 2007 for a contradictory result). Although ASC is linked to general patterns of reduced alpha-to-gamma PAC, it is evident that findings are heavily influenced by task requirements or developmental factors, making it very difficult to draw firm conclusions on whether excessive neural noise is present. Importantly, this remains an indirect metric of evaluating levels of neural noise in the neural system. For that reason, direct measurement of 1/f slopes of PSD is necessary to clarify whether noise-induced pathological undercoupling underpins neural dynamics in ASC.

1.7.3 Parameterisation of Power Spectral Density (PSD)

Careful parameterisation of the power spectrum is suggested to be a crucial step to be able to successfully isolate noise exponents of power spectra from task-related power influences. Multiple methods of separating oscillatory dynamics (central frequency and amplitude) from non-oscillatory dynamics (broadband offset and $1/f$ noise exponent) have been proposed in the literature. Voytek et al. (2015) originally utilised a regression-based model fitting method, according to which a line of best fit describing the relationship between PSD and frequency was fitted to the observed data and alpha band peaks (7-14Hz) of PSD were then subtracted. A limitation of this approach is that the width of the alpha band window remains fixed, therefore it is not accounting for individual differences in alpha peaks, an issue directly tackled in the present thesis by adjusting the window to capture the start and end of alpha band peak for each participant. More recently, Donoghue et al. (2020a) proposed parameterising PSD through an iterative model fitting process, using the 'Fitting Oscillations and One-Over- f ' (FOOOF) toolbox. This algorithm removes periodic activity via an iterative peak-finding process, where the peaks of residuals are identified and if they are above the noise threshold, a Gaussian is fitted and then subtracted from the original PSD (see p.3, Donoghue et al., 2020a). Other methods of parameterising power spectra involve parametric curve fitting based on the summation of alpha, modelled as a bell function instead of a Gaussian and $1/f$ noise, a method known as ' $\alpha+1/f$ ' (Ouyang et al., 2020). A very different method of disentangling periodic and aperiodic properties of the neural signal is suggested by Wen & Liu (2016), who propose extracting $1/f$ from resampled signal to deal with the issue of spectral leakage, a method known as Irregular-resampling auto-spectral analysis (IRASA, see Wen & Liu, 2016).

Taken together, in the present thesis the regression-based method was employed to remove periodic activity and this approach was further refined to adjust the width of the alpha bump by picking the start and end of the alpha peak for each participant individually. This method of parameterisation was preferred over other methods because it is a well-established way of parameterising power spectra in previous experimental studies (see Voytek et al., 2015; Dave et al., 2018). At this early stage of research, keeping such parameters constant allowed for greater comparability across studies and greater confidence in the interpretation of results.

1.8 Overlap of Autism Spectrum Conditions (ASC) and Attention Deficit Hyperactivity Disorder (ADHD)

ADHD is a neurodevelopmental condition shown to share behavioural features and genetic risk factors with ASC (McCarthy et al., 2014; Satterstrom et al., 2019). Although at surface the two diagnostic categories seem distinct, behavioural profiles of individuals with ASC and individuals with ADHD frequently overlap. From a phenotypic perspective, an ASC diagnosis is provided if social communication difficulties and repetitive and restricted patterns of behaviour are present, whereas core ADHD diagnostic symptoms include inattention, hyperactivity and impulsivity (American Psychiatric Association, 2013). However, social interaction difficulties and repetitive behaviours are often reported in individuals with a clinical diagnosis of ADHD (Antrop et al., 2000; Reiersen et al., 2008), whereas inattention and executive functioning difficulties are well-documented in ASC clinical samples (Sinzig et al., 2009; Demetriou et al., 2018). In addition, ASC and ADHD frequently co-occur; 28% of individuals with ASC are also diagnosed with ADHD (Simonoff et al., 2008) and 11- 12.4% of individuals with a primary diagnosis of ADHD hold a comorbid ASC diagnosis (Jensen & Steinhausen, 2015; Giacobini et al., 2018). Along those lines, an important hypothesis yet to be disentangled is whether those behavioural features are characterised by overlapping or distinct underlying pathophysiologies.

In an effort to shed light on the causal pathways of disorder manifestations in ASC and ADHD, genomic studies have further demonstrated that the two conditions share genetic risk factors. Clinical studies have shown that siblings of children with ASC are at higher risk of being diagnosed with ADHD (Jokiranta-Olkonemi et al., 2016) and that first-born offsprings of mothers with a clinical diagnosis of ADHD are at higher risk to be diagnosed with ADHD and ASC (Musser et al., 2014). Similarly, population-based twin studies have found that symptom domains of ASC and ADHD are distinct but show high genetic overlap (Ronald et al., 2008; Taylor et al., 2011; Ronald et al., 2014). From a molecular genetics standpoint, Genome-Wide Association studies (GWAS) have identified pleiotropic genes linked to both ASC and ADHD (Grove et al., 2017; Byrne et al., 2020), providing further supporting evidence for the partial genetic overlap of the two conditions.

Shared genetic risk factors imply that some underlying neurobiological mechanisms may also be common. Existing studies have revealed disorder-specific but also overlapping neural patterns (see Section 2.1.2 of Chapter 2 for a breakdown of studies and Lau-Zhu et al., 2019

for a review). Functional networks responsible for attentional control and executive functions as well as error and feedback processing, involving regions such as the prefrontal and the anterior cingulate cortex, are shown to be affected in both ASC and ADHD (Henderson et al., 2006; Lau-Zhu et al., 2019; Kaiser et al., 2020). Nevertheless, the very few existing comparative ERP studies indicate that ADHD is characterized by attentional orienting and inhibitory control abnormalities and ASC by conflict monitoring and response preparation difficulties (Tye et al., 2014). Distinct patterns of neural functioning also emerge with regards to functional connectivity patterns. ASC is associated with global hypoconnectivity, whereas ADHD demonstrates widespread patterns of global hyperconnectivity in large-scale networks during attentional control and social tasks (Shephard et al., 2019). In resting state conditions, there are reports of hypoconnectivity in ASC (Dickinson et al., 2018; Shephard et al., 2019) but the picture becomes more blurry in ADHD as studies report both patterns of hyperconnectivity (Barry et al., 2002; Robbie et al., 2016) and lack of alterations in global/local connectivity (Alba et al., 2016; Shephard et al., 2019). Atypicalities in oscillatory power are also reported in resting-state conditions, taking the form of decreased theta and alpha power in ASC and decreased delta power in ADHD (Shephard et al., 2018). Although the exact biological mechanisms giving rise to specific network abnormalities in the two conditions are still not very well understood, a growing number of studies attribute some of these differences to synaptic transmission imbalances in the brain of individuals with ASC and those with ADHD (Kim et al., 2020).

Despite the fact that both disorders are characterised by widespread neural communication abnormalities, neuroscientific data on the integrity of neural circuitry dynamics coming from comparative study designs in ASC and ADHD are scarce. With respect to neural noise, increased levels of neural noise in the form of reduced ITPC have been previously reported in both ASC and ADHD (Milne, 2011; Gonen-Yaacovi et al., 2016, see also Ostlund et al., 2021 about flatter 1/f slopes in ADHD). Nevertheless, there have been no direct studies to date measuring and comparing levels of neural noise in clinically diagnosed ASC and ADHD samples.

Understanding how neural noise manifests in the brain of participants with ASC and ADHD could provide new insights on the gene- brain- behaviour pathways and the causal mechanisms giving rise to phenotypic expressions in ASC and ADHD. Such direct comparisons could shed light on the ongoing debate of whether an overarching disorder underlies both conditions, thereby some individuals with a diagnosis of ASC and those with ADHD are expected to share

neural underpinnings or they are two distinct nosological entities, therefore ASC and ADHD are expected to be characterised by distinct underlying neurological features (Rommelse et al., 2010). Chapter 2 provides an in-depth discussion of how comparative study designs of ASC and ADHD could advance current knowledge of pathophysiological processes and aid biomarker discovery.

1.9 Experimental approach followed in the present thesis

Neural oscillations tune their phases to be at an optimal point in the excitatory cycle during the onset of a stimulus (Makeig et al., 2002). If some subtypes of ASC are indeed associated with an imbalance in E/I ratio, resulting in increased endogenous neural noise, as proposed by Rubenstein & Merzenich (2003) and Simmons et al. (2007), disproportionately high excitation or weak inhibition is expected to be affecting the ability of neural oscillations to reach this optimal point in the excitatory cycle and phase-reset effectively in response to external stimulation. In the neurotypical brain, levels of neural noise are usually quantified by measuring SNRs. Nevertheless, as it will be discussed in Section 1.5.4.3, metrics using trial averaging to calculate the amplitude of the signal may not reveal existing differences in ASC as compared to neurotypical samples. Therefore, failures in synaptic transmission are more likely to be captured by ITPC, as extracted from electrodes or Independent Components of interest. For that reason, the present thesis directly investigates neural noise in ASC in the form of ITPC. In those subgroups of individuals with ASC characterised by synaptic transmission abnormalities, phase angles of stimulus-evoked neural oscillations are expected to be “misaligned” from trial-to-trial in key electrode sites (e.g. in close proximity to the sensory cortices), with a phase distribution approaching uniformity, reflecting a more variable, noisier neural response.

Considering the inconsistencies in the literature, evident when spectral features are strictly studied within canonical frequency bands (see Section 1.7.2 about Phase/Amplitude Coupling), the present thesis also investigates neural noise in ASC from the perspective of $1/f$ noise of PSD, a metric not confined within a specific frequency band. Excessive noise in key neural circuits is suggested to lead to weakened interregional oscillatory coherence and manifest as pathological undercoupling in ASC, involving difficulties to establish neural communication (Voytek & Knight, 2015). If the pathological undercoupling hypothesis proposed by Voytek & Knight is true, $1/f$ slopes of PSD will be flatter in the ASC samples tested in the present thesis, as weaker oscillatory coupling from weaker dendritic outputs results in smaller numbers of simultaneously triggered spikes and therefore reduced temporal variability of spike timings.

In terms of spatial scale, an E/I imbalance manifesting in a large-scale circuit involves a change in the relative activity of different types of excitatory or inhibitory neurons within small-scale circuits, such that the threshold at which global balance is achieved changes (Sohal &

Rubenstein, 2019). Although it is also important to know what microscopic sources may be contributing to a global E/I imbalance as observed in larger scale circuits, small-scale neural network dynamics cannot be captured sufficiently by EEG as they are chaotic and non-linear in nature (Pritchard, 1996; Wright & Liley, 1996). For that reason, the focus of the present thesis is not small-scale network behaviour, but rather, the main objective is to explore whether global E/I balance is affected in specific regions (e.g. visual cortices), with metrics such as ITPC and in the whole brain, with metrics such as $1/f$ slope of PSD. In addition, this approach allows to directly interrogate periodic oscillatory dynamics but also aperiodic properties of the neural signal under scrutiny.

Given that ERP trial averaging may not reveal existing atypicalities in evoked responses of participants with ASC (see Section 1.5.4.3 for a discussion), single-trial analysis was performed to extract neural signal in the experimental studies of the present thesis measuring ITPC. Independent Component analysis was utilised to “blindly” separate distinct sources of signal, which are less contaminated with noise generated by other cortical and non-cortical sources. In addition, recent evidence by Van Diepen & Mazaheri (2018) demonstrated that ITPC computed from the same channel across participants is impacted by differences in dipole orientations, resulting in null findings when compared across samples. For that reason, ITPC was extracted from source reconstructed signal i.e. Independent Components projecting to the visual cortex, rather than EEG channels. This approach is well-documented and has previously been utilised in ASC (see Milne, 2011; Milne et al., 2019) and ADHD (Gonen-Yaacovi et al., 2016).

On the other hand, $1/f$ slopes were calculated from PSD recorded from scalp EEG signals. In contrast with ITPC, the study of aperiodic signal properties is a newly emerging field. Very few experimental studies have previously examined $1/f$ slope of PSD and as a result it is still unclear what signal source PSD should be extracted from (i.e ICs or EEG channels) and consequently which electrode cluster $1/f$ noise analysis should be performed on. Previous literature does not provide a clear picture, as the majority of the studies measuring noise exponents do not report on the signal source utilised to extract PSD from. In the present thesis, two methods of comparing levels of $1/f$ noise across groups were utilized with the aim to scrutinize whole-brain dynamics; either the grand average value of the aperiodic exponent was

extracted from all EEG channels and was compared across groups and/or single electrode comparisons were performed across the whole brain.

1.10 Aims of the present thesis

1.10.1 General aims

Following proposals that increased neural noise may serve as a biomarker of ASC, primary aim of the present thesis was to systematically investigate the increased neural noise hypothesis in ASC. Initial exploration of the literature indicated that levels of neural noise may be elevated not only in ASC but also in ADHD, a neurodevelopmental condition that shares genetic risk factors with ASC. However, current research findings are mixed and, despite the clear etiological link between ASC and ADHD, there are no previous studies that have directly compared patterns of neural noise in individuals with a clinical diagnosis of ASC and those with a diagnosis of ADHD. The experimental study summarised in Chapter 2 aimed to bridge this gap in knowledge and investigate whether levels of neural noise as measured by ITPC and 1/f slope of PSD are increased in adults with ASC as compared to adults with ADHD and typically developing (TD) adults (**Aim 1**).

Due to limitations related to the fact that many of the autistic adults were later diagnosed in adulthood and therefore may be characterised by less severe forms of autism, it was unclear how generalisable the findings of Chapter 2 were. In addition, it remained unclear whether levels of neural noise follow a similar pattern in childhood compared to adulthood. For that reason and in order to consolidate the findings of Chapter 2, the increased neural noise hypothesis was also tested in a child sample (**Aim 3**). The desire to recruit a large and representative sample to look at this hypothesis motivated the drive to set up a mobile EEG paradigm and collect data in children's homes (**Aim 2**). Methodological details on how this was achieved are presented in Chapter 3.

Similarly to the first experimental study, the child study indicated that only a subgroup of children with ASC are characterised by reduced ITPC. Further to the group comparisons, an important next step was to understand whether those reductions in ITPC occur in participants with a specific behavioural profile. In order to do this, we investigated whether levels of neural

noise can be predicted by core ASC symptoms but also extended the analysis beyond primary diagnostic symptoms and looked into secondary behavioural expressions such as sensory symptoms (**Aim 4**). Previous studies- albeit small in number- have not revealed a relationship between neural noise and global measures of ASC symptom severity (see Milne et al., 2019). Although core phenotypic expressions of ASC were previously assessed, sensory symptoms have not been previously examined in the literature. Therefore, Chapter 5 presents findings on the relationship between neural variability as indexed by ITPC and 1/f slope of PSD, and variability in ASC symptomatology across a range of cognitive domains.

1.10.2 Aim 1

If increased neural noise is capturing pathophysiological dynamics that are distinct in ASC- neural features prominent in the brain of individuals with ASC characterized by synaptic transmission abnormalities- it is important to know whether the neural correlate is possible to distinguish between ASC and other neurodevelopmental conditions such as ADHD. A key limitation of the studies outlined in Section 1.6.1 and Section 1.7.1 is that they have not examined neural noise in a comparative study design and as a result, we cannot draw firm conclusions regarding neural processes that differ or may be common. In addition, they use a wide variety of methods and analytical approaches to measure neural variability, which often leads to conflicting results within the literature. Therefore, the question of whether increased neural noise describes ASC alone or is a pathophysiological feature of other psychiatric conditions characterized by imbalances in synaptic transmission such as ADHD, remains unanswered.

The first aim of this thesis is to understand whether increased neural noise in the form of increased neural variability is likely to be specific to ASC, taking the form of an ASC biomarker as suggested by David et al. (2016), or whether it also characterises ADHD, therefore taking the form of a transdiagnostic marker that cuts through diagnostic boundaries. Recent research work proposes that ADHD is characterized by low ITPC and flatter 1/f slopes of PSD, indicating disrupted information processing which mirrors the pattern of neural functioning observed in ASC. Failures in synaptic transmission have been previously reported in both conditions, therefore it is plausible that increased neural noise is not exclusively a feature of the autistic brain. Section 2.1.4 of Chapter 2 discusses those studies in detail and elaborates on similarities and differences between the two clinical groups.

In the present thesis, using EEG, we examine neural noise as indexed by ITPC and 1/f slope of PSD, two variables that provide insight into both periodic and aperiodic brain dynamics. In order to test the above hypothesis, in Chapter 2, ITPC and 1/f slope of PSD are computed both in response to visual stimulation and during a resting state condition in three samples; a group of adults with ASC, a group of adults with ADHD and an age and ability-matched group of typically developing adults. Direct comparisons across the three groups using the same task and data processing pipeline are necessary to describe patterns of neural communication in ASC with greater precision. Considering previous experimental findings, it is expected that participants in both clinical groups will demonstrate increased neural noise, operationalised as reduced ITPC and flatter 1/f slopes of PSD, in line with a growing body of literature speaking for an E/I imbalance and pathological undercoupling in the two conditions.

1.10.3 Aim 2

Traditional laboratory-based EEG experiments, such as the one described above, are by nature less inclusive and less accessible by more severely affected individuals with ASC (Lau-Zhu et al., 2019). A significant barrier to their participation is that these experiments usually take place in a fixed location, the EEG laboratory, under demanding experimental conditions where participants have to communicate effectively with the experimenter, successfully follow a sequence of activities and limit movement during the experimental task. The transition to a new social environment to participate in unknown activities with an unfamiliar person i.e the researcher posits a substantial challenge for individuals with ASC and their carers. Social communication difficulties ranging from mild to more severe, extreme sensory sensitivities and repetitive behaviours, symptoms exacerbated by high levels of anxiety contribute to the difficulty individuals with ASC face to visit the EEG laboratory and comply with EEG experimental procedures. Comorbid intellectual disability further contributes to reduced participation rates. As a result, a selection bias is observed towards the inclusion of more able individuals with ASC in clinical studies aiming to investigate neurophysiological biomarkers of ASC and a lack of electrophysiological data recorded from more severely affected individuals with ASC (Russell et al., 2019). The systematic underrepresentation of these individuals in biomarker research ultimately hinders the identification of valid behaviour-brain-gene pathways in ASC and the opportunity to accurately describe neural patterns in the clinical group.

Enabling data collection to take place in a more familiar environment, e.g. at home, may increase access to research participation in this group. In Chapter 2 we present a new accessible method of studying brain activity of autistic individuals outside the laboratory in their home environment, using mobile EEG technology. The primary aim of this chapter is to test the feasibility of acquiring good quality EEG data from autistic children at home, assessed via a set of objective data quality metrics, and to develop a list of practical guidelines on how to successfully conduct an EEG experiment in such a naturalistic setting based directly upon participants' views.

1.10.4 Aim 3

In childhood, studies such as the one conducted by Milne (2011) indicate that ASC is associated with reduced alpha ITPC in response to visual stimulation, however, in an effort to replicate the study by Milne (2011), Butler et al. (2017) do not report significant differences in levels of ITPC between the ASC and TD group. Of note, these studies are characterized by small sample sizes ranging from 13-20 participants, raising questions about whether these findings can be generalised. Some useful mechanistic insights are provided by a well-powered study by Milne et al. (2019) who report low ITPC during visual processing only in a subsample of adults with ASC, a finding indicating that increased neural variability is likely to be characterising the brain of some participants with ASC but not all. Due to ASC heterogeneity, it is expected that such neurological differences between participants will be evident at any given sample, explaining some of the inconsistencies in the child studies. However, it is still unclear whether children with ASC show a similar pattern of neural functioning to the adults with ASC, as documented in Milne et al. (2019).

Considering the above, the third aim of the present thesis is to investigate patterns of neural noise in a much larger sample of children with ASC and clarify whether increased neural noise occurs in children with ASC. In addition, we aim to understand whether increased neural noise is a characteristic of evoked responses or ongoing oscillatory activity. Following a similar analytical approach to the experimental study outlined in Chapter 2, neural noise is measured by computing ITPC and changes in 1/f slope of PSD in a group of children with ASC and a group of typically developing children. Children were tested at their home environment using a gel-based mobile EEG system. Consistent with the experimental approach followed

throughout this thesis, these measures are extracted from both a visual task-based condition and a resting-state ‘eyes-closed’ condition.

1.10.5 Aim 4

The fourth aim of this thesis is to investigate the relationship between neural noise and core diagnostic symptoms of ASC. If increased neural noise is a neural signature of ASC, a measurable feature in the brain of those autistic individuals with synaptic transmission disruptions, it should also be linked to some aspect of the ASC phenotype (Carroll et al., 2021). Thus far, studies investigating neural noise in ASC have primarily focused on linking the variable indexing neural noise (i.e ITPC, SNRs etc.) with global measures of ASC symptom severity (see Dinstein et al., 2012). In addition such studies have not revealed any relationship between global measures of ASC symptom severity and neural noise (see Milne et al., 2019). However, this framework is somewhat simplistic as aspects of sensory perception, known to be integral to the pathophysiology of ASC, are neglected. In the visual modality, which is the focus of the present research work, reports of illusions and visual distortions in response to gratings with low spatial frequency such as black and white checkerboards are widespread in the ASC literature (Ludlow, Wilkins & Heaton, 2006; Ludlow & Wilkins, 2016; Ludlow et al., 2020). Given that the stimuli used to measure neural noise are likely to generate a hyper-active neural response in key regions, it is plausible that low ITPC would be more likely to be seen in those who are characterised by perceptual sensitivity to such patterns. However, the relationship between neural noise, as measured in response to visual stimulation, and the sensitivity of the visual cortex to such incoming stimuli has not been previously examined. Thus, Chapter 4 aims to systematically examine whether neural noise in the form of ITPC and $1/f$ slope of PSD is linked to clusters of symptoms specific to the autism phenotype. Phenotypic traits examined in the study include not only social communication impairments and restricted and repetitive patterns of behaviour but also sensory symptoms. Based on previous research by Milne et al (2019), it is hypothesised that social communication impairments and restricted patterns of behaviour will not predict levels of ITPC, as this is what was previously found in a group of autistic adults.

Chapter 2:

Neural noise in adults with Autism Spectrum Conditions (ASC) and Attention Deficit Hyperactivity Disorder (ADHD)

2.1 Introduction

Autism Spectrum Conditions (ASC) and Attention Deficit Hyperactivity Disorder (ADHD) are childhood onset neurodevelopmental disorders, which persist into adulthood and often co-occur (Ronald et al., 2008). ASC is diagnosed on the basis of social communication difficulties and repetitive and restricted patterns of behaviour, whereas diagnostic symptom domains for ADHD include inattention, hyperactivity and impulsivity (American Psychiatric Association, 2013). The distinct core diagnostic criteria for ASC and ADHD reflect a unique underlying genetic aetiology that leads to heterogeneous patterns of behavioural symptoms in both conditions. However, phenotypic profiles in ASC and ADHD frequently overlap; core ASC diagnostic symptoms such as social interaction difficulties (Reiersen, et al., 2008), language delay (Rohrer-Baumgartner et al., 2016), and repetitive and ritualistic behaviours (Antrop et al., 2000) often occur in ADHD. Similarly, primary ADHD symptom domains such as inattention (Sinzig et al., 2009), and executive functioning impairments frequently manifest in ASC (Demetriou et al., 2018). Prevalence rates of ASD-ADHD co-occurrence reach 28% in ASC samples (Simonoff et al., 2008) and range from 11- 12.4% in ADHD samples (Jensen & Steinhausen, 2015; Giacobini et al., 2018), suggesting that some genetic and neurobiological pathways may be common.

2.1.1 Genetic overlap

Indeed, a growing number of genetic studies suggest that genetic risk factors are partly shared, explaining the moderate degree of phenotypic overlap. Twin studies have shown overlapping genetic influences of ASC and ADHD trait measures in general population- based cohorts of children (Ronald et al., 2008) and adults (Reiersen et al., 2008). Large studies including clinically diagnosed samples however have been more scarce. Three large-scale birth registry studies have examined the familial transmission of ASC and ADHD. Musser et al. (2014) studied the genetic and phenotypic profiles of >35000 children and their mothers and found that first-born offsprings of mothers with a clinical diagnosis of ADHD are 6 times more likely to be diagnosed with ADHD and 2.5 times more likely to be diagnosed with ASC. Jokiranta-Olkonemi et al. (2016) showed that siblings of children with ASC are at higher risk of being diagnosed with ADHD. This is in line with Ghirardi et al. (2018) who also report that family members of individuals with ASC with varying degrees of genetic relatedness are at elevated risk of ADHD. Gene-specific candidate-driven and genome-wide association studies (GWAS) provide further support for the existence of genetic cross- disorder links. Deletions of *ASTN2*

and *TRIM32* genes in chromosome 9 are implicated in both ASC and ADHD (Lionel et al., 2014). After combined analysis of ASC and ADHD exome sequences, a recent study by Satterstrom et al. (2018) demonstrated that ASC and ADHD samples carry a strikingly similar number of protein-truncating variants (PTVs) and identified the novel gene *MAP1A* and the *DYNC1H1*, *POGZ*, *SCN2A* and *ANK2* genes as some of the primary loci where these mutations reside, further confirming the genetic overlap of two disorders. These results speak for a partially shared genetic aetiology between ASC and ADHD; we now understand that there are multiple gene-environment interactions contributing to the expression of complex traits in each disorder separately, however the above literature suggests that shared genetic factors give rise to particular aspects of disorder manifestations in both conditions.

2.1.2 Neurocognitive overlap

Shared genetic etiology suggests that some underlying neural pathways may also be common. Separate lines of work point towards altered structural and functional patterns of brain organisation in both conditions. These have so far revealed disorder-specific but also overlapping neural patterns. Based on evidence from structural MRI studies, a shared anatomical feature seems to be a smaller corpus callosum and cerebellum (ASC: Piven et al., 1997; Freitag et al., 2009, ADHD: Hutchinson et al., 2008; Stoodley, 2014). Other studies report reductions in grey matter density in the left temporal medial lobe-attributed to delayed brain maturation in the region- and an increase in the left inferior parietal cortex, potentially linked to attentional processing abnormalities (Brieber et al., 2007). Some morphological differences are also apparent; ASC is characterised by larger subcortical brain volume (Freitag et al., 2009), whereas ADHD by reduced whole- brain volume (Greven et al., 2015).

Functional networks implicated in attention and executive functioning are shown to be compromised in both ASC and ADHD. In the fMRI literature, diminished BOLD signal activation is consistently shown to occur in the fronto-parietal network during a wide range of executive functioning tasks. Both ASC and ADHD are associated with atypicalities in the amplitude and latencies of P300 ERP subcomponents, as demonstrated in EEG studies utilising visual or auditory oddball paradigms. Other lines of evidence indicate that both disorders are characterised by functional abnormalities in the anterior cingulate cortex and lateral prefrontal cortex, a network playing a key role in error and feedback processing. Using flanker tasks, ERP studies have shown differences in error-related negativity (ERN) and error-related positivity (Pe) amplitudes between clinical group and controls, in both ASC (Henderson et al., 2006) and

ADHD samples (McLoughlin et al., 2009). These suggest reduced capacity to monitor error responses in both conditions. Comparative study designs have revealed some disorder-specific patterns too, with ADHD showing more negative amplitude and shorter latency of the ERN during an illusory figure categorization task compared to ASC (Sokhadze et al., 2012). Shephard et al. (2019) also demonstrated that ASC is associated with global hypoconnectivity, whereas ADHD demonstrates widespread patterns of global hyperconnectivity in large-scale networks during attentional control and social tasks. Other studies have shown an absence of post-error slowing, which suggests difficulties to adjust subsequent behaviour in order to optimise outcomes (ASC: Vlamings et al., 2008; McMahon & Henderson, 2014, ADHD: Balogh, 2016). In contrast with ADHD, in ASC post-error slowing abnormalities are observed primarily in response to social stimuli (McMahon & Henderson, 2014). Early sensory processing of low-level auditory and visual stimuli is also shown to be abnormal in both conditions. This is reflected in atypicalities in the amplitude and latency of P1 in response to visual stimuli (ASC: Kovarski et al., 2016, ADHD: Kim et al., 2015; Nazhvani et al., 2013) and the mismatch negativity ERP component, elicited by deviant changes in the presentation of a sequence of standard sounds (ASC: Fan & Cheng, 2014, ADHD: Cheng et al., 2016).

In resting-state paradigms, power fluctuations of the EEG signal appear to be abnormal in both ASC and ADHD, however conflicting evidence is presented regarding the magnitude and the frequency band these atypicalities occur at. Some studies report a U-shape resting-state EEG profile in ASC (Machado et al., 2015) and others propose an elevated slow-wave, followed by reduced fast-wave activity pattern in ADHD (Kitsune et al., 2015). The increased theta/beta power ratio (TBR) is proposed to be a sensitive marker, differentiating ADHD from non-ADHD participants in several studies (Lubar, 1991; Monastra et al., 1999; Markovska-Simoska & Pop-Jordanova, 2017), although a meta-analysis by Arns and colleagues (2013) argues that excessive TBR only characterizes a subgroup of individuals of ADHD (also see Kiiski et al., 2020). In contrast with the above, the only comparative study design of resting-state neural correlates in ASC and ADHD has shown reduced theta and alpha power in ASC and reduced delta power in ADHD (Shephard et al., 2018). The same study reports limited evidence for elevated theta band activity in ADHD, questioning the reliability of the increased TBR finding as a diagnostic measure of ADHD. To conclude with, ASC and ADHD have shown divergent patterns of resting-state brain activity. However, more work is necessary to replicate the results by Shephard et al. (2018) and understand how these resting-state network alterations impact cognition.

Existing neuroscientific studies, including the ones reviewed above, do not address the two neurodevelopmental disorders in tandem, often include a single diagnostic group (either ASC or ADHD) and very rarely include a comparison group with comorbid ASC and ADHD or account for high ASC and ADHD traits. Notable exceptions include the studies by Bink et al. (2015), Saunders et al. (2016), Shephard et al. (2018), Shephard et al. (2019) and Bellato et al. (2020), who measured resting state dynamics in children with ASC and ADHD and Tye et al. (2013), Tye et al. (2014), Tye et al. (2014) and Shephard et al. (2019) who investigated attentional and social cognition mechanisms in children with ASC and ADHD. This problem is not trivial as existing evidence, stemming from divergent fields, provides a fragmented overall picture and does not allow for firm conclusions regarding the overlapping pathophysiological mechanisms underlying ASD and ADHD. The lack of evidence is mainly attributed to the fact that previous diagnostic criteria did not permit a dual diagnosis of ASC and ADHD in the same individual, therefore studies comparing ASC, ADHD and ASC+ADHD clinical samples were not feasible prior to the revisions of the Diagnostic and Statistical Manual of Mental Disorders in 2013 (American Psychological Association, 2013). In addition, neuroscientific data directly comparing ASC and ADHD brain architectures are limited or non-existent in some key functional domains, for example with respect to neural noise patterns. Addressing those issues will provide new insights on the shared and unique neural correlates underpinning both conditions, which will in turn inform biomarker research and nosological models.

Given the shared genetic influences, a key question is whether behavioural features in ASC and ADHD are based on overlapping or distinct underlying pathophysiologies. It is yet unclear whether ASC and ADHD are different manifestations of an overarching disorder as suggested by van der Meer (2012) or truly distinct clinical entities (Rommelse et al., 2010). If the latter is true, we would expect neural correlates linked to phenotypic features to be different in ASC vs ADHD, therefore independent from each other. If there is an interactive effect of ADHD on traits which depends on ASC (and vice versa), we would expect to observe the presence of subgroups with a similar neural profile in both conditions. This distinction is important to be made, in order to better characterize the gene-brain-behaviour pathways to ASC and ADHD. For this distinction to be clarified, it is necessary to employ study designs which directly compare the neural profiles of the two patient groups using the same neurophysiological measures. Identifying neural correlates that may be common or different in the two conditions will provide new insights on the causal pathways linking genetic variants to atypical neural

patterns and ultimately phenotypic expressions in ASC and ADHD. Importantly, this fine-grain approach will help disentangle etiological heterogeneity in ASC and ADHD (Hodgson, McGuffin & Lewis, 2017), regarded as one of the biggest obstacles in the identification of candidate susceptibility genes.

2.1.3 Neural variability

A recent review by Lau-Zhu et al. (2019) of the neurophysiological overlap and distinctions between ASC and ADHD, highlights the importance of investigating neural variability as a candidate neural substrate, likely to explain aspects of the phenotype i.e atypical sensory processing in both ASC and ADHD. In the present study we aim to fill this gap in the literature and investigate neural variability in ASC and ADHD. As outlined in Chapter 1, here we focus on neural variability- also referred to as “neural noise”- from two different perspectives; the degree of phase angle alignment across experimental trials, known as inter-trial phase coherence (ITPC) and the degree of variation of the spiking activity as indexed by 1/f noise slope of Power Spectral Density (PSD).

Effective communication between regions is known to depend upon the synchronization of oscillatory activity of neurons. For optimal information processing, groups of neurons tend to align the phase angles of their oscillations, so that spikes arrive at a time window of high excitability, rather than low. If spikes arrive at random phases of the oscillation cycle, the information stream will be characterised by greater neural variability or else greater “noise” and lower effective connectivity (Fries, 2015). It is important to note that noise, in the form of noisy, serially uncorrelated spikes arriving at a moment of low excitability, is often introduced in the healthy brain as a corrective mechanism to smooth the threshold of action potentials and prevent hypersynchronisation (Fries, 2005). However, excessive noise works to the expense of the system, resulting in weakened interregional oscillatory coherence and pathological undercoupling (Voytek & Knight, 2015). According to Voytek & Knight (2015), network communication disruptions in the brain can manifest either as a) “undercoupling”, involving difficulties to establish communication or as b) “overcoupling”, meaning that two clusters of neurons are too strongly synchronized and are both equally detrimental for information processing within the circuitry. This process is fundamental for information transmission and is a candidate mechanism for a pervasive network impairment in ASC and ADHD. It is therefore surprising that neural variability has not been previously investigated in a comparative study design of ASC and ADHD, particularly considering that both disorders are

characterised by functional brain connectivity abnormalities (see Hull et al., 2017 and Kowalczyk et al., 2021 for a review), which are not localised to a specific brain region but rather, they seem to be widespread, affecting interconnections between neural networks.

A well-established way of measuring neural variability is by computing the oscillatory phase angle alignment in single experimental trials- a variable known as inter- trial phase coherence (ITPC). ITPC is a particularly effective method of studying within subject trial- to trial variability of electrophysiological signal; it indicates whether the phase-angle of an oscillating sine wave at a specific time point is coherent across trials (Cohen, 2014). A reliable, precise, highly consistent evoked response exhibits high ITPC from trial to trial (David et al., 2016). The opposite happens when the evoked response is noisier or highly variable; lower ITPC is expected (David et al., 2016).

The $1/f$ slope component of Power Spectral Density (PSD) is another method of quantifying neural variability. As described in Section 1.4.4 and Section 1.7 of Chapter 1, $1/f$ slope of spectral power reflects variability of spike arrival timings at a local level in relation to the strength of interregional oscillatory coupling (Voytek & Knight, 2015). If spiking activity in the neural ensemble is highly synchronised with only a few spikes reaching the nearby neurons in their non-excitatory phases, then $1/f$ slope of PSD will be steeper, i.e. more negative. A more negative $1/f$ slope indicates that spike trains are highly correlated, therefore characterised by smaller amount of variability. On the other hand, if spike trains in the neuronal population are firing asynchronously, $1/f$ slope will be flatter. White noise is represented in a spectrogram as a flat line with a noise exponent of 0. The closer the $1/f$ slope is to 0, the flatter the line of the slope will be, indicating more variable, less synchronized spiking activity. As proposed in the relevant literature, there is an optimal balance between the two and extreme deviations from the mode- steeper or flatter slope- is strong evidence for disruptions in neural communication. In the context of Voytek & Knight's dynamic network communication framework (2015), it is possible that electrophysiological responses in ASC and ADHD are characterised by a flatter $1/f$ power slope, indicating undercoupling of oscillatory dynamics. In turn, a steeper $1/f$ slope of PSD would suggest overcoupling or hypersynchronisation, meaning that two clusters of neurons are too strongly synchronized (see Section 1.7.1 in Chapter 1 about the dynamic network communication framework).

We propose that ITPC and 1/f slope of PSD are two complementary ways of quantifying neural variability. ITPC characterises evoked neural activity in response to a stimulus presentation, therefore it is task-specific. It is also band-specific as it describes narrowband changes in phase synchrony and is computed locally. On the other hand, 1/f slope of PSD is a variable that can be computed from both task-based and resting-state data. It is not focused on a specific frequency band but rather describes how the distribution of power contained in a signal changes as a function of all frequencies. Compared to traditional spectral power analysis approaches, 1/f slope is focusing on broadband, rather than narrowband changes in power density, therefore it may be a better indicator of global neural synchrony and coherence. In addition, 1/f slope of PSD captures aperiodic features of the electrophysiological signal, which are largely ignored in other study designs. For that reason, we believe that 1/f slope of PSD is a more holistic way of conceptualising neural variability in the brain.

2.1.4 Neural variability in ASC and ADHD

In search for more concrete, quantifiable neural features indexing genetic susceptibility to ASC, a number of studies have examined neural variability as a promising neural correlate, believed to be capturing underlying network communication disruptions (Milne et al., 2019). In support of the undercoupling hypothesis (Voytek & Knight, 2015), multiple lines of research have shown that ASC is associated with excessive neural noise in the form of increased neural variability and poorer SNRs. Reduced ITPC occurs at both low and high frequency bands in response to a wide range of cognitive tasks, including visual, auditory, somatosensory and error-processing. In the visual domain, Milne (2011) analysed scalp EEG data of children with ASC and found lower ITPC in the alpha band during visual processing of Gabor patches. Similarly, Weinger et al. (2014) showed weak SNRs in electrophysiological responses of children with ASC, computed from steady state visual evoked potentials. Reductions in the Phase-Locking Factor (PLF) of beta rhythms in the occipital lobe is also reported during picture-naming (Buard et al., 2013). A more recent EEG study by Milne et al. (2019) found reduced ITPC in response to visual stimulation in a group of adults with ASC and concluded that increased neural variability is likely to be reflecting one of the many pathophysiological routes to ASC symptomatology. In the auditory domain, reduced ITPC and Phase-locking Factor (PLF) is reported in the gamma band in response to tones of various frequencies (Rojas et al., 2008; Edgar et al., 2015). Some contradictory results were presented by Yu and colleagues (2018), who found an increase in ITPC of theta oscillations computed

for the P1 time window, followed by a reduction in ITPC for the N2 time window during processing of pure tones and words. The authors concluded that slow waves in ASC tend to exhibit phase asynchrony 200ms after stimulus presentation but not before this time window, whereas faster waves show reduced synchrony in earlier time windows. Other lines of work have shown reductions in ITPC of theta oscillations in the frontal electrode site during feedback processing of rewards and errors (van Noordt et al., 2017). In line with the EEG and MEG literature, Dinstein et al. (2012) and Haigh et al. (2014) conducted three fMRI experiments measuring neural variability in response to simple visual, somatosensory and auditory stimuli and report low SNRs in all sensory modalities. Taken together, these findings highlight that short-range network communication patterns are altered in ASC. Increased neural noise in the form of neural variability is likely to be degrading the oscillatory activity of the neural circuit, affecting synchronisation-mediated information flow locally.

Increased neural variability is also reported in ADHD. Thus far, only five studies have examined the neural noise hypothesis in clinical ADHD samples (see *Table 2.1* for a summary of studies). Groom et al. (2010) report a reduction in early and late theta band ITPC, computed from fronto-central electrodes, in response to visual go/no-go trials. In a similar task design, Pertermann and colleagues (2019) showed that 1/f slope of PSD is significantly flatter in ADHD compared to controls in the NoGo trials but not in the go trials. They concluded that ADHD is not characterised by excessive neural noise as such, but rather it increases with increasing task demands and requirements for greater inhibitory control, a domain known to be impaired in ADHD. In extension to this finding, they demonstrated that 1/f slope of PSD becomes more negative, less flat, when methylphenidate is administered, a drug known to be restoring SNRs by increasing dopaminergic neurotransmission (Pertermann et al., 2019). It is important to mention that error-processing abnormalities of this nature are observed in both ADHD (Groom et al., 2010) and ASC (van Noordt et al., 2017). In line with these preliminary findings, Gonen-Yaacovi et al. (2016) showed that reductions in ITPC of theta and alpha oscillations occur not only in the visual but also the auditory modality. In this experiment, ITPC was reduced in pre and post stimulus intervals as well as in trials where there was no stimulus present. In contrast to the conclusions of Pertermann et al. (2019) however, the authors propose that ongoing, rather than stimulus-evoked neural activity is characterised by greater noise in ADHD. In support of this hypothesis, Ostlund et al. (2021) found flatter 1/f slopes in a large sample of adolescents with ADHD, as computed from resting state data (i.e eyes open and eyes closed conditions). In the auditory domain, contradicting findings are presented by Yordanova

et al. (2001) who found increased levels of phase-locking in the gamma band during auditory processing of tones. This contrasting result is likely to be explained by the use of a less conventional method of computing neural variability, known as ‘single-sweep wave identification’. In summary, converging evidence points towards reductions in phase synchrony of the theta and alpha rhythms in individuals with ADHD during sensory and error-processing tasks. It is still unclear whether excessive neural noise is a feature of stimulus-evoked neural activity, ongoing or both, or whether it characterises short-range or long-range network communication in ADHD. The majority of these studies utilise task designs targeting executive functioning processes and examine exclusively the fronto-central electrode site, providing limiting insights into whole-brain neural synchronisation patterns in ADHD.

Table 2.1

Studies measuring neural variability in individuals with a clinical diagnosis of ADHD

	Author	Year	Participants*	Modality	Stimulus	Method	Location	Frequency	Result**
EEG studies	Yordanova et al.	2001	Children (<i>n</i> =14)	Auditory	Non-target tones, high target tones	single-sweep wave identification	Electrode cluster F3, Fz, F4, C3, Cz, C4, P3, P4	Gamma	More strongly phase- locked gamma oscillations
	Groom et al.	2010	Adolescents (<i>n</i> =23)	Visual	Go/NoGo letters 'X', 'K'	ITPC ¹	Electrode FCz	Theta	Reduced ITPC
	Gonen-Yaacovi et al.	2016	Young adults (<i>n</i> =17)	Visual, auditory	Black triangles/circles, pure tones	ITPC	Electrode with the highest P1/N1 amplitude PO8 and FCz electrodes in all subjects ICA component that best captured the early sensory response	Theta, Alpha	Reduced ITPC in all conditions
	Pertermann et al.	2019	Children (<i>n</i> =29)	Visual	Go/NoGo words 'DRUCK', 'STOP'	1/f slope of PSD ²	Electrode cluster FC1, FC2, FCz, Cz	Theta, Beta	Flatter 1/f slope during NoGo trials in the ADHD group vs TD group but not during Go trials. Methylphenidate treatment improved the steepness of the 1/f slope.
	Ostlund et al.	2021	Adolescents (<i>n</i> =87)	N/A	8 min baseline period (eyes closed/open)	1/f slope of PSD ²	Not known	N/A	Smaller aperiodic exponents

*Sample size given for the ADHD group

**The result is reported for the ADHD group relative to the TD control group

¹ Inter-trial Phase Coherence² 1/f slope of Power Spectral Density

The wide range of tasks and data analysis techniques used in the above studies do not allow to draw conclusions regarding neural processes that differ or may be common in ASC and ADHD. A key limitation of the above studies is that they use a wide variety of neuroscientific methods (i.e EEG, MEG, fMRI) and analytical approaches to measure neural variability (i.e. ITPC, PLF, SDs, single-sweep wave identification etc), which may lead to conflicting results within the ASC and ADHD literature. In addition, samples with different characteristics (i.e age, developmental stage, IQ, diagnostic status, comorbid conditions) are recruited in each study, limiting the possibility of comparing findings in the ASC literature with that of the ADHD. Even when the same neurocognitive domain is investigated, task characteristics such as type of stimulus, duration of stimulus presentation, baseline measurements and input modality vary remarkably from one experiment to the other (Lau-Zhu et al., 2019). Linked to this, existing work focuses primarily on childhood ADHD and although ADHD is known to persist into adulthood, studies investigating neural underpinnings in older adults with ADHD are largely lacking. Hartman et al. (2016) explicitly highlight the need to “go beyond childhood” in a recent review. Importantly, there are currently no studies directly comparing neural variability in clinically diagnosed ASC and ADHD samples of any age. Evidence regarding neural variability in adult samples in specific is missing. Direct comparisons across disorders using the same methodology and design are necessary to determine distinct and overlapping neural patterns in ADHD and ASC.

2.1.5 Aims of the current study

In the present study, we aim to bridge this gap in the literature and investigate neural noise in a comparative study design of ASC and ADHD. Direct comparisons across the two clinical groups and a typically developing group using the same task and data processing pipeline will allow us to explore whether ASC and ADHD, two conditions that share genetic risk factors, demonstrate similar or distinct levels of neural noise. This comparison will ultimately allow us to describe with greater precision patterns of neural synchrony in the two conditions. For the purposes of the study, we utilized already existing data from a diagnosed group of adults with ASC published in Milne et al. (2019) (see Section 2.2.1 for further details), recruited an additional group of non-medicated adults with ADHD and a group of adults without a clinical diagnosis of mental health conditions. Using electroencephalography (EEG), we examine neural noise in the form of neural variability from two different perspectives; as indexed by ITPC and 1/f slope of PSD. Although numerous studies have measured neural variability by computing ITPC in ASC, there is no previous research on 1/f properties of PSD. To our knowledge this is the first study to examine 1/f slope of PSD in this clinical group. In order to clarify whether increased neural variability

manifests in stimulus-evoked activity, ongoing or both, we first compute ITPC and changes in 1/f slope of PSD in a visual task-based condition in the three groups and then measure 1/f slope of PSD in a resting-state ‘eyes-closed’ condition. Taking into account the relevant literature (see *Table 2.1* and *Table 2.2*), we hypothesise that the ASC and the ADHD group will exhibit lower ITPC in response to visual stimulation compared to the TD group. A recent study has shown flatter 1/f slope of PSD in NoGo trials in ADHD and a reduction of the 1/f noise exponent through methylphenidate treatment (Pertermann, et al., 2019). In addition, Ostlund et al. (2021) found flatter 1/f slopes as computed from eyes open and eyes closed conditions in a large sample of adolescents with ADHD. In this line of argument, we also expect to observe flatter slopes in the non-medicated ADHD group compared to the TD group. In addition, we hypothesise that both the ASC and ADHD group will show flatter 1/f slope of PSD compared to the TD group; if confirmed, this would indicate oscillatory undercoupling, as suggested by Voytek & Knight (2015). However, given that no studies have tested the 1/f noise hypothesis in ASC, it is difficult to predict with certainty the direction of the comparison between the ASC and the TD group or the comparison between the two clinical groups. As an exploratory analysis, we finally investigate the relationship between ITPC and 1/f slope of PSD to determine whether participants that exhibit low ITPC also exhibit flatter 1/f slope of PSD.

2.2 Materials and Methods

2.2.1 Participants

34 typically developing (TD) participants, 36 participants with ADHD and 28 participants with ASC were recruited for the study. The TD and ADHD data were primary data collected for the sole purpose of the study, however 71% of the ASC datasets (20 out of 28) were secondary data previously published (Milne et al., 2019). Participants were age, gender and cognitive ability-matched (*Table 2.2*). Groups did not differ in age, gender and IQ as determined by one-way ANOVA (age: $F(2, 91) = 0.10, p = 0.89$, gender: $F(2, 91) = 1.17, p = 0.31$, IQ: $F(2, 91) = 0.06, p = 0.93$). Participants with ADHD were primarily recruited via online advertisement on social media, TD participants were recruited via the University of Sheffield and the local community and the ASC sample via a volunteer emailing list maintained by the Sheffield Autism Research Lab and the Sheffield Adult Autism and Neurodevelopmental Service (SAANS). Participants in the ADHD group held a diagnosis of either ADHD ($n=29$) or ADD ($n=5$). Similarly, participants in the ASC group had a diagnosis of ASC or Asperger Syndrome provided by a private or NHS mental health service. Participants with ADHD did not have a comorbid ASC diagnosis and participants with ASC did not hold a co-occurring ADHD diagnosis. A comprehensive overview of the formally diagnosed co-occurring conditions in the three groups is provided in *Table 2.3*. Twenty-four participants in the ADHD group were on regular ADHD medication, however they all remained non-medicated for 16 hours prior to the experiment. Eight participants in the ASC group were medicated (*Table 2.4*). All participants had normal or corrected to normal visual acuity.

Table 2.2

Participant demographics

	TD (<i>n</i> =34)	ADHD (<i>n</i> =32)	ASC (<i>n</i> =28)
Gender			
Female	11	9	13
Male	23	23	15
Age			
Mean	41.2	39.8	41.0
SD	11.9	10.7	15.0
Range	18-69	18-64	18-67
MRS score^a			
Mean	59.1	59.6	59.7
SD	5.7	5.6	8.0
Range	43-70	47-72	29-72
SRS-2 score^b			
Mean	45.4	62.6	68.8
SD	4.8	10.6	11.1
Range	38-55	49-83	48-89
ASRS score^c			
Mean	8.5	19.4	13.4
SD	4.1	2.7	3.4
Range	2-19	13-24	8-20

^aMRS score, Matrix Reasoning Subscale score, Wechsler Abbreviated Scales of Intelligence (WASI, Wechsler, 1999)

^bSRS- 2, Social Responsiveness Scale (SRS-2, Constantino & Gruber, 2011)

^cASRS, Adult ADHD Self- Report Scale (ASRS, Kessler et al., 2005)

Table 2.3

Number of participants in each group with formal diagnosis of a co-morbid condition

	Major depressive disorder	Generalised Anxiety Disorder	Obsessive Compulsive Disorder	Dyspraxia	Dyslexia
TD (<i>n</i> =34)	0	0	0	0	0
ADHD (<i>n</i> =32)	8	9	1	1	0
ASC (<i>n</i> =28)	13	11	0	3	3

Table 2.4

Drug intake of participants recorded up to 16 hours prior to the EEG experiment

	Citalopram	Venlafaxine	Lansoprazole	Propranolol
TD (<i>n</i> =34)	0	0	0	0
ADHD (<i>n</i> =32)	0	0	0	0
ASC (<i>n</i> =28)	3	3	1	1

The following exclusion criteria were applied to all three groups: participants (a) with a known intellectual disability, that (b) did not speak English, (c) had epilepsy and/or (d) a mental health condition such as personality disorder, bipolar disorder, psychotic disorder did not take part in the study. Psychometric and neurophysiological data were initially collected from 98 participants, however, four participants from the ADHD group were excluded from the study, as there was a substantially large amount of noise in their EEG recordings. Data channel rejection for those participants crossed the cut-off of 25% (16 channels out of 64) and/or the amount of remaining artefact-free epochs was <75%, which rendered the quality of the EEG data inadequate for further analysis. Subsequently, data from a total of 94 participants was further analysed. Participant consent was provided in written form prior to the testing session and ethical guidelines were followed throughout according to the standards set by the Ethics Committee at the University of Sheffield. *Table 2.2* provides descriptive information about the three groups, TD, ADHD and ASC.

2.2.2 Psychometric assessments

Participants completed three standardized questionnaires aiming to assess their perceptual reasoning and the presence or absence of ADHD and ASC symptoms. The Matrix Reasoning subtest of the Wechsler Abbreviated Scales of Intelligence (WASI, Wechsler, 1999) (0.99) was used to measure non-verbal abstract reasoning. Subjects viewed a number of geometric patterns and were asked to identify the missing piece from a selection of four or six answers. Raw scores were converted into t-scores based on the participant's chronological age. Adult ADHD symptoms were measured using the Adult ADHD Self-Report Scale (ASRS, Kessler et al., 2005). The ASRS is a self-report questionnaire used to address ADHD symptoms in adults. Respondents were asked to rate the extent to which they meet six criteria, which are indicative of ADHD. Each question was answered on a 6-item Likert scale, ranging from "never" to "Very often". The Social Responsiveness Scale- Revised Adult Self Report version (SRS-2, Constantino & Gruber, 2011), a self-report questionnaire containing 65 4-point Likert scale items, was used to identify the presence and severity of social impairments associated with ASC.

The SRS “self-report” provides a t-score, which is indicative of the severity of the social communication impairments. The “other-report” version of the SRS was also completed. This version of the SRS is identical to the “self-report” but is designed to be completed by a parent, spouse, friend or other relative of the participant. The multiple perspectives approach with regards to behaviour facilitates validation of data through cross verification and therefore was preferred in the current study design. A two-way mixed intraclass correlation coefficient analysis indicated excellent agreement between the two raters (ICC = 0.89) (Cicchetti, 1994).

2.2.3 Procedure

Upon their arrival at the University of Sheffield, participants underwent a short background history interview. Information about demographics, medication intake and known mental health conditions was acquired for descriptive purposes. Participants then completed the ASRS, SRS-2 and the matrix-reasoning subtest of the WASI followed by the EEG recording.

2.2.3.1 Apparatus

A 64-channel BioSemi ActiveTwo EEG system and BioSemi ActiView Software (Biosemi Instrumentation BV, Amsterdam, The Netherlands) were used for EEG data acquisition. Visual stimuli were presented on a Viglen LCD display screen with a spatial resolution of 1280×1024 pixels and a temporal resolution of 60 Hz. Data acquisition took place in a shielded room to eliminate electrical interference in the measurement cables and the ground electrode DRL (Metting Van Rijn et al., 1990).

2.2.3.2 EEG experiment

The EEG experiment consisted of a task- based condition followed by a resting state condition, explained in detail at Section 2.2.3.4 and Section 2.2.3.5.

2.2.3.3 Data acquisition

EEG data was recorded continuously from 64 Ag/AgCl mounted in an elastic 64- channel cap. The data quality was ensured by keeping the impedance values of the electrodes below 25 k Ω . The signal was amplified (midband gain of 10^3), bandpass filtered at 0.01- 80Hz, then digitalised at a sampling rate of 2048Hz. ActiveTwo Biosemi system does not store signal in a referenced format, therefore the raw data was reference-free when acquired.

2.2.3.4 Task- based EEG

Stimuli

The first part of the EEG experiment involved presentation of a checkerboard stimulus on a display screen and lasted approximately ~13 minutes (see *Figure 2.1*). The checkerboard appeared on the screen for an average of 2000ms, jittered between 1500 and 2500ms, followed by an image of a red cross. The duration of the inter- stimulus interval (ISI) was 2000ms, jittered between 1500ms and 2500ms. The checkerboard stimulus was presented 200 times in 2 blocks of 100. Participants were instructed to press the spacebar when the checkerboard disappeared from the screen and the red cross appeared to ensure that they were continuously engaged and did not orient attention towards a different point.

Figure 2.1

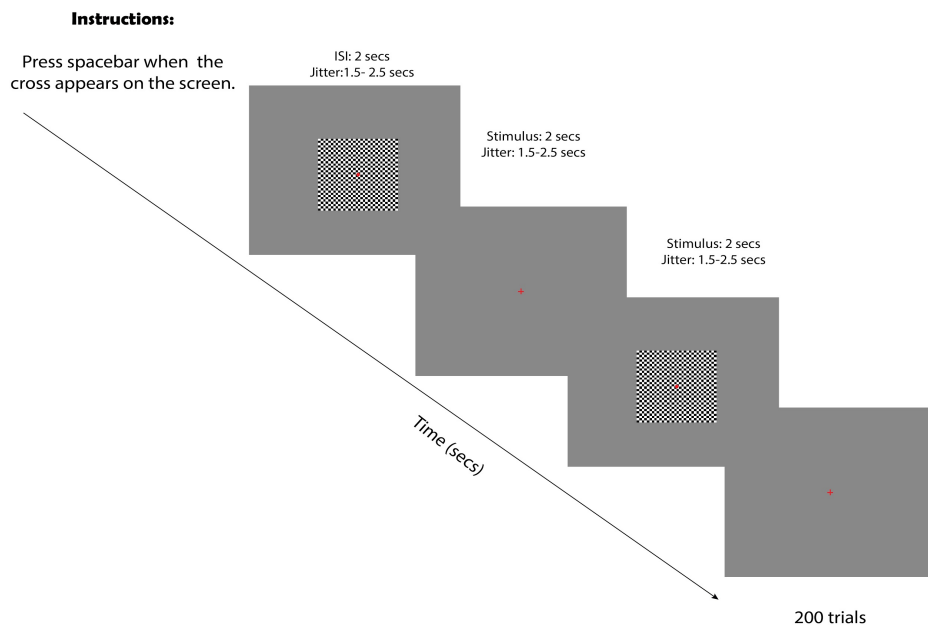


Figure 2.1: Schematic representation of the EEG experiment

2.2.3.5 Resting- state EEG

Following 200 trials, participants were instructed to close their eyes while EEG data was acquired for 120 secs. *Figure 2.2* provides a schematic representation of the resting- state condition.

Figure 2.2

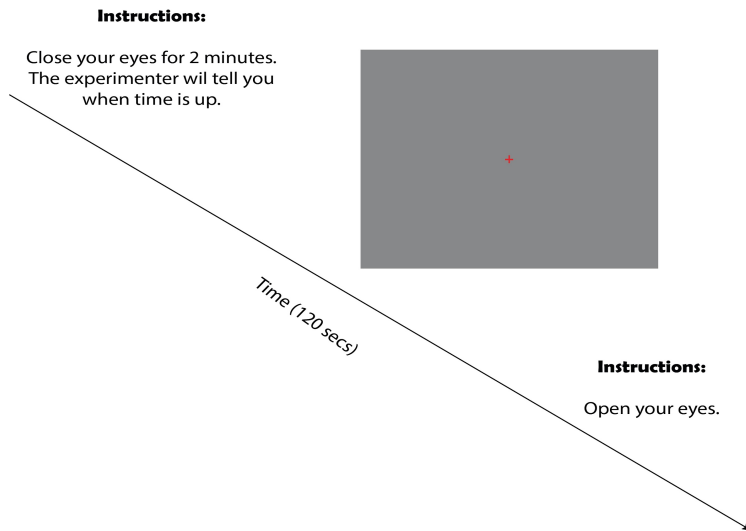


Figure 2.2: Schematic representation of the resting- state condition

2.2.4 General data preprocessing

All EEG datasets were analysed using EEGLAB (Delorme & Makeig, 2004) running on Matlab 2014a (The Mathworks, Inc.). A number of preprocessing pipeline steps were followed to ensure that high quality signal was extracted. Signal was downsampled from 2048Hz to 512Hz. For ITPC analysis, Cz was selected as the reference electrode, following previous work by Milne et al. (2019). In contrast, the preprocessing steps followed for 1/f slope analysis remained similar to the ones outlined by Voytek et al. (2015) and, for that reason, the average reference was used. In both analyses, a high- pass filter of 1Hz was applied to remove large drifts or signal deviations. Channels exhibiting noise due to poor scalp connection were removed from the analysis. Continuous data was visually inspected and noisy time segments containing muscle or eye movement artefacts affecting multiple channels were manually rejected. This resulted in fewer epochs being retained and used for further analysis than the initial number of trials. Independent Component Analysis (ICA) was then applied on the clean data, using the *runica* function of EEGLAB (see Section 2.2.6.2). *Figure 2.3* provides a summary of the preprocessing steps followed, in preparation for extraction of the variable of interest i.e. ITPC and 1/f slopes. Sections 2.2.6.1 and 2.2.8.1 provide a description of the analysis-specific preprocessing steps to extract ITPC and 1/f slopes of PSD respectively.

Figure 2.3

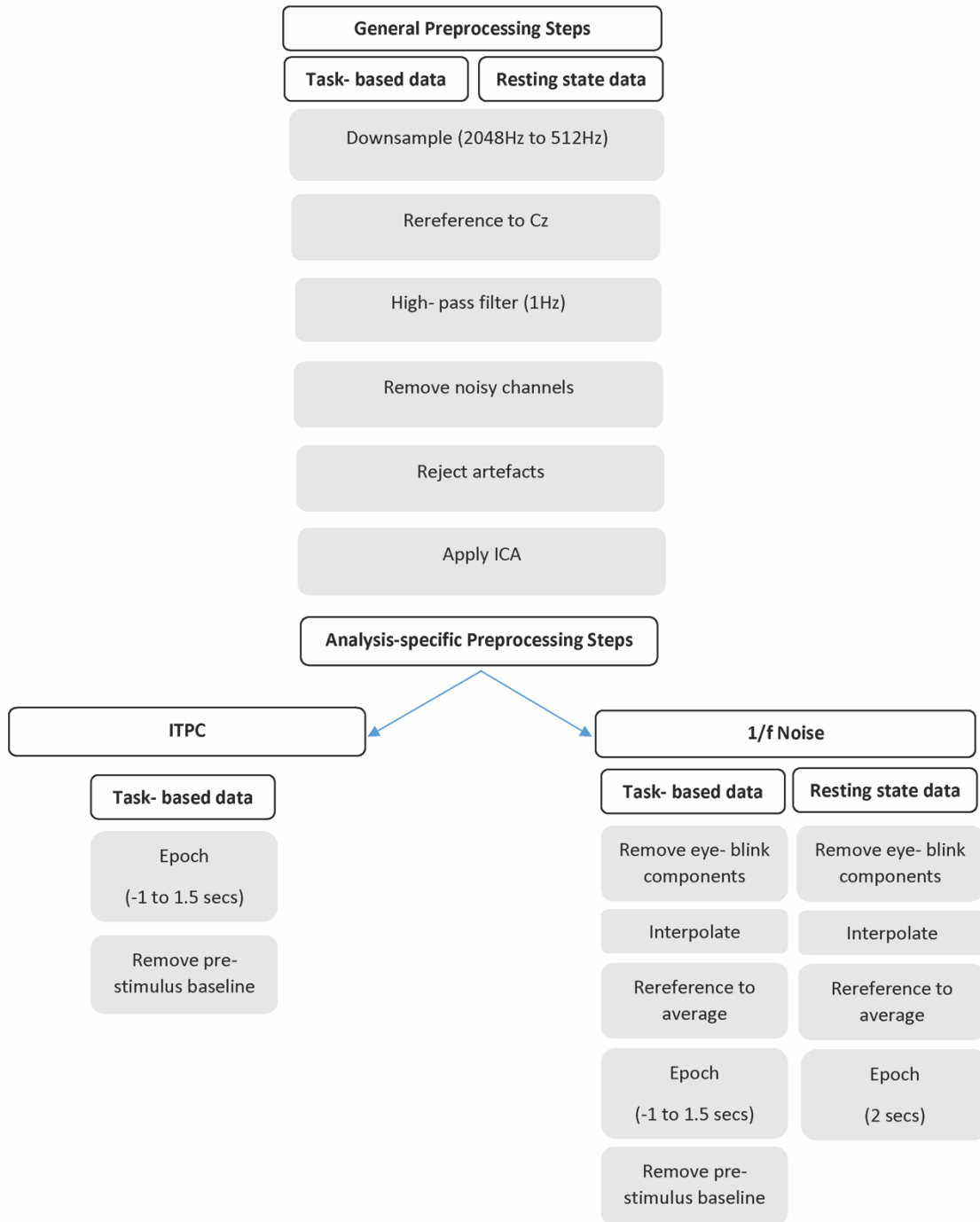


Figure 2.3: Summary of A) the general and B) analysis specific preprocessing steps followed.

2.2.5 Data integrity

Following the preprocessing analysis, a series of extra analysis steps were carried out in order to ensure that EEG data quality is adequate for further analysis, as well as similar across different datasets and amongst different groups. We first established that the number of epochs were the same in the final ITPC vs 1/f noise task-based datasets. Secondly, we ensured that the number of epochs was similar across groups. The mean number of epochs extracted from the task-based data (ADHD: 187 [170 200], ASC: 182 [100 198], TD: 188 [178 197]) did not differ significantly between groups as determined by a one- way ANOVA ($F(2,91) = 2.26$, $p = 0.11$). Thirdly, only signal from Independent Components or channels with signs of a visual evoked potential (VEP) (e.g. P1 or N1 deflection) was kept for further analysis. The ERP of the selected IC and the selected channel was examined, confirming that a VEP was present in the neural signal of all participants in the three groups (*Figure 2.4* and *Figure 2.5* for the ASC group and *Annex 1* for the TD and ADHD groups). In addition to the above, the ITPC values of the ASC group, which were falling below the minimum value of the ITPC distribution for the TD and ADHD group (see *Figure 2.10*), were examined in relation to the ERP trace of the respective IC or channel. Visual inspection of their topographic map and ERP image revealed that the signal quality was adequate.

Figure 2.4

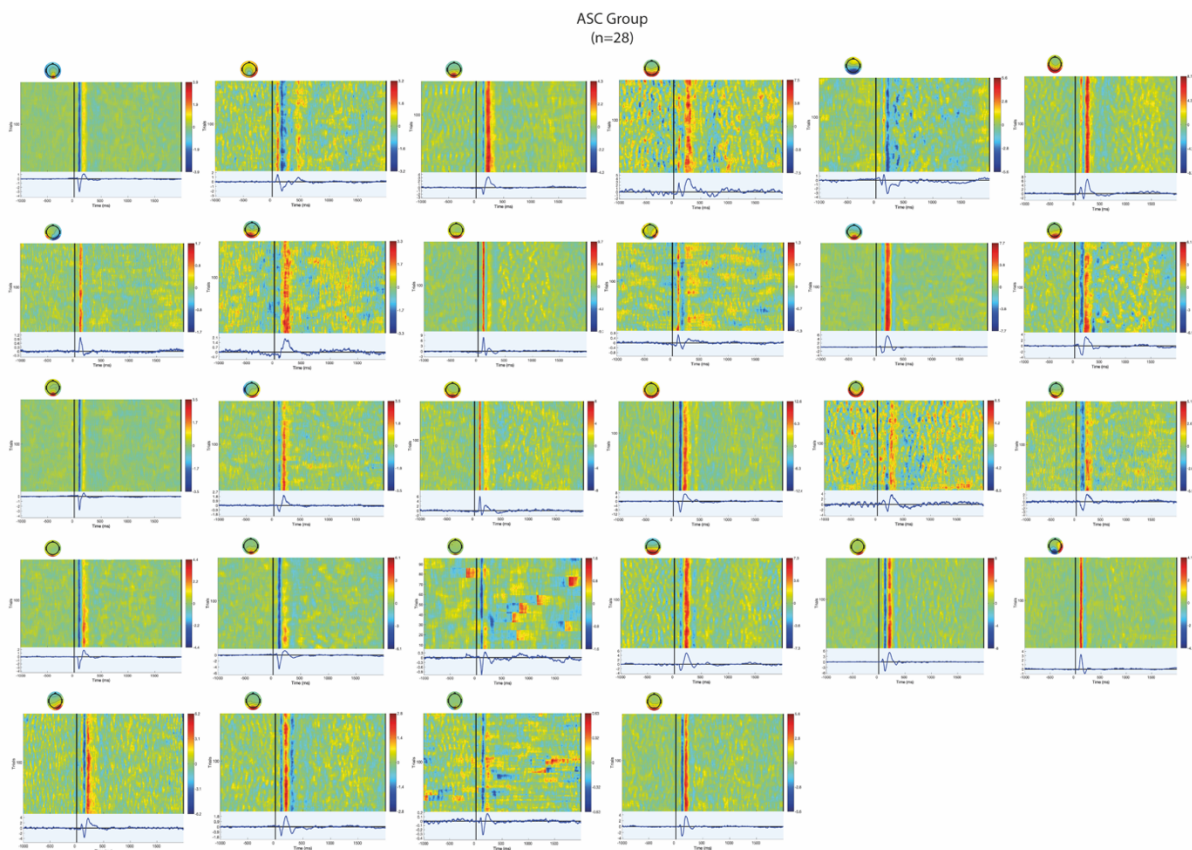


Figure 2.4: ERPs of the selected Independent Components (ICs) included in the group analysis, presented for the ASC group($n=28$).

Figure 2.5

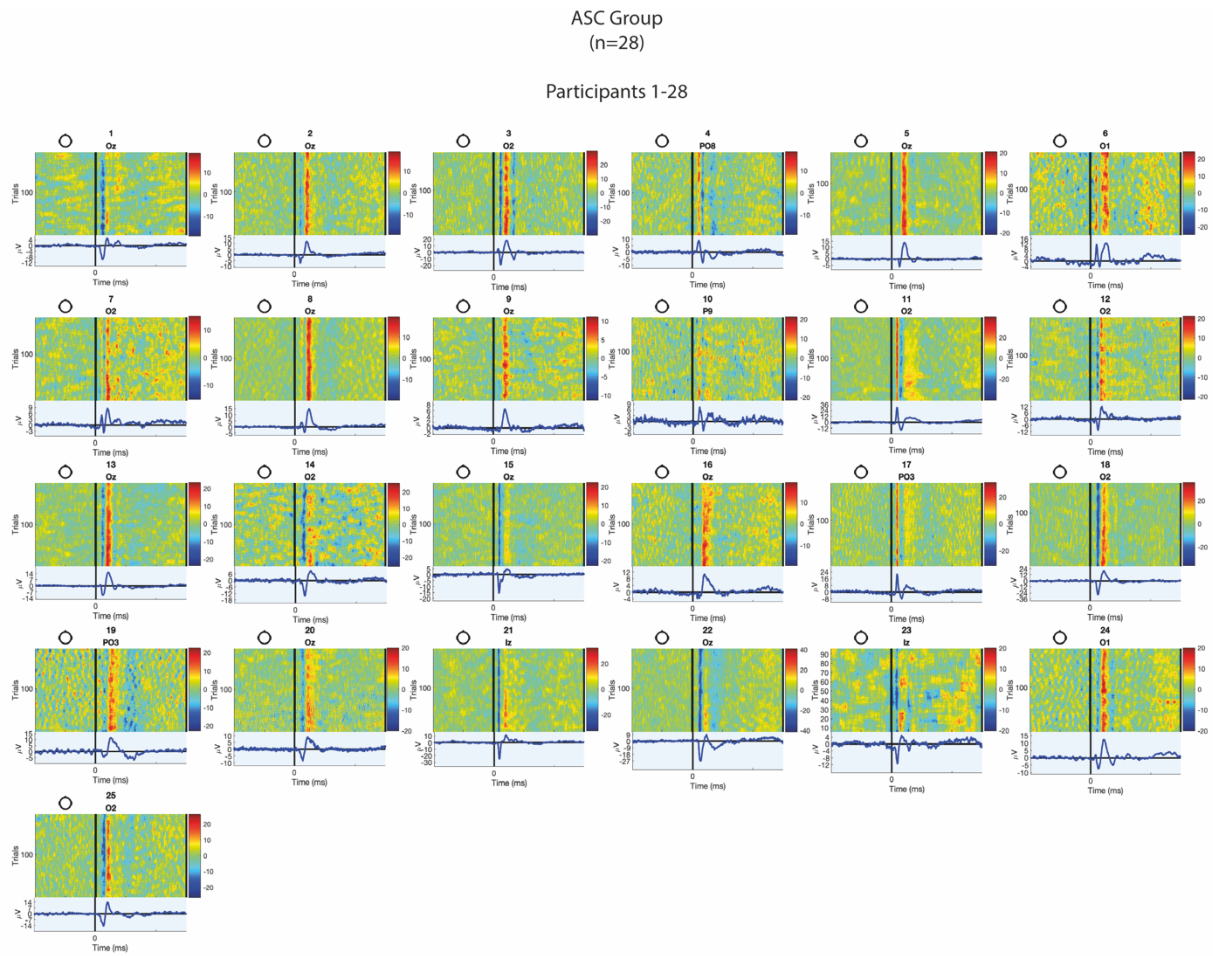


Figure 2.5: ERPs of the selected channels included in the group analysis, presented for the ASC group($n=28$).

2.2.6 EEG data preparation for Inter- Trial Phase Coherence analysis

2.2.6.1 Data preprocessing

Additional preprocessing steps were followed to prepare the task-based data for ITPC analysis (Figure 2.3). Data was segmented into epochs, from -1 to 1.5 secs around stimulus onset, and corrected to baseline, using the average signal between 1 sec before stimulus onset to stimulus onset.

2.2.6.2 Data selection

In the present chapter, ITPC was extracted from two distinct sources of signal, both from Independent Components (ICs) and EEG scalp electrodes.

Independent Component selection

Independent Component Analysis (ICA) is a method of blindly separating sources of signal, which are linearly mixed when recorded from several sensors of scalp EEG. The ICA algorithm separates the mixed signal into spatially independent components of source signal, which are less contaminated with noise generated by other cortical and non- cortical sources.

ICA decomposition was performed using the *runica* function of EEGLAB, which utilises the informax ICA algorithm of Bell & Sejnowski (1995) with the natural gradient characteristics suggested by Amari et al. (1996). ICs are computed using the following mathematical process: neural data X is defined as a matrix of n channels multiplied by t time points, $n \times t$. ICA decomposition produces a matrix U of ICs which is equal to a component ‘unmixing’ matrix W multiplied by the neural data matrix X :

$$U = W X$$

where U and X are equal dimension matrices ($n \times t$) and W is defined as $n \times n$ (Stone, 2002; Onton & Makeig, 2009). Therefore, the number of ICs recovered for each participant is always equal to the number of channel inputs. ICA, applied on individual participant scalp data, returned as many components as the number of channels kept for further analysis after preprocessing. Time-frequency analysis was then performed on all ICs (see Section 2.2.6.2). For each participant, we calculated ITPC for every IC and selected the single IC with maximum ITPC for further analysis. Visual inspection of the IC scalp maps of the IC selected from each participant revealed that the selected ICs were projected at the occipital lobe, suggesting that they were

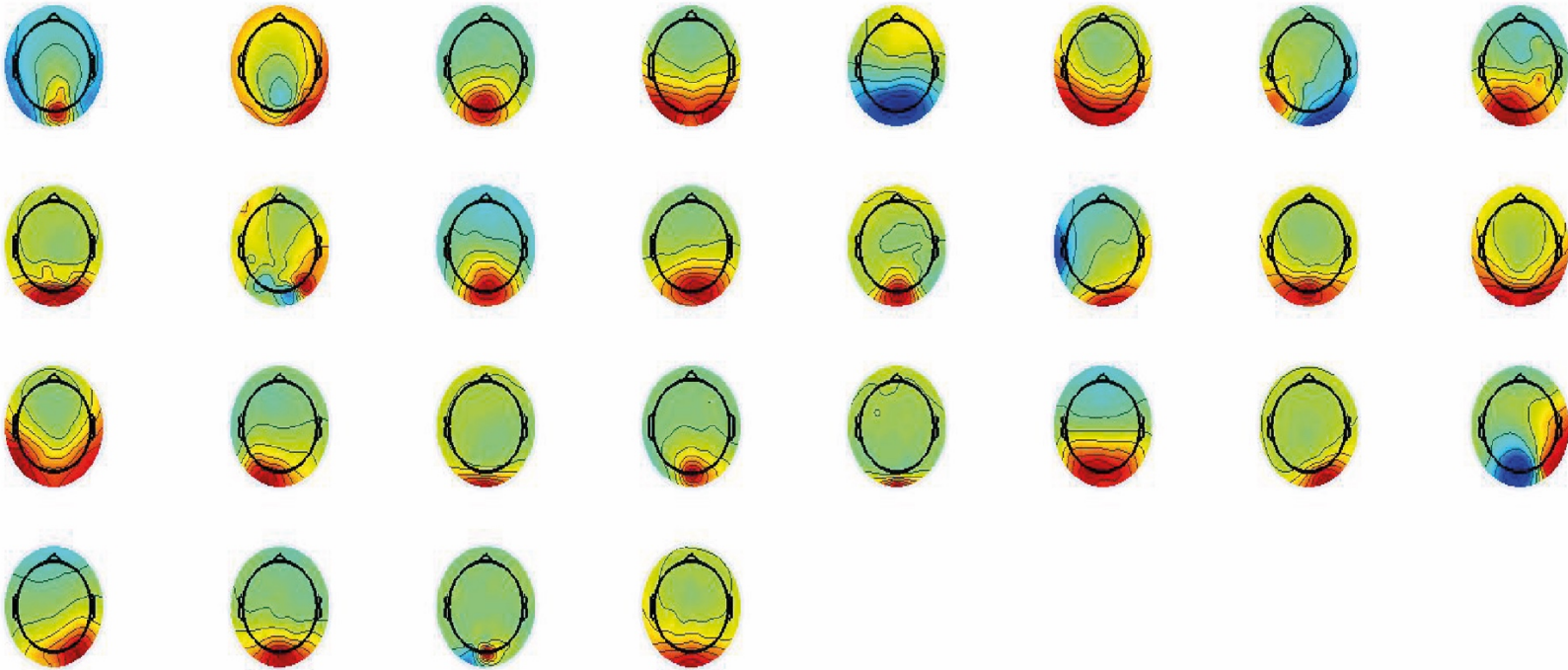
reflection activation of the visual cortex. Scalp maps of the IC with max ITPC chosen for each participant in the ASC group is presented in *Figure 2.6* (also see *Annex 2* for the TD and ADHD max ITPC IC scalp maps). The ERP of the selected components was also examined further confirming that the signal source was at the visual cortex.

Channel selection

Although signal from individual electrodes is known to be more contaminated with noise artefacts as compared to signal from ICs, we conducted supplementary channel analysis and extracted ITPC from an electrode cluster covering the occipital region of the brain. Following a similar approach to the IC selection, for each participant we calculated ITPC for every electrode in the cluster P9, P7, P5, P3, P1, Pz, P2, P4, P6, P8, P10, PO7, PO3, POz, PO4, PO8, O1, O2, Oz, O2, Iz and selected the single electrode with maximum ITPC for further analysis.

Figure 2.6

Independent Components with max ITPC



ASC Group

Figure 2.6: Scalp maps of the Independent Component with maximum ITPC selected for each participant ($n=28$) in the ASC group.

2.2.7 Data analysis

Time-frequency analysis

Time-frequency decomposition of EEG single-trial data was performed using the *newtimef* function of EEGLAB (Delorme & Makeig, 2004). The time series data was convolved with a complex Morlet wavelet, defined as a sinusoid with a Gaussian shape. The wavelet ranged from 3 to 12.5 cycles at 556.56ms intervals. The length of the average vector of the phase angles was computed for 200 evenly spaced time-frequency points, extracted from the epochs and for 47 frequencies, ranging from 4 to 50Hz. The result of the averaging was a complex number, containing information about the length and the angle of the average vector. ITPC, theoretically defined as a measure of how uniform the distribution of phase angles is in the polar space (Cohen, 2014), can be mathematically conceptualized as the absolute value of the averaging of complex vectors:

$$ITPC_p = \left| n^{-1} \sum_{t=1}^n (e^{ik_{pt}}) \right|$$

where n is the number of trials, $e^{ik_{pt}}$ is a complex number representing the position of a phase angle k on trial t at time frequency point p . If the distribution of phase angles is perfectly uniform, therefore less coherent, the average vector will have a length of 0, whereas if phase angles are closely clustered, the average vector will be closer to 1. A single ITPC value, representing the maximum ITPC generated from any independent component or any channel in the electrode cluster of interest at any frequency and at any time point, was extracted for each participant in the TD, ADHD and ASC group and used for group analysis.

2.2.8 EEG data preparation for 1/f noise analysis

2.2.8.1 Data preprocessing

Task-based and resting state data were further preprocessed in preparation for 1/f noise analysis (see *Figure 2.3* for a summary of steps). The preprocessing approach we followed here differs from the approach taken in the preparation of the task-based data for ITPC analysis. Main objective of the ITPC analysis pipeline was to separate the mixed signal and select one source of signal to analyse, whereas primary aim of the 1/f preprocessing analysis is to ensure that the mixed EEG signal is clean and free of noise artefacts so that power spectral estimations are accurate and attributed to brain functions rather than external sources of electrical interference.

Eye- blink components were visually identified from the ICA maps and removed as suggested in the 1/f analysis pipeline followed by Peterson et al. (2017). In order to replace the missing channels, all datasets were interpolated using the channel interpolation function from the EEGLAB gui. Data were then referenced to average reference and segmented into epochs. Task-based data were epoched from -1 to 1.5 secs around stimulus onset and pre- stimulus baseline removal was performed at 1 sec. Resting state data were segmented into 2 secs epochs as suggested in Milne et al. (2019).

2.2.8.2 Data selection

Power Spectral Density estimation

Power Spectral Density (PSD) was computed using the Welch's method (Welch, 1967). The Welch method is preferred over other methods i.e the Bartlett method as it improves the accuracy of the classic periodogram, which is biased towards assuming stationarity in the statistical properties of the signal- the signal in each time window is very rarely a sum of perfectly formed sines and therefore varies immensely. The Welch method minimises this variance by averaging out the spectral content of short windows of signal.

The original time- series data were segmented into blocks with 50% overlap between them. A modified periodogram was then computed for each block using a 2-second Hamming data window. The periodograms for each block were averaged out to produce the final PSD periodogram:

$$PSD = \log_{10} \left(N^{-1} \sum_{n=1}^N 2\tilde{g}'_i{}^2 \right) \quad (1)$$

where N represents the total number of Hamming windows and \tilde{g}' refers to the consecutive segmented windows of the original signal g' , transformed using the Discrete Fourier Transform (DFT).

A linear regression line was fitted to the data to model an inversely proportional relationship

between PSD and frequency, of the form $P_f = k \frac{1}{f^\alpha}$, where P_f is the power spectra per frequency interval f , k is a random constant and α is the scaling exponent:

$$P_f = k \frac{1}{f^a}$$

$$\log P_f = \log \frac{k}{f^a} \quad (1)$$

$$\log P_f = \log k - a \log f$$

$$\log P_f = -a \log f + c \quad (2)$$

Power spectra was plotted in log coordinates (Eq. 1). As shown above, the log- transform of the power function is a straight line with a negative slope α and an intercept c (Eq. 2, *Figure 2.7*, also see *Annex 3* for the slope of all electrodes as computed from Participant 6). It is important to note that 1/f slopes of PSD were estimated from frequencies between 2- 24Hz (Voytek et al., 2015). High frequency bands were excluded from the analysis, as they are more likely to reflect intrinsic channel noise, rather than neural processes. Alpha band power (7-14Hz) was also excluded as it represents changes in periodic EEG patterns, biasing estimations of the non-periodic properties of the signal i.e. 1/f noise (Voytek et al., 2015).

Figure 2.7

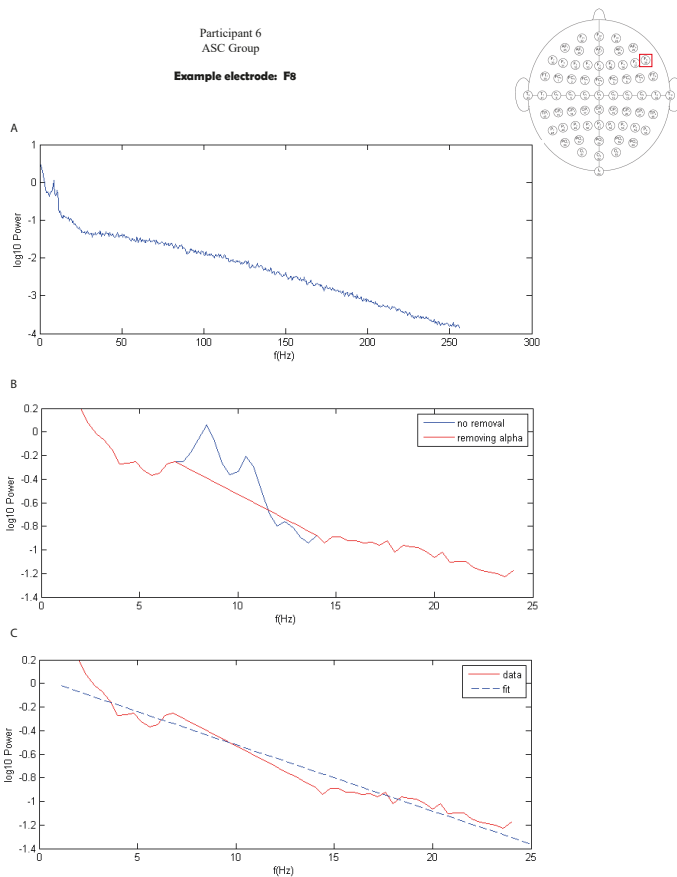


Figure 2.7: Log- transformed Power Spectral Density (\log_{10} Power) of signal coming from a single electrode F8, is presented here as a function of frequencies (f) ranging from A) 0-250Hz, B) 2-24 Hz including alpha band and C) 2-24 Hz excluding alpha band. A regression line with a negative slope $a = -0.056175$ is fitted to the data in graphs B and C.

2.2.9 Data analysis

A single value representing the 1/f slope of PSD at each electrode was first calculated for all electrodes and for all participants in the three groups, TD, ADHD, ASC. We followed two methods of preparing the data for group comparisons to be able to check and cross-validate the consistency of the findings. The first method involved computing the mean slope of all 64 electrodes for every participant and then calculating and comparing the grand mean slope for each group, TD, ADHD and ASC (*Figure 2.8*). However, such analysis is likely to mask location-specific group differences that may exist. Similarly, cluster specific analysis would require some arbitrary selection of electrode clusters to compare, which is also likely to mask other underlying location-specific differences. To deal with this problem, we followed a second method of analysing the data. The second method involved computing the mean slope for each electrode in one group, by adding the channel specific slopes, and comparing it to the mean slope of the same electrode in the other group, a process resulting in 192 electrode-specific slope comparisons in three pairs of groups, ADHD vs ASC, ADHD vs TD and ASC vs TD group (*Figure 2.9*).

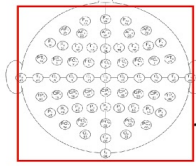
2.2.10 Statistical analysis

We utilised frequentist methods of hypothesis-testing throughout the present chapter. Frequentist statistics were conducted using IBM SPSS Statistics for Windows, version 25 (IBM Corp., Armonk, N.Y., USA). In the group comparisons of the key variables of interest ITPC and 1/f slopes- where appropriate and possible- Bayesian statistical analysis was also performed alongside frequentist statistical analysis (see Sections 2.3.1 and 2.3.2) using the free software JASP (JASP Team, 2017). This allowed us to evaluate with greater certainty which of the two hypotheses i.e the null hypothesis H_0 or the alternative hypothesis H_1 is more likely given the *experimental data* (H_0 : there is no overall group difference, H_1 : there is overall group difference). Bayes factors (BF) assessing the strength of evidence were presented, with 1-3 indicating weak evidence, 3-10 indicating moderate evidence and Bayes factors >10 indicating strong evidence in favour of H_1 (van Doorn et al., 2020). In the Bayesian ANCOVA analysis specifically, the inclusion probability of each component (i.e., model term) was computed across a number of different models; a) the null model, b) a model containing a single predictor variable and c) a model containing both predictor variables. The Bayes factor BF_M indicating the change from prior to posterior model odds is reported as well as the effect size for each predictor.

Figure 2.8

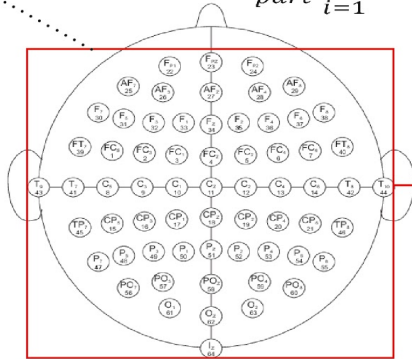
Method 1

$$\bar{x}_{Slope} = \frac{1}{n_{electr}} \sum_{i=1}^n x_i$$



Participant 1
n_{electr}= 64

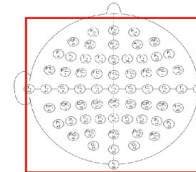
$$\bar{y}_{Slope} = \frac{1}{n_{part}} \sum_{i=1}^n y_i$$



Participant i
n_{part}= 32

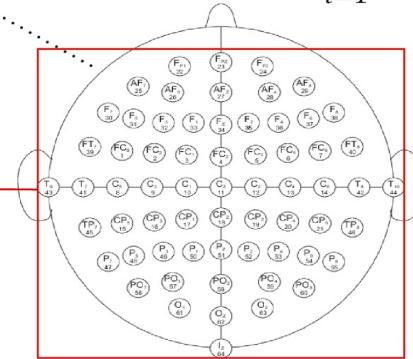
ADHD Group

$$\bar{x}_{Slope} = \frac{1}{n_{electr}} \sum_{i=1}^n x_i$$



Participant 1
n_{electr}= 64

$$\bar{y}_{Slope} = \frac{1}{n_{part}} \sum_{i=1}^n y_i$$



Participant i
n_{part}= 34

TD Group

**Comparison of
grand mean slopes**

Figure 2.8: Method 1 involved a) computing the mean slope of all 64 electrodes for every participant, b) calculating the grand mean slope for each group and c) comparing the grand mean slopes. Here we present the comparison between the ADHD and the TD group.

Figure 2.9

Method 2

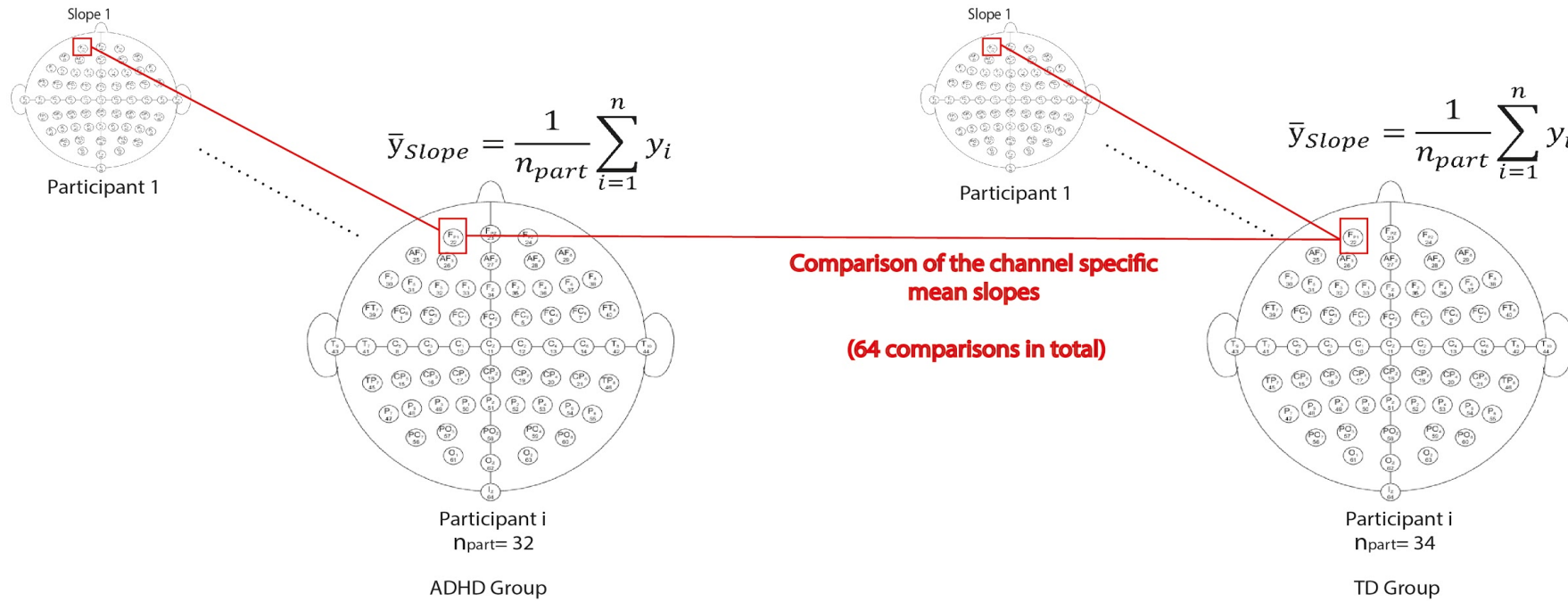


Figure 2.9: Method 2 involved a) computing the mean slope for each electrode in one group and b) comparing it to the mean slope of the same electrode in the other group. Here we present the comparison between the ADHD and the TD group.

2.3 Results

2.3.1 Group comparisons: Inter- Trial Phase Coherence

Independent Component Analysis

Descriptive statistics for the three groups are presented in *Table 2.5*.

Table 2.5

Mean values (M) and Standard Deviations (SD) of the max ITPC extracted from the Independent Components presented for the three groups ADHD, ASC and TD

	TD (n=34)		ADHD (n=32)		ASC (n=28)	
	<i>M</i>	<i>SD</i>	<i>M</i>	<i>SD</i>	<i>M</i>	<i>SD</i>
Max ITPC ^a	0.92	0.03	0.92	0.04	0.88	0.08

^aMax ITPC, Maximum Inter-Trial Phase Coherence extracted from the Independent Components

Parametric test assumptions such as the requirement of observations to be independent and the data to be normally distributed were met, however Levene's test for equality of variances showed that the three groups were characterized by unequal variances (see *Figure 10*, $F(2,91)=7.09$, $p=0.00$). Although extreme outliers were not present, ITPC values for two participants within the ASC group were falling below the interquartile range of the third quartile (*Figure 10*). ANCOVA-specific assumptions of the independence of the covariate (i.e lack of interaction between the "age" variable and the "group" variable) as well as the homogeneity of regression slopes were met.

A one-way ANCOVA was performed to assess whether the means of maximum ITPC are equal across groups, while also adjusting for age differences. The result showed that there were statistically significant differences in ITPC between the three groups after controlling for age effects ($F(2,90)=2.99$, $p=0.03$). However, further analysis showed that the two outliers in the ASC group had a significant impact on the group comparisons outcome. When the outliers were removed from the ANCOVA analysis, the significant result disappear ($F(2,89)=1.42$, $p=0.14$), therefore we do not consider this to be strong evidence for a group difference. Average maximum

ITPC maps computed separately for the TD, ADHD and ASC group are presented in *Figure 2.11* (also see *Annex 4* for maximum ITCP heat maps for all participants in the three groups).

Alongside frequentist statistics, we performed Bayesian analysis of covariance on ITPC values, including “group” as a fixed factor and “age” as a covariate. The Bayesian ANCOVA compared a few models with varying predictors of ITPC: a) a null model, b) a model containing only “age” as a predictor, c) a model containing only “group” as a predictor and d) a model containing both “group” and “age” as predictors. Only the null model had their model odds increased after observing the data ($BF_M = 3.6$). Analysis of effects demonstrated that the data were only 0.4 times more likely under models containing “group” as a predictor and 0.2 times as likely when including “age”. This is evidence in favour of the null hypothesis H_0 , in line with frequentist statistics, which demonstrated that the differences between groups were not significant when the outliers were removed from the analysis.

Figure 2.10

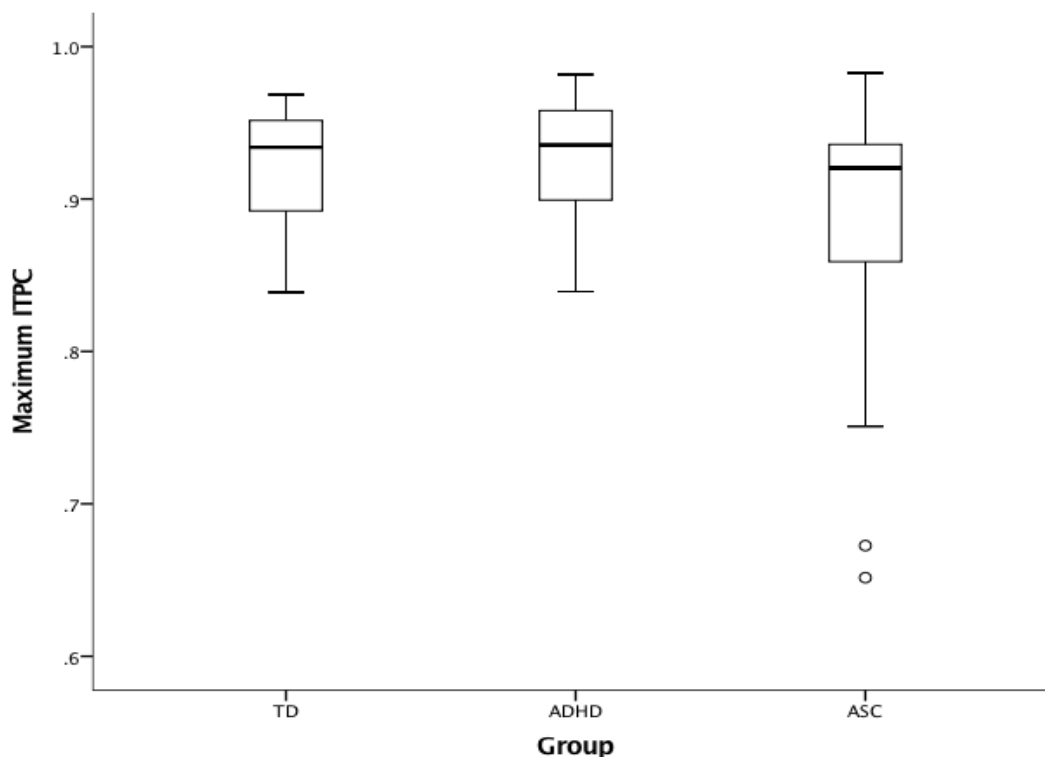


Figure 2.10: Boxplots of maximum ITPC for the three groups, TD, ADHD and ASC (range of values= 0-1), showing differences in central tendency between groups.

Figure 2.11

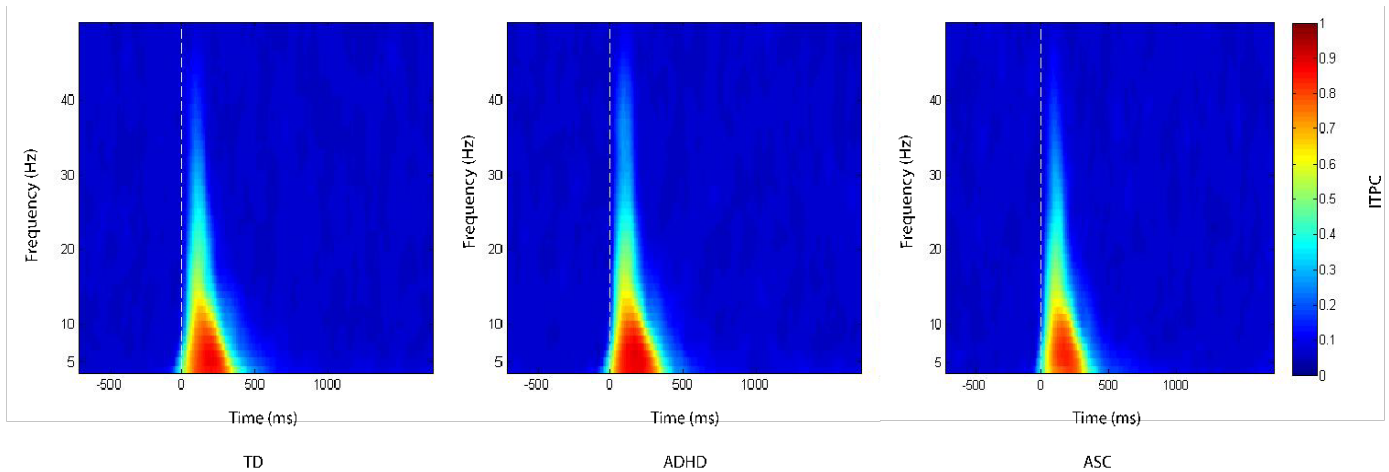


Figure 2.11: Average maximum ITPC maps computed for the TD, ADHD and ASC group.

Maximum ITPC extracted from the Independent Components was observed primarily in the theta band (4-7Hz) for all groups (Figure 2.12). Maximum ITPC for the ADHD group occurred at 4Hz for the majority of participants (43%) and for the ASC group it covered a wider range of frequencies compared to the TD group. However, the differences between groups were not significant as determined by a one-way ANOVA ($F(2,91)=1.01, p=0.36$). Bayes factors indicated that the data were about 4.66 times more likely under the null hypothesis H_0 than under the alternative hypothesis H_1 . This is strong evidence in favour of the null hypothesis and is in line with the results of frequential analysis.

Figure 2.12

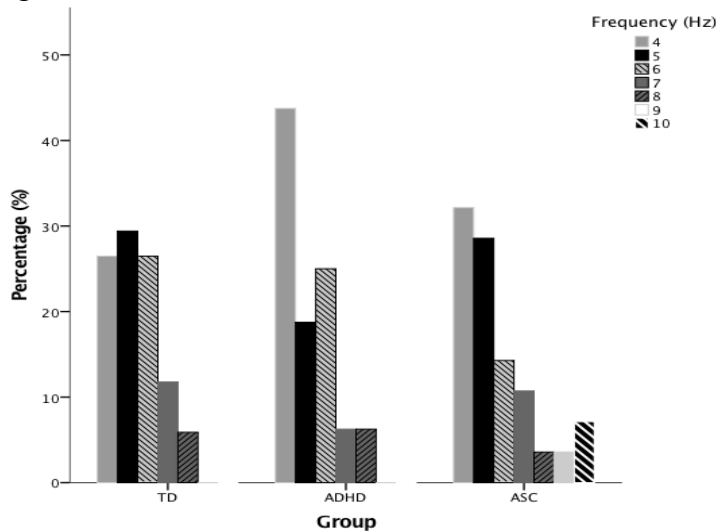


Figure 2.12: Frequency (Hz) where maximum ITPC was observed for each group, TD, ADHD, ASC

Channel Analysis

Descriptive statistics for the three groups are presented in *Table 2.6*.

Table 2.6

Mean values (M) and Standard Deviations (SD) of the max ITPC extracted from the occipital electrode cluster, presented for the three groups TD, ADHD and ASC

	TD (n=34)		ADHD (n=32)		ASC (n=28)	
	<i>M</i>	<i>SD</i>	<i>M</i>	<i>SD</i>	<i>M</i>	<i>SD</i>
Max ITPC ^a	0.83	0.09	0.86	0.06	0.82	0.09

^aMax ITPC, Maximum Inter-Trial Phase Coherence extracted from the Independent Components

Inspection of the ITPC distributions showed that the data were approximately normally distributed for the ADHD and ASC groups but not for the TD group, further confirmed by Shapiro-Wilk tests for normality (TD: $W(34)=0.92, p=0.01$, ADHD: $W(32)=0.94, p=0.09$, ASC: $W(28)=0.93, p=0.06$). Efforts to square root-transform the ITPC distributions did not change the normality test results (TD: $W(34)=0.91, p=0.00$, ADHD: $W(32)=0.94, p=0.09$, ASC: $W(28)=0.93, p=0.06$). Additionally, Levene's test for equality of variances showed that the three groups were characterised by unequal variances ($F(2,91)=4.45, p=0.01$). Data distributions are presented in the form of boxplots in *Figure 2.13*. ANCOVA-specific assumptions were met; regression slopes in the three groups were homogeneous and the variable of "age" was independent from the categorical predictor variable "group".

A one-way ANCOVA was performed to assess whether maximum ITPC extracted from the selected electrodes differs across groups, while also adjusting for age. The model did not indicate a statistically significant effect of "group" on levels of ITPC, therefore it is concluded that there are no differences in ITPC between the three groups ($F(2,90)=1.34, p=0.26$). Additionally, this analysis showed that age effect was negligible ($F(2,90)=1.36, p=0.24$). The above result was in agreement with Bayesian analysis of covariance on ITPC values with "group" added as a fixed factor and "age" as a covariate. This showed that only the null model had its model odds increased after observing the data ($BF_M=4.01$).

Figure 2.13

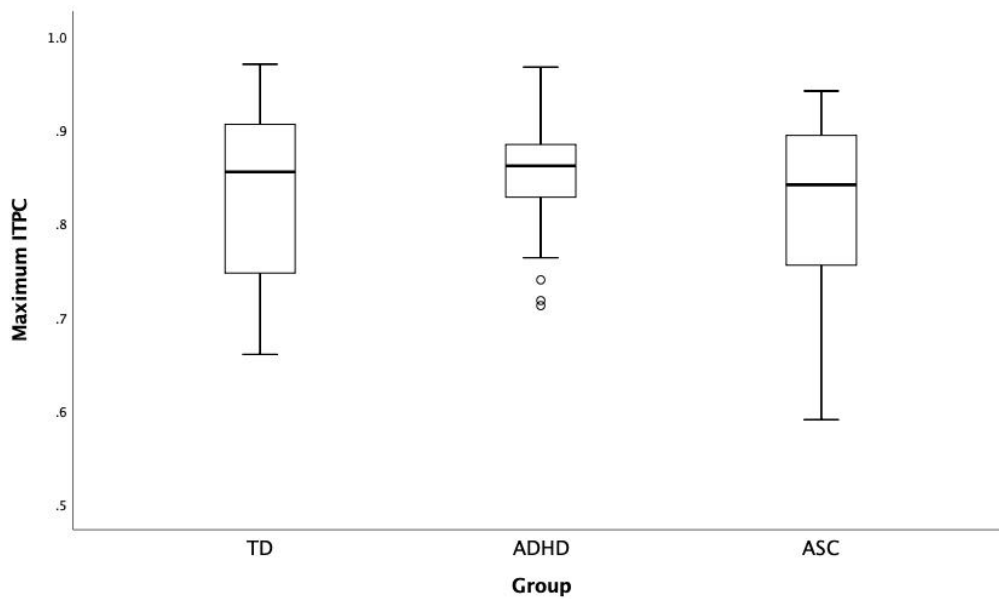


Figure 2.13: Boxplots of maximum ITPC for the three groups, TD, ADHD and ASC (range of values= 0-1), showing differences in central tendency between groups.

For all three groups, maximum ITPC was observed at the electrode Oz out of the electrode cluster P9, P7, P5, P3, P1, Pz, P2, P4, P6, P8, P10, PO7, PO3, POz, PO4, PO8, O1, O2, Oz, O2, Iz (TD: 56%, ADHD: 38%, ASC: 39%) and in the theta (4-7Hz) frequency band (TD: 91%, ADHD: 79%, ASC: 75%) (Figure 2.14, Figure 2.15). For the TD group, maximum ITPC occurred at 4Hz for the majority of participants (47%), whereas for the ADHD group, it occurred at 5 Hz (35%). For the ASC group, it covered a wider range of frequencies compared to the TD and ADHD groups, ranging from low theta to high alpha. A one-way ANOVA showed that the frequency where maximum ITPC is captured is not significantly different in the ASC group as compared to the TD and ADHD group ($F(2,91)=1.65, p=0.19$). In line with those results, Bayes factors indicated that the data were about 2.88 times more likely under the null hypothesis H_0 than under the alternative hypothesis H_1 , providing moderate evidence in favour of the null hypothesis (i.e there are no differences between groups).

Figure 2.14

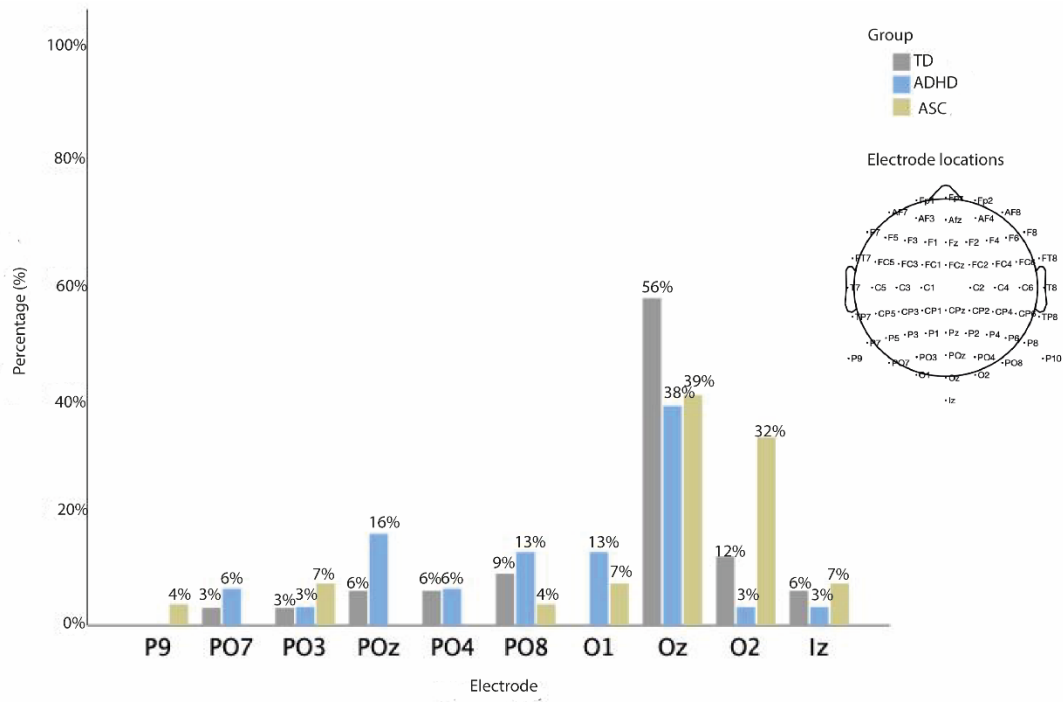


Figure 2.14: Electrode where maximum ITPC was captured for each group, TD, ADHD, ASC.

Figure 2.15

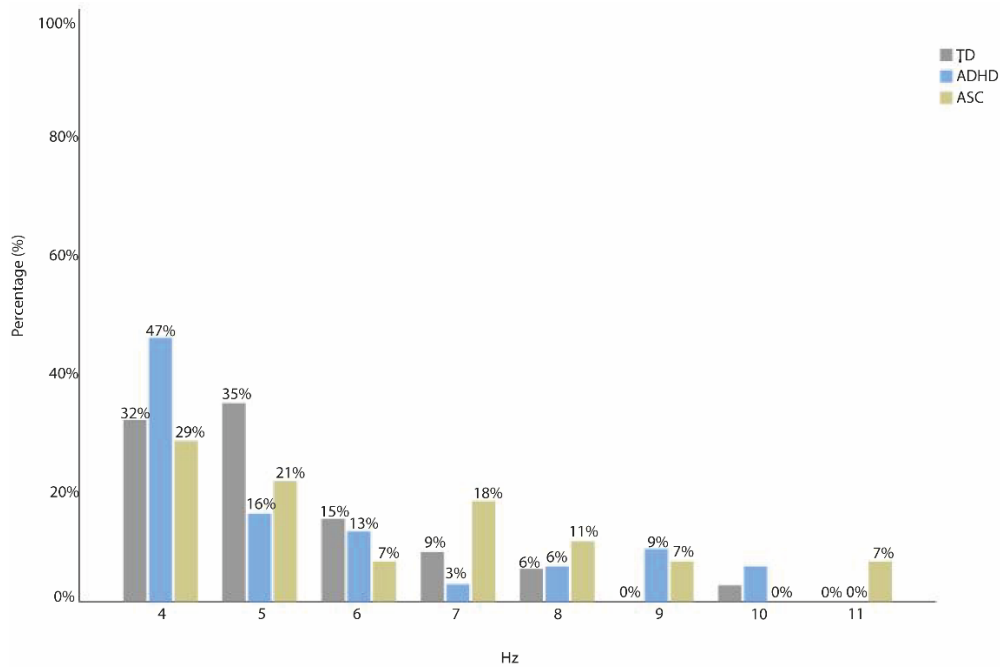


Figure 2.15: Frequency (Hz) where maximum ITPC was observed for each group, TD, ADHD, ASC.

2.3.2 Group comparisons: 1/f noise of Power Spectral Density

2.3.2.1 Method 1

Descriptive statistics of the 1/f slope of PSD were computed for the three groups TD, ADHD and ASC. A summary is presented in *Table 2.7*.

Table 2.7

Mean values (M) and Standard Deviations (SD) of the 1/f slope of PSD, computed for the three groups TD, ADHD and ASC

	TD (n=34)		ADHD (n=32)		ASC (n=28)	
	<i>M</i>	<i>SD</i>	<i>M</i>	<i>SD</i>	<i>M</i>	<i>SD</i>
Task- based EEG: Slope	-0.037	0.016	-0.036	0.016	-0.040	0.013
Resting- state EEG: Slope	-0.038	0.020	-0.037	0.018	-0.041	0.016

Outliers- observations within the inner and outer lower fence of the boxplot- were detected in both the task-based and resting-state data (see *Figure 2.16*). For that reason, parametric test assumptions and results were computed with and without the outliers. The outlier data points did not affect the assumptions and parametric test results; therefore, the analysis presented below includes these. Data was normally distributed as shown by the Shapiro-Wilk test in both the task-based (TD: $W(34)=0.97$, $p=0.58$, ADHD: $W(32)=0.97$, $p=0.56$, ASC: $W(28)=0.98$, $p=0.90$) and the resting-state condition (TD: $W(34)=0.95$, $p=0.12$, ADHD: $W(32)=0.97$, $p=0.49$, ASC: $W(28)=0.98$, $p=0.91$). The three groups had equal variances as determined by the Levene's test (Task-based Condition: $F(2,90)=0.18$, $p=0.83$, Resting-state Condition: $F(2,90)=0.38$, $p=0.68$).

Given that the data satisfied the assumptions of independence of observations, normality and homogenous variance, parametric methods of hypothesis-testing were used. In the task-based condition, a one-way ANCOVA with age added as a covariate in the linear model, revealed no significant differences in 1/f slope between the TD, ADHD and ASC group ($F(2,90)=0.64$, $p=0.52$) (*Figure 2.16*). Similar analysis in the resting- state condition, revealed that there is no difference in the steepness of 1/f slope between groups ($F(2,90)= 0.40$, $p=0.67$) (*Figure 2.16*). However, as expected, age was found to be significantly interacting with 1/f slope in both the task-based ($F(1,90)=15.41$, $p=0.00$) and the resting-state condition ($F(1,90)=11.15$, $p=0.00$).

In line with the above findings, Bayesian analysis indicated that only models containing “age” as a predictor had their model odds increased in presence of the experimental data (Task-based condition: $BF_M = 17.84$, Resting state condition: $BF_M = 16.92$). Analysis of effects demonstrated that in the task-based condition the data were 134.7 times more likely under models containing “age” as a predictor but only 0.16 times as likely when including “group”. Similarly, in the resting state condition the data were 25.36 times more likely under models containing “age” as a predictor but only 0.13 times as likely when including “group”. This is in agreement with frequentist statistics, which demonstrated that the effect of “age” was large and that the main effect of “group” on “1/f slope” was not significant. Scalp maps representing the 1/f slope measured from all electrode locations for the three groups in the two conditions, task-based and resting state, are presented in *Figure 2.17*.

Figure 2.16

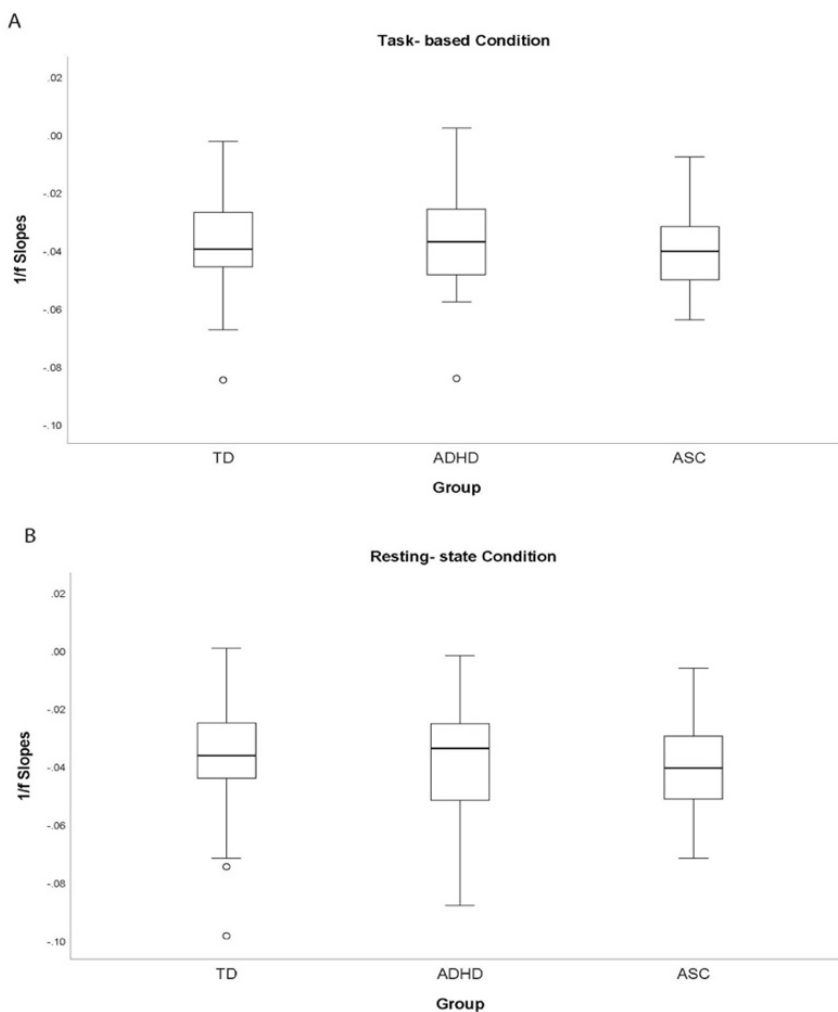


Figure 2.16: Boxplots of 1/f slopes for the three groups, TD, ADHD and ASC, showing central tendency group differences in the task-based (A) and resting-state condition (B).

Figure 2.17

1/f slopes

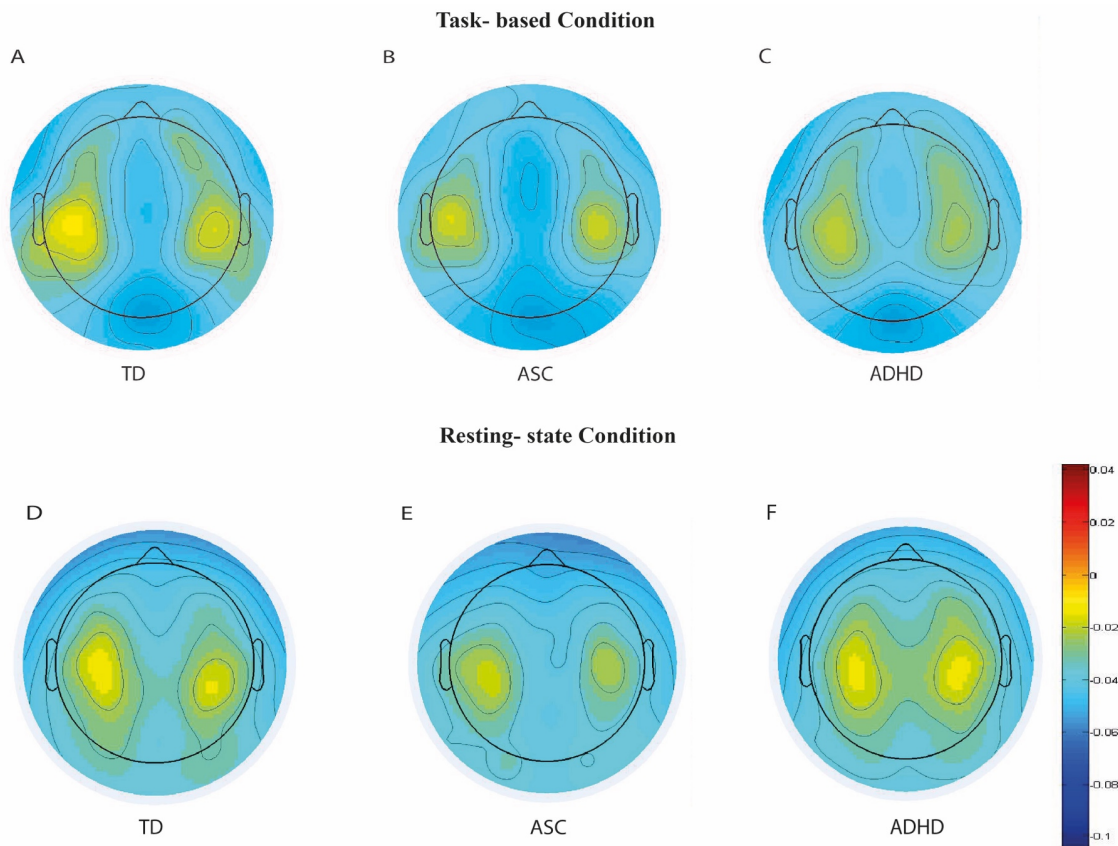


Figure 2.17: Scalp maps representing the mean slope computed from different electrode locations for the TD (A), ASC (B) and ADHD (C) group in the task-based condition and for the TD (D), ASC (E) and ADHD (F) group in the resting-state condition.

2.3.2.2 Method 2

64 independent samples t-tests were performed comparing individual electrode slopes between the ADHD and TD group, ASC and TD group, ADHD and ASC group in both the task-based and resting-state conditions (192 tests in total for all groups and all conditions). This process generated 192 raw p-values, which did not cross the 0.05 significance cut-off (Figure 2.18). Multiple comparisons are known to increase the probability of Type I error and the observation of false positives. To ensure that the above result is robust, we controlled for the False Discovery Rate (FDR) by implementing the Benjamini-Hochberg procedure (1995). We compared each individual p value to its Benjamini-Hochberg critical value, $(i/m)Q$, where i is the rank, m is the total number of tests, and Q is the FDR value set at 0.05. Following the Benjamini-Hochberg procedure, none of the raw p-values approached significance.

Figure 2.18

Uncorrected p- values

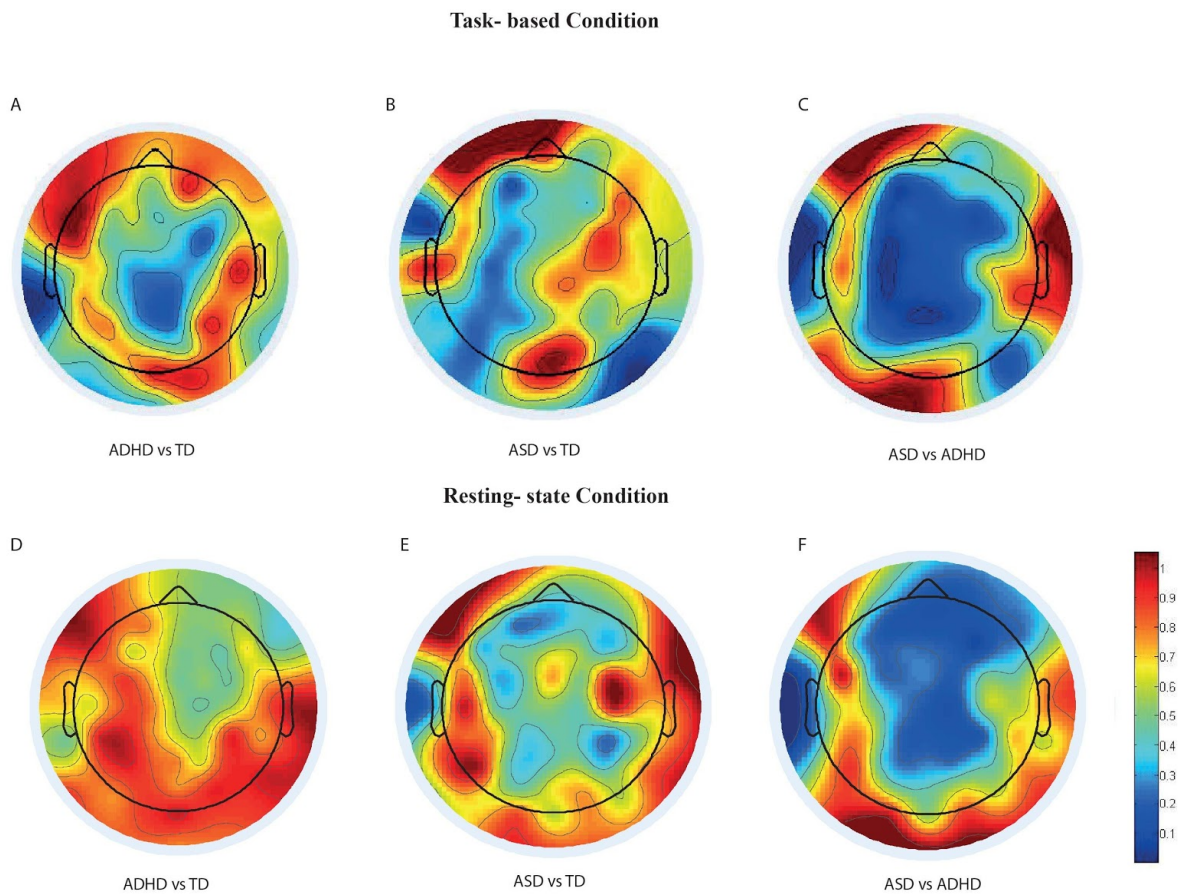


Figure 2.18: Scalp maps representing uncorrected p-values produced from the comparison of individual electrode slopes in the ADHD vs TD group (A), ASD vs TD group (B), ASD vs ADHD group (C) in the task- based condition and the ADHD vs TD group (D), ASD vs TD group (E), ASD vs ADHD group (F) in the resting- state condition.

2.3.3 Association between age and ITPC

Spearman's rank-order correlation analysis was performed to determine the relationship between age and ITPC (*Figure 19*). The correlation analysis was performed a) for all participants and b) the three groups TD, ASC and ADHD separately. Age and ITPC were not found to be associated in the full sample ($r_s=0.08$, $p=0.40$). Similarly, the two variables were not correlated in the TD ($r_s=0.23$, $p=0.18$), ASC ($r_s=0.02$, $p=0.88$) and ADHD group ($r_s=0.08$, $p=0.66$).

Figure 2.19

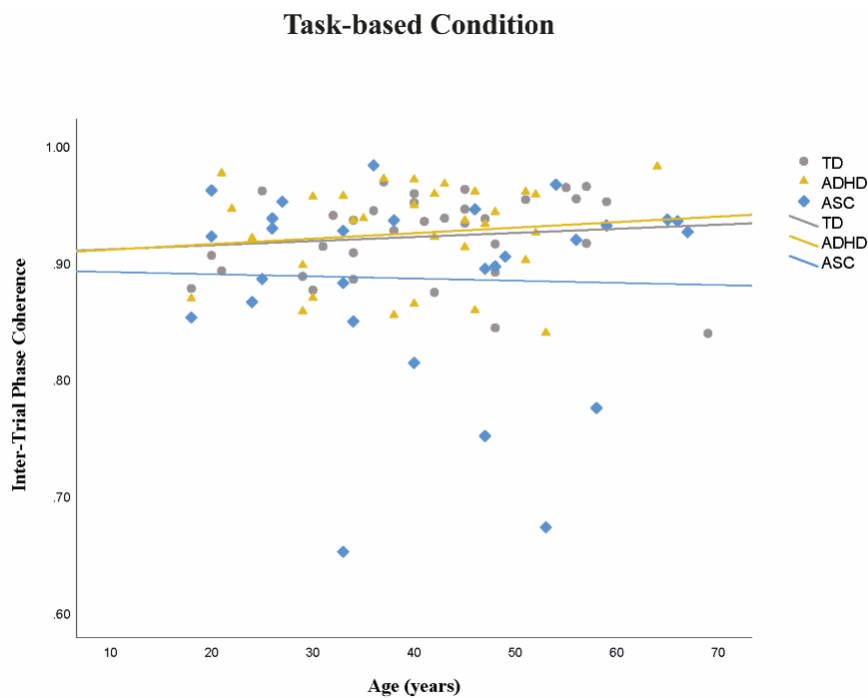


Figure 2.19: Scatterplot of age and maximum ITPC computed from the task-based data and plotted for the TD, ADHD and ASC group.

2.3.4 Association between age and 1/f slope of PSD

Spearman's rank-order correlation analysis was performed to determine the relationship between age and the average 1/f slope of PSD computed from the task-based and the resting state data using *Method 1* (Figure 2.20). In the task-based condition, age and 1/f slope were correlated in the full sample ($r_s=0.35, p=0.00$). Further analysis showed that the two variables were highly correlated in the TD ($r_s=-0.51, p=0.00$) and the ADHD group ($r_s=0.54, p=0.00$) but not the ASC group ($r_s=-0.00, p=0.99$). In the resting state condition, age and 1/f slope of PSD were correlated in the full sample ($r_s=0.29, p=0.00$). When the full sample was split into groups, the two variables were found to be correlated in the TD ($r_s=0.43, p=0.01$) and the ADHD group ($r_s=0.42, p=.01$) but not the ASC group ($r_s=0.03, p=0.84$).

Figure 2.20

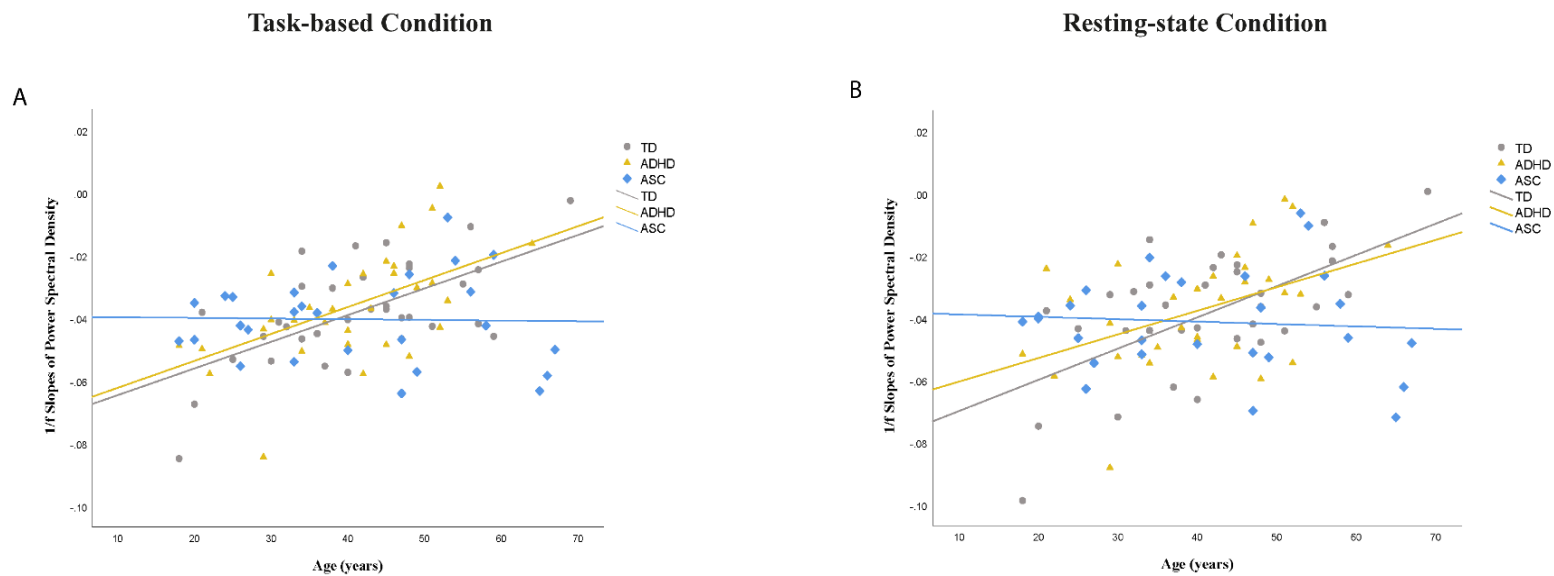


Figure 2.20: Scatterplots of age and average 1/f slope of PSD computed from the task-based (A) and resting state data (B) and plotted for the TD, ASC and ADHD groups.

2.3.5 Association between ITPC and 1/f noise

Spearman's rank-order correlation analysis was performed to determine the relationship between ITPC and 1/f noise of PSD (*Figure 2.21*). The two variables ITPC and the mean slope of PSD computed from all participants ($n=94$) in the task- based condition using *Method 1*, were not found to be correlated ($r_s=0.05, p=0.59$).

Figure 2.21

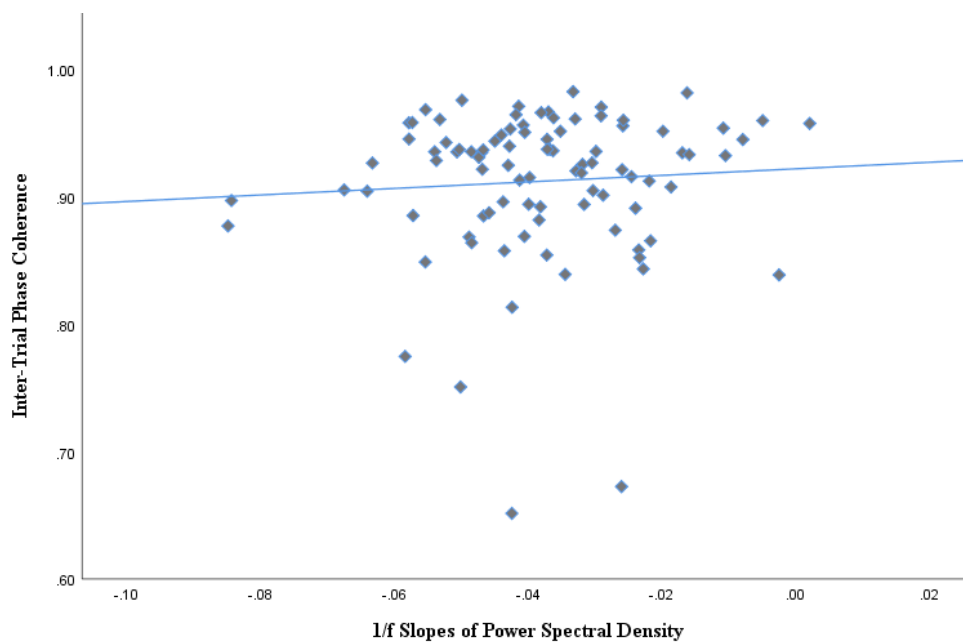


Figure 2.21: Scatterplot of ITPC and 1/f mean slope of PSD computed from individual channels for all participants ($n=94$).

It is important to note that, in the above analysis, the source of signal for the 1/f noise slopes was individual channels (see *Method 1*). To ensure this result is robust, 1/f slope of PSD was also computed from the independent component identified to have maximum ITPC for each participant and was compared to the ITPC values extracted, as above. This analysis step confirmed that the ITPC and 1/f slopes of PSD are not correlated ($r_s=0.01, p=0.86$) (*Figure 2.22*).

Figure 2.22

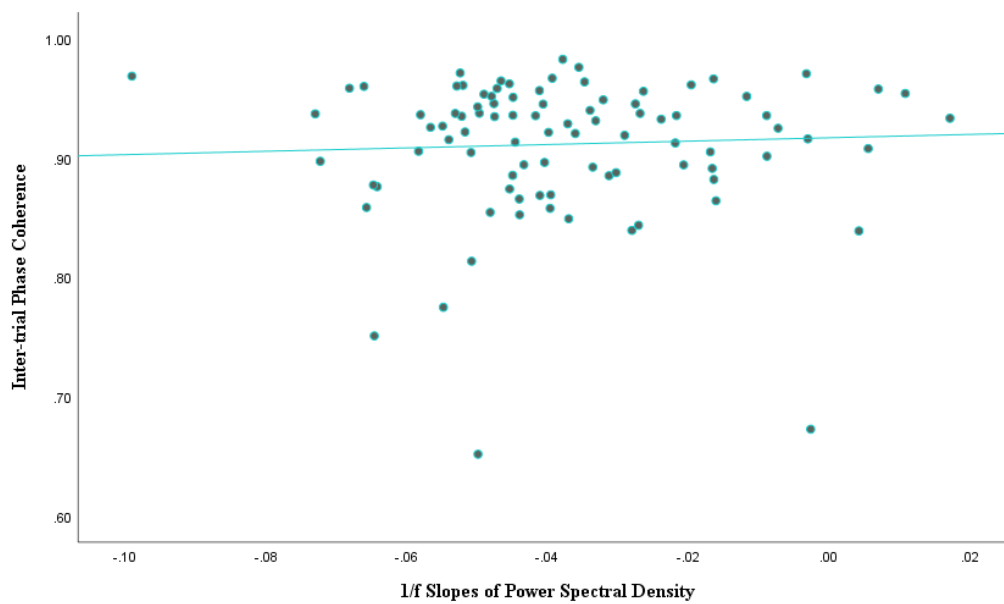


Figure 2.22: Scatterplot of ITPC and 1/f mean slope of PSD computed from Independent Components for all participants ($n=94$).

2.4 Discussion

The primary aim of this study was to establish whether adults with ASC and adults with ADHD demonstrate similar or different levels of neural noise, in the form of neural variability, compared to typically developing adults. Neural variability was measured by computing ITPC and 1/f slope of PSD in a visual task condition, involving the presentation of checkerboard stimuli. 1/f slope was also computed in a resting ‘eyes-closed’ condition. In the task-based condition, we did not observe significant differences between groups in levels of maximum ITPC as extracted from selected ICs and selected occipital electrodes. Maximum ITPC was primarily observed in the theta band for all groups, but for the ASC group it covered a wider range of frequencies. In addition, 1/f slope of PSD did not differ between the ASC, ADHD and TD group in the task-based condition. When neural variability was examined in the ‘eyes-closed’ condition, the steepness of the 1/f slope was also found to be similar across groups. The strength of association between age and neural variability as measured by ITPC and 1/f noise of PSD was also examined. The two variables were found to be associated in the TD and the ADHD group but not the ASC group. Finally, the strength and direction of association between ITPC and 1/f slope of PSD was assessed. No association between the two variables was found and therefore it was concluded that ITPC and 1/f slope of PSD are not related.

It is important to note that in the present study adults with ASC exhibited similar levels of ITPC to the ADHD and TD adult samples. This finding is in line with previous reports of no difference in ITPC between the ASC and the TD group (Butler et al., 2017) but does not agree with other research efforts which document reductions in ITPC locally in the visual cortex of adults and children with ASC (Milne, 2011; Weinger et al., 2014; Milne et al., 2019). In a similar study design, Milne (2011) found lower alpha ITPC during visual processing of Gabor patches in children and adolescents with ASC. Using a slightly different analytical approach but similar stimulus characteristics (i.e check patterns), Weinger et al. (2014) showed reduced SNRs in electrophysiological responses of children with ASC, computed from steady state visual evoked potentials. On the other hand, EEG studies such as the one conducted by Butler et al. (2017), in an effort to replicate the study by Milne (2011), do not report differences in levels of ITPC between groups, as extracted from selected ICs. Given the small sample sizes ranging from 11-22 participants for the above studies and the issue of ASC heterogeneity, these inconsistencies in existing published work are not surprising; underpowered studies are known

to have a reduced chance of detecting a true effect and there is also a reduced likelihood that a statistically significant result reflects a true effect (Button et al., 2013). Taken together, the present study showed that neural variability in the form of low ITPC is not increased in adults with ASC, a finding speaking against accounts of phase-alignment difficulties and disrupted interregional synchrony during visual processing in ASC. Nevertheless, given that outliers determined the group comparisons outcome, this finding should be interpreted with caution and further replication is necessary to consolidate those results.

To our surprise, the study of Milne et al. (2019)- which shares 71% of the ASC data with the present study but includes a different TD cohort- report significant differences in levels of ITPC between adults with a diagnosis of ASC and TD adults, in contrast to the findings presented here. Although the methodological approach of extracting ITPC in the two pieces of work was identical and subsequent unpublished analysis indicated that inter-rater reliability was high, the inclusion of additional 16 participants with ASC in the ASC group and a different control group substantially influenced the outcome of the group comparisons. This difference further demonstrates that low statistical power in the present study may have increased the probability of Type II error.

The above finding also suggests that reduced ITPC is not possible to accurately differentiate participants with ASC from participants without ASC. Therefore, ITPC lacks the necessary specificity and sensitivity to be used as a diagnostic tool. In extension to this, it is unlikely that it can serve as a valid endophenotype of the condition, as suggested by David et al. (2016). Efforts to detect endophenotypes or neural signatures of ASC assume that there is a single, independent pathophysiological mechanism in the brain with clear genetic connections, which is altered in the affected individuals. Yet, current understanding of how psychiatric conditions occur, suggests that behavioural manifestations of such disorders are very rarely the result of a single disease process but rather, they arise from multi- factorial gene- environment interactions resulting in heterogeneous behavioural profiles (Beauchaine & Constantino, 2017). Behavioural manifestations of autism are attributed to multiple genetic and environmental etiologic factors (Amaral, 2017); therefore, it is unlikely that there is a single pathophysiological route to the large range of phenotypic expressions in ASC. Linked to this, recent advances in autism research speak against a single neural profile underlying ASC (Milne

et al., 2019); multiple authors recognize the existence of sub-groups within the autism spectrum with clear neurological differences (Ousley & Cermak, 2014).

In the present study, maximum ITPC was primarily observed at electrodes O2 and Oz and, for both channel and IC analyses, the strongest ITPC was captured primarily in the theta band for the majority of participants. Multiple lines of work suggest that theta band oscillations facilitate sensory encoding. The phase of theta oscillations, in particular, is shown to act as an endogenous “clock”, able to partition spike trains efficiently and provide a temporal reference point in the oscillatory cycle signaling a dynamic change in the sensory environment i.e the onset of an event (Kayser, Ince & Panzeri, 2012). In addition, animal studies have demonstrated that visual stimulation triggers strong phase-locking of theta oscillations locally in early visual areas such as V1 and V2 through to V4, which receives feedforward input from V1/V2 (Spyropoulos, Bosman & Fries, 2018; Kienitz et al., 2021). Studies have also shown that strong phase-locking to the theta rhythm in visual cortices is coupled with an increase in gamma amplitude (Canolty et al., 2006), allowing for information to travel through the visual hierarchy and reach higher-order areas (Fries, 2015). Considering the above, strong trial-to-trial phase-locking in the theta band of the visual cortices may occur in order to facilitate long-range communication.

Other lines of work posit that theta oscillations facilitate episodic memory formation through the integration of sensory representations from different sensory modalities (Herweg et al., 2020). In support of this hypothesis, Klimesch et al. (2004) demonstrated that increased phase-locking in the occipital and parietal electrode sites (O2 and P4 electrodes) is associated with the P1 and N1 ERP components and is linked to memory performance. From that perspective, strong theta phase-locking in the visual cortex, may be providing a mechanism that allows for the synchronous activation of the hippocampal circuitry, responsible for forming memory associations between sequential visual inputs (Hasselmo et al., 2002).

In the ASC group, maximum ITPC was observed in a wide range of frequencies, from low theta to high alpha. This is in contrast to the TD and ADHD participants, whose strongest phase-locked activity trial-on-trial was concentrated in the theta band alone. Alpha oscillations are proposed to play a critical role in the gating information flow to sensory cortices by selectively suppressing task-irrelevant input, thereby facilitating processing of task-relevant input (Jensen & Mazaheri, 2010; Palva & Palva, 2011). Studies in typically developing

populations have shown that top-down attentional influences, in anticipation of an expected stimulus, modulate the phase of ongoing alpha oscillations and shift it so that it is at an optimal point in the cycle at the arrival of the stimulus (Tallon-Baudry et al., 1996; Klimesch, Sauseng & Hanslmayr, 2007; Jensen & Mazaheri, 2010; Bennefond & Jensen, 2012). It is therefore plausible that in some participants, top-down attentional influences are greater, reflected in stronger ITPC of alpha rhythms locally.

When the steepness of $1/f$ slope of PSD was examined, we did not find a difference in $1/f$ slope of PSD across the three groups. The above result contradicts Voytek and Knight's theory about pathological undercoupling in ASC, which was suggested to reflect weakened interregional oscillatory coherence in the clinical group. This is a surprising finding, particularly given the large number of studies pointing towards disrupted short-range and long-range synchronous activity in the brain of individuals with ASC.

Our effort to understand the nature of those disruptions generates discussion about what underlying neural processes may be captured by background $1/f$ noise dynamics and raises important questions about what the best method of conceptualising neural noise might be. Further analysis showed that the two variables used here to index neural noise, ITPC and $1/f$ slope of PSD, are not associated, which indicates that they may be measuring two different constructs. Indeed, it can be argued that $1/f$ slope of PSD is computed by measuring the total energy distribution of the signal which is a real-valued quantity and does not contain phase information, whereas ITPC is calculated by averaging phase angles at each time point over trials, therefore is independent of power. In addition, $1/f$ slope was extracted from all electrodes in the cortex, in contrast to ITPC, which was calculated from visual ICs or the occipital electrode cluster, therefore was more localised to a specific region. Another key difference highlighted in the $1/f$ literature relates to the signal periodicity. Electrophysiological signal consists of periodic and aperiodic activity, the former referring to neural oscillations, where ITPC is extracted from and the latter referring to $1/f$ noise dynamics. The two components are fundamentally different constructs, likely to explain the lack of association between ITPC and $1/f$ slope in the present study.

Perhaps the finding that adds most value to the literature, is the outcome of the ADHD-ASC group comparison as it is the first time that has been reported and answers an important

theoretical question regarding the underlying neurobiology of the two conditions. This comparison did not reveal significant ASC-ADHD group differences in the levels of neural noise as measured by ITPC and 1/f noise of PSD. This result was confirmed using two different variables indexing neural variability, ITPC (as extracted from both ICs and scalp electrodes) and 1/f slope of PSD and replicated in two different conditions, task-based and eyes-closed.

Using a larger sample size than previous studies, a robust methodology and statistical approach, it was shown that neither ongoing nor stimulus-evoked oscillatory activity is characterised by increased neural noise in the ADHD sample tested in the present study. The adults with ADHD tested here demonstrated intact ITPC patterns locally in the visual cortex and 1/f slopes of PSD of comparable steepness to the TD group. This finding contradicts previous work by Ostlund et al (2021) who found flatter 1/f spectral slopes, computed from resting state data, in adolescents with ADHD as compared to their typically developing counterparts. This discrepancy in findings however may be explained by differences in the way PSD was parameterised; in the present study the regression-based method was used, whereas Ostlund et al. (2021) utilised the FOOF algorithm. Studies such as the one by Pertermann et al. (2019), who used the same method of parameterising PSD, indicated that the brain of adolescents with ADHD is not characterised by flatter 1/f slopes per se but rather, slopes become flatter when there is greater demand for inhibitory control. Therefore, it may be that, as shown by Pertermann et al. (2019), neural responses become less reliable and more variable in affected areas such as the prefrontal region during tasks targeting neurocognitive processes known to be deficient in ADHD (eg. executive functions). Differences between groups may be apparent as task demands increase and requirements for executive function control become greater (Pertermann et al., 2019).

In addition to the above, it was established that 1/f slope of PSD and age were associated in the TD and the ADHD group but not the ASC group. This finding is in line with studies demonstrating that aging is associated with flatter spectral slopes in TD samples (Voytek et al, 2015). Voytek et al. (2015) showed that older adults are characterised by a flatter 1/f slope of PSD compared to younger adults and that 1/f slope mediates the relationship between age and cognitive decline in a visual working memory task. The fact that this relationship was not evident in adults with ASC may suggest differences in neural aging in ASC.

A few parameters are considered, which may influence the interpretation and generalization of the research findings. The current study used a large sampling interval, with participant age starting from 18 years old (late adolescent) ranging up to 69 years old (late adulthood). The broad age range implies that participants were at different developmental stages at the date of testing; in the younger samples, brain maturation may not have been complete (Somerville, 2016), whereas in the older cases, the brain may have been characterised by age-related decline (Lodato & Walsh, 2019) known to be affecting the speed of neural encoding and overall effectiveness of information processing (Ishii et al., 2017). The present study did not focus on developmental trajectories as such, however participants in each group were age and cognitive ability-matched with participants in the other two groups, therefore such differences were accounted for in the statistical analysis.

Another important limitation of the current study is the medication effects that may have influenced the EEG neural dynamics measured by ITPC. This is a common problem in neuroscientific studies of this nature. Although, participants with ADHD remained medication-free for 12 hours prior to the experiment, 3 participants with ASC were on regular medication for generalized anxiety disorder and depressive disorder (i.e. selective serotonin reuptake inhibitors such as Citalopram and serotonin-norepinephrine reuptake inhibitors such as Venlafaxine). Without baseline measurements, it is impossible to accurately determine what effects pharmacological intervention may have had on neural functioning and levels of ITPC in those participants. Serotonergic stimulation is known to be increasing P3a amplitude in a No/Go paradigm (Fischer et al., 2015), however serotonin neurotransmission is not likely to be a central mechanism influencing phase synchrony of EEG dynamics and to our knowledge, there are currently no studies available having investigated the effect of SSRIs on ITPC. Future studies should put in place stringent exclusion criteria and recruit non-medicated participants or conduct relevant statistical analysis to isolate interaction effects.

In the current study, we used self-report instruments to confirm diagnostic status and obtain phenotypic information about participants with ADHD and ASC. Score discrepancies have been reported between self and carer/teacher's ratings of behaviour in ASC, which questions the validity of self-assessment tools and suggests caution when using self-report measures in ASC (Mazefsky et al., 2011). To ensure that the data provided a reliable representation of the clinical profile of the participants with ASC, we compared the total score calculated from the

SRS self-report questionnaire with the total score computed from the SRS- other report, a questionnaire completed by a close relative or friend of the participant with ASC. The result of this analysis showed symptom overlap, confirming that the information provided by the participants with ASC was valid. Second, the SRS rather than a clinician- administered observational tool such as the commonly used Autism Diagnostic Observation Schedule (ADOS), was chosen as the optimal tool for measuring autism symptoms in the current sample for a number of reasons. Empirical evidence has shown that ADOS is less sensitive to detect autism symptoms in adult populations (Bastiaansen et al., 2011). The majority of the adults with ASC recruited for this study were later diagnosed in adulthood and exhibited less severe forms of ASC symptomatology, symptoms often missed in a short clinical interview such as the ADOS. Linked to this, adults with less severe ASC often camouflage their symptoms in social situations (Hull et al., 2017), which means that ASC symptoms are less likely to surface in a clinical one-to-one interview with the experimenter. Future studies aiming to include samples of adults with ASC, should utilise a combination of methods- both self-report and observational tools- to ensure comprehensive and accurate assessment of ASC symptoms (Pearl & Mayes, 2015).

An important future direction is to include a larger sample size to tackle sampling errors and investigate whether low ITPC characterises the brain of individuals with more severe forms of ASC. Given that the presence of outliers in the current study determined the direction of group comparisons and considering the contradictory results by Milne et al (2019), it is important to replicate the ITPC finding in a larger group of adults with ASC. In addition, the hypothesis about increased neural variability in ASC emerged primarily from studying the brain of individuals with high-functioning autism, it is therefore strongly biased towards less impaired individuals. Inadequate representation of those severely affected in studies exploring subtypes of ASC, leads to a blurry picture of the neural profiles that may exist and their characteristics (Stedman et al., 2019).

Chapter 3:

Investigating neural dynamics in Autism Spectrum Conditions (ASC) outside of the laboratory using mobile EEG

3.1. Introduction

EEG is a commonly used neuroimaging method for those with neurodevelopmental conditions. Although despite being one of the more accessible neuroimaging methods, it is not without barriers to participation, including the requirement to visit a specific, usually unfamiliar location and the requirement to limit movement during the recording. For individuals with ASC, entering a new environment to take part in unknown activities with an unfamiliar social partner- the experimenter- can be a daunting prospect. This can pose challenges for both the individual and the experimenter, as well as caregivers who accompany the participant to the appointment. Consequently, there is a tendency for research to be biased towards the inclusion of more able autistic individuals and a paucity of EEG data recorded from more severely affected individuals with ASC. This bias ultimately hinders the identification of behaviour-brain-gene pathways and limits opportunity to fully describe and understand variations in neural dynamics in ASC. Here we describe a new accessible method of studying the brain of autistic individuals at home, using mobile EEG technology.

An understanding of how mobile EEG hardware and software interact with specific features of the ASC phenotype is necessary to maximise the likelihood that individuals with ASC can participate in EEG research and allow for the acquisition of low-noise EEG signal (Webb et al., 2015). Certain elements of EEG hardware have previously been systematically assessed and solutions for capturing high-quality data proposed (Ratti et al., 2017; Kam et al., 2019). Aspects important for ASC research include the material of the cap, the speed with which the cap can be applied and engineering elements that allow for good SNRs. For example, soft lightweight fabric EEG caps are likely to be more tolerable than caps made of hard plastic. Head caps with integrated “hidden” electrodes look less intimidating than caps with protruding wires and can also reduce the length of time required for preparation. Similarly, it’s important to balance the length of time it takes to prepare the participant for the recording, with the number of channels used to record data. Active electrodes show better SNRs and require fewer trials to detect significant effects compared to passive electrodes (Mathewson et al., 2017).

Researchers should strive to maintain the fine balance between procedural adaptation and standardisation. Although processes should be adapted to meet the autistic individual’s needs, which will ultimately allow for better quality of EEG data, this should not be to the expense of standardisation of procedures, which allows for comparability across non-clinical and clinical

groups (Kylliäinen et al., 2014; Webb et al., 2015). Shared understanding on how to achieve this is currently limited. In an effort to address the need for practical guidelines, Kylliäinen et al. (2014) and Webb et al. (2015) have presented guidelines to consider when planning and implementing an EEG experiment with children with ASC. However, these are based on empirical data and the authors' personal recommendations and focus on data acquisition in the laboratory. To shed light on best practice when collecting data outside of the laboratory environment, it is important to define what consists of an optimal home-testing protocol for this group and develop practical guidelines that directly map onto the experiences of the children and adults with ASC that take part in such studies, rather the perspective of the researcher alone.

Considering the above, the primary aim of the present study was to test the feasibility of acquiring high quality EEG data from autistic children at home using mobile EEG technology and to explore children's views on the experimental process, which would in turn inform practical guidelines for EEG experimentation at home. To the best of our knowledge, this study is the first to directly record EEG signal from individuals with ASC in their own homes and also the first to systematically gather data on user-experience regarding children's participation in EEG research.

To demonstrate the utility of this method, a simple visual paradigm, based on the paradigm used in Chapter 2 to measure neural noise in autistic adults and adults with ADHD was administered, designed to elicit visual evoked potentials across multiple trials. This approach was selected as it is similar to many paradigms that are used to investigate neural dynamics in ASC and related conditions (Milne et al., 2009). EEG data were recorded from 69 children with ASC who had diverse neurocognitive profiles (see Methods section). There is currently no consensus on a single method of assessing EEG data quality (Clayson, 2020). Therefore, in an attempt to objectively define the quality of data obtained via this method, we evaluated the EEG signal by computing five key indicators of data quality: a) the proportion of artefact-free channels, b) the proportion of artefact-free epochs, c) the number of components to which dipole models could be fitted with residual variance below 15% after ICA decomposition, d) the presence of P1 and N1 Event Related Potential (ERP) deflections- common ERP components that one would expect to be elicited by this paradigm, metrics previously used in the literature to evaluate EEG data quality in ASC (Milne et al., 2009) and in validation of other mobile EEG devices (Badcock et al., 2015; Raduntz, 2018), and e) an indicator of

reliability based on the comparison of the aggregated standard error of the mean of trials for each subject to the variance of mean ERP response across subjects (Luck et al., 2021). We also explored the user experience of the participants by asking each participant to rate specific aspects of the protocol and to comment on what they liked and disliked about the procedure. This information is essential to refine the ideas by Killiainen and colleagues (2014) and Webb et al. (2015) and promote experimental practices taking into account the experiences of the individuals with ASC participating in mobile EEG experiments.

3.2 Materials and Methods

3.2.1 Participants

Seventy-three children with ASC were initially recruited for the study. From this cohort, four participants could not tolerate the EEG process. EEG data were therefore acquired from sixty-nine children with a diagnosis of ASC. Of these participants, thirteen were using limited or no language and could not complete the user experience survey. Fifty-six participants completed the evaluation questionnaire. Participants were recruited via online advertisement on social media, the local community and special schools. Participant demographics are presented in *Table 3.1*. Parents of all participants confirmed that their child had been given a diagnosis of ASC from a qualified clinical professional. A comprehensive overview of the formally diagnosed co-occurring conditions in the group is provided in *Table 3.2*, as reported by the carers. Thirteen participants were taking medication at the time of the testing session (see *Table 3.3*). All participants had normal or corrected to normal visual acuity. Consent from both the child and the carer was acquired in written form. The study was approved by the Department of Psychology Ethics Committee of the University of Sheffield.

Table 3.1

Participant demographics

ASC (n=69)	
Gender	
Female	17
Male	52
Age	
Mean	11.0
SD	2.3
Range	6-15
WASI Performance IQ score^a	
Mean	109.0
SD	14.7
Range	78-147
SRS-2 T-score^b	
Mean	84.0
SD	6.7
Range	68- >90

^aWASI Performance IQ score, *Wechsler Abbreviated Scales of Intelligence (WASI, Wechsler, 1999)*

^bSRS- 2, *Social Responsiveness Scale (SRS-2, Constantino & Gruber, 2011)*

Table 3.2

Number of participants with a diagnosed comorbid condition

Diagnosis	Frequency	Percent (%)
Total	42	62.68
Sensory Processing Disorder	7	10.44
ADHD	7	10.44
Dyspraxia	4	5.97
Anxiety Disorder	6	8.95
Social Communication Disorder	2	2.98
Intellectual Disability	1	1.49
ADHD & Sensory Processing Disorder	2	2.98
ADHD & Intellectual Disability	1	1.49
ADHD & Dyspraxia	1	1.49
ADHD & Anxiety Disorder	1	1.49
Intellectual Disability & Sensory Processing Disorder	1	1.49
Intellectual Disability & Dyspraxia	1	1.49
Sensory Processing Disorder & Dyspraxia	1	1.49
Sensory Processing Disorder & Anxiety Disorder	1	1.49
Anxiety disorder & Depressive Disorder	1	1.49
Sensory Processing Disorder, Dyspraxia & Anxiety Disorder	2	2.98
Sensory Processing Disorder, Intellectual Disability & Dyspraxia	1	1.49
Intellectual Disability, Social Communication Disorder & Anxiety Disorder	1	1.49
Tourette's Syndrome, Sensory Processing Disorder, Dyspraxia & Anxiety Disorder	1	1.49
Tourette's Syndrome, ADHD, PDA, Sensory Processing Disorder & Motor Disorder	1	1.49

Table 3.3

Drug intake of participants recorded up to 24 hours prior to the EEG experiment

	Frequency	Percent (%)
Total	13	19.38
ADHD medication		
Lisdexamfetamine	1	1.49
Atomoxetine	1	1.49
Methylphenidate	2	2.98
Depression medication		
SSRIs	2	2.98
Sleeping disorder medication		
Melatonin	6	8.95
Antipsychotic medication		
Risperidone	1	1.49

3.2.2 Psychometric assessments

64 participants completed the Matrix Reasoning and the Block Design subtests of the Wechsler Abbreviated Scales of Intelligence (WASI, Wechsler, 1999), a tool used to measure cognitive abilities of individuals aged 5-85 years old. The Matrix Reasoning and the Block Design scores combined form the Performance Scale and yield a Performance IQ (PIQ) score, summarised in *Table 3.1* for the present sample. All caregivers completed an online version of the Social Responsiveness Scale-Revised Child/Adolescent version (SRS-2, Constantino & Gruber, 2011). A T-score of 59 or below is not associated with clinically significant symptoms of ASC, whereas T-scores above 60 are indicative of clinically significant deficiencies in reciprocal social behaviour associated with ASC, symptoms ranging from moderate ($n=9$) to severe ($n=60$) for the present sample.

3.2.3 Procedure

3.2.3.1 Apparatus

A 32-channel Eego™ sports ANTneuro EEG system and ANTneuro Eego™ Software were used for EEG data acquisition. Stimuli were presented on a Dell Latitude 5490 with an Intel® Core™ i5-8250U CPU at 1.60GHz processor, running on a Windows 10 and a 64-bit operating system. Visual stimuli were presented on an LCD display screen with a spatial resolution of 1920 × 1080 pixels, refresh rate of 60 Hz, bit depth of 6-bits and colour space of Standard Dynamic Range (SDR). The screen was connected to an Intel® UHD Graphics 620.

To solve the problem of sending triggers without a parallel port, the Lab Streaming Layer (LSL) was utilised for trigger transmission. The core transport library *liblsl* and its Matlab application programming interface (API), was used to transmit event marker data (*Figure 3.1*). A single hardware system, a Dell Latitude 5490, was used to send and receive data. LSL transmitted data through the Local Area Network (LAN) using a UDP protocol (Kothe, 2014). Matlab executables (.mex files) provided in the downloaded folders were recompiled using a 64-bit C/C++ compiler. All relevant *liblsl* folders and subfolders were added to the path of the Matlab script file of the experimental task. A new stream outlet was created by declaring a new *lsl_streaminfo* object, storing core information about the data stream (i.e name, type, channel count, sampling rate, channel format, source ID). Event markers were pushed into the inlet chunk-by-chuck (using the function *outlet.push_sample*).

Figure 3.1

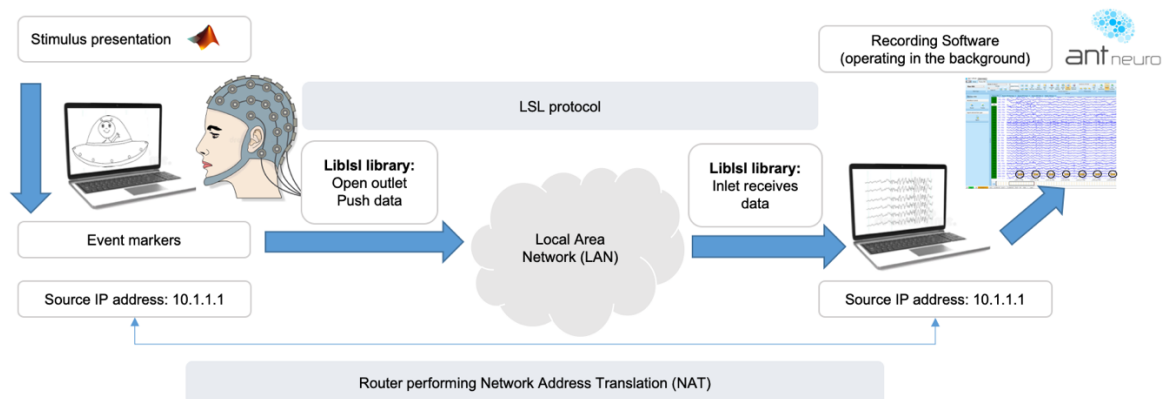


Figure 3.1: Schematic representation of the Lab Streaming Layer (LSL) protocol.

3.2.3.2 Visual task

A checkerboard stimulus was presented 100 times on the display screen (2 blocks of 50). Each sub-block consisted of a random number of checkerboard presentations each time ranging between 5-7, followed by an image of a red cross. The checkerboard appeared on the screen for an average of 1250ms, jittered between 1000 and 1500ms. The duration of the inter-stimulus interval (ISI) was a uniform distribution between 1000 and 1500ms. Similarly, the inter-trial interval (ITI) varied randomly between 1000 and 1500ms. At the end of each sub-block a black and white image of a spaceship was shown on the screen (deviant stimulus), in order to provide some interest for the participant and thus facilitate engagement. Participants were instructed to press the spacebar when the spaceship image appeared on the screen (*Figure 3.3*). Following 100 trials, participants were instructed to close their eyes while resting-state data were acquired for 120 secs.

3.2.3.3 User experience measures

Participants were asked to complete a brief user experience questionnaire at the end of the study when both parts of the experiment, the EEG task and the questionnaires were completed (*Figure 3.2*). A few participants had a shower to remove the gel and then completed the user experience questionnaire. Participants pointed at the right answer for Questions 1 to 3 and verbally provided an answer for Questions 4 and 5. In the first two questions children were asked to rate specific elements of the EEG equipment on a smiley face Likert 6-point scale, corresponding to “*Very poor*”, “*Poor*”, “*Okay*”, “*Good*”, “*Very good*”, “*Excellent*”. Question 3 asked children to rate how they felt about the experiment taking place at home. The last two questions were open-ended, aiming to understand more about the child’s overall experience of the EEG session, without biasing their responses. Children were asked to comment freely on aspects of the EEG session they liked (Question 4) and disliked (Question 5), questions that aimed to provide richer information about their individual experience.

Figure 3.2

Participant number _____

EVALUATION

How did the **material of the cap** feel?



How did the **gel** feel?



How did you feel about the experiment taking place at **home**?



What did you **like** about the EEG?

What did you **NOT like** about the EEG?

THANK YOU!

Figure 3.2: User experience questionnaire.

Figure 3.3

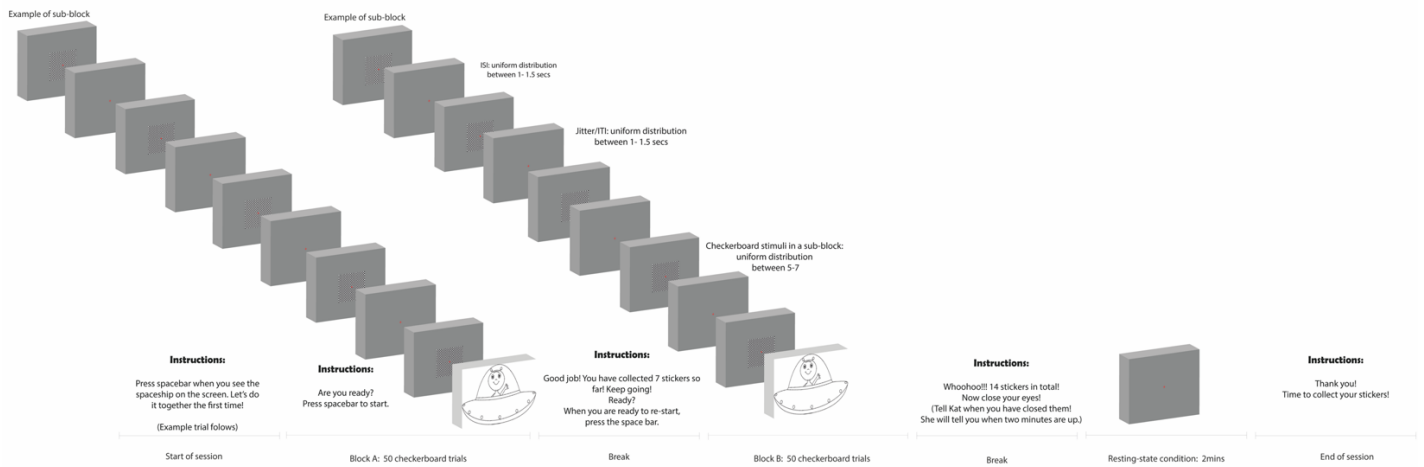


Figure 3.3: Schematic representation of the EEG experiment.

3.2.3.4 Standardisation of study parameters

Carers were instructed to turn off all electrical devices in close proximity of the location of testing to minimise power line noise interference. To avoid inter-site biases and minimise sources of variability, known to impact EEG outcomes (Farzan et al., 2017), the time of data acquisition and environmental conditions during data acquisition were kept as consistent as possible across sites. All children were tested in the evening after school (between 4pm and 7pm). To ensure consistency of environmental conditions across sites, the EEG experiment took place in a darkened room, where curtains were closed and lights were turned off. Caregivers were instructed to remain silent and outside the participant’s visual reach but remained present during the testing session.

The visual task remained the same for all participants. However, the task was designed so that it could be either active or passive depending on the ability of the participant. Participants with greater developmental delay were encouraged to look at the red cross on the screen only ($n=5$), whereas more able participants were instructed to press spacebar when the spaceship image appeared on the screen ($n=64$).

3.2.3.5 Adaptation of procedures

The home visit involved a warming-up phase, aiming to familiarise participants with the communication style of the experimenter and allow for preparation of the testing environment. The length and content of the warm-up period differed from one child to the other, depending on their developmental level and need at the time of testing. The session was presented as a “science lesson” to more able participants, during which they could learn more about the human brain. For less able children, the experimenter engaged the child in active play, using their favourite toys (e.g building Lego blocks). Communication style involved exaggerated body, facial and vocal expressions, imitation, short sentences, very simple words and/or communication cards (see *Annex 5*). The experimenter introduced each element of the equipment and explained what the study would involve. During the warm-up period, the child chose their preferable seating arrangement. Cap preparation started as soon as the experimenter judged the participants to be engaged and relaxed to reduce the risk of the child getting bored. The time taken for the electrodes to reach the desirable scalp impedance levels of 20kohms or less ranged from 15 to 45 mins, depending on the individual’s skin properties as well as their sensitivity to sensory input.

Clear instructions about the experimental process were given to all participants. Language was adjusted to establish a stream of communication between the experimenter and the participant. Prior to the visit, caregivers were asked whether their child uses alternative and augmentative communication techniques prior to the visit. For those participants ($n=9$) as well as for younger children aged 6-7 years old ($n=6$), the experimenter utilised laminated Picture Exchange Communication System (PECS) flash cards to communicate the exact steps of the process. Both verbal instructions and visual aids were utilised to ensure that the child understood task requirements. Visual cues were used to make the process predictable and help with transitions. The user interface of the EEG acquisition system was used in most cases as a visual aid to show how movement affects the EEG signal in real time and the number of electrodes subjected to impedance check (see *Annex 6* for pictures illustrating experimenter-participant interactions during the testing session).

For children demonstrating sensitivity to tactile input, we gradually exposed the child to the gel and the cap until they felt comfortable with it. The desensitisation procedure lasted from 5 mins to 20 mins, depending on the child’s needs. The experimenter first put gel on their own

hand, then on the child's hand and encouraged them to touch it. Similarly, we asked the child to touch the material of the cap before wearing it. On some occasions, the cap was put on their favourite teddy bear or was placed on the carer's scalp. The EEG cap was presented as being similar to a "swimming hat", which helped some children relate previous experiences of wearing a tight hat to the new. A 3cc syringe with a blunt tip was utilised which ensured minimal noise during gel application. Rewards and positive reinforcement were the behavioural strategies used to increase motivation. Children could choose from a pool of rewards such as stickers, LEGO minifigures or time with their favourite toy at the end of the EEG experiment.

3.2.4 Data analysis

3.2.4.1 Temporal accuracy of LSL triggers

In order to validate the temporal precision of LSL event markers, the hardware clock of the data acquisition device was used to compute the temporal error, also known as jitter, between scheduled time and actual time of triggers being recorded in the hardware. LSL event markers were fired at different time points: when the checkerboard and spaceship stimulus appeared and disappeared from the screen, when the participant pressed space bar in response to the spaceship stimulus and when the resting state period started and ended. Every time one of the above markers was fired, the start stopwatch timer- in-built within Matlab- recorded the elapsed time between the two time points. Jitter time was computed for all triggers and all participants in the experiment.

3.2.4.2 Evaluation of EEG data quality

EEG data preprocessing

A number of preprocessing steps were followed to separate physiological signal of interest from sources of noise, non-neuronal in origin (Makeig & Onton, 2012). All EEG datasets were analysed using EEGLAB (Delorme & Makeig, 2004) running on Matlab 2014a (The Mathworks, Inc.). Electrode *Cz* was selected as the reference electrode. A high-pass filter of 1Hz was applied to the continuous data in order to remove large drifts or signal deviations. Channels exhibiting noise due to poor scalp connection were identified by visual inspection

and were removed from the analysis. Channels visually identified as having unusual peaks following high-pass filtering were also excluded from the analysis. Continuous data were visually inspected and noisy time segments containing muscle or eye movement artefacts affecting multiple channels were manually rejected. This resulted in fewer epochs being retained and used for further analysis than the initial number of trials. Independent Component Analysis (ICA) was then applied using the *runica* function of EEGLAB. Data were interpolated and dipole source localisation of Independent Components (ICs) was performed using the *dipfit* plug-in of EEGLAB (Oostenveld & Oostendorp, 2002; Delorme et al., 2012). Data were segmented into epochs, from -1 to 1 secs around stimulus onset, and corrected to baseline, using the average signal between 1 sec before stimulus onset to stimulus onset.

EEG data quality measures

The first indicator of data quality was the number of good channels retained for further analysis after the artefact rejection procedures described above. The greater the number of channels maintained for downstream analysis, the smaller the EEG signal loss. The second metric was the number of epochs retained after artefact rejection. This is a good indicator of how contaminated the raw EEG signal was with motion, or other, artefacts. As a third indicator of signal quality, we measured the number of Independent Components (ICs) to which dipole models could be fitted with residual variance below 15%. It is expected that a single equivalent dipole is projected onto ICs, representing neuronal activity within a cortical area. For this reason, the goodness of fit of the dipole model fitted for each IC is an indicator of signal quality as low residual variance of the model fit suggests that ICA has successfully resolved neural signals that can be localised to a single source (Makeig & Onton, 2012).

The fourth metric of signal quality was the reliable detection of the visual P1 and N1 event-related potential (ERP) components. As early visual ERP components are more prominent in signal recorded from electrodes placed at or near the visual cortex (Novitskiy et al., 2011), we measured P1 and N1 amplitude and latency of a cluster of channels (P3, P4, Pz, POz, O1, Oz, O2) covering the occipital and posterior regions of the brain. First, the mean amplitude of the baseline period (-100–0ms) was computed for each electrode in the electrode cluster of interest and for each participant (Step 1). Second, we computed the mean amplitude of each electrode for each participant in two time windows which correspond to P1 and N1 deflections (Step 2). These time windows were based on previous literature and were defined as 130-200ms for P1

and 220-280ms for N1. We then identified the number of participants who did not show P1 and N1 deflections in at least one of the occipital and posterior electrodes (Step 3). If the mean value of the P1 window was greater than the mean +2 standard deviations of the baseline period, then P1 was considered as being present. Similarly, if the mean value of the N1 window was lower than the mean -2 standard deviations of the baseline period, then N1 deflection was considered as being present.

The fifth metric was a ‘reliability’ measure which compares the aggregated standard error of the mean of trials for each subject to the variance of mean ERP response across subjects (Luck et al., 2021). In order to find out what proportion of the participants’ amplitude or latency score variability (Var_{total}) is due to true variability i.e true signal of interest rather than measurement error, we computed the ‘psychometric reliability’ of the scores obtained from the ERP waveform, as proposed by Luck and colleagues (2021, p.25, Equation 8):

$$Reliability = \frac{(Var_{total} - \text{mean square (SME)})}{Var_{total}}$$

This gives an indication as to whether any differences in ERP magnitude or latency across subjects are due to genuine inter-subject variability or due to inter-trial variability within a subject. If the inter-trial variability is greater than that observed between subjects, data quality is considered to be poor. Values returned range between 0 and 1, with values closer to 1 indicating higher reliability.

3.2.4.3 Statistical analysis of user experience measures

We used a mixed method approach to analyse the questionnaire data. A percentage frequency distribution of responses is presented for Questions 1-3. We present the percentage of children who felt positive (“*Excellent*”, “*Very good*”), neutral (“*Good*”, “*Okay*”) and negative (“*Poor*”, “*Very poor*”) about a) the material of the cap, b) the gel and c) taking part in an experiment at their home environment. Open-ended survey questions (Questions 4 and 5) were manually analysed using thematic analysis, a data-driven approach, which captures the richness of information provided by the participants (Braun et al., 2019). Key themes were assigned to the data using a coding frame that was not pre-defined but rather, it emerged from the participant text entries (inductive coding) (Thomas, 2006). Codes were first assigned to the raw data and text entries were re-coded to ensure test-retest reliability (Roberts et al., 2019). Given the exploratory nature of this work, the experimenter encouraged children to elaborate on their experience and there was no limit in the number of given answers. Similar codes were put

under the same thematic category, which allowed the emergence of main and overarching themes and subthemes.

3.3 Results

3.3.1 Temporal accuracy of LSL triggers

23.866 LSL event markers were fired in total. The latency distribution between scheduled time and actual time of triggers being recorded in the hardware, presented in *Figure 3.4*, demonstrates that temporal accuracy of LSL trigger markers is high, within millisecond precision or better ($M=0.0003s$, $SD=0.0007$, $Min=0.00004s$, $Max=0.02s$).

Figure 3.4

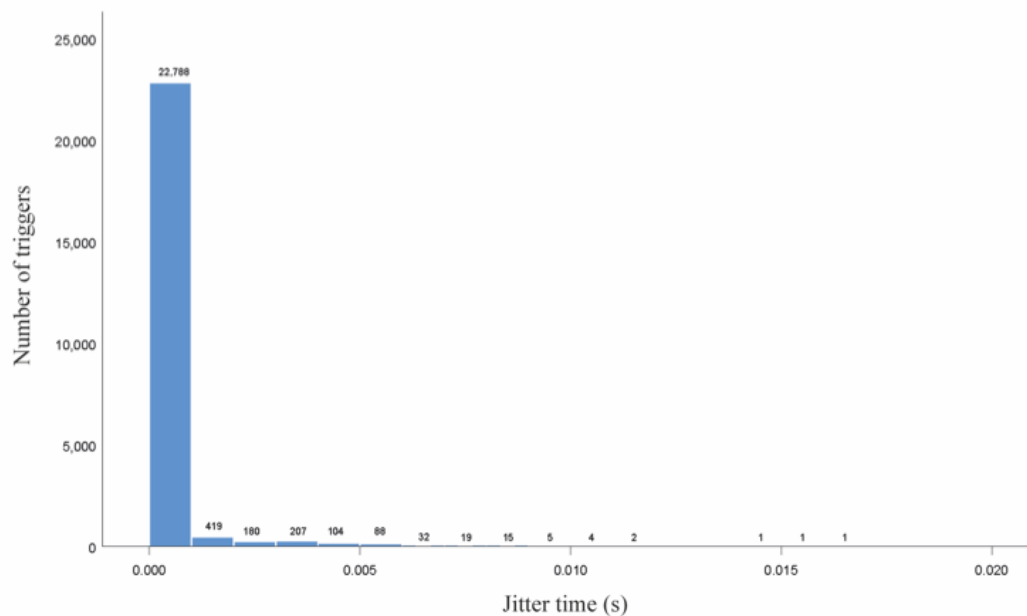


Figure 3.4: Histogram of jitter time (x axis), presented in seconds (s) for all triggers (y axis).

3.3.2 EEG data quality assessment

The number of channels and epochs retained after artefact rejection, extracted from the data recordings using the Eego Sports mobile system, is presented in *Table 3.4*.

Table 3.4

Mean (M), Standard Deviation (SD), Minimum (Min) and Maximum (Max) number of EEG channels and epochs retained, as computed from data acquired using the 32-channel Eego Sports mobile system

Metric	<i>M</i>	<i>SD</i>	<i>Min</i>	<i>Max</i>
1. EEG channels retained	26	2.93	16	30
2. Epochs retained	89	5.35	71	96

ICA applied on individual participant scalp data, returned as many components as the number of channels kept for further analysis after preprocessing.

The number of ICs with residual variance lower than 15% was also computed from the EEG recordings. We found that dipole scalp projections adequately fit the IC scalp maps for an average of 18 ICs per participant ($M=18$, $SD=3$, $Min=10$, $Max=25$). A previous laboratory-based study using similar methods to those reported here found a mean number of retained components of ~ 10 , extracted from signal acquired from children with ASC using a static wet electrode EEG system that is frequently used in neurodevelopmental research (Milne et al., 2009). The number of ICs that likely reflect neural sources extracted from the mobile EEG signal is therefore comparable to laboratory-based alternatives. *Figure 3.5* shows a single IC from each participant to highlight the topographic projection of the IC to the EEG data in sensor space. For each participant, we selected an IC that projected at the occipital lobe, to demonstrate the consistency of these components across participants.

Figure 3.5

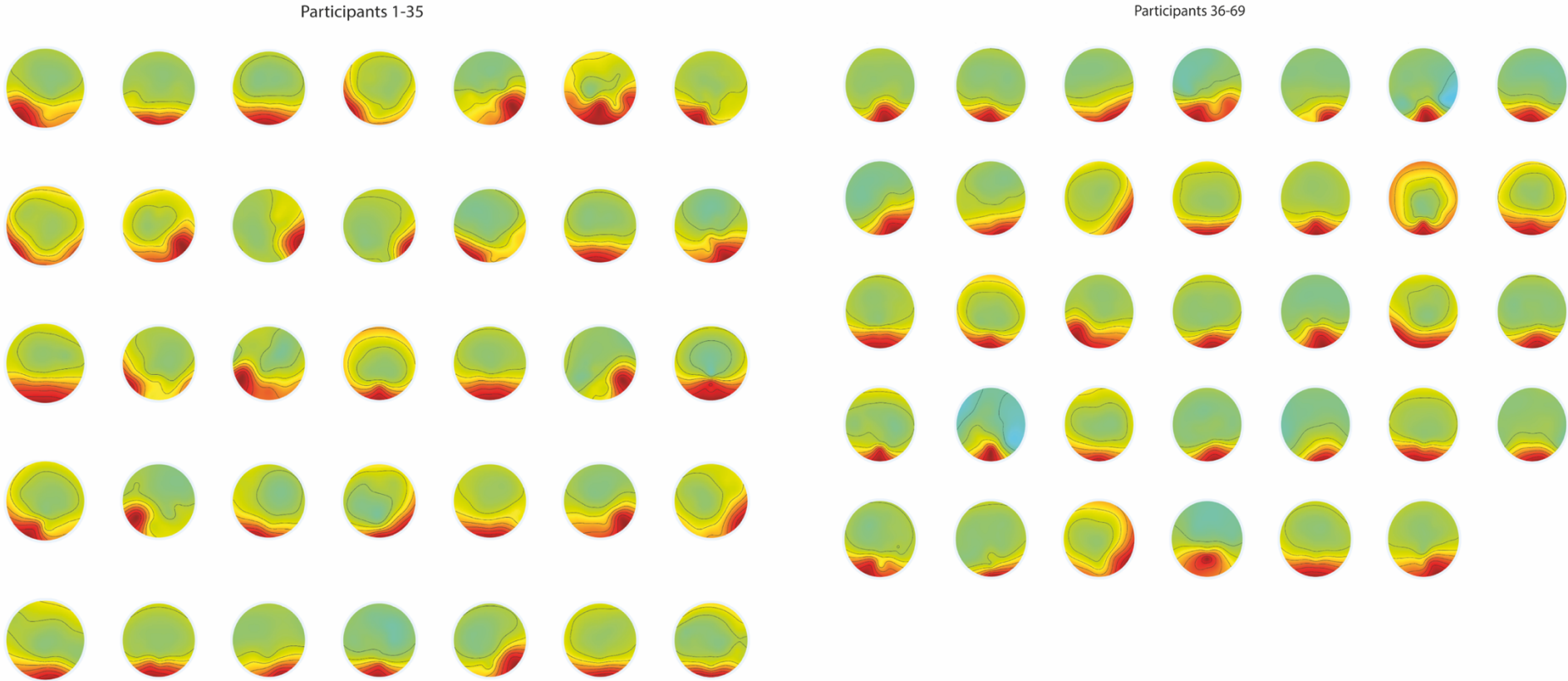


Figure 3.5: Example Independent Component (IC) scalp maps.

Further to this analysis, we identified which electrode, from the electrode cluster P3, P4, Pz, POz, O1, Oz, O2, showed the largest P1 and N1 deflection (see *Table 3.5*). For most participants, the largest P1 deflection occurred at electrode O2 around 175ms and the largest N1 amplitude occurred at electrode O1 around 246ms. For 91% of the group, maximum P1 amplitude was observed in one of the three channels O2, Oz and O1, whereas for maximum N1 amplitude, the spread was greater, across all posterior channels.

We also computed reliability values for all electrodes in the cluster P3, P4, Pz, POz, O1, Oz, O2. Reliability values were computed for the peak amplitude and peak latency of the P1 and N1 deflections. Reliability values range between 0 and 1, with those closer to 1 indicating higher reliability of ERP components. Reliability values for the peak amplitude of P1 and N1 ERP components at electrodes P3, P4, Pz, POz, O1, Oz, O2 are close to 1, ranging from 0.907 to 0.966 for P1 ‘peak’ and 0.825 to 0.965 for N1 ‘peak’. Similarly, the latency where the peak amplitude for P1 and N1 occurs shows reliability ranging from 0.666 to 0.902 for P1 and 0.824 to 0.922 for N1 (*Table 3.5*). Therefore, it is established that both P1 and N1 ERP components show high reliability.

Table 3.5

P1 and N1 Amplitude (uV) and Latency (ms) computed from electrodes P3, P4, Pz, POz, O1, Oz, O2 from all participants (Mean, Minimum, Maximum) and the reliability values (R) given for the peak P1 and N1 Amplitude and Latency.

Electrode	Amplitude (uV)				Latency (ms)			
	P1	R	N1	R	P1	R	N1	R
P3	6.99	0.907	-5.67	0.825	172.20	0.733	243.74	0.824
	[0.09 17.72]		[-17.86 1.35]		[134 200]		[220 280]	
P4	5.81	0.937	-4.16	0.883	176.46	0.715	245.88	0.840
	[0.10 16.72]		[-13.98 3.82]		[108 200]		[220 278]	
Pz	8.05	0.911	-6.39	0.876	170.67	0.666	241.45	0.828
	[1.92 24.05]		[-18.38 5.90]		[132 200]		[220 274]	
POz	13.11	0.945	-5.47	0.925	177.01	0.836	248.67	0.892
	[1.21 33.12]		[-24.00 12.82]		[100 200]		[220 280]	
O1	19.79	0.955	-7.17	0.926	175.04	0.874	246.67	0.919
	[0.99 47.40]		[-40.59 7.02]		[130 200]		[220 280]	
Oz	21.21	0.966	-4.96	0.955	177.04	0.897	251.10	0.922
	[1.06 47.87]		[-40.50 14.20]		[130 200]		[220 280]	
O2	22.14	0.964	-6.40	0.956	175.42	0.902	249.48	0.920
	[1.10 50.51]		[-41.23 14.56]		[132 200]		[220 280]	

As *Figure 3.6* demonstrates, P1 and N1 deflections are evident in grand-average ERP traces computed from occipital and posterior electrodes as well as the ERPs of individual channels- here we present ERP traces computed from electrode O2. This figure shows that visual ERPs were reliably detected in the signal. *Table 3.6* presents the number of participants showing P1 and N1 deflections at each electrode of the electrode cluster covering the occipital and posterior locations of the head. The majority of participants (99% and 97% respectively) showed clear P1 and N1 deflections in at least one electrode from the electrode cluster. Overall, P1 voltage deflections were completely absent in only one participant, whereas two participants did not show N1 ERP traces in any of the aforementioned channels.

Table 3.6

Number and percentage of participants in the group showing P1 and N1 deflections at each of the electrodes P3, P4, Pz, POz, O1, Oz, O2

Electrode	ERP Component			
	P1		N1	
	Frequency (n=69)	Percent (%)	Frequency (n=69)	Percent (%)
P3	53	77	65	94
P4	53	77	58	84
Pz	61	88	66	96
POz	60	87	50	72
O1	63	91	46	67
Oz	60	87	23	33
O2	62	90	44	64

Figure 3.6

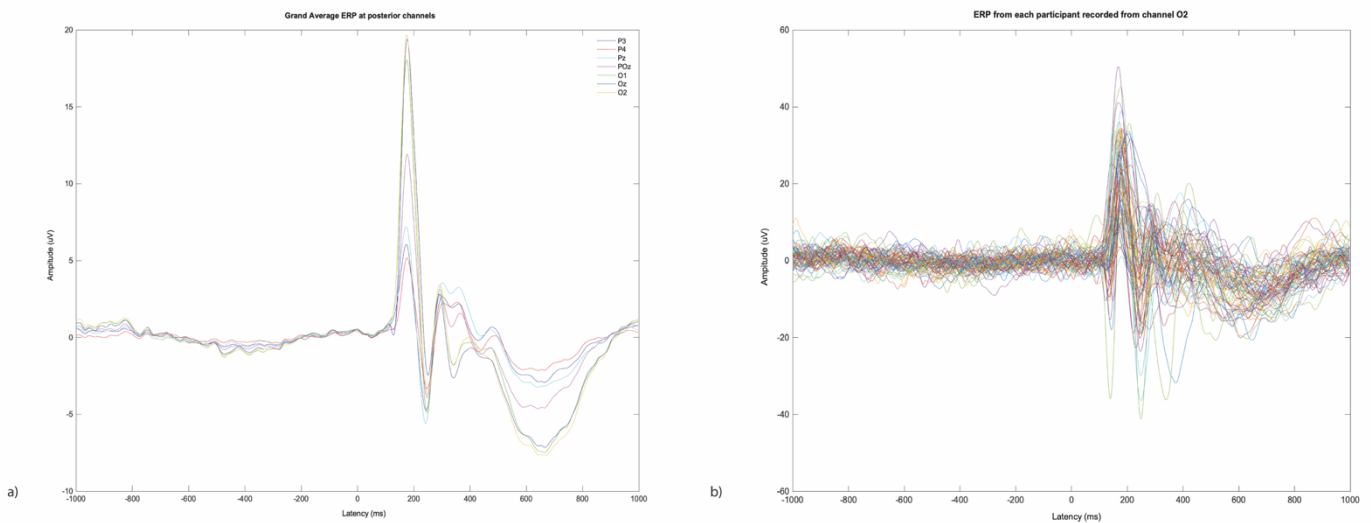


Figure 3.6: a) Grand-average ERPs computed from electrodes P3, P4, Pz, POz, O1, O2, OZ for all participants and b) ERP traces plotted for the example electrode O2, as extracted for all participants.

3.3.3 User experience

The majority of children found the EEG cap pleasant and felt positive about the experiment taking place at home, but the responses to the electrolyte gel were more mixed. *Figure 3.7* summarises children's responses to Questions 1-3.

Figure 3.7

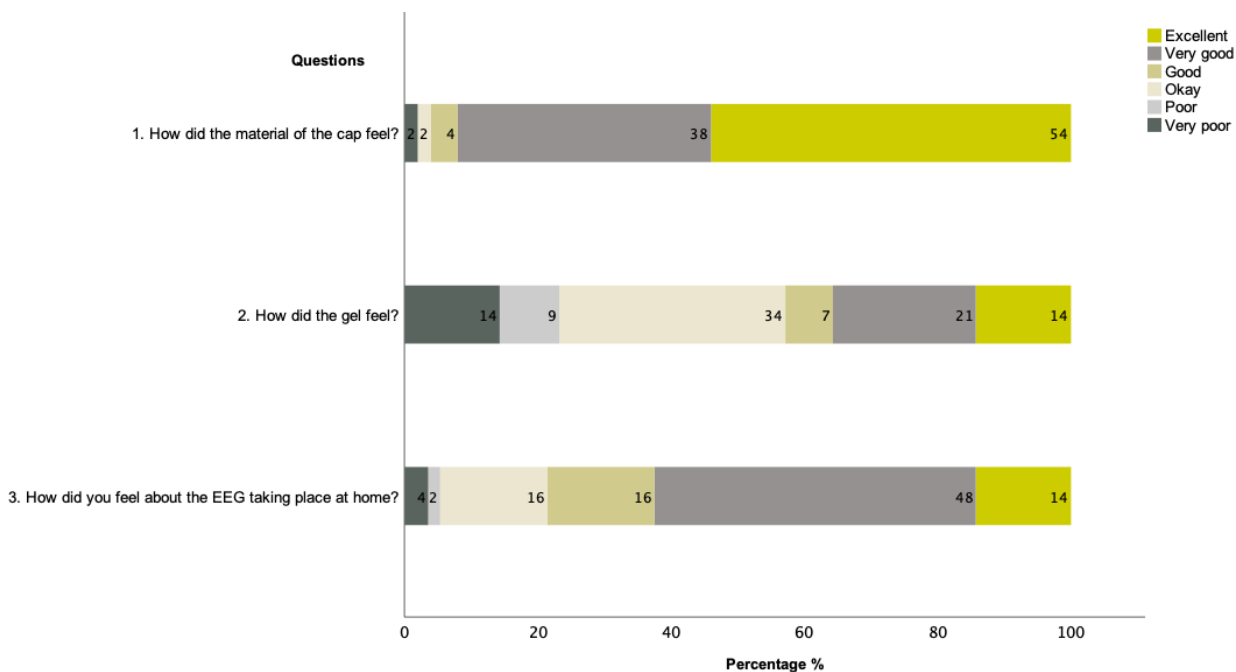


Figure 3.7: Proportion of children that responded positively (“Excellent”, “Very good”), neutrally (“Good”, “Okay”) and negatively (“Poor”, “Very poor”) to Questions 1-3

Five themes emerged from Question 4 (“What did you like about the EEG session?”, see Table 3.7 for a summary). The first theme relates to aspects of the equipment. A large number of children ($n=25$) pointed out that they were fascinated by software features of the EEG such as the interactive screen showing a) EEG data in real time and b) the impedance check view feature (e.g “I liked seeing my brain waves”). A smaller number of participants commented on the design of the cap ($n=3$) and the overall technology ($n=2$). A small number of children enjoyed the tightness of the cap and the cold feeling of the gel on the scalp ($n=2$).

The second theme that emerged relates to aspects of the experimental task. A large number of children found the task very engaging; incorporating play into the process made the experimental task very appealing ($n=13$). They explicitly commented on the alien/spaceship picture and pointed out that “the game was fun”. Others mentioned that the task was “easy” and “not stressful” ($n=2$) and that they liked the rewards offered by the experimenter ($n=2$).

The third theme encompasses aspects of the environment. Children enjoyed taking part in a scientific experiment at home ($n=2$) and in a quiet environment ($n=1$).

The fourth theme relates to intrinsic motivation. Some children mentioned that they enjoyed improving their sense of social responsibility by taking part in the research study, “*knowing that they are helping others*” ($n=2$). This highlights the importance of communicating the aim and purpose of the study in an accessible way. Linked to this, the fifth theme relates to the experimenter. A subset of children ($n=3$) commented on the accessible and inclusive communication style of the researcher (e.g. “[*Name of the experimenter*] *communicated well the information*”).

Five themes emerged from Question 5 (“*What did you not like about the EEG session?*”). The first theme relates to the equipment used during testing. Some children found the sensation of the gel touching their skin uncomfortable (“*I didn’t like it when the gel wet my hair*”) ($n= 23$). Other children did not like the experience of wearing the tight cap ($n=3$), fastening the strap around their chin ($n=1$) or having the wire touching their neck ($n=1$). Other children commented negatively on the “*squirting noise*” of the liquid dispenser/syringe used to inject gel. The second theme relates to the subject preparation and equipment set-up. Some children found the time taken to prepare the wet electrodes very long ($n=4$). They report that “*it took so long*” and “*I didn’t like waiting to get ready for the spaceship*”. The third theme relates to the task itself. Two of the children found the task boring due to its repetitiveness (“*It was boring, I was drifting off*”). The fourth theme is about the environment. Even though all children chose freely their sitting arrangement, in one occasion, the child found the chair uncomfortable to sit for a long time. The fifth theme relates to the participant’s physical state during the experiment. One child reported difficulty staying still during the EEG and another child found keeping their eyes closed in the resting-state condition challenging. To strengthen this point, five children could not complete the eyes-closed condition because they were unable to keep their eyes closed for two minutes.

Table 3.7

Key themes and subthemes, as emerged from children's responses to Question 4 and 5

Questions	Theme	Subtheme	Example answers	
4. "What did you like about the EEG session?"	Equipment	Interactive screen- Software	"I liked seeing my brain waves", "I liked watching the dots changing colour"	
		Design- Cap	"I liked the style of the hat"	
		Sensory experience- Cap	"I liked the tight cap"	
		Sensory experience- Gel	"I liked the gel going into the hair", "I liked the gel being cold"	
		Overall technology	"It had brilliant technology"	
		Task	Engaging task/use of play	"Spaceship was fun", "I liked the alien picture", "I liked the game"
			Easy task	"Task wasn't too hard", "The EEG wasn't stressful to do"
	Environment	Use of rewards	"I was offered stickers"	
		Being tested at home	"I liked that it took place at home"	
	Intrinsic motivation	Quiet	"I liked that it was quiet"	
		Altruism	"I might be helping people"	
	Experimenter	Fascination with science	"I liked the science of it"	
		Accessible communication style	"[Name of the experimenter] communicated well the information", "[Name of the experimenter] was really nice to me"	
5. "What did you not like about the EEG session?"	Equipment	Sensory experience- Cap	"The cap was too itchy", "I didn't like the colours of the cap"	
		Sensory experience- Strap	"The strap around the chin was uncomfortable", "The bottom bit of the cap was too loose"	
		Sensory experience- Wire	"I didn't like the wire at the back of the head"	
		Sensory experience- Gel	"I didn't like it when the gel wet my hair"	
		Sensory experience- Syringe	"I didn't like the needle squirting"	
	Task	Boring task	"It was boring, I was drifting off"	
		Environment	Uncomfortable sitting arrangement	"Back was hurting half way through, I had bad chair"
	Subject preparation/equipment set-up	Length of time	"It took so long", "I didn't like waiting to get ready for the spaceship"	

3.4 Discussion

The present study was the first to use mobile EEG technology to record data from children with ASC in their home environment. The primary aim of the present study was to test the feasibility of acquiring good quality EEG data from autistic children in such a setting. We evaluated the EEG signal quality recorded from 69 children with ASC at their home environment using a gel-based Eego Sports mobile EEG system. In order to evaluate the quality of data obtained via this method, we examined the number of channels and epochs retained after artifact rejection, the number of returned independent components with residual variance of the fit of the dipole to the scalp map that is smaller than 15%, detection of P1 and N1 ERP deflections in the visual task-based data the reliability of these ERP deflections. The majority of participants showed clear P1 and N1 deflections in at least one electrode from the electrode cluster covering the posterior and occipital sites. N1 deflections were absent in 3% of the group, whereas only 1% did not show P1 deflections. In addition, both P1 and N1 ERP deflections demonstrated high reliability of close to 1. These values are comparable with reliability measures of EEG data collected in a lab-setting from neurotypical adults (Luck et al., 2021). We therefore established that visual ERP deflections can be reliably measured in the signal. Furthermore, the fact that many of the independent components derived from the continuous data could be fit with a dipole model with <15% residual variance, and no participants generated data from which less than 10 components where the dipole models were fit with residual variance of < 15%, suggests high quality of the EEG signal and its potential utility in studying a range of neural processes in this group.

Based on the above metrics, it was demonstrated that the EEG signal quality acquired using the Eego Sports mobile system and collecting data in the participants' homes was satisfactory to perform EEG analysis such as ICA decomposition and ERP examination. It was also demonstrated that the LSL protocol can be reliably used to send trigger markers through the network, enabling more complex task-based EEG designs to be implemented at home or other settings, where parallel port technology is not available.

Taking a more holistic approach to experimentation, the present study was also the first to explore the user experience of children with ASC in relation to the mobile EEG experiment; this is crucial to understand how experimenters could acquire optimal signal quality from participants with ASC at home. Based directly upon the views and experiences of the children

who participated in this experiment, we identified important aspects to consider when planning and implementing an EEG experiment with children with ASC at their homes.

In our sample, certain elements of the EEG cap interacted with individual differences in sensory sensitivity. A subsample of the children found the EEG cap, the chin strap and the wire connecting the cap with the amplifier to be uncomfortable, whereas a different subgroup enjoyed the tightness of the EEG cap. Therefore we suggest that EEG systems relying heavily on chin straps to ensure the electrodes are in place should be avoided. Wireless EEG systems may also be a good solution, solving the problem of the back wire touching the child's neck.

Due to heightened tactile sensitivity, the electrolyte gel was uncomfortable or just about tolerable for a third of the children tested in the present study. Considering the neurocognitive profile of participants with ASC, this is not surprising. In the present study, wet electrodes were chosen over dry electrodes to maintain low skin-electrode impedances and therefore achieve high signal quality. In addition, EEG signal recorded using dry electrodes is shown to be more prone to movement artefacts (Meziane et al., 2013), a parameter to be taken into consideration when testing young participants with neurodevelopmental conditions. As dry EEG technology is rapidly evolving, dry electrodes may be a good option to be used with children with ASC to minimise sensory reactions and maximise rates of participation in the future. Preliminary evidence has shown that dry electrodes can record EEG signal of similar quality to wet electrodes in a laboratory setting (Kam et al., 2019), although these results are necessary to be extended to a naturalistic setting such as the home environment and to clinical groups such as ASC.

In the present study, it is likely that the familiar environment together with the manipulation of experimental parameters helped children tolerate the EEG and cope with the experimental procedure. Although a hypothesis not directly tested in this research work, low levels of emotional arousal are likely to have played an important role in the successful acquisition of low-noise signal. In support of this proposition, a recent study by DiStefano et al. (2019) showed that elevated participant state, captured as vigilance or agitation displayed during testing, is linked to lower EEG data retention rates and greater reduction in alpha spectral power in a sample of children with ASC of various cognitive abilities. We therefore suggest that conducting the EEG experiment in a familiar environment such as the home setting has the potential to be a very effective method of achieving low levels of emotional arousal, allowing

for higher quality EEG data acquisition from subjects with ASC, particularly those with more challenging behaviour that would not otherwise comply with experimental processes.

Mobile EEG technology is a rapidly developing field and there are a number of different options available for experimentation, including wireless EEG systems and systems utilising dry electrode technology (see *Table 3.8* for a summary). Multiple research lines have compared dry-wet electrode EEG solutions (Marini et al., 2019). An important next step for future research is to compare the performance of dry and wet electrodes on similar metrics in a naturalistic environment such as the home setting, where access to a shielded room is not possible and the environmental conditions are more variable. Future work should also aim to test the functionality of using a wireless system instead of a wired EEG device, shown to exacerbate sensory sensitivities in our ASC sample and restrict participant's mobility in other studies.

A strength of this study is the sample size ($n=69$), however potential sampling bias remains an important limitation of the work. Of the seventy-three participants who originally consented to take part, four children were not able to comply with the experimental process due to severe communication deficits, hindering effective communication between the experimenter and the participant. As our recruitment method was an opt-in method (i.e. we were contacted by parents who wanted their child to take part after seeing advertisement of the study) it is likely that the high success rate of successful recordings is due, in part, to the sample being this will have skewed towards children who were more able to engage with the protocol. Therefore, the limitation of increasing accessibility to research for children who are profoundly affected by ASC remains. Nevertheless, anecdotally, our impression of the data collection phase was that being able to complete the testing session in the participants' homes increased uptake to the study and allowed us to gain data from a larger sample than has been possible in previous studies where data collection is consigned to the lab. In conclusion, here we provided evidence and developed guidelines to support EEG data collection at home, potentially opening up possibilities for increased access to research for a range of participants.

Table 3.8

Available mobile EEG systems and their technical specifications

Hardware											Overall device							
Model/Company	Electrodes				Amplifier						Head cap		General characteristics					
	Number	Type	Sensor shielding	Material	Max sampling rate (Hz)	Bandwidth (Hz)	Resolution (bit)	CMRR (dB)	Input impedance (M Ω)	Input noise (mV)	Material	Cable shielding	Weight (gr)	Battery life (h)	CE mark	Price*	Prep time (mins)	
MindWave (NeuroSky)	1	dry	passive	stainless steel	512	1-100	12	N/A	20	Not stated	plastic, rubber	yes	90	6-8	no	low	0	
4S JellyFish (Mindo)	4	dry	passive	spring-loaded pins	256	0.23-1300	24	110	3	<1.25	plastic	no	95	10	no	low	Not stated	
BR8 (BRI)	8	dry	passive	spring-loaded pins, polymer foam	500	0.12-125	24	Not stated	Not stated	Not stated	plastic	no	269	10	no	low	Not stated	
EPOC ^X (EMOTIV)	14	wet (saline)	passive	gold-plated, felt	256	0.16-43	14-16	85	1	N/A passive amplifier	plastic	no	1000	6-12	no	low	10-15	
B-Alert (ABM)	X24	20	wet (gel)	passive	polymer foam	256	0.1-100	16	105	>10 ²	1.5	plastic	no	110	8-15	yes	high	Not stated
Smarting (mBrainTrain)	24	wet (gel)	passive	sintered Ag/AgCl	550	0-250	24	>140	>10 ³	<1	soft fabric	no	60	5	no	low	5-10	
EPOC ^{Flex} (EMOTIV)	32	wet (saline or gel)	passive	sintered or electroplated Ag/AgCl	1024	0.16-43	14	85	30	N/A passive amplifier	soft fabric	no	500 (saline) 1500 (gel)	9	no	low	20	
32 Trilobite (Mindo)	32	dry	passive	spring-loaded pins, polymer foam	512	0.23-1300	24	110	3	<1.25	plastic	no	578	10	no	low	Not stated	

actiCAP Xpress, V-amp (BrainProducts)	32	dry	active	gold-plated	20.000	0-320	24	100	$>10^2$	<1	soft fabric	no	430	Not stated	no	medium	Not stated
ENOBIO (Neuroelectronics)	8, 20, 32	dry or wet (gel)	passive	Ag/AgCl (dry, wet)	500	0-125	24	115	$>10^3$	<1	thick elastic fabric	no	<97	5.5-24	yes	low, medium	1-3 (dry), 10-30 (wet)
SAGA (TMSI, BIOPAC)	32, 64	wet (gel or water)	passive	Ag/AgCl	4096	0-800	24	100	$>10^2$	<0.8	soft fabric	yes	700	8-10	yes	medium	10-20
Eego Sports (Ant-neuro)	32, 64	wet (gel)	passive	Ag/AgCl	2048	0-532	24	>100	$>10^3$	<1	soft fabric	yes	<500	5	yes	medium	10-15
g.NAUTILUS RESEARCH (g.tec)	8,16,32, 64	dry or wet (gel)	active	spring-loaded graphene pins (dry) or sintered Ag/AgCl (wet)	500	0- 10^4	24	>90	$>10^2$	<0.6	hard fabric	no	<140	>10	no	medium	5-10
g.NAUTILUS PRO (g.tec)	8, 16, 32	dry or wet (gel)	active	spring-loaded graphene pins (dry) or sintered Ag/AgCl (wet)	500	0- 10^4	24	>90	$>10^2$	<0.6	hard fabric	no	<110	>10	yes	high	5-10
Mobile (Cognionics)	64, 128	wet	active	Ag/AgCl	1000	0-131/262	24	Not stated	Not stated	<1	hard fabric	no	460	6-8	yes	high	10-40

*low <6000 GBP, medium 6000-15000 GBP, high >15.000 GBP

3.5 Conclusions

The present study demonstrated that it was possible to record high quality EEG signal from children with ASC at a home environment. Here, we used a gel-based Eego Sports mobile system to record EEG signal and the LSL protocol was successfully used to send trigger markers through the network, paving the way for more complex EEG experiments to be implemented at home by ASC researchers. In addition, we developed a protocol for home visits in ASC. The user experience survey flagged up a few areas experimenters should take into consideration when designing an EEG experiment aiming to acquire EEG data from children with ASC at a home setting.

Chapter 4:

Neural noise in children with Autism Spectrum Conditions (ASC)

4.1 Introduction

1/f noise dynamics have not been systematically investigated in ASC. ASC studies examining neural noise in the form of 1/f noise of PSD are limited to the work presented in the present thesis. Chapter 2 demonstrated that visual-evoked and resting state electrophysiological responses of adults with ASC are not characterized by a flatter 1/f slope of PSD compared to typically developing adults, contradicting theories about pathological undercoupling in ASC. What remains unclear is whether spike trains behave similarly in younger ASC populations. It is still unclear whether the slope of power decay follows the trajectory of neurotypical development in children with ASC or shows distinct patterns of functioning. Initial evidence suggests that 1/f slope of PSD is unlikely to be capturing neurophysiological underpinnings that are distinct in ASC compared to typically developing populations, however there is some evidence that alpha-to-gamma phase coupling is reduced in the visual cortex of children with ASC (Seymour et al., 2019). Further research in children is necessary to understand whether there is a different developmental trajectory of power decay in autism; although no difference was seen in 1/f slope of PSD between adults with and without ASD in previous chapters, this difference may be observable in autistic children.

In contrast to 1/f noise, a greater number of ASC studies have investigated neural noise in the form of ITPC. The majority of these indicate that ASC is associated with reduced ITPC across all developmental stages, although some contradicting results are also reported (see *Table 1.1* of Chapter 1 for a summary). In childhood, existing evidence is inconclusive. Milne (2011) reports reduced ITPC in the alpha band during visual processing of Gabor patches in a sample of children and adolescents with ASC. On the other hand, Butler et al. (2017), using a similar methodology, do not report differences in levels of ITPC between groups. Similarly, Yu and colleagues (2018) found an increase in ITPC of theta oscillations computed for the P1 time window, followed by a reduction in ITPC for the N2 time window during processing of pure tones and words. In early adulthood, reductions in ITPC of theta oscillations are observed in the frontal electrode site during feedback processing of rewards and errors (van Noordt et al., 2017). In mid and late adulthood, Milne et al. (2019) found reduced ITPC in response to visual stimulation but only in a subgroup of adults with ASC and concluded that increased neural variability is likely to be reflecting one of the many pathophysiological routes to ASC symptomatology. This conclusion may also explain some of the inconsistencies in the rest of the literature, particularly evident in the child studies. It is likely that due to low power (sample sizes ranging from 13-20) and the large variability in neural profiles of participants with ASC, these neurological differences are

captured in the brain of children recruited for some studies i.e Milne (2011) but not others i.e Butler et al. (2017).

4.1.2 Aims of the current study

Considering the above, the present research work seeks to extend the findings of Chapter 2 and establish whether atypical patterns of neural noise are observed in children with ASC. The primary aim of the present study was to investigate whether children with ASC demonstrate similar or distinct levels of neural variability compared to their typically developing counterparts. In order to clarify this, a group of children with a clinical diagnosis of ASC and a group of typically developing children were recruited for the present study. Children were tested at their home environment using a gel-based mobile EEG system (see Chapter 3 for a detailed description of the methodology followed). To ensure consistency and facilitate comparisons of findings between studies, children took part in an adapted version of the visual task utilized in Chapter 2. Following a similar approach to the study outlined in Chapter 2, neural noise in the form of neural variability was measured by computing ITPC and changes in 1/f slope of PSD from the signal recorded from both groups. Consistent with the experimental approach followed thus far, these measures were extracted from both a visual task-based condition and a resting-state ‘eyes-closed’ condition.

4.2 Materials and Methods

4.2.1 Participants

Seventy-three participants with ASC and twenty-five typically developing (TD) children were initially recruited for the study. From this cohort, four participants with ASC could not tolerate the EEG process and parents of two participants did not complete the psychometric assessments, therefore sixty-seven participants with ASC were included in the present study. Participants were recruited via online advertisement on social media, mainstream and special schools and the local community. Participants in the ASC group held a diagnosis of either Autism Spectrum Disorder/Condition ($n=56$) or Asperger’s Syndrome ($n=11$). A comprehensive overview of the formally diagnosed comorbid conditions in both groups is provided in *Table 4.2*. Descriptive information for the two groups are provided in *Table 4.1*. A few participants from the ASC and TD groups were on regular medication at the time of testing (see *Table 4.3* for a detailed breakdown), however all participants remained non-medicated for twenty-four hours prior to the experiment. All participants had normal or corrected to normal visual acuity.

Participants that (a) their carers did not speak English to a sufficient level to be able to complete the questionnaires, (b) had epilepsy and/or (c) a mental health condition such as personality disorder, bipolar disorder, psychotic disorder did not meet the eligibility criteria for participation in the study. In addition to the above exclusion criteria, TD participants had to not hold a diagnosis of ASC, Asperger's Syndrome, Atypical Autism and Pervasive Developmental Disorder. This was confirmed both by parental report for each participant and by a T-score of 60 or below in the Social Responsiveness Scale (SRS-2, Constantino & Gruber, 2011), indicating that TD participants did not have clinically significant difficulties in reciprocal social behaviour, suggestive of ASC (see *Table 4.1* and *Table 4.4*). Consent from both the child and the carer was acquired in written form. Ethical guidelines were followed throughout according to the standards set by the Ethics Committee at the University of Sheffield.

Table 4.1

Participant demographics

	ASC Group (<i>n</i> =67)	TD Group (<i>n</i> =25)	t-statistic	Hedges' g
Gender				
Female	15	2		
Male	52	23		
Age				
Mean	11.0	9.56	2.74***	0.64
SD	2.3	2.48		
Range	6-15	5-14		
WASI score^a				
Mean	109.0	113.54	-3.74***	0.88
SD	14.7	14.15		
Range	78-147	84-144		
SRS-2 T-score^b				
Mean	84.0	44.32	27.31***	5.89
SD	6.7	6.76		
Range	68- >90	36-59		

^aWASI Performance IQ score, Wechsler Abbreviated Scales of Intelligence (WASI, Wechsler, 1999)

^bSRS- 2, Social Responsiveness Scale (SRS-2, Constantino & Gruber, 2011)

p*<0.5, *p*<0.01, ****p*<0.001

Table 4.2

Number of participants with a diagnosed comorbid condition

Diagnosis	Frequency	
	ASC Group (<i>n</i> =67)	TD Group (<i>n</i> =25)
Total	42	0
Sensory Processing Disorder	7	0
ADHD	7	0
Dyspraxia	4	0
Anxiety Disorder	6	0
Social Communication Disorder	2	0
Intellectual Disability	1	0
ADHD & Sensory Processing Disorder	2	0
ADHD & Intellectual Disability	1	0
ADHD & Dyspraxia	1	0
ADHD & Anxiety Disorder	1	0
Intellectual Disability & Sensory Processing Disorder	1	0
Intellectual Disability & Dyspraxia	1	0
Sensory Processing Disorder & Dyspraxia	1	0
Sensory Processing Disorder & Anxiety Disorder	1	0
Anxiety disorder & Depressive Disorder	1	0
Sensory Processing Disorder, Dyspraxia & Anxiety Disorder	2	0
Sensory Processing Disorder, Intellectual Disability & Dyspraxia	1	0
Intellectual Disability, Social Communication Disorder & Anxiety Disorder	1	0
Tourette's Syndrome, Sensory Processing Disorder, Dyspraxia & Anxiety Disorder	1	0
Tourette's Syndrome, ADHD, PDA, Sensory Processing Disorder & Motor Disorder	1	0

Table 4.3

Regular drug intake of participants in the ASC and TD group

Drug intake	Frequency	
	ASC Group (n=67)	TD Group (n=25)
Asthma medication		
Ventolin	0	2
Corticosteroids (i.e Pulmicort, Montelukast, Beclometasone)	2	1
ADHD medication		
Methylphenidate (i.e Equasym, Delmosart)	2	0
Lisdexamfetamine	1	0
Atomoxetine	1	0
Sleeping disorder medication		
Melatonin (i.e Circadian)	6	0
Diabetes medication		
Insulin	1	0
Depression medication		
SSRIs	2	0
Antipsychotic medication		
Risperidone	1	0
Constipation medication		
Sodium picosulfate	2	0

4.2.2 Psychometric assessments

Cognitive abilities

Participants completed the Matrix Reasoning and the Block Design subtests of the Wechsler Abbreviated Scales of Intelligence (WASI, Wechsler, 1999), a tool used to measure cognitive abilities of individuals aged 5-85 years old. The Matrix Reasoning and the Block Design scores combined form the Performance Scale and yield a Performance IQ (PIQ) score, summarised in *Table 4.1* for the present sample.

Social communication

All caregivers completed an online version of the Social Responsiveness Scale-Revised Child/Adolescent version (SRS-2, Constantino & Gruber, 2011). The SRS-2, consisting of sixty-five 4-point Likert scale items, was used to identify the presence and severity of social impairments associated with ASC. A single raw score was produced by summing the scores of the “Social Awareness”, “Social Cognition”, “Social Communication”, “Social Motivation” and “Restricted Interests and Repetitive Behaviour” treatment subscales. The raw score was then converted into a T-score for every participant, taking into account their gender and age. *Table 4.4* indicates the severity of social communication impairments associated with ASC in the ASC and TD group, as measured by the SRS-2. A T-score of 59 or below is not associated with clinically significant symptoms of ASC, whereas T-scores above 60 are indicative of clinically significant deficiencies in reciprocal social behaviour associated with ASC, symptoms ranging from mild (60-65) and moderate (66-75) to severe (76 or higher).

Table 4.4

Severity of social communication impairments in the ASC and TD group as indicated by the SRS-2

	<i>SRS-2^a T-score</i>			
	59 or below (no association with ASC)	60-65 (mild)	66-75 (moderate)	76 or higher (severe)
ASC Group (n=67)	0	0	11	56
TD Group (n=25)	25	0	0	0

^aSRS-2, Social Responsiveness Scale (SRS-2, Constantino & Gruber, 2011)

4.2.3 Procedure

4.2.3.1 Apparatus

A 32-channel Eego™ sports ANTneuro EEG system and ANTneuro Eego™ Software were used for EEG data acquisition. The experiment was presented on a Dell Latitude 5490 with an Intel® Core™ i5-8250U CPU at 1.60GHz processor, running on a Windows 10 and a 64-bit operating system. Visual stimuli were presented on an LCD display screen with a spatial resolution of 1920×1080 pixels, refresh rate of 60 Hz, bit depth of 6-bits and colour space of Standard Dynamic Range (SDR). The screen was connected to an Intel® UHD Graphics 620.

4.2.3.2 EEG experiment

The EEG experiment consisted of a task- based condition followed by a resting state condition, explained in detail at Section 4.2.3.4.

4.2.3.3 Data acquisition

EEG data was recorded continuously from a 32-channel ANTneuro cap. The data quality was ensured by keeping the impedance values of the electrodes below 25 k Ω . The signal was digitalised at a sampling rate of 512Hz. Eego™ sports ANTneuro EEG system does not store signal in a referenced format, therefore the raw data was reference-free when acquired.

4.2.3.4 EEG task

A checkerboard stimulus was presented 100 times on the display screen (2 blocks of 50). Each sub-block consisted of a random number of checkerboard presentations each time ranging between 5-7 ($U_{(5, 7)}$), followed by an image of a red cross. The checkerboard appeared on the screen for an average of 1250ms, jittered between 1000 and 1500ms. The duration of the inter-stimulus interval (ISI) was a uniform distribution between 1000 and 1500ms. Similarly, the inter-trial interval (ITI) varied randomly between 1000 and 1500ms. At the end of each sub-block a black and white image of a spaceship was shown on the screen (deviant stimulus). Participants were instructed to press spacebar when the spaceship image appeared on the screen (*Figure 4.2*). The task-based part of the experiment lasted for approximately ~5 minutes. Following 100 trials, participants were instructed to close their eyes while EEG data was acquired for 2 minutes. *Figure 4.1* provides a schematic representation of both the task-based and resting- state part of the EEG experiment.

Figure 4.1

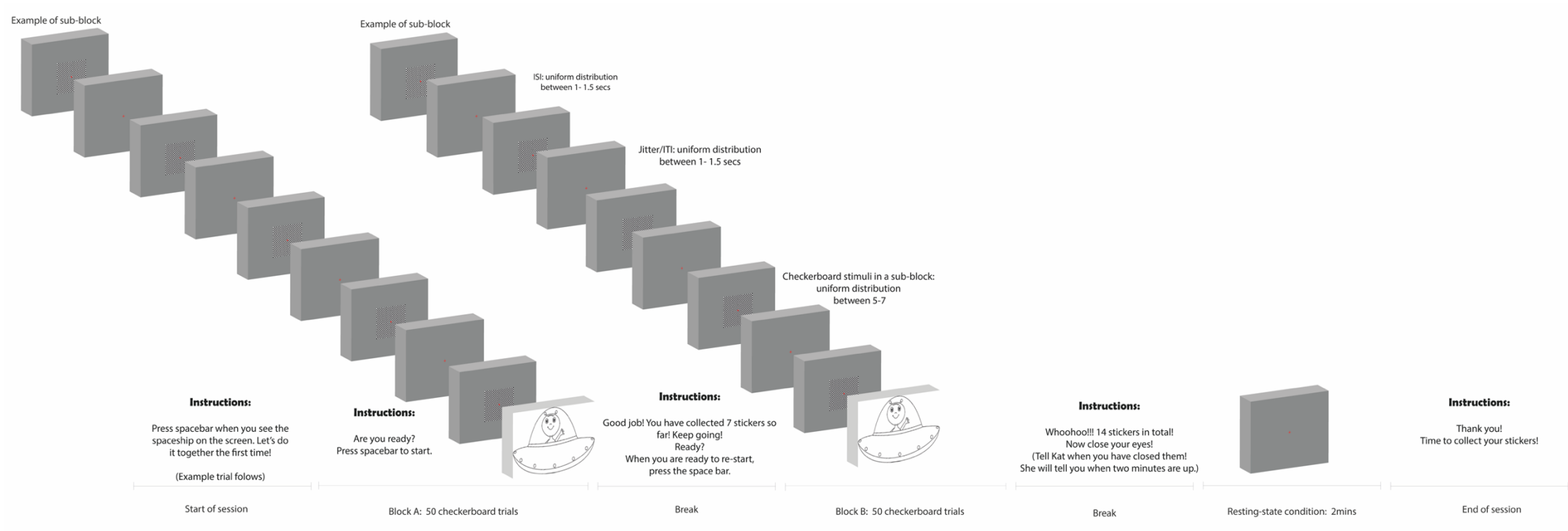


Figure 4.1: Schematic representation of the EEG experiment.

4.2.4 General data preprocessing

EEG datasets were analysed using EEGLAB (Delorme & Makeig, 2004) running on Matlab 2014a (The Mathworks, Inc.). A number of preprocessing pipeline steps were followed to ensure that high quality signal was extracted. For ITPC analysis, Cz was selected as the reference electrode, based on previous literature (Milne et al., 2019). In contrast, the preprocessing steps followed for 1/f slope analysis remained similar to the ones outlined by Voytek et al. (2015) and, for that reason, the average reference was used. In both analyses, a high-pass filter of 1Hz was applied to remove large drifts or signal deviations. Channels exhibiting noise due to poor scalp connection were removed from the analysis. Continuous data were visually inspected and noisy time segments containing muscle or eye movement artefacts affecting multiple channels were manually rejected. This resulted in fewer epochs being retained and used for further analysis than the initial number of trials. Independent Component Analysis (ICA) was then applied on the clean data, using the *runica* function of EEGLAB (see Section 4.2.6.2). *Figure 4.2* provides a summary of the preprocessing steps followed in preparation for extraction of the variable of interest i.e. ITPC and 1/f slope of PSD.

Figure 4.2

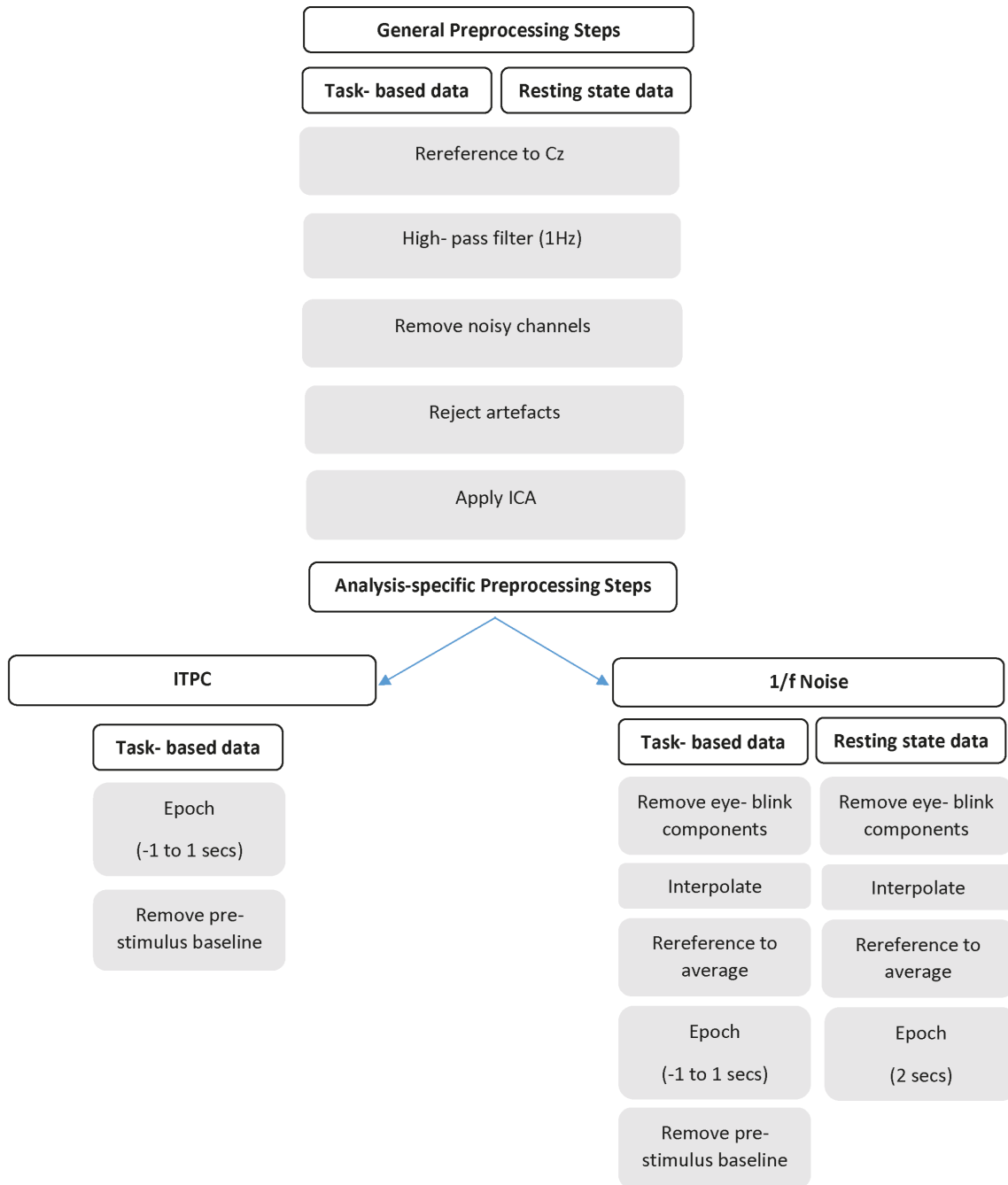


Figure 4.2: Summary of A) the general and B) analysis specific preprocessing steps followed

4.2.5 Data integrity

Following the preprocessing analysis, a series of extra analysis steps were carried out in order to evaluate whether EEG data quality was similar across different datasets and amongst different groups. We first established that the number of epochs were the same in the final ITPC vs 1/f noise task-based datasets. Secondly, we assessed whether the number of epochs was similar across groups. The mean number of epochs extracted from the task-based data did not differ significantly between groups (see *Table 4.5*).

Third, similarly to the analysis in Chapter 2, the ERPs of the Independent Component and the channel selected for further group analysis were examined to assess the quality of the signal for each participant. This step confirmed that signs of a visual evoked potential (VEP) (e.g. P1 or N1 deflection) was present in the neural signal of sixty-five out of sixty-seven participants in the ASC group and all twenty-five participants in the TD group (*Figure 4.3* for ASC group and *Annex 7* for the TD group). Two participants in the ASC group did not show a clear VEP (see *Figure 4.3* in red), therefore their data were excluded from the group analysis. For the channel analysis, a VEP was present in all selected channels and for that reason all participants were included in the analysis (*Figure 4.4* for ASC group and *Annex 7* for the TD group). In addition to the above, the ITPC values of the ASC group, which were falling below the minimum value of the ITPC distribution for the TD group (see *Figure 4.11*), were examined in relation to the ERP trace of the respective IC or channel. Visual inspection of their topographic map and ERP image revealed adequate signal quality.

Figure 4.3

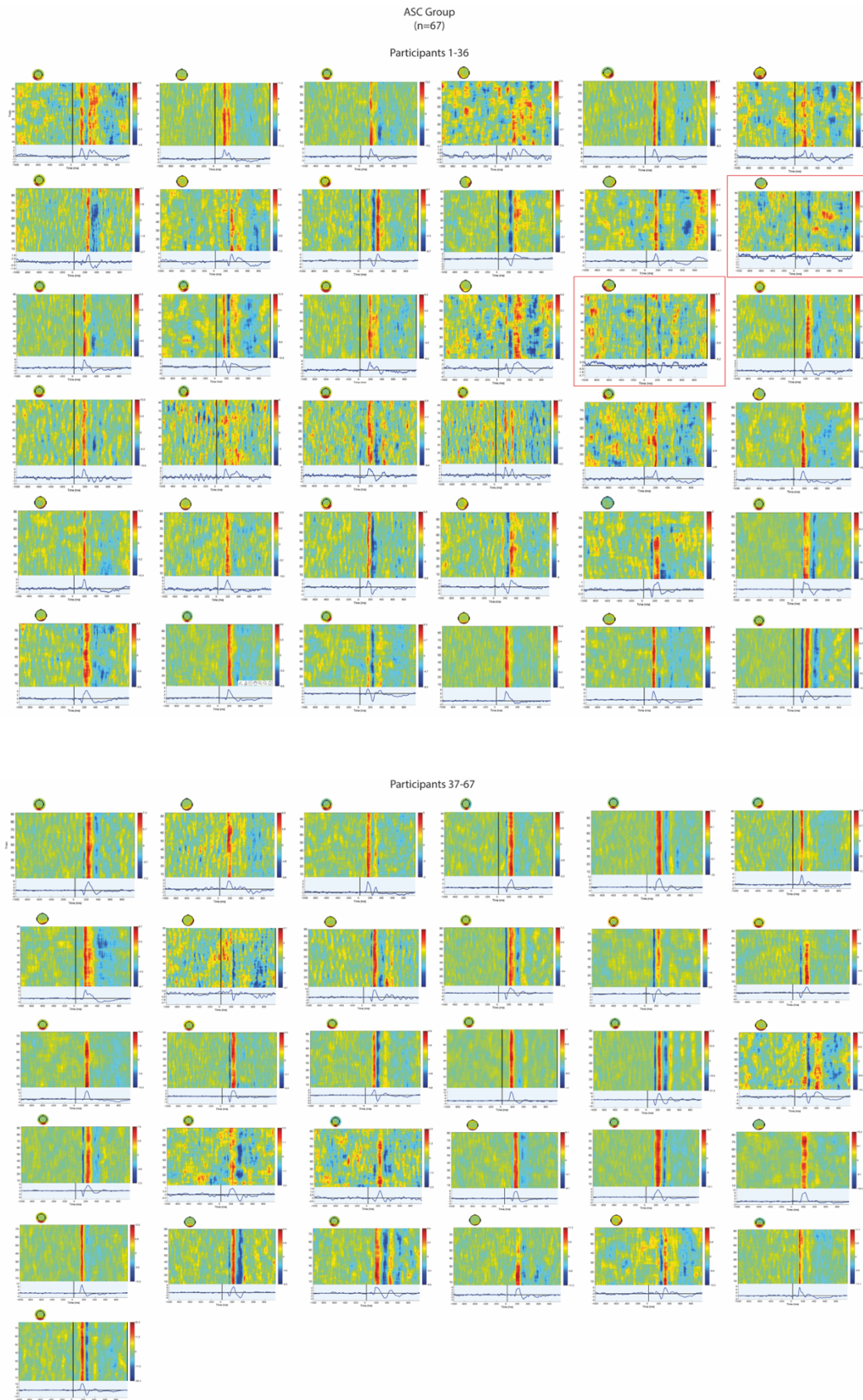
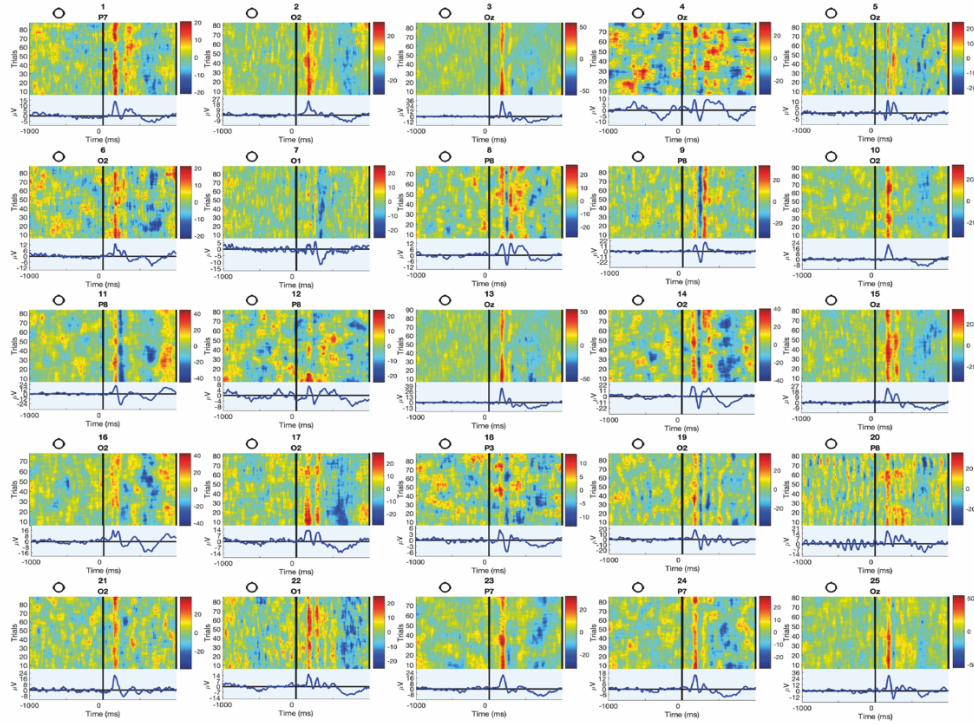


Figure 4.3: ERPs of the selected Independent Components (ICs) included in the group analysis ($n=65$), presented for the ASC group. Participants with a less clear VEP were excluded from the group analysis and are marked in red ($n=2$).

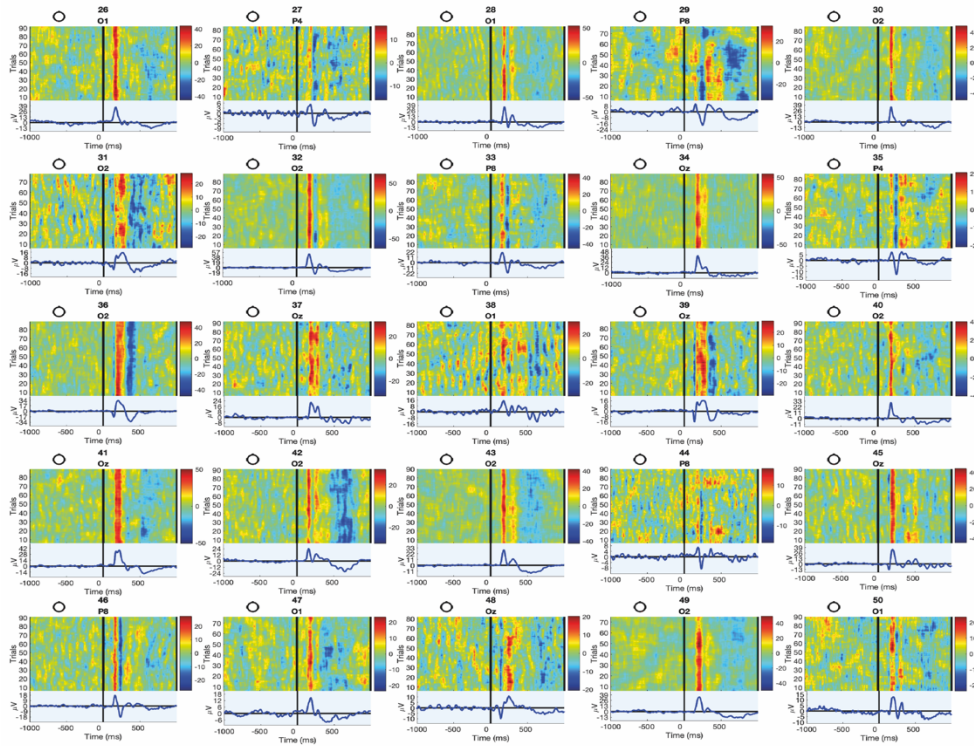
Figure 4.4

ASC Group
(n=67)

Participants 1-25



Participants 26-50



Participants 51-67

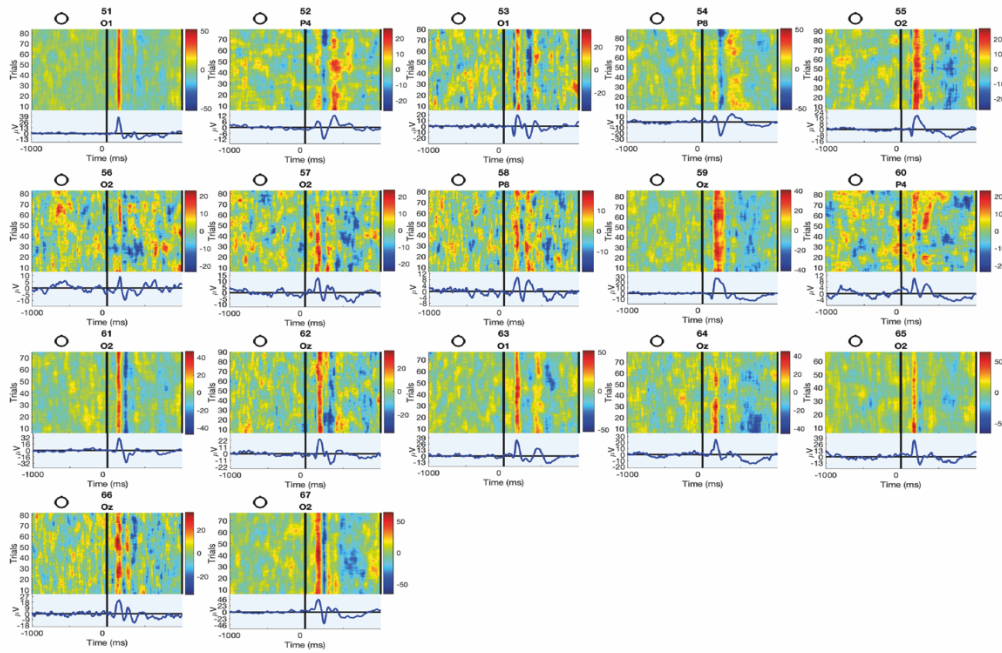


Figure 4.4: ERPs of the selected channels included in the group analysis ($n=67$), presented for the ASC group.

Table 4.5

Mean (M), Standard Deviation (SD), Range of artefact-free EEG channels and experimental trials and the t -statistic presented for the comparison of the means in the ASC and TD group

	ASC Group ($n=67$)	TD Group ($n=25$)	t -statistic
EEG channels retained			
Mean	26	26	0.44
SD	2.8	2.7	
Range	16-30	20-30	
Experimental trials retained			
Mean	88.54	86.52	1.35
SD	5.60	7.70	
Range	71-96	67-96	

* $p < 0.5$, ** $p < 0.01$, *** $p < 0.001$

4.2.6 EEG data preparation for Inter- Trial Phase Coherence analysis

4.2.6.1 Data preprocessing

Additional preprocessing steps were followed to prepare the task-based data for ITPC analysis (*Figure 4.2*). Data was segmented into epochs, from -1 to 1 secs around stimulus onset, and corrected to baseline, using the average signal between 1 sec before stimulus onset to stimulus onset.

4.2.6.2 Data selection

In the present chapter, ITPC was extracted from two distinct sources of signal, both from Independent Components (ICs) and EEG scalp electrodes.

Independent Component selection

ICA decomposition was performed using the *runica* function of EEGLAB, which utilises the infomax ICA algorithm of Bell & Sejnowski (1995) with the natural gradient characteristics suggested by Amari et al. (1996). ICA, applied on individual participant scalp data, returned as many components as the number of channels kept for further analysis after preprocessing. Time-frequency analysis was then performed on all ICs (see Section 4.2.6.2). For each participant, we calculated ITPC for every IC and selected the single IC with maximum ITPC for further analysis. Inspection of the IC scalp maps of the IC selected from each participant revealed that the selected ICs were projected at the occipital lobe and had clear signs of a visual evoked potential, suggesting that they were reflection activation of the visual cortex. Scalp maps of the IC with max ITPC chosen for each participant in the ASC group is presented in *Figure 4.5* and *Figure 4.6*. The ERP of the selected components was also examined further confirming that the signal source was at the visual cortex.

Channel selection

Although signal from individual electrodes is known to be more contaminated with noise artefacts as compared to signal from ICs, maximum ITPC was also extracted from an electrode cluster covering the occipital region of the brain to provide greater confidence in the direction of the results. Following a similar approach to the IC selection, for each participant we calculated ITPC for every electrode in the cluster P7, P3, P2, P4, P8, POz, O1, Oz, O2 and selected the single electrode with maximum ITPC for further analysis.

Figure 4.5

ASC Group

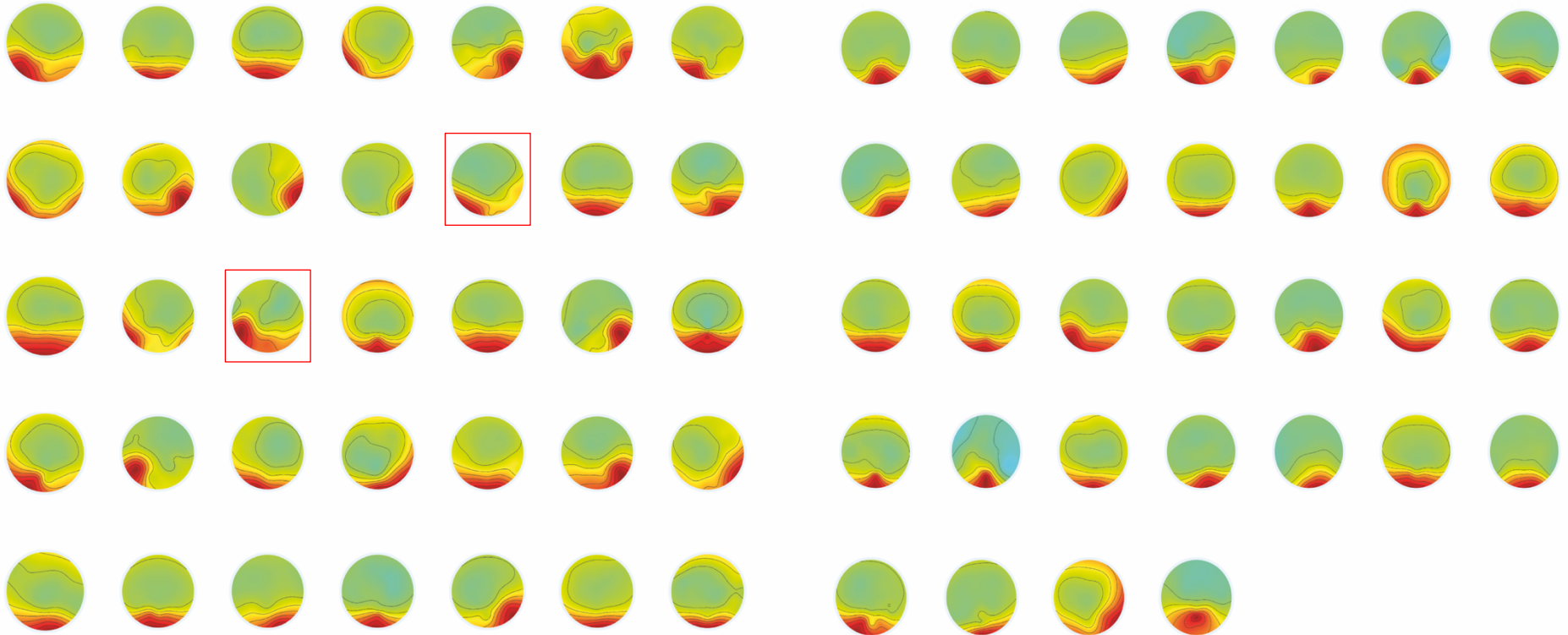


Figure 4.5: Scalp maps of the Independent Component with maximum ITPC for participants 1-67 in the ASC group. Data of two participants outlined in red were excluded from further analysis.

Figure 4.6

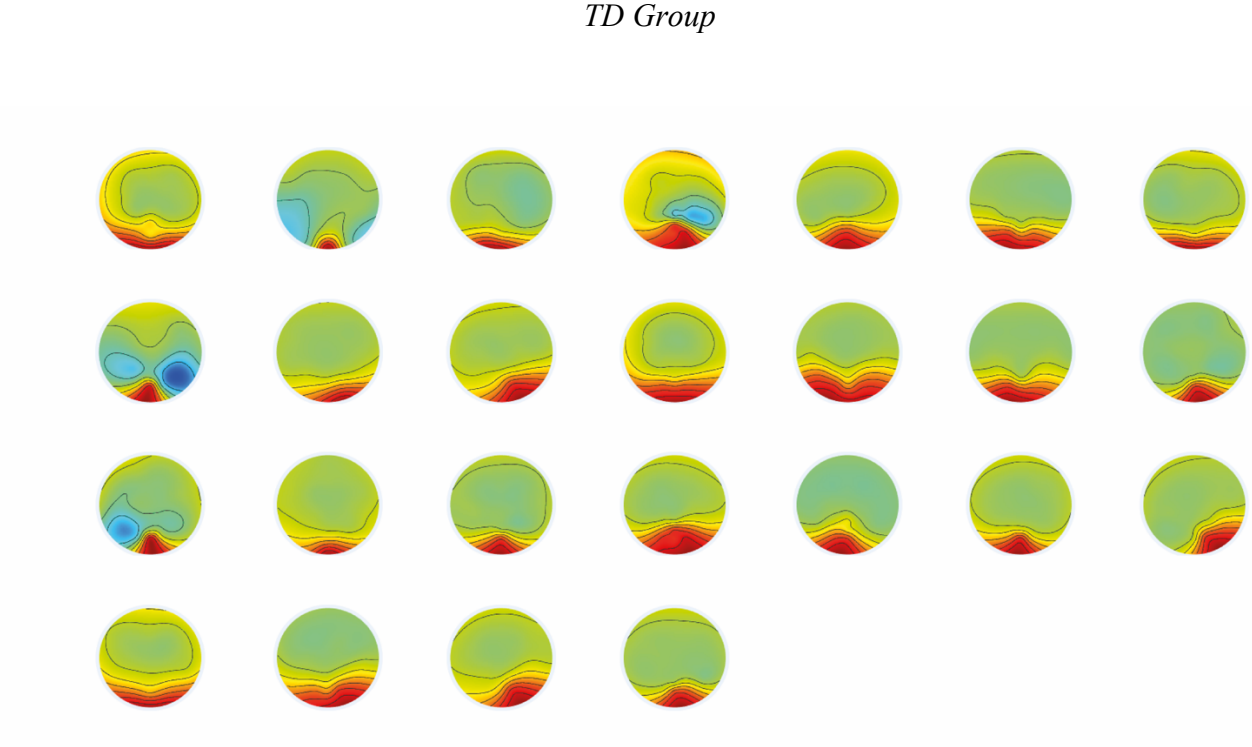


Figure 4.6: Scalp maps of the Independent Component with maximum ITPC selected for participants 1-25 in the TD group.

4.2.7 Data analysis

Time-frequency analysis

Time-frequency decomposition of EEG single-trial data was performed using the *newtimef* function of EEGLAB (Delorme & Makeig, 2004). The time series data was convolved with a complex Morlet wavelet, defined as a sinusoid with a Gaussian shape. The wavelet ranged from 2 to 12.5 cycles at 558 ms intervals (equivalent to 279 samples). The length of the average vector of the phase angles was computed for 200 evenly spaced time-frequency points (-720.7 to 720.7 ms) and was estimated for 23 log-spaced frequencies, ranging from 4 to 50Hz (see Chapter 2, Section 2.2.7 for a detailed explanation of time-frequency analysis). A single ITPC value, representing the maximum ITPC generated from any independent component or any channel at any frequency and at any time point, was extracted for each participant in the group and was used for group analysis.

Epoch length was shorter in the adapted version of the paradigm used in Chapter 2 to accommodate for the short attention span of young children and render the paradigm more child-friendly. For that reason, compared to the methodology followed in Chapter 2, frequencies were logarithmically rather than linearly spaced. This allowed to capture the lower end of the frequency spectrum, which could not be captured if linear scaling had been used (see *p.165*, Cohen, 2014 for a discussion on logarithmic vs linear scaling). An independent samples t-test confirmed that there were no significant differences between ITPC derived from logarithmically spaced vs linearly spaced frequencies in the ASC and TD group (ASC: $F(132)=0.23$, $p=0.34$, TD: $F(48)=0.19$, $p=0.36$).

4.2.8 EEG data preparation for 1/f noise analysis

4.2.8.1 Data preprocessing

Task-based and resting state data were further preprocessed in preparation for 1/f noise analysis. The preprocessing approach we followed here differs from the approach taken in the preparation of the task-based data for ITPC analysis. The main objective of the ITPC analysis pipeline was to separate the mixed signal and select one source of signal to analyse, whereas primary aim of the 1/f preprocessing analysis was to ensure that the mixed EEG signal is clean and free of noise artefacts so that power spectral estimations are accurate and attributed to brain functions rather than external sources of electrical interference.

Eye-blink components were visually identified from the ICA maps and removed as suggested in the 1/f analysis pipeline followed by Peterson et al. (2017). In order to replace the missing channels, all datasets were interpolated using the channel interpolation function from the EEGLAB gui. Data were then referenced to average reference and segmented into epochs. Task-based data were epoched from -1 to 1 secs around stimulus onset and pre-stimulus baseline removal was performed at 1 sec. Similar to the methodology followed in experimental Study 1, resting state data were segmented into 2 secs epochs.

4.2.8.2 Data selection

Power Spectral Density estimation

Welch's method (Welch, 1967) was used for Power Spectral Density (PSD) estimation. The Welch's method is explained in detail in Chapter 2. In brief, the Welch method minimises this variance by averaging out the spectral content of short windows of signal. Each dataset was segmented into blocks with 50% overlap between them. A modified periodogram was then computed for each block using a 2-second Hamming data window. The periodograms for each block were averaged out to produce the final PSD periodogram. A linear regression line was then fitted to the data to model an inversely proportional relationship between PSD and frequency, of the form $P_f = k \frac{1}{f^\alpha}$, where P_f is the power spectra per frequency interval f , k is a random constant and α is the scaling exponent. Power spectra was plotted in log coordinates. The log-transform of the power function is a straight line with a negative slope α and an intercept c (Figure 4.7, also see Annex 8 for the 1/f slope of all electrodes computed from Participant 26). 1/f slopes of PSD were estimated from frequencies between 2-24Hz (Voytek et al., 2015), effectively excluding high frequency bands from the analysis, as they are more likely to reflect intrinsic channel noise, rather than neural processes. Alpha band power (7-14Hz) was also excluded prior to 1/f slope estimation, as it represents changes in periodic EEG patterns, biasing estimations of the non-periodic properties of the signal i.e. 1/f noise (Voytek et al., 2015). Alpha band power was not excluded a priori (for example by band pass filtering) instead an identical method to previous research (Voytek et al., 2015) was used in which the alpha component of the calculated power spectra was removed simply by replacing the characteristic peak of the alpha wave with a straight line between the data points of the power associated with 7 and 14Hz frequencies.

Figure 4.7

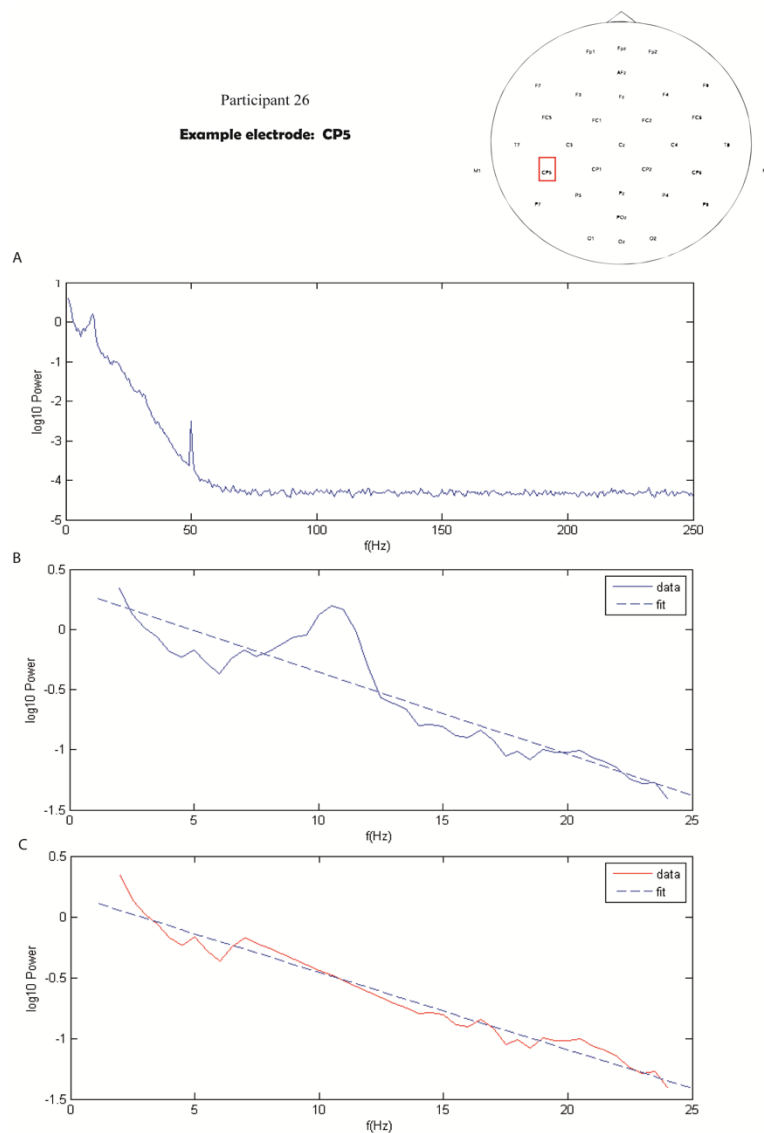


Figure 4.7: Log-transformed Power Spectral Density (\log_{10} Power) of signal coming from a single electrode CP5 from a participant in the ASC group, is presented here as a function of frequencies (f) ranging from A) 0-250Hz, B) 2-24 Hz including alpha band and C) 2-24 Hz excluding alpha band. A regression line with a negative slope $a = -0.063614$ is fitted to the data in graphs B and C.

4.2.9 Data analysis

In contrast with ITPC, there are very few studies having previously measured 1/f slopes of PSD, therefore there is very limited prior knowledge on what consists of an optimal analytical approach of analysing 1/f slopes of PSD. In Chapter 2, we followed two distinct methods of preparing the data for group comparisons, the first analytical method compared grand average 1/f slope values across groups, whereas the second method involved single electrode comparisons. In this chapter, we utilised the former method only, so that age effects can be taken into consideration in subsequent analysis. As demonstrated in Section 4.2.1 (*Table 4.1*), the two samples differed significantly in age. In addition, further analysis in Section 4.3.2 showed that 1/f slope of PSD is associated with age, therefore the age difference between the samples should be accounted for. To the best of our knowledge, there is not an analytical approach that can adjust for multiple comparisons and add age as a covariate. For that reason, in the present study only the first method of computing 1/f noise is utilised (comparison of grand average 1/f slope values across groups). A single value representing the 1/f slope of PSD at each electrode was first calculated for all electrodes and for all participants in the ASC and TD groups. The mean slope of all 32 electrodes for every participant was then computed and the grand mean slope was calculated for each group, ASC and TD (*Figure 4.8*).

4.2.10 Statistical analysis

We utilised frequentist methods of hypothesis-testing throughout the present chapter. Frequentist statistics were conducted using IBM SPSS Statistics for Windows, version 25 (IBM Corp., Armonk, N.Y., USA). In the group comparisons of the key variables of interest ITPC and 1/f slopes- where appropriate and possible- Bayesian statistical analysis was also performed alongside frequentist statistical analysis in Sections 2.3.1 and 2.3.2, in order to decide with greater certainty which of the two hypotheses i.e the null hypothesis H_0 or the alternative hypothesis H_1 is more likely given the *experimental data* (H_0 : there is no overall group difference, H_1 : there is overall group difference) (van Doorn et al., 2020). Bayes factors (BF) assessing the strength of evidence were presented, with 1-3 indicating weak evidence, 3-10 indicating moderate evidence and Bayes factors >10 indicating strong evidence in favour of H_1 (van Doorn et al., 2020). In the Bayesian ANCOVA analysis, the inclusion probability of each component (i.e., model term) was computed across a number of different models; a) the null model, b) a model containing a single predictor variable and c) a model containing both predictor variables. The Bayes factor BF_M indicating the change from prior to posterior model odds is

reported as well as the effect size. Bayesian statistics were conducted using the free software JASP (JASP Team, 2017).

Figure 4.8

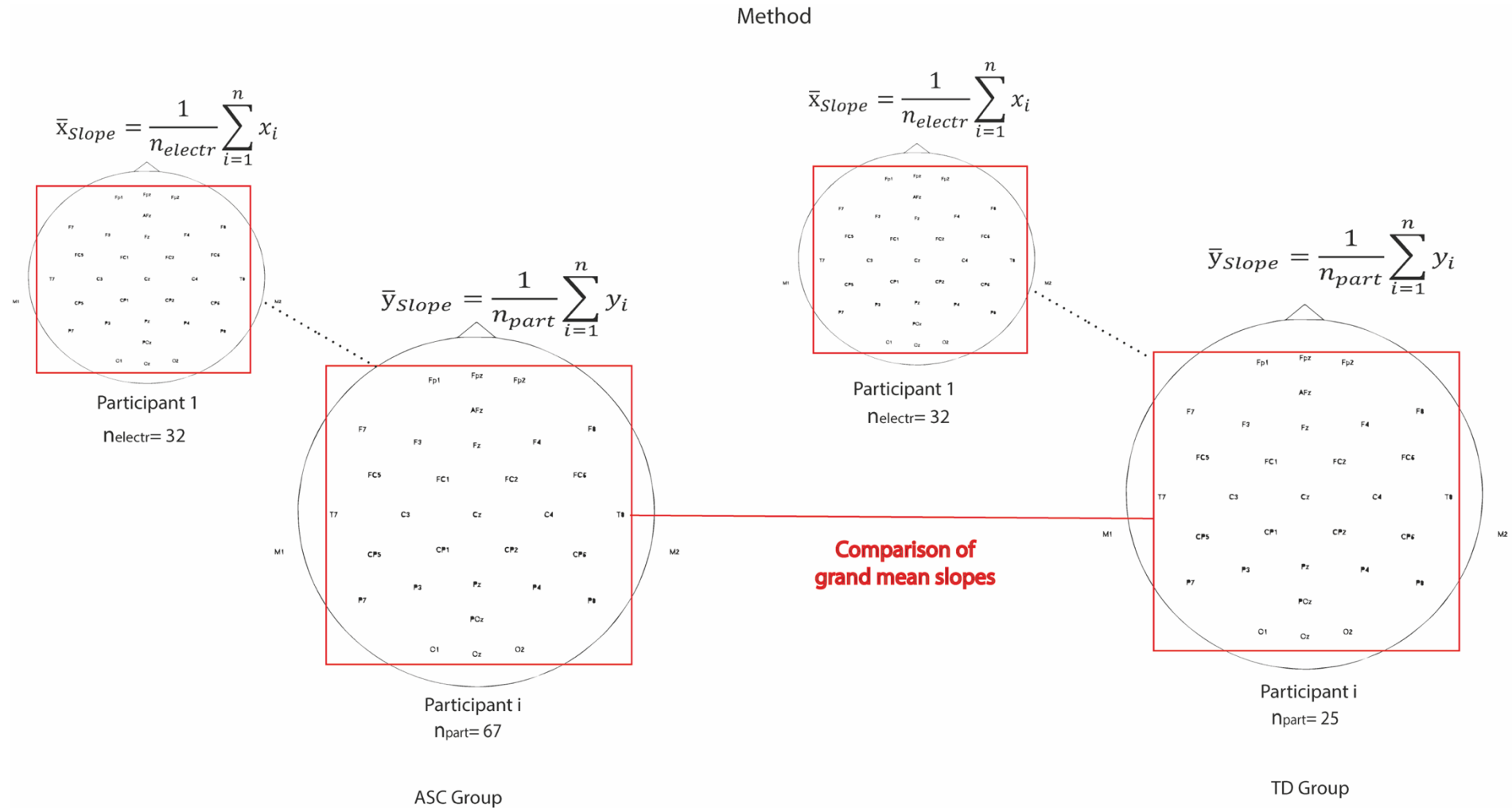


Figure 4.8: Method 1 involved a) computing the mean slope of all 32 electrodes for every participant in the ASC and TD group, b) calculating the grand mean slope for each group and c) comparing the grand mean slopes.

4.3 Results

4.3.1 Group comparisons: Inter-Trial Phase Coherence

Independent Component Analysis

Descriptive statistics of the maximum ITPC extracted from the Independent Components presented for the ASC ($n=65$) and TD groups ($n=25$) is presented in *Table 4.6*.

Table 4.6

Mean values (M) and Standard Deviations (SD) of the max ITPC extracted from the Independent Components presented for the ASC and TD groups

	ASC ($n=65$)		TD ($n=25$)	
	<i>M</i>	<i>SD</i>	<i>M</i>	<i>SD</i>
Max ITPC ^a	0.77	0.13	0.86	0.09

^aMax ITPC, Maximum Inter-Trial Phase Coherence extracted from the Independent Components

Kendall's tau-b correlation analysis was performed to determine the relationship between age and ITPC (*Figure 4.9*). The correlation analysis was performed a) for all participants and b) the two groups ASC and TD separately. Age and ITPC were not found to be associated in the full sample ($\tau_b=0.10, p=0.18$). The two variables were correlated in the TD group ($\tau_b =0.35, p=0.02$) but not in the ASC group ($\tau_b =0.14, p=0.12$).

Figure 4.9

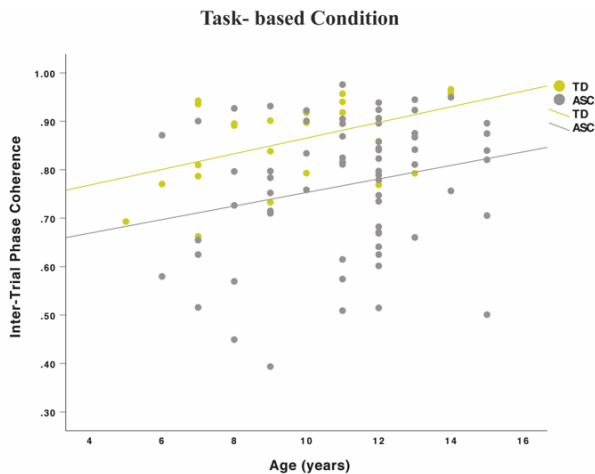


Figure 4.9: Scatterplot of age and maximum ITPC computed from the task-based data and plotted for the ASC and TD group.

Additionally, Kendall’s tau-b correlation analysis was performed to determine the relationship between Performance IQ and ITPC (*Figure 4.10*). Performance IQ and ITPC were not found to be associated in the full sample ($\tau_b=0.10, p=0.16$). When analysis was performed on the specific groups, the two variables were not found to be statistically dependent, neither in the TD group ($\tau_b=0.07, p=0.64$) nor in the ASC group ($\tau_b=0.00, p=0.98$) (see *Table 4.7*). Taking into account the above results, we accounted for the effect of age but not IQ in the group comparisons.

Figure 4.10

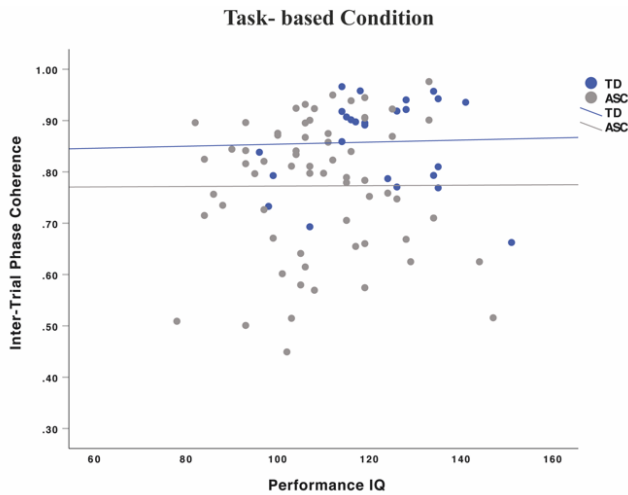


Figure 4.10: Scatterplot of Performance IQ and maximum ITPC computed from the task-based data and plotted for the ASC and TD group.

Average maximum ITPC maps computed separately for the ASC and TD group are presented in *Figure 4.12* (also see *Annex 9* for maximum ITPC heat maps for all participants in the two groups). Exploration of the ITPC boxplots revealed that the ASC group was characterized by a larger range, standard deviation and variance compared to the TD group (*Figure 4.11*). Levene’s test for equality of variances indicated that the two groups were characterized by unequal variances ($F(88)=4.35, p=.04$). The data in both the ASC and TD group were not normally distributed as indicated by the Kolmogorov-Smirnov (ASC: $D(65)=0.94, p=0.04$) and the Shapiro-Wilk test of normality (TD: $W(25)=0.91, p=0.03$). Square root-transformation of the data did not change ITPC distributions sufficiently (TD: $W(25)=0.90, p=0.02$, ASC: $D(65)=0.13, p=0.00$).

Because the TD group was younger, on average, than the ASC group, a one-way ANCOVA was performed so that age can be added as a covariate in the linear model. This analysis allowed us to evaluate whether maximum ITPC differs across groups, while also adjusting by the confounding variable “age”. Assumptions that underlie the use of ANCOVA were met.

Inspection of the “age” vs “ITPC” scatterplots, split by group, indicated that the strength and direction of association between the covariate and the outcome variable were similar across the two groups. Regression slopes were homogeneous and the covariate “age” was shown to be independent from the categorical predictor variable “group”. As expected, “age” significantly adjusted the association between “group” and “ITPC” ($F(1,87)=6.35, p=0.01$). Further to this, the corrected model indicated that there were statistically significant differences in ITPC between the two groups when controlling for age effects and that the effect size of this result was large ($F(1,87)=7.53, p=0.00, \text{partial } \eta^2 = 0.15$).

The Bayesian ANCOVA compared a few models with varying predictors of ITPC: a) a null model, b) a model containing only “age” as a predictor, c) a model containing only “group” as a predictor and d) a model containing both “group” and “age” as predictors. Only models c and d had their model odds increased after observing the data ($BF_M=0.96$ and $BF_M=7.27$ respectively). To account for model uncertainty, we performed Bayesian model averaging to test the effects of both predictors. The data were 19.05 times more likely under models containing “group” as a predictor but only 2.6 times as likely when including “age”, demonstrating that Bayesian analysis was in line with frequentist statistical analysis.

Figure 4.11

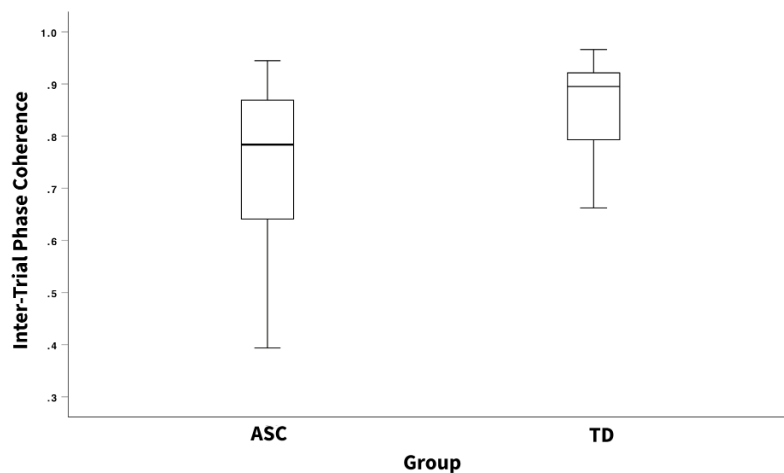


Figure 4.11: Boxplots of maximum ITPC for the ASC and TD group, showing differences in central tendency between groups.

Figure 4.12

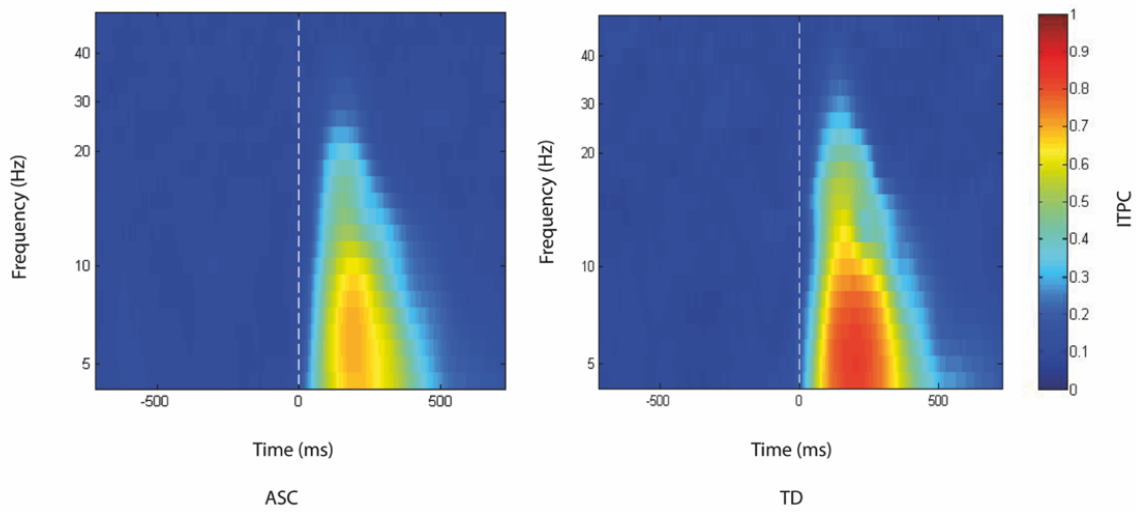


Figure 4.12: Average maximum ITPC maps computed for the ASC and TD group.

Maximum ITPC extracted from the Independent Components was observed primarily in the theta band (4-7Hz) in both groups (Figure 4.13). Maximum ITPC occurred at 4Hz for the majority of participants (ASC: 45%, TD: 56%). However as illustrated in Figure 4.13, for the ASC group it covered a wider range of frequencies compared to the TD group. An independent samples t-test indicated that the mean frequency where maximum ITPC was captured was significantly different between groups ($t(78.47)=-2.05, p=0.04$). Bayes factors indicated that this finding was equally likely under both hypotheses H_0 and H_1 ($BF_{01}=1.39$).

Table 4.7

Mean values (*M*), Standard Deviations (*SD*), Minimum (*Min*) and Maximum (*Max*) of the frequency, where maximum ITPC occurred at, presented for the ASC and TD groups

	ASC (<i>n</i> =65)				TD (<i>n</i> =25)			
	<i>M</i>	<i>SD</i>	<i>Min</i>	<i>Max</i>	<i>M</i>	<i>SD</i>	<i>Min</i>	<i>Max</i>
Frequency	5.70	2.13	4	14	4.99	1.14	4	8

Figure 4.13

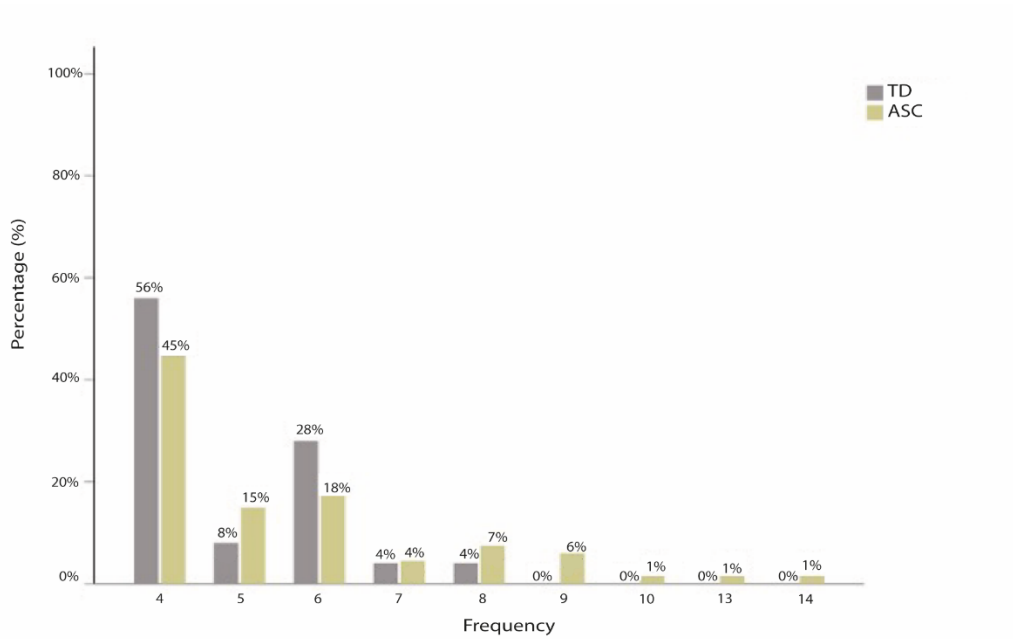


Figure 4.13: Frequency (Hz) where maximum ITPC was observed for the TD and ASC group.

Channel Analysis

Descriptive statistics for the two groups are presented in Table 4.8.

Table 4.8

Mean values (*M*) and Standard Deviations (*SD*) of the max ITPC extracted from the occipital electrode cluster, presented for the ASC and TD groups

	ASC (<i>n</i> =67)		TD (<i>n</i> =25)	
	<i>M</i>	<i>SD</i>	<i>M</i>	<i>SD</i>
Max ITPC ^a	0.72	0.11	0.78	0.10

^aMax ITPC, Maximum Inter-Trial Phase Coherence

Parametric test assumptions were partially met. Outliers were not detected in the data (see Figure 4.14). Levene’s test for equality of variances indicated that the groups were characterised by equal variances ($F(1,90)=0.23, p=0.63$). Although the data were approximately normally distributed in the ASC group ($D(67)=0.07, p=0.20$), the data were not normally distributed in the TD group, as shown by the Shapiro-Wilk test ($W(25)=0.92, p=0.04$). Square root-transformation of the data did not change ITPC distributions sufficiently (TD: $W(25)=0.91,$

$p=0.02$, ASC: $D(67)=0.08$, $p=0.20$). ANCOVA-specific assumptions were met; regression slopes i.e the covariate coefficients were homogeneous and the interaction term between the covariate “age” and the categorical predictor variable “group” was not significant.

Considering the above, a one-way ANCOVA was performed to assess whether maximum ITPC extracted from the selected electrodes differs across the ASC and TD groups, while also adjusting for age. This analysis showed that the covariate “age” was not significantly adjusting the association between “group” and “ITPC” ($F(1,89)=0.26$, $p=0.60$). The corrected model showed that there was a statistically significant effect of the “group” variable on levels of ITPC, after controlling for “age” ($F(1,89)=3.39$, $p=0.03$).

Bayesian analysis of covariance was also performed on ITPC values with “group” added as a fixed factor and “age” as a covariate. As above, the Bayesian ANCOVA compared a few models with varying predictors of ITPC: a) a null model, b) a model containing only “age” as a predictor, c) a model containing only “group” as a predictor and d) a model containing both “group” and “age” as predictors. Only the model containing “group” as a predictor had their model odds increased after observing the data ($BF_M=5.45$). Bayesian model averaging demonstrated that the data were 3.94 times more likely under models containing “group” as a predictor but only 0.23 times as likely when including “age”. This is in line with frequentist statistics, which demonstrated that the effect of “age” was negligible and that the main effect of “group” was significant.

Figure 4.14

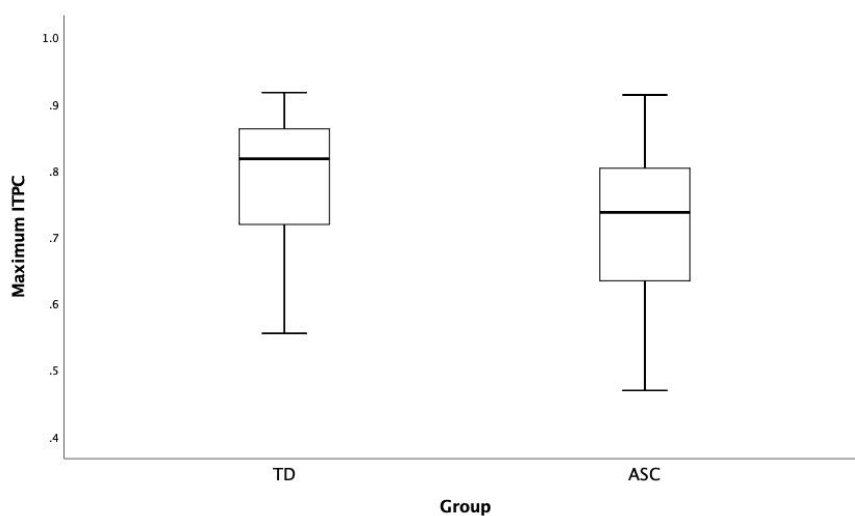


Figure 4.14: Boxplots of maximum ITPC for the TD and ASC (range of values= 0-1), showing differences in central tendency between groups.

For the majority of participants in both groups, maximum ITPC was observed at the electrode O2 (TD: 40%, ASC: 39%) and in the theta (4-7Hz) frequency band (TD: 91%, ASC: 60%) (see *Figure 2.14, Figure 2.15*). For 47% of the TD group, maximum ITPC occurred at 4Hz ($M=5.28$, $SD=1.46$). In contrast, the ASC group showed a very different frequency profile; for the majority of participants maximum ITPC occurred either at 4Hz (19%) or 7Hz (19%) but for many participants it was captured at higher frequency bands (i.e alpha and beta), as compared to the TD group ($M=7.52$, $SD=5.28$). An independent samples t-test indicated that the frequency where maximum ITPC was captured was significantly different between groups ($t(90)=1.01$, $p=0.00$). In line with this analysis, Bayes factors showed that this was strong evidence for the alternative hypothesis H_1 i.e there is a difference between groups ($BF_{01}=0.03$).

Figure 4.15

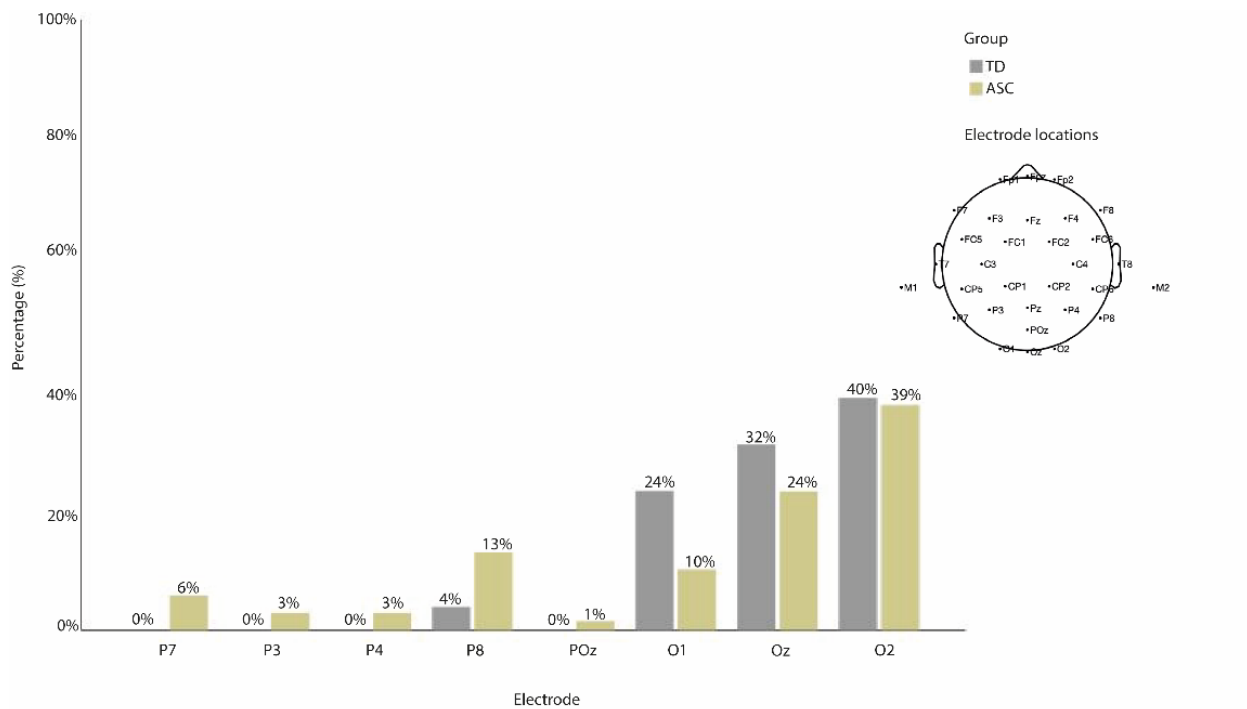


Figure 4.15: Electrode where maximum ITPC was captured for each group, TD and ASC.

Figure 4.16

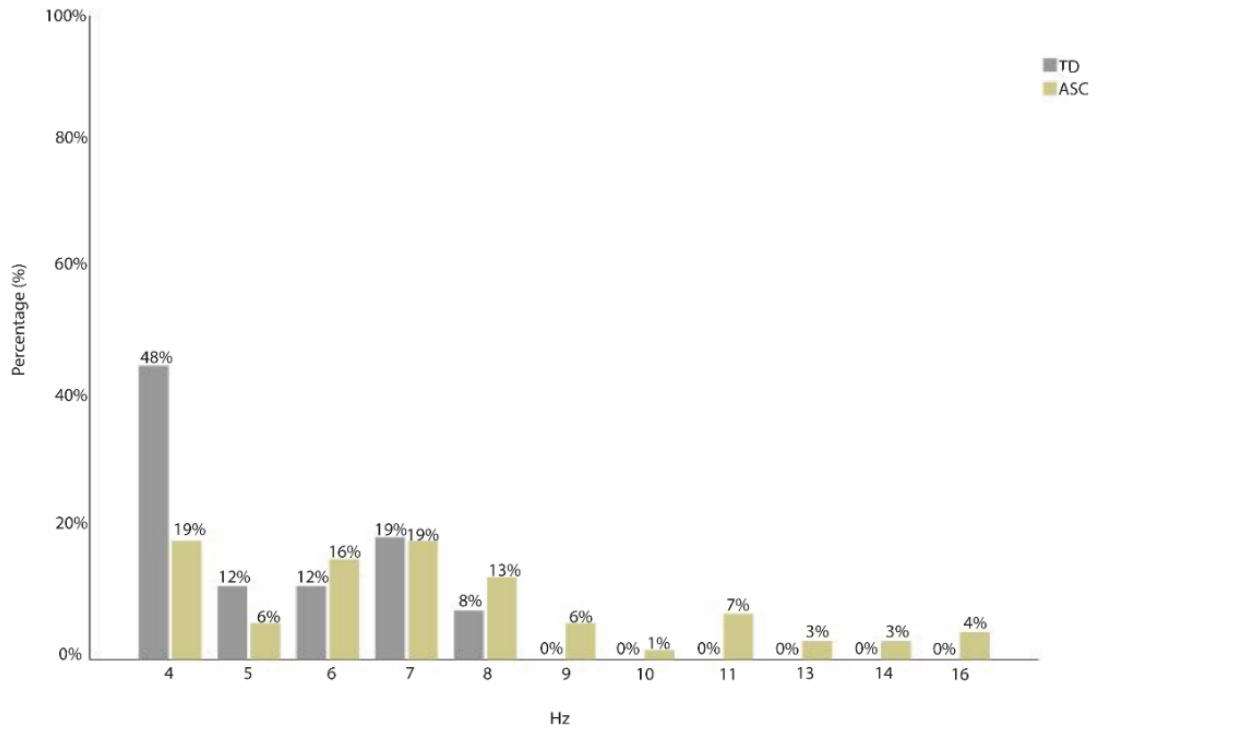


Figure 4.16: Frequency (Hz) where maximum ITPC was observed for each group, TD and ASC.

4.3.2 Group comparisons: 1/f noise of Power Spectral Density

Descriptive statistics of the 1/f slope of PSD for the two groups ASC (Task-based condition: $n=67$, Resting state condition: $n=62$) and TD ($n=25$) are presented in Table 4.9.

Table 4.9

Mean values (M), Standard Deviations (SD), Minimum (Min) and Maximum (Max) of the 1/f slope of PSD computed for the task-based and resting-state condition, for the ASC and TD group

	ASC ($n=67, n=62$)				TD ($n=25$)			
	M	SD	Min	Max	M	SD	Min	Max
Task-based EEG: 1/f Slope	-0.07	0.01	-0.1	-0.04	-0.07	0.01	-0.09	-0.05
Resting-state EEG: 1/f Slope	-0.07	0.02	-0.12	-0.04	-0.08	0.02	-0.11	-0.05

Kendall's tau-b correlation analysis was performed to determine the relationship between age and the average 1/f slope of PSD computed from the task-based and the resting state data (see Figure 4.17). In the task-based condition, age and 1/f slope were correlated in the full sample ($\tau_b=0.41, p=0.00$). Further analysis showed that the two variables were associated in both the ASC ($\tau_b=0.36, p=0.00$) and the TD group ($\tau_b=0.41, p=0.01$).

In the resting state condition, age and 1/f slope of PSD were positively correlated in the full sample ($\tau_b=0.45, p=0.00$). Similarly, the two variables were found to be statistically dependent in the ASC ($\tau_b=0.40, p=0.00$) and TD group ($\tau_b=0.49, p=0.00$).

Figure 4.17

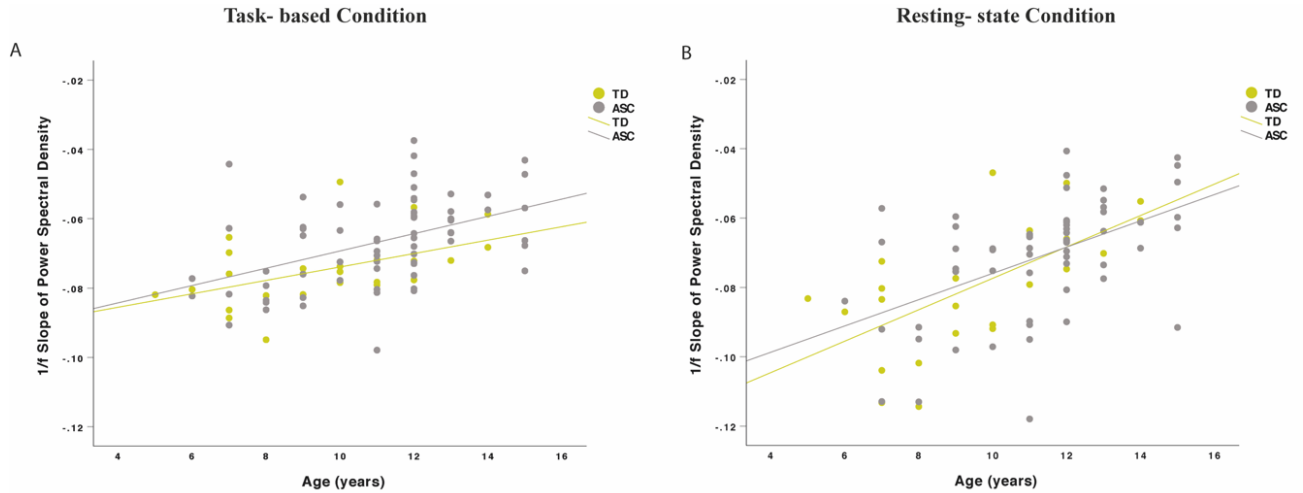


Figure 4.17: Scatterplots of age and average 1/f slope of PSD computed from the task-based (A) and resting state data (B) plotted for the ASC and TD group.

Kendall's tau-b correlation analysis was also performed to determine the relationship between Performance IQ and the average 1/f slope of PSD computed from the task-based and the resting state data (see Figure 4.18).

In the task-based condition, Performance IQ and 1/f slope were not correlated in the full sample ($\tau_b=-0.09, p=0.24$). Further analysis showed that the two variables were not associated, neither in the ASC ($\tau_b=0.03, p=0.75$) nor the TD group ($\tau_b=-0.13, p=0.37$).

In the resting state condition, Performance IQ and 1/f slope of PSD were not correlated in the full sample ($\tau_b=-0.12, p=0.11$). Similarly, the two variables were not found to be correlated in the ASC ($\tau_b=-0.03, p=0.74$) and TD group ($\tau_b=-0.24, p=0.09$).

Given that age and the average 1/f slope of PSD were associated in both conditions but Performance IQ and the average 1/f slope of PSD were not, we accounted for the group difference in age but not IQ in all subsequent analyses.

Figure 4.18

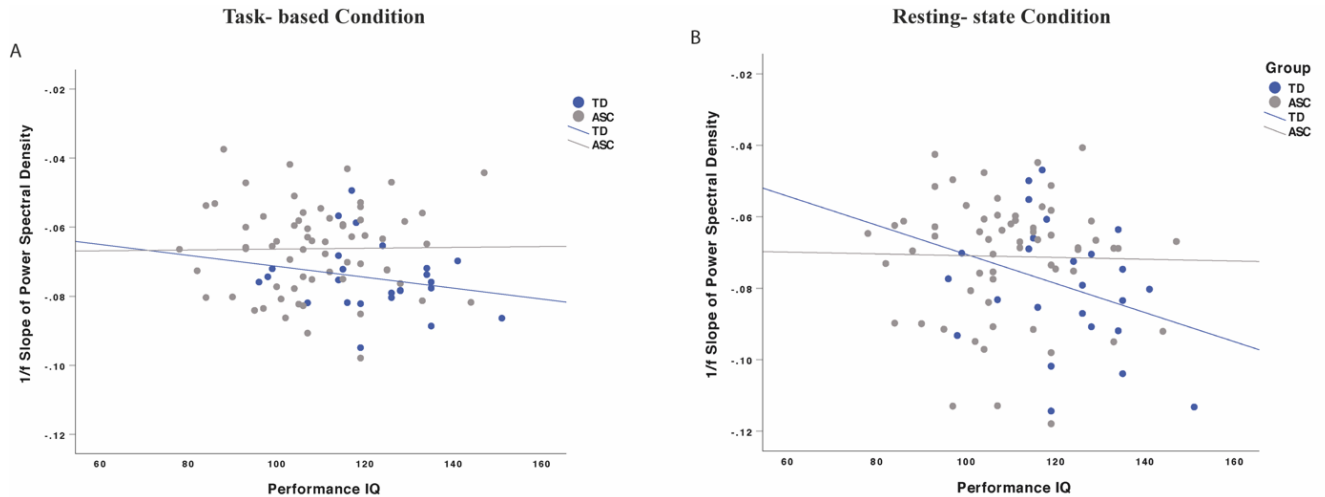


Figure 4.18: Scatterplots of Performance IQ and average 1/f slope of PSD computed from the task-based (A) and resting state data (B) plotted for the ASC and TD group.

The two groups had equal variances as determined by the Levene’s test (Task-based Condition: $F(90)=3.49$, $p=0.06$, Resting-state Condition: $F(85)=0.22$, $p=0.64$). The Kolmogorov-Smirnov test showed that the resting state data of the ASC group were not normally distributed (Task-based condition: $p=0.20$, Resting-state condition: $p=0.00$), however the data of the TD group were shown to be normally distributed in both conditions (Task-based condition: $p=0.40$, Resting-state condition: $p=0.91$). In line with the ITPC finding, the boxplots in the task-based condition indicated that the ASC group was characterized by a larger range, standard deviation and variance compared to the TD group (Figure 4.19). Although extreme outliers were not present, 1/f slope values for four participants within the TD group in the task-based condition and two participants within the ASC group in the resting state condition were falling below the interquartile range of the third quartile (Figure 4.19). Further analysis showed that those values did not have a significant impact on the group comparisons outcome and for that reason they were included in the ANCOVA analysis.

In both the task-based and resting state condition, a one-way ANCOVA was performed to compare mean 1/f slope in the ASC and TD group, whilst controlling for the confounding effects of age, a variable added as a covariate in the linear model. Scalp maps representing the 1/f slope measured from all electrode locations for the ASC and TD group in the two conditions are presented in Figure 4.20. Neither in the task-based condition nor in the resting state condition the model indicated any significant differences between groups (Task-based condition: $F(1,89)=3.09$, $p=0.08$, Resting state condition: $F(1,84)=0.13$, $p=0.71$). Similarly, Bayesian analysis showed that only the model including “age” and the model containing both “age” and

“group” as predictor variables had their model odds increased in light of the experimental data ($BF_M = 2.90$ and $BF_M = 3.09$ respectively). Bayesian model averaging demonstrated that the data were 7339.47 times more likely under the model containing “age” as a predictor but only 1.03 times as likely when including “group”. Considering both analyses, it is therefore concluded that 1/f slope of PSD is not different in the ASC group as compared to the TD group but age is a predictor of the steepness of 1/f slope.

Figure 4.19

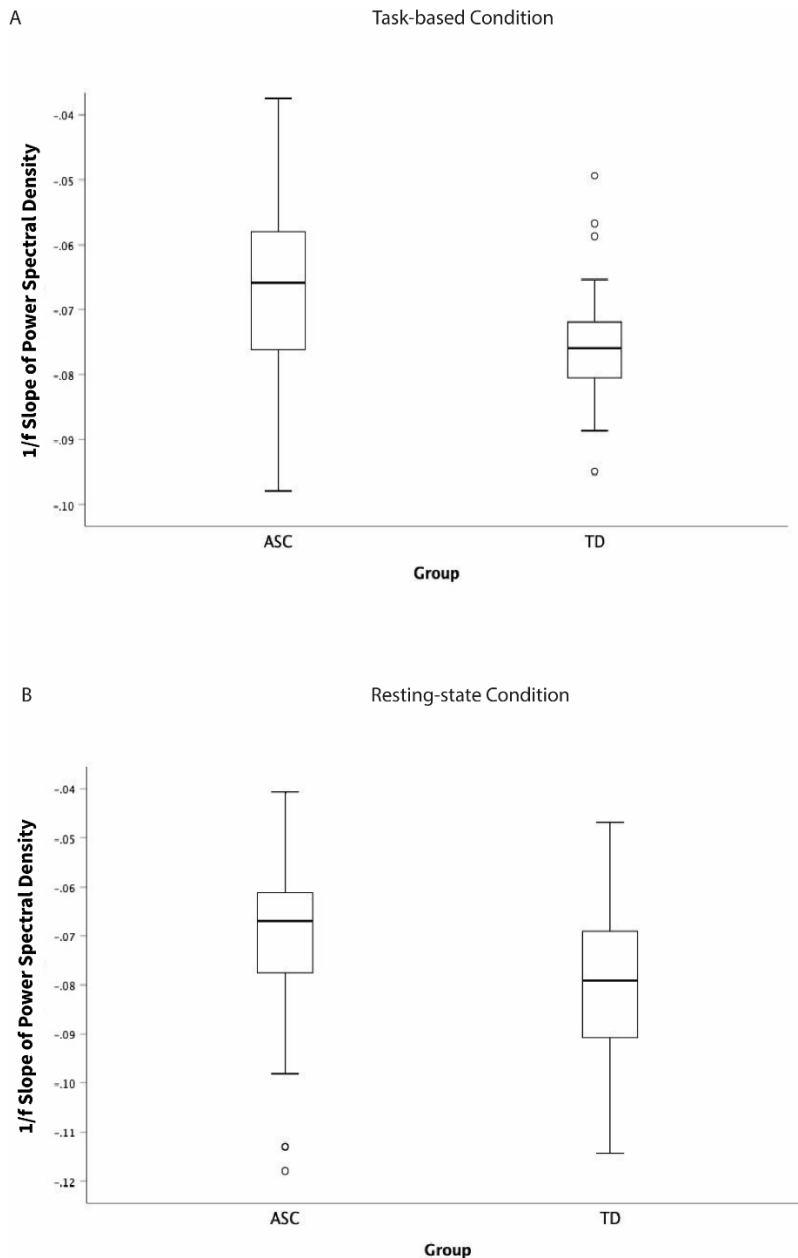


Figure 4.19: Boxplots of 1/f slopes for the two groups, ASC and TD, in the task-based (A) and resting-state condition (B).

Figure 4.20

1/f slopes

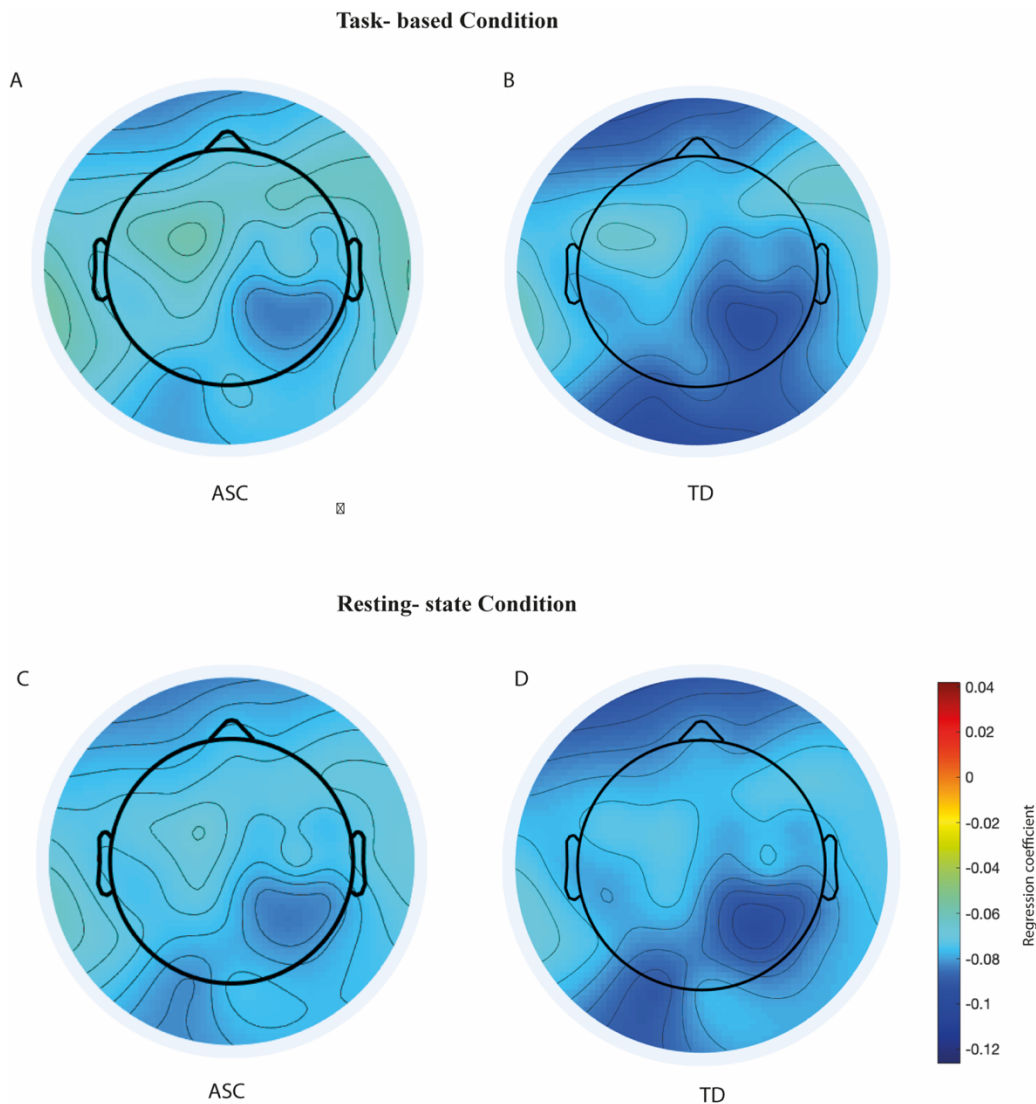


Figure 4.20: Scalp maps representing the mean slope computed from different electrode locations for the ASC (A) and TD group (B) in the task-based condition and for the ASC (C) and TD group (D) in the resting-state condition.

In addition to the analysis presented in Sections 4.3.1 and 4.3.2, the relationship between neural noise and comorbid conditions was further examined in the samples tested (*Appendix 1*). Inspection of the scatterplots of ITPC and 1/f noise of PSD did not reveal any clear relationship between variables indexing neural noise and the number and type of comorbid condition in the ASC group (see *Figure 1* in *Appendix 1*).

4.4 Discussion

The present study aimed to investigate whether the atypical patterns of neural noise observed in adults with ASC in Chapter 2 are also observed in children with ASC. Following a similar method to the study outlined in Chapter 2 and benefitting from home-testing protocol described in Chapter 3, neural noise was measured by computing ITPC and changes in 1/f slope of PSD in a visual task condition, involving the presentation of checkerboard stimuli. Consistent with the experimental approach followed in Chapter 2, 1/f slope was also computed in a resting-state condition. In the present study, the ASC group consisted of somewhat older children with lower cognitive abilities compared to the TD group. Further analysis showed that age significantly correlated with 1/f slope of PSD and ITPC, so it was controlled for in the group-comparison analysis. After controlling for age effects, maximum ITPC, as extracted from both selected ICs and electrodes, was significantly lower in the ASC group compared to the TD group. In addition, it covered a wider range of frequencies from theta to beta rhythms for the ASC participants, in contrast to the TD participants, whose strongest ITPC was consistently found in the theta and alpha band. With regards to the 1/f analysis, ASC participants did not show differences at a group level in the steepness of 1/f slope of PSD compared to the TD participants, neither in the task-based nor in the resting state condition.

Using a similar experimental approach and method of quantifying neural noise to previous chapters, the current study established that increased levels of neural noise, demonstrated as reductions in ITPC, manifest in children and adolescents with ASC. This result agrees with previous accounts of low ITPC during visual processing in groups of children and adolescents with ASC (Milne, 2011). In line with the findings of the present study, Milne (2011) report reduced alpha ITPC in children with ASC during visual processing of Gabor patches and Milne et al. (2019) in adults with ASC during processing of checkerboard stimuli. The authors conclude that low ITPC is capturing atypical neural features prominent in the brain of some individuals with ASC, indicating that reduced ITPC is likely to be one of many neurological features that is associated with ASC. On the other hand, EEG studies such as the one conducted by Butler et al. (2017), in an effort to replicate the study by Milne (2011), do not report differences in levels of ITPC between groups. As discussed in Chapter 2, the lack of consistency in experimental findings can be partially explained by ASC heterogeneity, which often results in disparate findings in groups of participants with a clinical diagnosis of ASC and the small sample sizes ranging from 11-20 participants for the aforementioned studies (Button et al., 2013).

For the ASC group the strongest phase-alignment was observed in a wide range of frequencies ranging from low theta to low beta (4-16Hz), whereas for the TD group maximum ITPC occurred in the theta and alpha band (4-8Hz) alone. Through the coordination of local and regulation of inter-regional neuronal interactions, slow oscillations are “context-defining” and play a fundamental role in early sensory encoding and attention (Palva, Palva & Kaila, 2005). Therefore, strong phase entrainment of theta/low alpha oscillations may reflect dynamic visual input processing, which is stimulus-driven (Kietel, Thut & Gross, 2017). Given that alpha oscillations are biasing the probability of a weak signal to be detected, subsequently enhancing the attended stimulus, strong phase-alignment of alpha rhythms may also indicate a greater effort to suppress unattended stimuli (Palva & Palva, 2011; Zareian et al., 2020; Lemi et al., 2021).

The fact that a small number of participants with ASC demonstrated strong phase-locking in the beta rhythm, captured consistently at the electrode O2 in the channel analysis, is striking. Beta oscillations are previously shown to exert top-down influences on the visual cortices (i.e from high to low-order visual areas or from fronto-parietal to visual cortices) (Spitzer & Haegens, 2017; Richter, Coppola & Bressler, 2018) and to be associated with functional aspects of sensory gating (Kisley & Cornwell, 2006), sensorimotor coordination (Kilavik et al., 2013) and working memory (Kulashekhar et al., 2016). It is possible that stronger alignment of the phase of beta oscillations in areas in close proximity to the visual cortices indicate greater effort to maintain the current sensorimotor state of the brain (Engel & Fries, 2010) and highlight if the visual stimulus presented on the screen is novel or salient (Kisley & Cornwell, 2006). Another possibility is that beta oscillations strongly align their phases in preparation of the movement execution i.e spacebar presses in anticipation of the deviant spaceship stimulus (see Kilavik et al. 2013), therefore strong phase-locking may reflect contextual gating of information related to visual action feedback (Limanowski, Litvak & Friston, 2020).

Building upon the above finding, it is still unclear what the primary biological source contributing to increased neural variability in the ASC group might be, however a few plausible theories have been suggested in the literature. Difficulties to synchronise the activity of neurons consistently across experimental trials may be explained by an increase in E/I ratio locally, resulting from a glutamatergic/GABA-ergic imbalance (Rubenstein & Merzenich, 2001). In an effort to maintain optimal information flow, this is likely to result into increased firing rates in local microcircuits of the visual cortex. Other lines of work suggest that astrocytes and microglia- two types of glial cells known to play a central role in synaptic formation and function- interfere with neural circuit development in ASC, affecting neural synchrony and connectivity (Kanner et

al., 2018; Rosso et al., 2018). Nonetheless, there is currently no experimental evidence directly linking the reductions in ITPC with the above theories. Oscillatory processes are dynamic in nature and phase-alignment of neural oscillations to a rhythmic stimulus can be affected by numerous factors such as pathophysiology, state of arousal, task characteristics and attention (Uhlhaas et al., 2009).

Despite the significant ITPC reductions at a group level, the steepness of 1/f slope of PSD did not differ between the ASC and TD group. Further to this and in contrast to the findings in adults with ASC presented in Chapter 2, we found a significant relationship between 1/f slope of PSD and age in the samples of children tested here, irrespective of whether they were in the ASC or TD group. This is in line with previous research by Dave et al. (2018) who found a significant relationship between 1/f slope and age in both younger and older adults and a flatter slope in the older group tested in response to two language comprehension tasks.

To our knowledge, this is the first study to explore 1/f properties of PSD in children with ASC. Here, we demonstrated that ASC participants show a 1/f slope of similar steepness to TD controls, a finding which replicates the result reported in adults reported in Chapter 2. As outlined in Chapter 2, this experimental finding contradicts theoretical accounts proposing that ASC is likely to be characterised by pathological undercoupling, involving an excess number of temporally decorrelated spikes occurring in the background.

A number of limitations characterise the research work summarised here. The present study did not adopt common group-matching design approaches to eliminate confounding factors such as the effect of age and cognitive ability. However, we followed the approach suggested by Jarrold & Brock (2004) as optimal in ASC and assessed the extent to which significant group differences occur after controlling for the factors interacting with the variable of interest (i.e age). In addition, this methodology allowed us to deal with the problem of the large sampling interval ranging from 6 to 15 years old for the ASC group and 5-14 years old for the TD group and statistically account for the significant difference in age between groups in the analysis. Another limitation relates to the use of carer-reported measures to confirm ASC diagnostic status and obtain information about participants' comorbid conditions as well as drug intake. This information was acquired from carers, who were instructed to complete a number of questionnaires online via the platform Qualtrics. Therefore, we cannot rule out response biases related to tiredness, distraction and/or confusion when interpreting the questions but also personal attitudes affecting perceptions of the child's behaviour. Nevertheless, this study design allowed us to balance clinical accuracy

and speed of data acquisition. A strength of the present study is the inclusion of a large number of participants with ASC ($n=67$), which would not be possible if tools requiring longer administration time had been employed. Future work however should incorporate direct measures of evaluation to confirm both ASC symptom severity and comorbidity status.

An important next step for future research is to explore whether low ITPC is linked to a specific aspect of the ASC behavioural phenotype. Theoretical accounts propose that increased neural noise in the sensory systems explain individual differences in sensory sensitivities (Simmons et al., 2007). However, previous studies investigating neural noise in the form of low ITPC have not provided adequate mechanistic insight on this process. Milne et al (2019) demonstrated that although increased neural noise, measured in the form of low ITPC is observed in the cortex in response to visual stimulation, these variables are not associated with core diagnostic domains of ASC as assessed by the Social Responsiveness Scale (SRS-2, Constantino & Gruber, 2011) and the Adult Repetitive-Behaviors Questionnaire (RBQ-2A, Barrett et al., 2015). Despite the fact that the study was designed to evoke neural responses in the sensory cortices, Milne et al. (2019) did not investigate the relationship between neural noise and sensory sensitivity, an integral aspect of the ASC phenotype. It still unknown how neural noise manifests in relation to the subjective sensory experience and/or behavioural sensitivity to the sensory stimuli presented. Particularly with regards to ITPC, more evidence is needed to understand whether low ITPC in response to sensory stimuli is associated with sensory sensitivities in ASC. The relationship between neural noise and autism symptoms, including sensory symptoms, will be directly investigated in Chapter 5.

Chapter 5:

The relationship between neural noise and the Autism Spectrum Conditions (ASC) phenotype

5.1 Introduction

ASC includes large variations in clinical profiles, often explained by distinct genetic etiologies (Betancur, 2011). There is now growing recognition that ASC is a heterogeneous condition (Happé & Ronald, 2008) and the phenotypic traits associated with it are the result of a complex interaction between genetic and environmental factors (Bill & Geschwind, 2009). The identification of autism subtypes or subgroups that share common genetic causes has been suggested as an alternative approach to the current classification system (Grzadzinski et al., 2013) ultimately allowing for more targeted interventions and predictive power over treatment outcomes. In order to disentangle the complex relationship between genotype and phenotype in ASC and understand how gene-environment interactions give rise to such variable clinical manifestations, it is paramount to understand individual differences. A more dimensional approach, linking phenotypic variations with distinct patterns of neural functioning could potentially aid the discovery of endophenotypes, a subset of heritable biological traits indicative of genetic vulnerability to ASC (Beauchaine & Constantino, 2017).

5.1.1 Neural variability as a marker of ASC

Although on a theoretical basis, it has been previously suggested that ASC may be associated with flatter $1/f$ noise slope of PSD, indicating pathological undercoupling of oscillatory dynamics, evidence provided in previous experimental chapters showed that visual-evoked and resting state electrophysiological responses of participants with ASC are not characterized by a flatter $1/f$ slope of PSD compared to typically developing and ADHD participants. In two separate experimental studies (Chapter 2 and Chapter 4), the slope of the $1/f$ noise function did not differ between individuals with and without ASC. No other studies have previously investigated $1/f$ noise dynamics in ASC, meaning that these results should be generalized with caution. Nevertheless, the above evidence suggests that $1/f$ slope of PSD is unlikely to be capturing neurophysiological underpinnings that are distinct in ASC, therefore it may not be meaningful to examine the variable in the context of a neural signature of ASC.

On the other hand, multiple lines of research have shown that ASC is associated with excessive neural noise in the form of low ITPC. This is a well-replicated finding both in the present thesis and in the wider literature, raising the question of whether it could indeed serve as a valid marker of ASC (David et al., 2016). Reduced ITPC is observed in response to a wide range of cognitive tasks targeting the visual and auditory modality. In the visual domain, Milne (2011) and Milne et al. (2019) report low ITPC in children and adults with ASC during low level visual stimulation.

This is in line with Edgar et al. (2015) and van Noordt et al. (2017), who also found that ITPC reductions occur in response to tones of various frequencies and during feedback processing of rewards and errors respectively. Nevertheless, contrasting evidence is coming from Butler et al. (2017) and Yu et al. (2018) (see *Table 1.1* of Chapter 1 for an overview of studies measuring ITPC in ASC and Section 1.5.5 for a discussion of studies investigating ITPC in clinical ASC samples). In summary, low ITPC is reported in the majority of the studies investigating electrophysiological dynamics in ASC.

Despite these promising first findings, a closer inspection of the existing literature reveals that ITPC may not meet the target levels of sensitivity and specificity to be utilised as a diagnostic tool. In previous chapters it was demonstrated that participants with ASC exhibit significantly lower ITPC in response to repeated visual stimulation at a group level as compared to an ADHD and a typically developing group, both in childhood and adulthood. After careful examination of the ITPC distributions, it is evident that at an individual level, some participants with ASC demonstrate low ITPC but other participants exhibit similar levels of ITPC to controls, a consistent finding suggesting that the variable may not be possible to accurately differentiate between participants with and without ASC, despite differing between those with and without ASC at a group level. This is in line with a growing body of literature speaking against a single neural profile underlying ASC (Milne et al., 2019) but rather recognizes the existence of sub-groups within the autism spectrum with clear neurological differences (Ousley & Cermak, 2014). Along this argument and as it was demonstrated above, difficulties to synchronise the activity of local neurons consistently from trial to trial are reported in some ASC studies but not all. Increased neural variability in the form of low ITPC only characterises electrophysiological responses of a subgroup of individuals with ASC. Regarding the specificity of the neural correlate, low ITPC in response to sensory stimulation is also reported in multiple studies in schizophrenia. For instance, patients with schizophrenia have shown reduced alpha band phase-locking at occipital brain regions in response to repeated visual stimulation (Basar-Eroglu et al., 2008) and reduced gamma band phase-locking in response to both auditory (Light et al., 2006; Perez et al., 2013; Tada et al., 2014) and visual stimulation (Koychev et al., 2011).

Therefore, it may not be meaningful to study ITPC in the context of an ASC marker as it lacks the relevant sensitivity and specificity to a single disorder, but rather in the context of a transdiagnostic marker that cuts through diagnostic boundaries and is linked to clusters of symptoms common in a number of conditions. Most importantly, the transdiagnostic marker may be indicative of subgroups within clinical groups characterised by neural substrates and

phenotypic traits, that are unique to, or more prevalent, in that subgroup. Linked to this, a common phenotypic feature amongst the aforementioned clinical groups exhibiting low ITPC is the sensory perceptual abnormalities. Sensory symptoms are well-documented in both ASC and schizophrenia. Sensory overload (Jones et al., 2003; Javitt & Freedman, 2015), heightened perception (Ashburner et al., 2013; Javitt & Freedman, 2015; Zeljic et al., 2021), hallucinations (Waters et al., 2014), sensory distortions (Bogdashina, 2003; Davis et al., 2006), altered local-global processing (Coleman et al., 2009; van der Hallen et al., 2016), are only some of the sensory perceptual abnormalities regularly reported in both conditions. It is yet to be confirmed whether the presence of more severe sensory symptoms explains why some participants exhibit low ITPC as compared to participants that exhibit high ITPC. Further research is necessary to test this theory; first establish whether a relationship between sensory symptoms and neural variability exists and secondly investigate whether the neural correlate can be used to identify subgroups with unique brain-behaviour ‘fingerprints’ within and across clinical groups.

5.1.2 Neural variability and the ASC phenotype

A few studies have previously explored the relationship between neural variability and core ASC symptoms but yielded inconsistent results. For example, Dinstein et al. (2012) found moderate correlations between ASC symptom severity, as assessed by the Autism Diagnostic Observation Schedule (ADOS), and SNRs in three sensory domains, visual ($r=-0.24$), somatosensory ($r=-0.3$), auditory ($r=-0.36$), providing some evidence that a relationship between trial to trial neural variability and ASC phenotypic severity may be present- although this result did not reach significance, possibly due to sample size related limitations ($n=14$). In support of this hypothesis, Ethridge et al. (2017) showed that decreased gamma band phase-locking in response to auditory stimuli was associated with behavioural measures of sensory sensitivities and social communication impairments in a Fragile X Syndrome sample, a single-gene disorder known to be linked with high rates of ASD comorbidity (Belmonte & Bourgeron, 2006). In contrast to these findings, a recent, larger-scale and more statistically powerful study by Milne et al. (2019) found no association between ITPC and cardinal ASC features, including social communication difficulties and repetitive and restricted patterns of behaviour, contradicting the above results. This study however did not measure sensory symptoms in detail.

A key limitation of the above studies is that they use a wide variety of neuroscientific methods (i.e EEG, fMRI) and different analytical approaches to measure neural variability (i.e. ITPC, PLF, SNRs etc). Linked to this, Milne et al. (2019) only examined the relationship between ITPC and the ASC phenotype in adults with ASC. In addition, as discussed in Chapter 2, the ASC

sample recruited by Milne et al. (2019) may not be entirely representative of the ASC profile. Therefore, an important next step would be to identify whether there is a relationship between ASC symptomatology and ITPC in a potentially more representative sample. It is also important to point out that no studies have previously investigated the relationship between 1/f slope of PSD and ASC symptoms. Given the inconsistencies of the literature and the gaps in knowledge, it is still unclear whether the severity of core diagnostic symptoms influence levels of neural noise, therefore more evidence is necessary to clarify this.

As shown above, a key aspect of the ASC phenotype that has not been previously studied in relation to neural variability, are the sensory symptoms. From a behavioural perspective, atypical response to sensory stimulation is a well-established finding in ASC research, shown to predict not only the severity of socio-communicative impairments and repetitive patterns of behaviours but also diagnostic outcomes (Turner-Brown et al., 2013). Atypical sensory processing is studied primarily in the realm of hyper-reactivity (e.g. aversion to lights, hypersensitivity to sounds, avoidance of tactile stimuli, other sensory avoiding behaviours) and hypo-reactivity to incoming sensory stimuli (e.g. diminished response to sensory information in the environment, insensitivity to pain, tolerance of extreme heat, cold or pressure, visual fascination with bright lights, other sensory seeking behaviours) (Baum et al., 2015). However, this framework is somewhat simplistic and limiting as other aspects of sensory perception are neglected and not integrated into the wider picture. Recently, anomalous perception has received attention, with findings suggesting that anomalous sensory experiences are highly prevalent in ASC (Milne et al., 2017). Those are assessed in the form of perceptual distortions, hallucinations and unusual sensory experiences covering a range of sensory domains.

In the visual modality, this new body of literature came to compliment findings about the increased vulnerability of subjects with ASC to pattern-induced illusions and visual distortions (Ludlow et al., 2006; Ludlow & Wilkins, 2016; Ludlow et al., 2020); a phenomenon widely known as sensitivity to pattern glare (Wilkins & Evans, 2001; Evans & Stevenson, 2008). Pattern glare, also known as “visual stress”, refers to a group of visuoperceptual symptoms experienced in response to striped and/or checkerboard patterns with specific spatial and temporal characteristics (Wilkins et al., 1984; Wilkins, 1995; Wilkins & Evans, 2001; Evans & Stevenson, 2008). These are taking the form of visual discomfort, headaches, eyestrain and illusions of colour, motion and/or shape (Evans & Stevenson, 2008). The strength of discomfort can vary and depends on parameters such as the properties of the visual image as well as the person’s susceptibility to pattern glare (Evans & Stevenson, 2008). Sensitivity to pattern glare is shown

to become greater when patterns have a spatial frequency greater than 3 cycles per degree (cpd), a 50% duty cycle and a high contrast (Wilkins et al., 1984; Wilkins, 1995; Evans & Stevenson, 2008, see *Figure 5.1*). Such images are “unnatural”, with greater contrast flicker and luminance structure deviating from the natural range i.e a Fourier amplitude spectrum of different slope and shape to that of natural images (Fernandez & Wilkins, 2008; Penacchio et al., 2015). *Figure 5.2* provides an example of natural and unnatural patterns in the environment; text is a common striped pattern known to be eliciting visual perceptual distortions (Wilkins et al., 2007). It has been further proposed that uncomfortable images are associated with inefficient encoding in the visual cortex manifesting as over-activation of neurons locally (O’Hare & Hibbard, 2011). A failure to modulate run-away excitation is suggested to be leading to an E/I imbalance, causing the symptoms of visual distortions and discomfort (Evans & Stevenson, 2008; Takarae & Sweeney, 2017). In support of this hypothesis, several studies have demonstrated that the magnitude of haemodynamic response in the visual cortex is greater when susceptible individuals are processing uncomfortable patterns (Migraine: Huang et al., 2003, Photophobia: Alvarez-Linera Prado et al., 2007, General population: Haigh et al., 2013; Haigh et al., 2015), requiring greater metabolic load and that the use of precision tints reduces the strength of cortical activation (Migraine: Huang et al., 2011). Multiple lines of research have now shown that coloured lenses and coloured overlays can alleviate symptoms of visual discomfort (Evans et al., 2002; Ludlow et al., 2008; Evans & Allen, 2016), potentially redistributing excitation in the visual cortex (Wilkins, 2021).

Linked to this, a closer look at the literature shows that Gabor patches and checkerboard stimuli are frequently used to trigger electrophysiological responses in ASC studies measuring ITPC (e.g. Milne, 2011; Milne et al., 2019). As demonstrated above, such visual patterns with high spatial frequency and high contrast are shown to cause increased discomfort and induce anomalous visual perceptual distortions in individuals susceptible to pattern glare (Wilkins & Evans, 2001; Evans & Stevenson, 2008). Additionally, it has been previously established that those symptoms are more prevalent in some clinical groups such as patients with photosensitive epilepsy (Wilkins et al., 1975; Soso et al., 1980; Radhakrishnan et al., 2005; Millichap, 2005; Wilkins et al., 2005), migraine (Harle et al., 2006; Conlon et al., 2012; Shepherd et al., 2013; Hayne & Martin, 2019) but also ASC and Tourette’s Syndrome (Ludlow & Wilkins, 2016). It has also been previously suggested that cortical hyperexcitability in response to uncomfortable patterns is further captured by reduced SNRs in EEG and fMRI studies (O’Hare & Hibbard, 2011). It is therefore possible that a relationship between neural noise and anomalous visual experiences exists. Given that the stimuli used to measure ITPC are likely to generate a

“hyperexcitable” visual response in susceptible individuals, it is plausible that atypical levels of ITPC would be more likely to be seen in those who are characterised by perceptual sensitivity to such patterns. However, this relationship has not been previously examined.

Figure 5.1

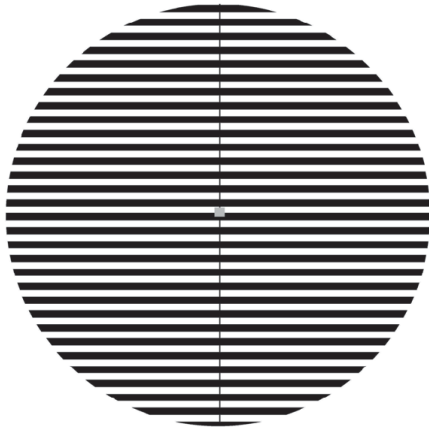


Figure 5.1: A striped pattern of high spatial frequency and high contrast. Reproduced with the kind permission of Prof Arnold Wilkins and Prof Bruce Evans.

Figure 5.2



Figure 5.2: “Natural” (A) vs “Unnatural” (B) patterns in the environment

5.1.3 Aims of the current study

In the present study, we aim to bridge this gap in the literature and investigate the relationship between neural variability and core diagnostic symptoms of ASC in a group of children with ASC. This will allow us to systematically examine whether neural variability is linked to clusters of symptoms specific to the autism phenotype. Phenotypic traits assessed in the study include not only social communication impairments and restricted and repetitive patterns of behaviour but also sensory symptoms. The analysis presented in this chapter therefore uses the data presented in Chapter 4 regarding potential group difference in ITPC and 1/f slope between children with and without ASC and uses regression analysis to investigate whether either of these two variables predict ASC symptomatology. Although Milne et al (2019) has previously shown that social communication impairments and restricted patterns of behaviour do not predict a significant proportion of the variance in ITPC in a group of adults with ASC, the present study is the first to investigate the relationship between core ASC symptoms and neural noise in children with ASC. The present study is also the first to explore the relationship between sensory symptoms and neural noise. For that reason, it is not clear what the direction of predictions would be. In Chapters 2 and 4, it was demonstrated that the steepness of 1/f slope of PSD does not differ in ASC participants compared to typically developing and ADHD sample groups. For that reason and in contrast with ITPC, we do not expect autistic traits to be good predictors of 1/f slope of PSD.

The relationship between neural variability and sensory symptoms specific to the visual modality is also examined. Task characteristics of the EEG study i.e the spatial frequency of checkerboard stimuli repeatedly presented on a screen, are likely to be triggering perceptual distortions better measured in the context of anomalous perceptual experiences specific to the visual stream, rather than the overall sensory symptomatology. Sensory symptoms, as measured in the first hypothesis, cover a wide range of sensory modalities i.e visual, auditory, tactile and others, providing a general picture of sensory processing abnormalities in the sample. Vision-related sensory symptoms in the second hypothesis refer to perceptual distortions, hallucinations and unusual sensory experiences specific to the visual domain. These are measured in the present study in the form of visual symptoms and pattern-induced visual distortions. By focusing specifically on anomalous visual experiences, one can assess whether increased neural variability in the form of low ITPC is associated with subclusters of sensory symptoms that are not specific to ASC, but rather they occur in other clinical and nonclinical populations characterised by visual cortical hyperexcitability, such as migraine and photosensitive epilepsy (Haigh et al., 2012; Wilkins et al., 1984). To our knowledge this is the first study to investigate the relationship

between neural variability as measured by two distinct variables, ITPC and 1/f noise slope of PSD, and anomalous visual symptoms. Given that no studies have previously examined this relationship, it is difficult to predict with certainty the outcome of this analysis. Nevertheless, there is abundant evidence that participants with ASC are more sensitive to pattern glare, which is biologically attributed to cortical hyperexcitability of the visual cortex and on this basis, we expect a relationship between neural variability, visual symptoms and visual distortions to exist.

5.2 Materials and Methods

5.2.1 Participants

Seventy-three participants with ASC were initially recruited for the study. From this cohort, four participants could not tolerate the EEG process and parents of two participants did not complete the psychometric assessments, therefore sixty-seven participants were included in the present study in total. The flow of participants from recruitment to final participation is shown in *Figure 5.3*. Descriptive information for the group is provided in *Table 5.1*. Participants were primarily recruited via online advertisement on social media, mainstream and special schools and the local community. Participants held a diagnosis of either Autism Spectrum Disorder/Condition ($n=56$) or Asperger's Syndrome ($n=11$). A comprehensive overview of the formally diagnosed comorbid conditions in the group is provided in *Table 5.3*. The majority of the participants remained non-medicated for twenty-four hours prior to the experiment ($n=55$). However, twelve participants were taking medication at the time of data collection (*Table 5.2*). All participants had normal or corrected to normal visual acuity.

The following exclusion criteria were applied to the group: participants that (a) their carers did not speak English to a sufficient level to be able to complete the questionnaires, (b) had epilepsy and/or (c) a mental health condition such as personality disorder, bipolar disorder, psychotic disorder did not take part in the study. Neurophysiological data were collected and analysed from sixty-seven participants in total. Five participants did not complete the resting-state part of the experiment (see *Figure 5.3*). For that reason, the task-based EEG analysis was performed on data acquired from sixty-seven participants and the resting-state EEG analysis on data acquired from sixty-two participants. Consent from both the child and the carer was acquired in written form. Ethical guidelines were followed throughout according to the standards set by the Ethics Committee at the University of Sheffield.

Table 5.1

Participant demographics

ASC (n=67)	
Gender	
Female	15
Male	52
Age	
Mean	11.0
SD	2.3
Range	6-15
WASI Performance IQ score ^a	
Mean	109.0
SD	14.7
Range	78-147
SRS-2 score ^b	
Mean	84.0
SD	6.7
Range	68- >90

^aWASI Performance IQ score, Wechsler Abbreviated Scales of Intelligence (WASI, Wechsler, 1999)

^bSRS-2, Social Responsiveness Scale (SRS-2, Constantino & Gruber, 2011)

^cCPRS-R:S, Conners' Parent Rating Scale- Revised, Short version (CPRS-R: S, Conners, 1997)

Table 5.2

Regular drug intake of participants

Drug	Frequency	Percent (%)
Asthma medication		
Corticosteroids (i.e Pulmicort, Montelukast, Beclometasone)	2	2.98
ADHD medication		
Methylphenidate (i.e Equasym, Delmosart)	2	2.98
Lisdexamfetamine	1	1.49
Atomoxetine	1	1.49
Sleeping disorder medication		
Melatonin (i.e Circadian)	6	8.95
Diabetes medication		
Insulin	1	1.49
Depression medication		
SSRIs	2	2.98
Antipsychotic medication		
Risperidone	1	1.49
Constipation medication		
Sodium picosulfate	2	2.98

Table 5.3

Number of participants with a diagnosed comorbid condition

Diagnosis	Frequency	Percent (%)
Total	42	62.68
Sensory Processing Disorder	7	10.44
ADHD	7	10.44
Dyspraxia	4	5.97
Anxiety Disorder	6	8.95
Social Communication Disorder	2	2.98
Intellectual Disability	1	1.49
ADHD & Sensory Processing Disorder	2	2.98
ADHD & Intellectual Disability	1	1.49
ADHD & Dyspraxia	1	1.49
ADHD & Anxiety Disorder	1	1.49
Intellectual Disability & Sensory Processing Disorder	1	1.49
Intellectual Disability & Dyspraxia	1	1.49
Sensory Processing Disorder & Dyspraxia	1	1.49
Sensory Processing Disorder & Anxiety Disorder	1	1.49
Anxiety disorder & Depressive Disorder	1	1.49
Sensory Processing Disorder, Dyspraxia & Anxiety Disorder	2	2.98
Sensory Processing Disorder, Intellectual Disability & Dyspraxia	1	1.49
Intellectual Disability, Social Communication Disorder & Anxiety Disorder	1	1.49
Tourette's Syndrome, Sensory Processing Disorder, Dyspraxia & Anxiety Disorder	1	1.49
Tourette's Syndrome, ADHD, PDA, Sensory Processing Disorder & Motor Disorder	1	1.49

Figure 5.3

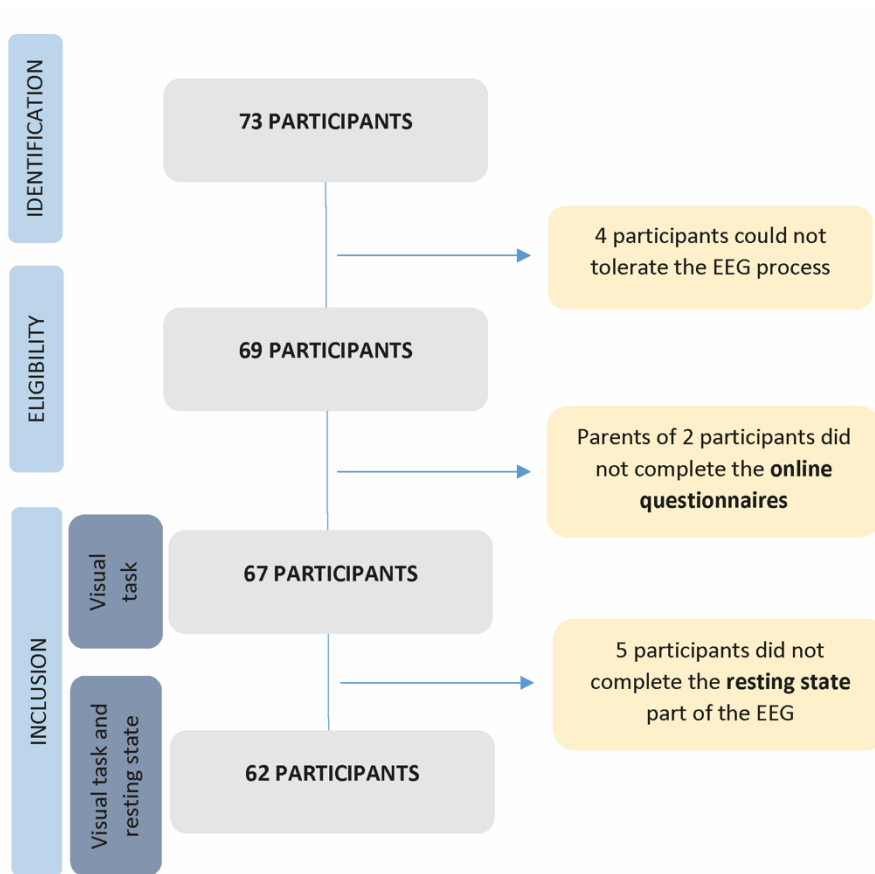


Figure 5.3: Number of participants included in the study after exclusion criteria was applied

5.2.2 Psychometric measures

Caregivers completed four online questionnaires assessing social communication deficits, restricted and repetitive patterns of behaviour and sensory symptoms associated with ASC: the Social Responsiveness Scale-Revised Child/Adolescent (SRS-2, Constantino & Gruber, 2011), the Repetitive Behaviours Questionnaire (RBQ-2, Leekam et al., 2007), the Sensory Behaviour Questionnaire (SBQ, Neil, Green & Pellicano, 2017) and the “Hallucinations” subscale of the Specific Psychotic Experiences Questionnaire (SPEQ, Ronald et al., 2013).

Participants completed three tasks aiming to assess their perceptual reasoning and the degree of visual distortions experienced. The Matrix Reasoning and the Block Design subtests of the Wechsler Abbreviated Scales of Intelligence (WASI, Wechsler, 1999) were used to measure performance IQ and the Pattern Glare Test (Wilkins & Evans, 2001) was used to assess the degree of sensitivity to pattern glare.

Social communication impairments

The Social Responsiveness Scale-Revised Child/Adolescent version (SRS-2, Constantino & Gruber, 2011), containing sixty-five 4-point Likert scale items, was used to identify the presence and severity of social impairments associated with ASC. A single raw score for social communication and interaction was produced by summing the scores of the “Social awareness”, “Social Cognition”, “Social Communication” and “Social Motivation” treatment subscales (53 items in total). The raw score produced, was converted into a T-score for every subject, taking into account the gender and age.

Repetitive and restricted patterns of behaviour

The Repetitive Behaviours Questionnaire (RBQ-2, Leekam et al., 2007), a 20-item questionnaire was used to assess the severity of restricted and repetitive patterns of behaviour linked with the autism phenotype. A total score, indexing the severity of restricted and repetitive behaviours was calculated from the three factors “repetitive motor movements”, “rigidity/adherence to routine”, “preoccupation with restricted patterns of interest” (15 items in total). Items referring to sensory symptoms (factor 4) were not included in the total score to ensure the assumption of multicollinearity is not violated in the multiple regression analysis. Sensory symptoms are assessed by a separate variable in the regression model (see *Sensory symptoms (general)* section below).

Sensory symptoms (general)

In addition to the above, caregivers completed the Sensory Behaviour Questionnaire (SBQ, Neil et al., 2017), a 50-item carer report instrument designed to measure both the frequency and intensity of twenty-five sensory symptoms in a number of different sensory modalities: auditory, visual, vestibular, proprioceptive, tactile, gustatory and olfactory. SBQ has been standardised in an ASC child sample and has shown excellent internal consistency and concurrent validity (Neil et al., 2017). The tool assesses unusual reactions to a number of sensory stimuli, rather than just hypo, hyper- sensitivity to sensory input, and therefore is a good indicator of the presence of sensory processing abnormalities. Each question is scored on a 6-point Likert scale with lower scores showing greater frequency/intensity of sensory symptoms (ranging from “All the time- Never” for the frequency part, “An extreme problem-Not at all” for the intensity part). The frequency subscale scores were used to calculate a total score, which is indicative of the unusual sensory behaviours occurring in the sample tested.

Visual symptoms (domain specific)

The 9-item “Hallucinations” subscale of the Specific Psychotic Experiences Questionnaire (SPEQ, Ronald et al., 2013) was used to measure anomalous sensory experiences of each subject, as reported by their caregiver. Given the lack of reliable anomalous perception instruments, developed for children in specific, the SPEQ is the only existent tool measuring- amongst other constructs- anomalous experiences in the form of hallucinations in young individuals.

SPEQ was initially designed to assess both positive and negative psychotic symptoms in typically developing adolescence, the former via self-report and the latter via caregiver-report. The Hallucinations subscale in specific, was developed as a self-report measure, however in the present study it is used as a caregiver measure. This is because individuals with ASC are known to experience difficulties with self-report (Mazefsky et al., 2011) and SPEQ questions can present as difficult and confusing, particularly to younger children with ASC, some of which have limited communicative abilities or have comorbid intellectual disability.

For the purposes of the present study, a composite score, providing an indication of the sensory symptoms specific to the visual modality of the individual was computed from the SBQ and the SPEQ, by summing the visual items of each scale (4 and 2 items respectively).

Visual distortions (domain specific)

The Pattern Glare Test (Wilkins & Evans, 2001) was used to measure the degree of visual distortions experienced by participants in response to three square wave gratings, each one presented in a different spatial frequency, 0.5, 3 and 12 cycles per degree (cpd). Gratings are shown in *Figure 5.4*. During the testing session, participants were asked to fixate on a dot in the middle of the striped pattern and report the number of visual distortions experienced post pattern presentation. The total sensitivity to pattern glare was calculated by summing the number of reported distortions on the three gratings (Wilkins & Evans, 2001).

Figure 5.4

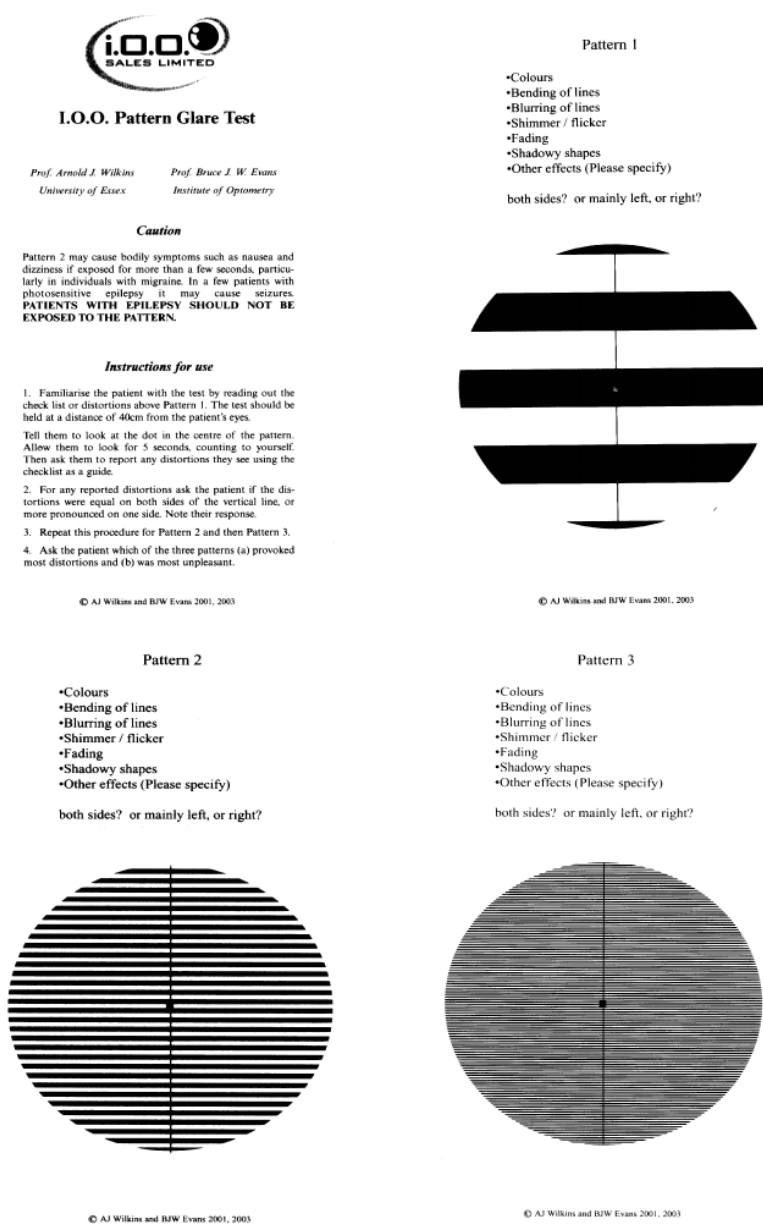


Figure 5.4: The Pattern Glare Test. Reproduced with the kind permission of Prof Arnold Wilkins and Prof Bruce Evans

It is important to note that comprehensive investigation was initially conducted to ensure that the psychometric tools used to measure the variables of interest (predictor variables) are age and gender appropriate and are standardised in ASC samples. For example, a comprehensive overview of the current psychometric tool availability and the caveats associated with each tool is presented for the sensory domain in *Annex 10*. Reliability statistics for the scores used for further analysis are presented below (*Table 5.4*).

Table 5.4

Reliability statistics for the predictor variables Social Communication Impairments (SCI), Repetitive and Restricted Patterns of Behaviour (RRB), Sensory Symptoms (SS) and Visual Symptoms (VS) used for further analysis

Subscale	Scale	Predictor variable	No. items	Cronbach's Alpha	<i>M</i>	<i>SD</i>
SCI t-score	SRS-2 ^a	SCI	53	0.90	83.37	7.15
Total of Factor 1,2,3	RBQ-2 ^b	RRB	15	0.83	41.48	8.53
Total of "Frequency" subscale	SBQ ^c	SS	25	0.90	62.45	22.26
Composite score for visual items	SBQ, SPEQ ^d	VS	6	0.77	8.21	6.13

^aSRS-2, *Social Responsiveness Scale (SRS-2, Constantino & Gruber, 2011)*

^bRBQ-2, *Repetitive Behaviours Questionnaire (RBQ-2, Leekam et al., 2007)*

^cSBQ, *Sensory Behaviour Questionnaire (SBQ, Neil, Green & Pellicano, 2017)*

^dSPEQ, *Specific Psychotic Experiences Questionnaire (SPEQ, Ronald et al., 2014)*

5.2.3 Procedure

Upon arrival, the experimenter explained in detail what the EEG process entails. The participant then completed a test-trial to familiarise themselves with the EEG task. Participants first completed the EEG experiment, followed by the Pattern Glare test, the matrix-reasoning and the block-design subtest of the WASI. Parents were asked to complete the questionnaires online on the same day of the testing session via the online platform Qualtrics.

5.2.4 EEG experiment

The EEG experiment consisted of a task-based condition followed by a resting state condition, explained in detail in Section 4.2.3 of Chapter 4.

5.2.5 Data preprocessing

A summary of the preprocessing steps followed in this study to extract the variables indexing neural noise are presented in Section 4.2.4 of Chapter 4.

5.2.6 Data integrity

A series of extra analysis steps were carried out in order to ensure that EEG data quality was similar across different datasets. For each participant, it was established that the number of epochs were the same in the final ITPC vs 1/f noise task-based dataset.

Table 5.5

Mean (M), Standard Deviation (SD), Range of artefact-free EEG channels and experimental trials retained for further analysis

EEG channels retained	
Mean	26
SD	2.9
Range	16-30
Experimental trials retained	
Mean	88.48
SD	5.53
Range	71-96

** $p < 0.5$, ** $p < 0.01$, *** $p < 0.001$*

5.2.7 EEG data preparation for Inter- Trial Phase Coherence analysis

5.2.7.1 Data preprocessing

Additional preprocessing steps were followed to prepare the task-based data for ITPC analysis. Data was segmented into epochs, from -1 to 1 secs around stimulus onset, and corrected to baseline, using the average signal between 1 sec before stimulus onset to stimulus onset.

5.2.7.2 Data selection

Independent Component selection

ITPC was extracted from Independent Components (ICs) rather than channels (Milne, 2011; Milne, Gomez, Giannadou & Jones, 2019). Independent Component Analysis (ICA) is a method of blindly separating sources of signal, which are linearly mixed when recorded from several sensors of scalp EEG. The ICA algorithm separates the mixed signal into spatially independent components of source signal, which are less contaminated with noise generated by other cortical and non-cortical sources. For that reason, we performed further analysis on ICs rather than channels, which are known to be sensitive to such noise artefacts.

ICA decomposition was performed using the *runica* function of EEGLAB, which utilises the infomax ICA algorithm of Bell & Sejnowski (1995) with the natural gradient characteristics suggested by Amari, Cichocku & Yang (1996). ICA, applied on individual participant scalp data, returned as many components as the number of channels kept for further analysis after preprocessing. Time-frequency analysis was then performed on all ICs (see Section 5.2.7.2). For each participant, we calculated ITPC for every IC and selected the single IC with maximum ITPC for further analysis. Visual inspection of the IC scalp maps of the IC selected from each participant revealed that the selected ICs were projected at the occipital lobe, suggesting that they were reflection activation of the visual cortex. Scalp maps of the IC with max ITPC chosen for each participant is presented in *Figure 5.5* and *Figure 5.6*. The ERP of the selected components was also examined further confirming that the signal source was at the visual cortex.

Figure 5.5

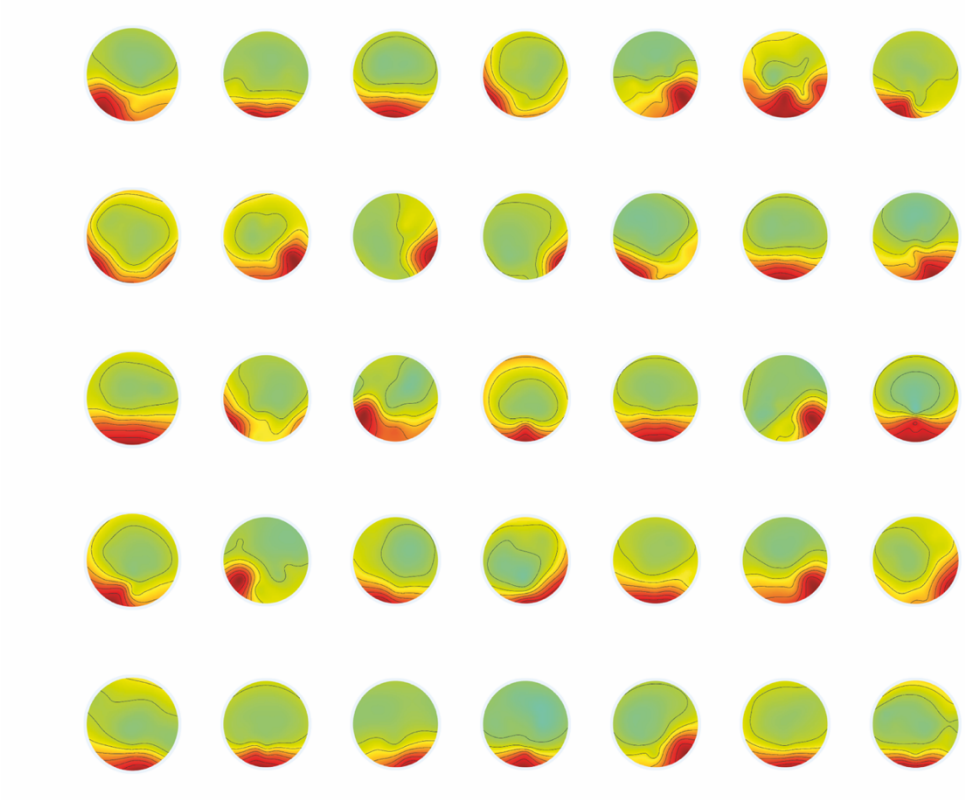


Figure 5.5: Scalp maps of the Independent Component with maximum ITPC selected for participants 1-35.

Figure 5.6

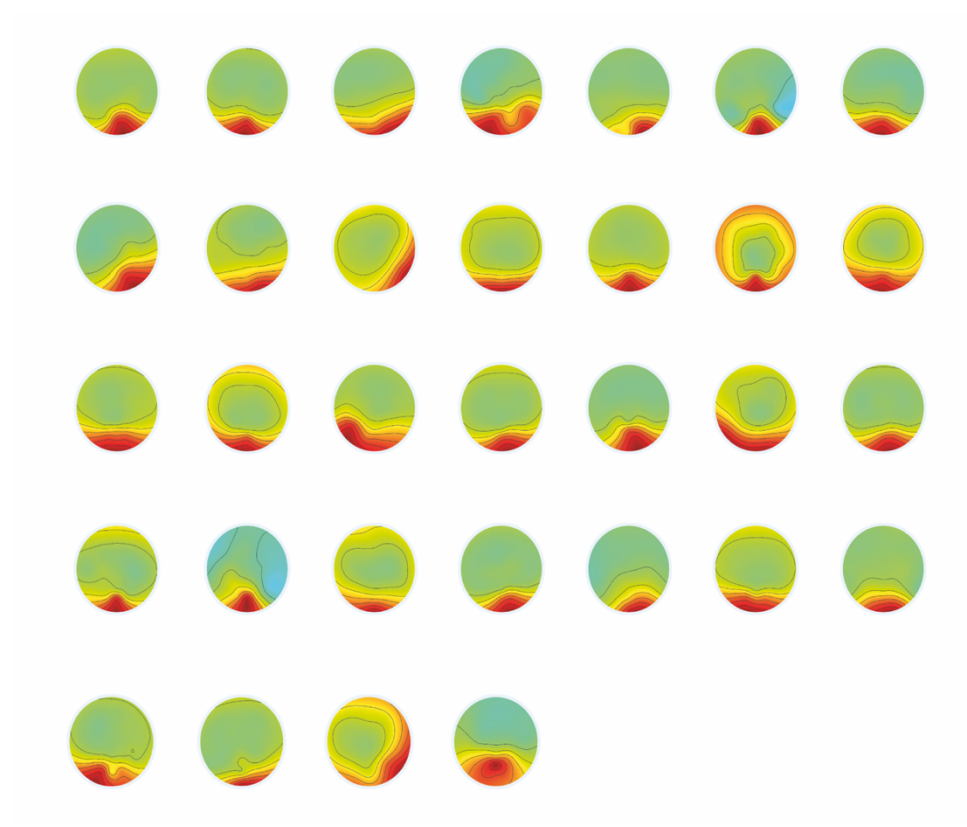


Figure 5.6: Scalp maps of the Independent Component with maximum ITPC selected for participants 36-67.

5.2.7.3 Data analysis

Time-frequency analysis

Time-frequency decomposition of EEG single-trial data was performed using the *newtimef* function of EEGLAB (Delorme & Makeig, 2004). The time series data was convolved with a complex Morlet wavelet, defined as a sinusoid with a Gaussian shape. The wavelet ranged from 2 to 12.5 cycles at 558 ms intervals (equivalent to 279 samples). The length of the average vector of the phase angles was computed for 200 evenly spaced time-frequency points (-720.7 to 720.7 ms) and was estimated for 23 log-spaced frequencies, ranging from 4 to 50Hz (see Section 2.2.6.2 for a detailed explanation of time-frequency analysis). A single ITPC value, representing the maximum ITPC generated from any independent component at any frequency and at any time point, was extracted for each participant in the group and was used for group analysis.

Compared to the methodology followed in Chapter 2, frequencies were logarithmically rather than linearly spaced. This allowed to capture the lower end of the frequency spectrum, which could not be captured if linear scaling had been used (see *p.165*, Cohen, 2014 for a discussion on logarithmic vs linear scaling). To ensure that this step did not change maximum ITPC values we measured maximum ITPC using both logarithmic and linear scaling and compared the results. An independent samples t-test showed that there was no difference between the maximum ITPC computed using linear versus logarithmic scaling ($F(132)=0.22, p=0.33$).

Table 5.6

Mean (M), Standard Deviation (SD), Minimum (Min) and Maximum (Max) value of maximum ITPC and the average Frequency (Hz) it occurs at, as computed from a) linearly and b) logarithmically spaced frequencies

	M	SD	Min	Max	Frequency (Hz)
max ITPC using linear scaling	0.74	0.14	0.40	0.96	7
max ITPC using logarithmic scaling	0.76	0.13	0.39	0.97	4

5.2.8 EEG data preparation for 1/f noise analysis

5.2.8.1 Data preprocessing

Task-based and resting state data were further preprocessed in preparation for 1/f noise analysis (see Section 4.2.4 in Chapter 4 for a summary of steps). The preprocessing approach we followed here differs from the approach taken in the preparation of the task-based data for ITPC analysis. The main objective of the ITPC analysis pipeline was to separate the mixed signal and select one source of signal to analyse, whereas primary aim of the 1/f preprocessing analysis is to ensure that the mixed EEG signal is clean and free of noise artefacts so that power spectral estimations are accurate and attributed to brain functions rather than external sources of electrical interference.

Eye-blink components were visually identified from the ICA maps and removed as suggested in the 1/f analysis pipeline followed by Peterson et al. (2017). In order to replace the missing channels, all datasets were interpolated using the channel interpolation function from the EEGLAB gui. Data were then referenced to average reference and segmented into epochs. Task-based data were epoched from -1 to 1 secs around stimulus onset and pre-stimulus baseline removal was performed at 1 sec. Similar to the methodology followed in experimental study 1, resting state data were segmented into 2 secs epochs.

5.2.8.2 Data selection

Power Spectral Density estimation

The Welch's method (Welch, 1967) was used for Power Spectral Density (PSD) estimation. The Welch's method is explained in detail in Chapter 2. In brief, the Welch method minimises this variance by averaging out the spectral content of short windows of signal. Each dataset was segmented into blocks with 50% overlap between them. A modified periodogram was then computed for each block using a 2-second Hamming data window. The periodograms for each block were averaged out to produce the final PSD periodogram. A linear regression line was then fitted to the data to model an inversely proportional relationship between PSD and frequency, of the form $P_f = k \frac{1}{f^\alpha}$, where P_f is the power spectra per frequency interval f , k is a random constant and α is the scaling exponent. Power spectra was plotted in log coordinates. The log-transform of the power function is a straight line with a negative slope α and an intercept c (Figure 5.7). 1/f slopes of PSD were estimated from frequencies between 0- 24Hz (Voytek et al., 2015),

effectively excluding high frequency bands from the analysis, as they are more likely to reflect intrinsic channel noise, rather than neural processes. Alpha band power (7-14Hz) was also excluded prior to 1/f slope estimation, as it represents changes in periodic EEG patterns, biasing estimations of the non- periodic properties of the signal i.e. 1/f noise (Voytek et al., 2015). Alpha band power was not excluded a priori (for example by band pass filtering) instead an identical method to previous research (Voytek et al., 2015) was used in which the alpha component of the calculated power spectra was removed simply by replacing the characteristic peak of the alpha wave with a straight line between the data points of the power associated with 7 and 14Hz frequencies (*Figure 5.7B* versus *Figure 5.7A*, previous chapter too). Spectral slopes of all electrodes for participant 26 are presented in *Annex 8*.

Figure 5.7

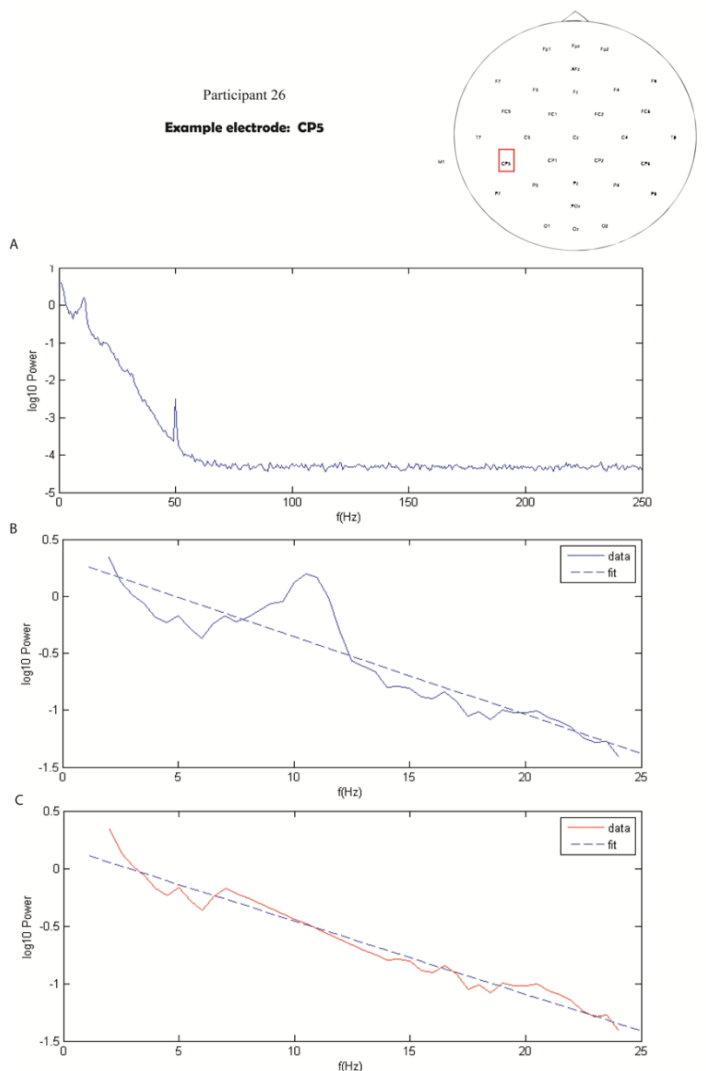


Figure 5.7: Log-transformed Power Spectral Density (\log_{10} Power) of signal coming from a single electrode CP5, is presented here as a function of frequencies (f) ranging from A) 0-250Hz, B) 2-24 Hz including alpha band and C) 2-24 Hz excluding alpha band. A regression line with a negative slope $a = -0.063614$ is fitted to the data in graphs B and C.

5.2.8.3 Data analysis

A single value representing the 1/f slope of PSD at each electrode was calculated for all electrodes and for all participants in the group. The mean slope of all 32 electrodes was computed for every participant as shown in *Figure 5.8*. The same approach was followed to extract the value of the slope from both the task-based and the resting state datasets.

Figure 5.8

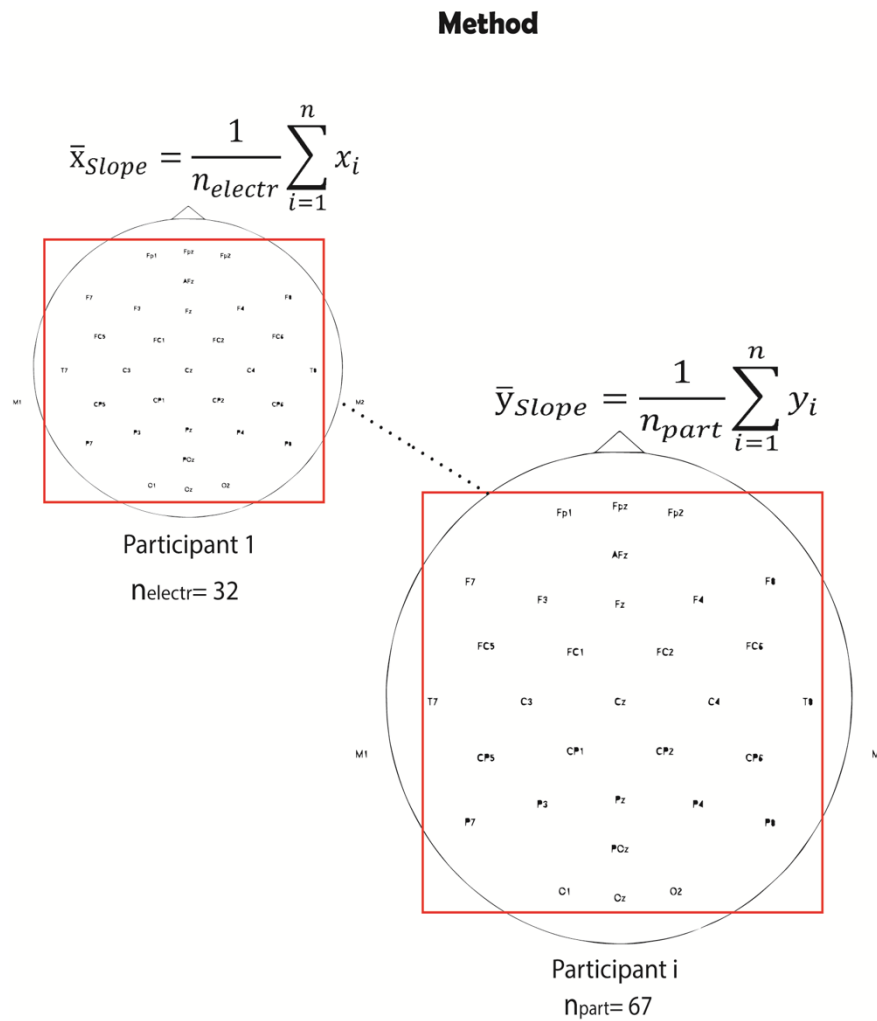


Figure 5.8: The mean slope of all 32 electrodes was computed for every participant

5.2.9 Regression analysis

Task-based condition

A series of multiple regression analyses were performed to examine the relationship between neural noise (dependent variable) and core diagnostic symptoms of ASC (independent variables). To investigate the extent to which social communication impairments (SCI), repetitive and restricted patterns of behaviour (RRB) and sensory symptoms (SS) can predict levels of neural noise, two regression models were fitted into the data. Model 1 examined the relationship between neural noise, as measured by ITPC and core diagnostic symptoms of ASC. Model 2 examined the relationship between neural noise, as indexed by 1/f slope of PSD (extracted from the task-based data) and core diagnostic symptoms.

Multiple regression analysis was also conducted to investigate the relationship between neural noise (dependent variable) and sensory symptoms specific to the visual modality (independent variables). Visual perceptual symptoms were represented in the regression equation by two predictor variables, visual symptoms (VS) as measured by a composite score derived from SBQ and SPEQ and visual distortions (VD) as measured by the Pattern Glare test (see Section 4.2.2 for a detailed description). To investigate the extent to which VS and VD can predict neural noise, two models were constructed; maximum ITPC was entered as a dependent variable in Model 3 and 1/f slope of PSD was entered as a dependent variable in Model 4.

Resting state condition

Following the same approach as above, model 5 examined the relationship between neural noise, as measured by 1/f slope of PSD (extracted from the resting state data) and core diagnostic autism symptoms. Model 6 examined the relationship between neural noise, as measured by 1/f slope of PSD (extracted from the resting state data) and sensory symptoms specific to the visual modality.

5.3 Results

5.3.1 Descriptive statistics

Descriptive statistics for the dependent and independent variables used in the regression analysis are presented in Table 5.7. Further details about the specific psychometric measures used are provided in Section 4.2.2.

Table 5.7

Number of participants (N), Mean values (M), Standard Deviations (SD), Minimum (Min) and Maximum (Max) values of the variables used in the regression analysis

	<i>n</i>	<i>M</i>	<i>SD</i>	<i>Min</i>	<i>Max</i>
Independent Variables					
Social Communication Impairments	67	83.37	7.15	66	90
Repetitive and Restricted Behaviours	67	41.48	8.53	25	58
Sensory Symptoms	67	62.45	22.26	2	115
Visual Symptoms	65	8.29	6.18	0	22
Visual Distortions	65	7.20	3.39	0	15
Dependent Variables					
Maximum ITPC (task-based)	67	0.76	0.13	0.39	0.97
1/f slope of PSD (task-based)	67	-0.06	0.01	-0.09	-0.03
1/f slope of PSD (resting state)	62	-0.07	0.01	-0.11	-0.04

Maximum ITPC extracted from the Independent Components was observed primarily in the theta band (4-7Hz) (*Figure 5.9*). Average maximum ITPC maps computed for the group are presented in *Figure 5.10*. Scalp maps representing the mean 1/f slope of PSD computed for the task-based condition and the resting-state condition are presented in *Figure 5.11*. Individual maximum ITPC heat maps computed for all participants are presented in *Annex 9* (see ASC group).

Figure 5.9

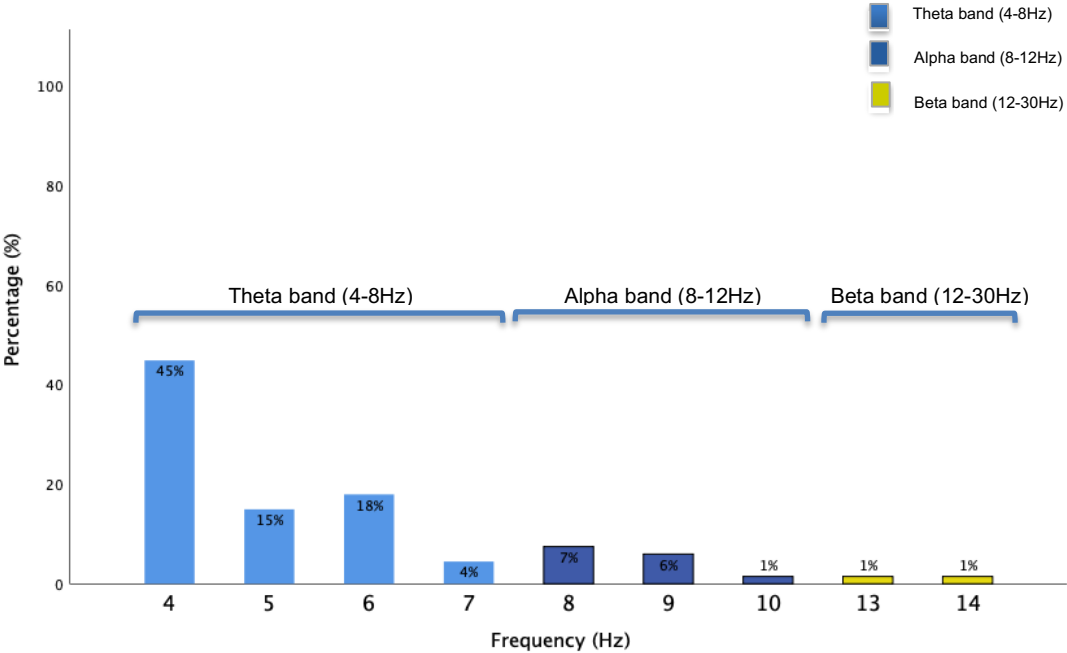


Figure 5.9: Frequency (Hz) where maximum ITPC was observed

Figure 5.10

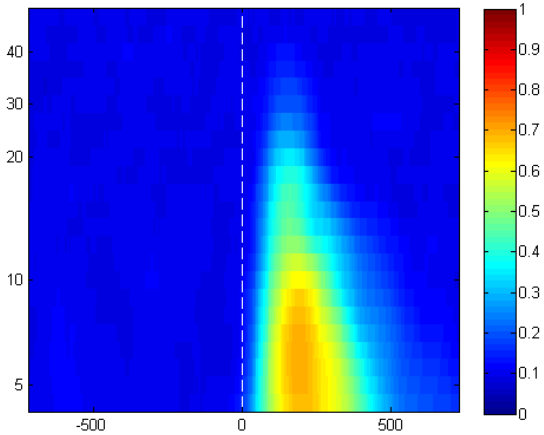


Figure 5.10: Average maximum ITPC maps computed for all participants (n=67)

Figure 5.11

1/f slopes

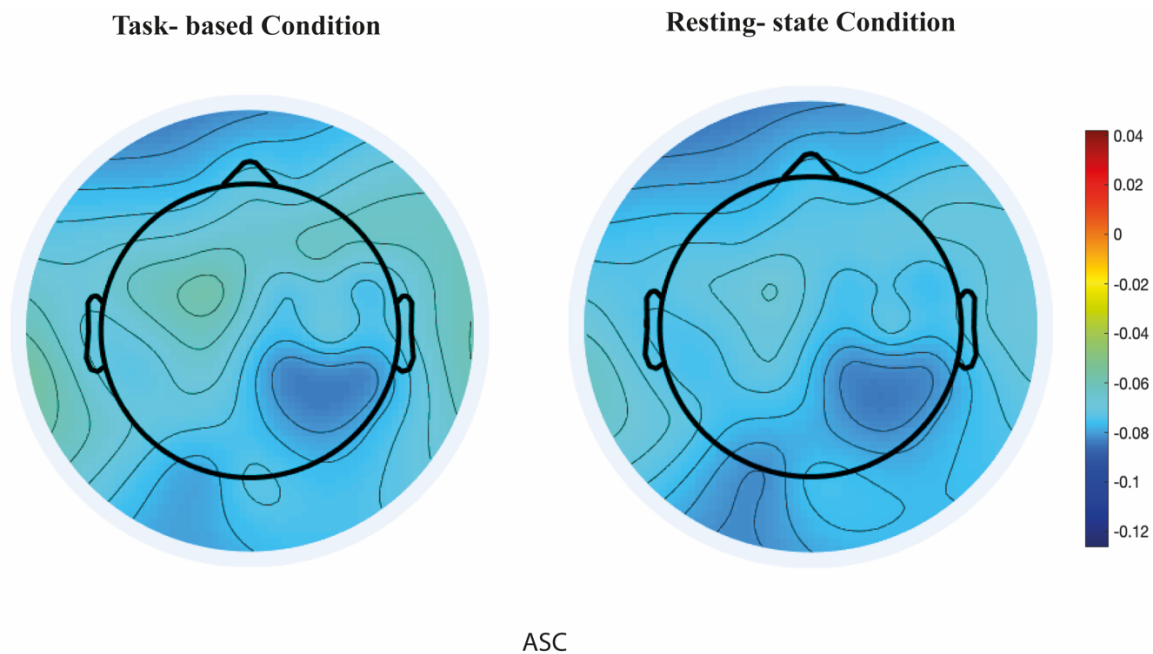


Figure 5.11: Scalp maps representing the mean slope computed for the task-based condition ($n=67$) and the resting-state condition ($n=62$).

5.3.2 Regression Analysis

Task-based condition

Model 1

Scatterplots revealed that the relationship between maximum ITPC (dependent variable) and SCI, RRB and SS scores (independent variables) was linear. Inspection of both the histogram and the normal Q-Q plot of the residuals showed that the errors between observed and predicted values were approximately normally distributed. Residuals versus predicted values were plotted and showed that residual variance is homoscedastic. The Durbin-Watson test, as a measure of autocorrelation, was also computed and confirmed that the assumption of independence of residuals was met ($d=1.58$). The assumption of multicollinearity was also tested a) by estimating a Pearson's bivariate correlation matrix amongst the SCI, RRB and SS scores (independent variables) and b) by computing the Variance Inflation Factor (VIF). Collinearity statistics indicated that the predictor variables were not too highly correlated. The

correlation matrix of the independent variables produced small eigenvalues of the range 0.00-0.06. Eigenvalues close to 0 indicate that an exact linear dependence exists. Correlation coefficients were below 0.8 and VIF scores were below 10 with tolerance scores above 0.2 (Table 5.8).

Table 5.8

Pearson's correlation coefficients, Tolerance and Variation Inflation Factors (VIF), for the independent variables included in Model 1, Model 2 and Model 5

Variable	1	2	3	Tolerance	VIF
1. Social Communication Impairments				0.70	1.42
2. Repetitive and Restricted Behaviours	0.51**			0.38	2.60
3. Sensory Symptoms	0.51**	0.77**		0.38	2.61

*indicates $p < 0.05$, **indicates $p < 0.001$

The above indicated that all assumptions for regression analysis were satisfied. Multiple regression analysis was performed to investigate the relationship between maximum ITPC and core diagnostic symptoms of ASD. The results of the multiple regression analysis indicated that the overall Model 1 fitted to the data was not significant and therefore the SCI, RRB and SS scores together were not good predictors of maximum ITPC ($F(3, 63) = 1.17, p = 0.32, R^2 = 0.05$). A non-significant result was also yielded when each independent variable was isolated from all others in the model (see p-values, Table 5.9).

Table 5.9

Regression analysis summary of core diagnostic symptoms of ASC predicting maximum ITPC (Model 1)

Variable	B	95% CI	β	t	p
1. Social Communication Impairments	-0.00	[-0.01, 0.00]	-0.21	-1.48	0.14
2. Repetitive and Restricted Behaviours	-0.00	[-0.00, 0.00]	-0.06	-0.31	0.75
3. Sensory Symptoms	0.00	[-0.00, 0.00]	0.04	0.21	0.83

*indicates $p < 0.05$, **indicates $p < 0.001$

Model 2

Having established that the assumption of multicollinearity was not violated, scatterplots of 1/f slope of PSD (dependent variable) and SCI, RRB and SS scores (independent variables) were visually inspected to assess whether the assumption of linearity in the model was met. These revealed a linear relationship between dependent and independent variables. Subsequent inspection of the histogram and the normal Q-Q plot of the residuals showed that the residuals were normally distributed. A scatterplot of the residuals plotted against the predicted values indicated that the error term was the same width for all values of the predicted data and therefore homoscedastic. The Durbin-Watson test showed that autocorrelation in the residuals were within the acceptable levels, in the range of 1.5 to 2.5 ($d=1.62$).

Given that all assumptions were met, multiple regression analysis was performed to examine the relationship between 1/f slope of PSD (extracted from the task-based data) and core diagnostic symptoms of ASD. The probability value for Model 2 did not reach the threshold of 0.05, indicating that the SCI, RRB and SS scores together can only explain a very small amount of the variance of the dependent variable 1/f slope of PSD ($F(3, 63)=0.34, p=0.79, R^2=0.01$). The results remained non-significant both when the overall model was fitted and when the independent variables were considered separately (*Table 5.10*).

Table 5.10

Regression analysis summary of core diagnostic symptoms of ASC predicting 1/f slope of PSD as extracted from the task-based data (Model 2)

Variable	B	95% CI	β	t	p
1. Social Communication Impairments	0.00	[0.00, 0.00]	0.09	0.65	0.51
2. Repetitive and Restricted Behaviours	0.00	[-0.00, 0.00]	-0.10	-0.50	0.61
3. Sensory Symptoms	-0.00	[0.00, 0.00]	-0.05	-0.28	0.77

*indicates $p < 0.05$, **indicates $p < 0.001$

Model 3

Scatterplots revealed that the relationship between maximum ITPC (dependent variable) and VS and VD scores (independent variables) was linear. Inspection of both the histogram and the Q-Q plot of the residuals showed that the errors between observed and predicted values were approximately normally distributed. A scatterplot of the residuals versus predicted values showed that residual variance was homoscedastic. The Durbin-Watson test confirmed that the assumption of independence of residuals was met ($d=1.85$). Collinearity statistics indicated that the assumption of multicollinearity was satisfied. The predictor variables were not too highly correlated; the correlation matrix of the independent variables produced small eigenvalues of the range 0.09-0.24, correlation coefficients were below 0.8 and VIF scores were below 10 with tolerance scores above 0.2 (Table 5.11).

Table 5.11

Pearson's correlation coefficients, Tolerance and Variation Inflation Factors (VIF), for the independent variables included in Model 3, Model 4 and Model 6

Variable	1	2	Tolerance	VIF
1. Visual Symptoms			0.95	1.04
2. Visual Distortions	0.20		0.95	1.04

*indicates $p < 0.05$, **indicates $p < 0.001$

The above shows that all assumptions for regression analysis were satisfied. Multiple regression analysis was performed to investigate the relationship between maximum ITPC and sensory symptoms specific to the visual modality. The results indicated that VS and VD scores combined were moderately predicting maximum ITPC ($F(2, 62)=6.84, p=0.00$), accounting for 18% of the total variance in maximum ITPC ($R^2=0.18$). When the effects of these predictor variables were examined separately, VD was a statistically significant predictor of maximum ITPC, explaining 15% of the variation in maximum ITPC, but VS did not account for a significant amount of variance in the dependent variable (Table 5.12). The relationship between maximum ITPC and VD is captured by the scatterplot in Figure 5.12. Although Model 3 reaches statistical significance, only, leaving a large amount of variance unexplained.

Table 5.12

Regression analysis summary of sensory symptoms specific to the visual modality predicting maximum ITPC (Model 3)

Variable	B	95% CI	β	t	p
1. Visual Symptoms	-0.00	[-0.01, 0.00]	-0.18	-1.56	0.12
2. Visual Distortions	0.02	[0.00, 0.03]	0.42	3.61	0.00**

*indicates $p < 0.05$, **indicates $p < 0.001$

Figure 5.12

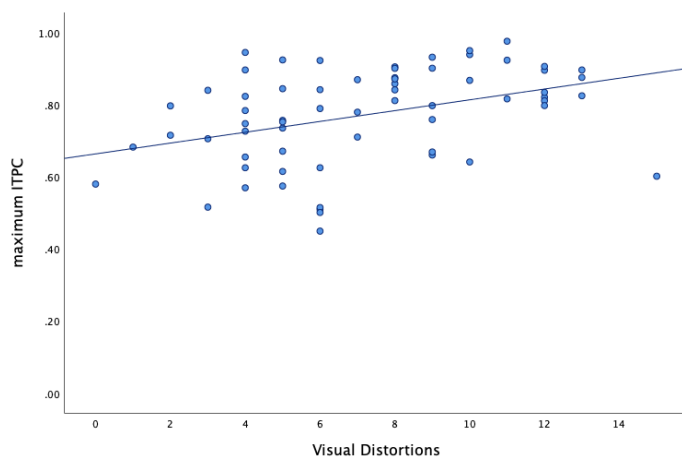


Figure 5.12: Scatterplot showing the relationship between maximum ITPC and Visual Distortions.

Model 4

Scatterplots revealed that the relationship between 1/f slope of PSD (dependent variable) and VS and VD scores (independent variables) was linear. Inspection of both the histogram and the Q-Q plot of the residuals showed that the errors between observed and predicted values were approximately normally distributed. A scatterplot of the residuals versus predicted values showed that residual variance was homoscedastic. The Durbin-Watson test confirmed that the assumption of independence of residuals was met ($d=1.67$).

Subsequently, multiple regression analysis was performed to examine the relationship between 1/f slope of PSD (extracted from the task-based data) and sensory symptoms specific to the visual modality. Model 4 did not reach significance, indicating that VS and VD combined can only explain a very small amount of the variance of the dependent variable 1/f slope of PSD ($F(2, 62)=0.22, p=0.66, R^2=0.02$). The results remained non-significant both when the overall model was fitted and when effects of the independent variables were isolated (*Table 5.13*).

Table 5.13

Regression analysis summary of sensory symptoms specific to the visual modality predicting 1/f slope of PSD as extracted from the task-based state data (Model 4)

Variable	B	95% CI	β	t	p
1. Visual Symptoms	0.00	[-0.00, 0.00]	0.13	1.00	0.31
2. Visual Distortions	0.00	[-0.00, 0.00]	-0.09	-0.76	0.44

*indicates $p < 0.05$, **indicates $p < 0.001$

Resting state condition

Model 5

Scatterplots of 1/f slope of PSD (dependent variable) plotted against SCI, RRB and SS scores (independent variables) revealed a linear relationship between them. A histogram with a superimposed normal curve and a normal Q-Q plot of the residuals showed that they are approximately normally distributed. A scatterplot of the residuals plotted against the predicted values indicated that the data is homoscedastic. The Durbin-Watson statistic showed that the assumption of independence of residuals was also met ($d=1.76$).

Given that all the relevant assumptions were satisfied, multiple regression analysis was performed to examine the relationship between 1/f slope of PSD as extracted from the resting state data and core diagnostic symptoms of ASD. Model 5 was not statistically significant, indicating that the SCI, RRB and SS scores together can only explain a very small amount of the variance of the dependent variable 1/f slope of PSD ($F(3, 58)=0.45, p=0.71, R^2=0.02$). The results remained non-significant both when the overall model was fitted and when the independent variables were considered separately (Table 5.14).

Table 5.14

Regression analysis summary of core diagnostic symptoms of ASC predicting 1/f slope of PSD as extracted from the resting-state data (Model 5)

Variable	B	95% CI	β	t	p
1. Social Communication Impairments	0.00	[-0.00, 0.00]	-0.04	-0.28	0.78
2. Repetitive and Restricted Behaviours	0.00	[-0.00, 0.00]	-0.17	-0.80	0.42
3. Sensory Symptoms	0.00	[0.00, 0.00]	0.24	1.16	0.24

**indicates $p < 0.01$

Model 6

Scatterplots revealed that the relationship between 1/f slope of PSD (dependent variable) and VS and VD scores (independent variables) was linear. Inspection of both the histogram and the Q-Q plot of the residuals showed that the errors between observed and predicted values were approximately normally distributed. A scatterplot of the residuals versus predicted values showed that residual variance is homoscedastic. The Durbin-Watson test confirmed that the assumption of independence of residuals was met ($d=1.96$).

Given that all the relevant assumptions were satisfied, multiple regression analysis was performed to examine the relationship between 1/f slope of PSD as extracted from the resting state data and sensory symptoms specific to the visual modality. Model 6 did not reach significance, indicating that VS and VD combined can only explain a very small amount of the variance of the dependent variable 1/f slope of PSD ($F(2, 59)=1.60, p=0.21, R^2=0.05$). The results remained non-significant both when the overall model was fitted and when effects of the independent variables were isolated (Table 5.15).

Although not statistically significant, results showed a trend which suggested that VS may be a predictor of 1/f slope of PSD. Nevertheless, further analysis showed that VS can predict less than 10% of the variance in 1/f slope. The lack of a relationship between the two variables was further confirmed by a scatterplot, presented in Figure 5.13.

Table 5.15

Regression analysis summary of sensory symptoms specific to the visual modality predicting 1/f slope of PSD as extracted from the resting-state data (Model 6)

Variable	B	95% CI	β	t	p
1. Visual Symptoms	0.00	[0.00, 0.00]	0.22	1.75	0.08
2. Visual Distortions	-0.00	[-0.00, 0.00]	-0.00	-0.02	0.98

*indicates $p < 0.05$, **indicates $p < 0.001$

Figure 5.13

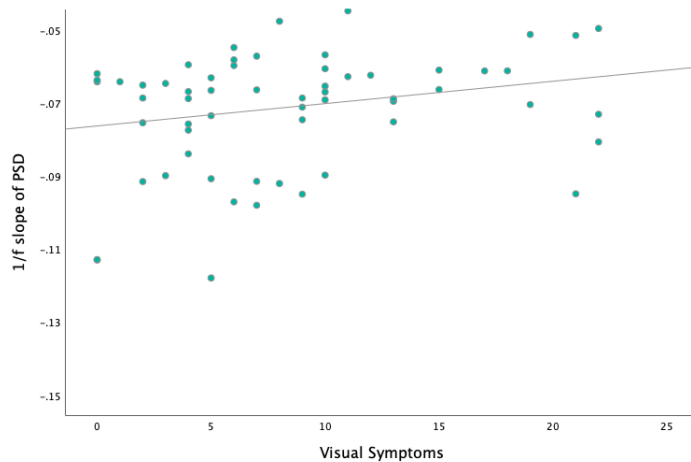


Figure 5.13: Scatterplot showing the relationship between 1/f slope of PSD as computed from resting state data and Visual Symptoms.

5.4 Discussion

In the context of previous research proposing that neural noise may be a biomarker of ASC, the present study aimed to investigate in greater detail the relationship between neural noise and core diagnostic symptoms of ASC in a group of children with ASC. Neural noise was indexed by two variables, ITPC and 1/f slope of PSD and was computed using EEG from a visual task involving repeated presentation of a checkerboard stimulus. 1/f slope of PSD was also computed from a resting state, eyes closed condition. Core diagnostic symptoms of ASC were assessed in the realm of social communication impairments, restricted and repetitive patterns of behaviour and sensory symptoms covering a wide range of sensory modalities. As the data illustrated, we found no relationship between neural variability and phenotypic traits associated with ASC. Most importantly, it was established that in the sample tested, there was no association between neural variability and general sensory sensitivity, an aspect of the ASC phenotype not previously examined in the literature.

At a second level, the relationship between neural variability and sensory symptoms specific to the visual modality was examined, taking into account participants' perceptual sensitivity to the stimulus presented during the experimental task. Domain specific sensory symptoms were quantified in the context of anomalous visual symptoms and visual distortions, measured via

the pattern glare test. The work presented here shows that there is no association between 1/f slope of PSD, as computed from the task-based data and visual symptoms. A similar conclusion was reached about the 1/f slope of PSD measured from the resting state data; although visual symptoms predicted some of the variance in 1/f slope of PSD (5%), this relationship was not strong enough to cross significance. We also found no relationship between 1/f slope of PSD, as measured from both task-based and resting-state data, and visual distortions. Nevertheless, results showed that visual symptoms and visual distortions together can predict a significant proportion of the variance of ITPC (18%). Visual distortions in particular was the variable driving this relationship, explaining 15% of the variance; the more visual distortions a participant reported in our sample, the higher the ITPC value was, indicating lower levels of neural noise in the cortex.

Neural noise as measured by ITPC and 1/f slope of PSD, was found not to be associated with core diagnostic features of ASC, as shown by the lack of a significant relationship between the variables indexing neural noise and either SRS scores or RRB scores. This suggests that ITPC is not likely to be a biomarker of ASC, as previously proposed in the literature (David et al., 2016). The finding about the lack of relationship between ITPC and core diagnostic features of ASC is not surprising and is in line with previous research work by Milne et al. (2019). Using a similar task design, Milne et al. (2019) demonstrated that ITPC is not related to the two main ASC symptom domains, social communication impairments and repetitive and restricted patterns of behaviour. In addition, the present work also established that ITPC cannot be explained by sensory perceptual abnormalities. Adding to the above finding, this is the first study to show the lack of a relationship between 1/f slope of PSD and core phenotypic traits of ASC. One of the strengths of the present work compared to other studies, is that it included participants with very diverse neurocognitive profiles, covering a wide range of abilities within the autism spectrum, therefore is much more representative of the ASC population. Using two different methods of computing neural variability in a very diverse sample, we demonstrated that autism severity does not determine levels of ITPC, nor does levels of 1/f slope of PSD. For that reason, literature referring to neural noise as a biomarker of ASC should be interpreted with caution.

Moving away from primary phenotypic symptoms and the idea of a single pathophysiological route to ASC, the second hypothesis allowed us to evaluate whether levels of neural noise can be predicted by clusters of secondary symptoms, commonly found in other clinical and non-

clinical groups. Indeed, this is the first study to report a link between ITPC, anomalous visual experiences and visual distortions, a group of visuoperceptual symptoms shown to occur not only in individuals with ASC but also patients with photosensitive epilepsy (Wilkins et al., 1975; Soso et al., 1980; Radhakrishnan et al., 2005; Millichap, 2005; Wilkins et al., 2005), migraine (Harle et al., 2006; Conlon et al., 2012; Shepherd et al., 2013; Hayne & Martin, 2019) and others in the general population (Braithwaite et al., 2013). Stripes and checkerboard patterns such as the ones utilised in the EEG task of the present study are shown to cause increased discomfort and induce anomalous visual perceptual distortions in some individuals- potentially those with a hyperexcitable visual cortex- but not in others; some people remain relatively unaffected by pattern glare (Wilkins & Evans, 2010). This is evident in the number of illusions reported in the present study by the participants in the Pattern Glare Test, ranging from zero to fifteen (the maximum amount of visual distortions a participant can report). It was also established that the total number of visual distortions reported in response to gratings with 0.5, 3 and 9 cpd is the strongest predictor of ITPC, meaning that the total sensitivity to pattern glare can partially predict the strength of phase-locking of neurons in the visual cortex. In the present study, the greater sensitivity to pattern glare a participant demonstrated, the higher their ITPC was in response to the checkerboard stimulus, translated into a less variable neural response. This further suggests that EEG stimulus characteristics may have a direct effect on ITPC, although it is still unclear what task parameters specifically might drive this relationship. In addition, we found no association between the steepness of the $1/f$ slope of PSD as computed from the same task-based data and anomalous visual symptoms. Subsequently, this suggests that different variables have predictive power over $1/f$ slope of PSD as compared to ITPC, strengthening the argument that they are likely to be capturing distinct processes.

From a biological perspective, the exact processes behind the ITPC- anomalous visual symptoms link remain poorly understood. The primary visual cortex (V1) comprises of arrays of vertical columns of cells with different orientation preferences and different spatial tuning for sine-wave gratings, producing a highly selective response to specific stimulus features. Checkerboard patterns of a particular orientation and spatial frequency are expected to activate some highly specialized columns of cells at V1 but not others (Wood et al., 2017). In a scenario of extreme cortical stimulation, it is likely that automatic homeostatic mechanisms at a local network level in these columns are disrupted; inhibitory interneurons, which are shared with adjacent columns, may fail to regulate excessive levels of neural excitation in these neural areas leading to an imbalance in the ratio of E/I locally (Evans & Stevenson, 2008; Wilkins, 2021).

It has been previously suggested that if the excessive activity remains contained within the cortical columns, it could cause visual distortions at a cognitive level (Meldrum & Wilkins, 1984; Evans & Stevenson, 2008). It has also been established that coloured lenses can reduce distortions, potentially “redistributing” excitation in the visual cortex (Evans et al., 2002; Wilkins & Evans, 2010; Ludlow et al., 2020; Wilkins, 2021). Although the underlying neural mechanisms are not yet understood, increased phase-locking in response to a high-contrast checkerboard pattern with a spatial frequency of 3 cpd and above, viewed binocularly, may reflect cortical hyper-reactivity of neurons locally in the visual cortex of participants demonstrating greater sensitivity to pattern glare. It is likely that ITPC as a method of measuring phase angle alignment of neurons in a specific electrode site, can capture this biological process occurring locally in the visual cortex. In contrast, 1/f slope of PSD as a measure of variability in the whole brain and an indicator of global neural synchrony and coherence, is connected to a specific ratio of E/I in the whole brain (Lombardi et al., 2017) and is less sensitive to local changes in neurotransmission. Despite the above, the link between cortical hyperexcitability and ITPC remains speculative. At this stage, due to limitations of EEG, it is not possible to draw definite conclusions with regards to the exact microscopic processes underlying the ITPC-anomalous visual experiences relationship solely based on EEG recordings.

The present study is subject to a few limitations. Although participants with known eyesight issues had corrected vision during the experiment, it is possible that visual distortions are attributed to undiagnosed ophthalmological pathologies rather than atypical functioning of the visual cortex in some subjects. Given the remarkably high prevalence of ophthalmological anomalies in individuals with ASC (Little, 2018), future research endeavours should include a comprehensive optometric examination as part of their study design to ensure that atypical visual responses to gratings are not due to underlying ophthalmological impairments.

In addition, there are some limitations regarding the method used to assess visual symptoms. The Hallucinations subscale of the SPEQ was completed by the caregiver and not the participant with ASC, despite the fact that the tool was initially developed as a self-report measure. This is because subjects with ASC are known to experience difficulties with self-report (Hill et al., 2004; Mazefsky et al., 2011) and questions about anomalous experiences can present as difficult and confusing to young children with ASC, some of which had limited communicative abilities or have comorbid intellectual disability. Along this line of argument,

a few participants could not complete the Pattern Glare Test, as they could not communicate effectively with the experimenter about the visual distortions they were experiencing during active viewing of gratings, strengthening the argument that caregiver-report was a more reliable measure to be used in the present study. Linked to this, it is important to point out that there is a lack of standardised tools designed to assess perceptual abnormalities in specific sensory modalities of children with ASC, therefore any effort to capture anomalous visual experiences is likely to be based upon a mixture of questions deriving from other tools and will be of questionable reliability. Nevertheless, in the present study, Cronbach's alpha for the composite score constructed to assess visual symptoms showed acceptable internal consistency/reliability. Another limitation concerns the sample size used to estimate the multiple regression models. Although the minimum sample size requirements of the initial power analysis were met, meaning that the sample size is regarded as adequate to detect a relationship between variables and provide a reasonably precise estimate of the strength of that relationship, the adjusted R-squared is a biased, very rough estimate of how well the regression prediction approximates the real data points and its accuracy depends upon the size of the sample. A larger sample size is likely to have provided greater precision in our parameter estimation and a more accurate estimate of R-squared. More data points would reduce the existing amount of error variance around the line of best fit in the histograms of ITPC and visual distortions (see Section 4.3.2, *Figure 5.12*). A greater sample size could also shed more light on the relationship between 1/f slope of PSD as computed from the resting state condition and visual symptoms, which approached but did not cross the probability cut-off of 0.05 ($p=0.08$).

Future studies should investigate in greater detail the relationship between ITPC and visual distortions. For example, it is still unclear whether manipulation of the parameters of the stimulus i.e orientation and spatial frequency, will have an impact on ITPC. In the present thesis, stimulus parameters were kept constant across experimental studies so that results are comparable- parameter manipulation goes beyond the scope of the present work. Nevertheless, the literature on pattern glare suggests that in order to trigger maximum pattern glare, the gratings should have a spatial frequency of 3 cpd, a 50% duty cycle, high contrast and should be viewed binocularly. Do gratings that don't meet these characteristics and are of a lower spatial frequency induce a less excitable neural response in the visual cortex and is this reflected on levels of neural variability as indexed by ITPC? It will be informative to compute ITPC in response to the standardised Pattern Glare test gratings of 0.5, 3 and 12 cpd to assess the behaviour of the local neural networks in the visual cortex. Linked to this, an important future

direction would be measuring ITPC in populations susceptible to pattern glare that are known to be characterised by a hyperexcitable visual cortex such as individuals with migraine (Palmer et al., 2000; Harle & Evans, 2006), photosensitive epilepsy and/or individuals with a diagnosis of Meares-Irlen Syndrome (Chouinard et al., 2012). Thus far, there are no studies having investigated levels of ITPC in the visual cortex of these populations in response to repeated visual stimulation and compared it with individuals without sensitivity to pattern glare. Research efforts should also focus on recruiting a larger sample and narrowing down the age range of the children with ASC. Visual distortions elicited by the Pattern Glare Test are known to reduce with age but remain stable across genders (Evans & Stevenson, 2008), therefore it is important to examine whether the relationship between ITPC and visual distortions changes in different age groups, for example young children compared to older children and/or adolescents.

Chapter 6:
Discussion

6.1 Summary of key findings

Building upon early theoretical work by Simmons et al. (2009) and Rubenstein & Merzenich (2003), an overarching aim of the present thesis was to experimentally investigate the increased neural noise hypothesis of ASC. Using Electroencephalography (EEG), neural noise was examined by measuring the degree of phase-alignment across experimental trials occurring in response to visual stimulation as indexed by ITPC and the degree of variation of the spiking activity in the aperiodic signal as indexed by $1/f$ noise slope of PSD. The experimental approach followed throughout this thesis involved interrogating signal recorded from both a visual task-based condition and a resting-state condition. Across experimental studies, ITPC and $1/f$ slope of PSD were computed from evoked neural responses generated during repeated presentation of black and white checkerboard stimuli. In addition, $1/f$ slope of PSD was computed from spontaneous brain activity recorded while participants had their eyes closed, in absence of an experimental event.

The first aim of this thesis was to investigate whether ASC and ADHD- two conditions that share genetic risk factors and behavioural features- are characterized by increased neural noise in the form of low ITPC and flatter $1/f$ slopes of PSD. Increased levels of neural noise in the form of reduced ITPC have been previously reported in separate studies in ASC and ADHD (Milne, 2011; Gonen-Yaacovi et al., 2016). $1/f$ noise slope of PSD has previously been examined in ADHD (Ostlund et al., 2021) but not in ASC. Importantly, to date, there have been no direct studies measuring and comparing levels of neural noise in clinically diagnosed ASC and ADHD samples. Although further work is required to consolidate this finding, in Chapter 2, it was demonstrated that ITPC was not significantly different in a group of adults with ASC compared to a group of TD adults and a group of adults with ADHD. This result suggests that low ITPC is not possible to accurately differentiate participants with ASC from participants without ASC, despite differing between those with and without ASC at a group level. In addition, it is important to note that the strongest phase-alignment from trial-to-trial was observed in the theta band for the majority of participants. For the ASC group in specific it covered a wider range of frequencies, extending from theta to the alpha band.

The lack of difference between the ASC group and the TD and ADHD groups in the strength of phase-locking agrees with previous accounts of no difference in levels of ITPC in response to visual stimulation (Butler et al., 2017), however this finding is contradictory to research

efforts reporting significant reductions in ITPC at a group level in adults and children (Milne, 2011; Milne et al., 2019). To illustrate this, in a similar study design, Milne (2011) found lower alpha ITPC during visual processing of Gabor patches in children and adolescents with ASC. Similarly, the study by Milne et al. (2019), using the same datasets in their ASC group as the ones utilised in Chapter 2 of the present thesis (71% of the data were previously published in Milne et al., 2019) but different datasets for their TD cohort, report significant differences in levels of ITPC between adults with ASC and TD adults. In contrast, EEG studies such as the one conducted by Butler et al. (2017), in an effort to replicate the study by Milne (2011), do not report ITPC differences between groups. These discrepancies can be explained by the small sample sizes in some of these studies and the issue of ASC heterogeneity, which means that the probability of recruiting participants with similar neurological profiles is diminished in any given set of studies. Notably, Milne et al. (2019) conclude that only a small subsample of the ASC group demonstrates low ITPC in the cortex. This highlights the need for larger sample sizes to be able to identify subgroups demonstrating distinct patterns of neural functioning in the first place and for more detailed reporting in published work to characterise variation and tease out individual differences at a second stage. As Trembath & Vivanti (2014) eloquently point out individual differences in ASC can be “*problematic but predictive*” of outcomes, therefore it is essential to understand how they manifest.

On the other hand, the lack of significant group difference in levels of ITPC between the ADHD and TD group is striking. Studies measuring ITPC in the visual modality of individuals with a clinical diagnosis of ADHD are scarce, which minimizes the ability to draw firm conclusions and explain our results within the realm of existing literature. A study by Gonen-Yaacovi et al. (2016) has previously examined ITPC in response to visual stimulation and in contrast to our finding, it reports low ITPC in the ADHD group compared to typical development. This study reports reduced ITPC in both the ICA component that best captured the early sensory response and the electrode with the strongest P1/N1 amplitude in young adults with ADHD. These discrepancies however may be explained by a difference in the way ICA components were isolated and selected for further analysis (ICA component with maximum ITPC in the present thesis vs ICA component that best captured the early sensory response in Gonen-Yaacovi et al., 2016). The smaller sample size in Gonen-Yaacovi et al. (2016) and the age difference of the samples may have also played a role in these divergent results.

When the steepness of 1/f slope of PSD was examined, a difference in 1/f slope of PSD was not evident across the ASC, ADHD and TD groups in either the visual-evoked or spontaneous neural activity. This is the first time this finding is reported in ASC and contradicts theoretical accounts of pathological undercoupling in ASC (Voytek & Knight, 2015), suggested to reflect weakened interregional oscillatory coherence in the clinical group. In ADHD, it is the first time 1/f slopes of PSD were examined as extracted from visual-evoked responses. In line with the experimental findings presented here, Pertermann et al. (2019) employed a Go/NoGo paradigm and found that children with ADHD do not generally show flatter 1/f spectral slopes but slopes appear to become flatter in NoGo trials as task demands increase and the requirements for inhibitory control become greater. In contrast to the findings presented in the present thesis, Ostlund et al. (2021) demonstrated that adolescents with ADHD show smaller aperiodic exponents in their ongoing oscillatory activity compared to their typically developing counterparts, however methodological differences in the way PSD was parameterised may have played a role in these divergent results (regression-based method in the present thesis vs FOOF algorithm in Ostlund et al., 2021).

In summary, adults with ASC displayed similar amounts of neural noise in the cortex to TD adults and adults with ADHD, a result confirmed using two different variables indexing neural variability, ITPC and 1/f slope of PSD and replicated in two different conditions, visual task-based and eyes-closed. Considering Pertermann et al.'s study (2019), it is very likely that atypicalities in levels of neural noise surface in ADHD only in paradigms that engage networks known to be deficient in the condition (i.e executive functions) and become prominent in trials that require greater executive function control (Pertermann et al., 2019). This remains an important aspect to disentangle in future work.

The second aim of this thesis was to test the feasibility of acquiring good quality EEG data from autistic children at home using a gel-based mobile EEG system and to develop a list of practical guidelines on how to successfully conduct an EEG experiment in such a naturalistic setting based directly upon participants' views. This was important to facilitate EEG data acquisition from children with ASC and a more diverse set of participants compared to the cohort recruited in Chapter 2. Based on a number of objective metrics, in Chapter 3 it was demonstrated that the signal acquired was of high quality and it was possible to perform not only basic ERP analysis but also more complex signal processing analysis such as ICA decomposition. It was also demonstrated that the LSL protocol can be reliably used to send

trigger markers through the network, enabling more complex task-based EEG designs to be implemented at home or other settings, where parallel port technology is not available. In addition, the user experience survey identified areas of good practice, which researchers should take into consideration when designing mobile EEG studies aiming to acquire data from children with ASC at home.

The third aim of the present thesis was to investigate whether the atypical levels of neural noise are observed in children with ASC. Using a similar experimental approach and method of quantifying neural variability, in Chapter 4 it was established that, in contrast to adults with ASC, reductions in ITPC do manifest in children and adolescents with ASC. Of note is that the strongest phase-locking in the ASC group was observed in a wide range of frequencies ranging from theta to beta band, an experimental finding previously reported in Chapter 2 for adults with ASC. Additionally, in line with the findings of Chapter 2, it was demonstrated that despite the ITPC reductions, the steepness of $1/f$ slope of PSD did not differ between the ASC and TD groups, after controlling for age effects. Taken together, it is concluded that $1/f$ noise dynamics during processing of simple visual stimuli and as measured from spontaneous neural activity were intact in our ASC samples.

In the context of previous work proposing that increased neural noise may be a biomarker of ASC (David et al., 2016), the fourth aim of the present thesis was to investigate in greater detail the relationship between neural noise and core diagnostic symptoms of ASC, including sensory symptoms. In Chapter 5, ITPC and $1/f$ slope of PSD were found not to be associated with primary diagnostic features of ASC such as social communication impairments and repetitive and restricted patterns of behaviour in a group of children with ASC. The finding about the lack of relationship between ITPC and core diagnostic features of ASC is in line with previous research work by Milne et al. (2019). Not directly comparable but perhaps complimentary findings are coming from the fMRI literature. Dinstein et al. (2012) also did not find a significant relationship between ASC symptom severity, as assessed by the ADOS, and SNRs extracted from BOLD signal in response to visual, auditory and somatosensory stimuli. Taken together, the result of the present thesis consolidated previous findings speaking against a relationship between neural noise and primary diagnostic symptoms of ASC, further suggesting that low ITPC is not likely to be a biomarker of ASC (David et al., 2016).

Although core phenotypic symptoms of ASC did not predict levels of neural noise as indexed by the two variables of interest, it was established that levels of neural noise as measured by ITPC can be partially predicted by clusters of secondary symptoms (18% of the variance explained), commonly found in other clinical and non-clinical groups. Indeed, this is the first study to report a link between ITPC, anomalous visual experiences and visual distortions, a group of visuoperceptual symptoms shown to manifest with varying prevalence in individuals with ASC, patients with photosensitive epilepsy (Wilkins et al., 1975; Soso et al., 1980; Radhakrishnan et al., 2005; Millichap, 2005; Wilkins et al., 2005), migraine (Harle et al., 2006; Conlon et al., 2012; Shepherd et al., 2013; Hayne & Martin, 2019) and other individuals in the general population (Braithwaite et al., 2013). In our ASC sample, the greater sensitivity to pattern glare and the greater number of anomalous visual symptoms a participant with ASC demonstrated, the more phase-aligned their neuronal response was to the checkerboard stimulus- a relationship likely to be reflecting cortical hyper-reactivity of neurons locally in the visual cortex in response to that stimulus (although see Section 6.2 for a discussion on the relationship between ITPC and cortical hyperexcitability). In addition, we found no relationship between the steepness of the $1/f$ slope of PSD and the same cluster of visual symptoms. This result indicates that different variables have predictive power over $1/f$ slope of PSD as compared to ITPC.

In conclusion, the two variables ITPC and $1/f$ slope of PSD are likely to be capturing distinct neural processes. In support of this, it was also shown that ITPC and $1/f$ slope of PSD are not associated, further demonstrating that the two metrics are tapping upon different neural mechanisms. This finding may be explained by methodological differences in spatial scale; $1/f$ slope was extracted from all electrodes in the cortex, in contrast to ITPC, which was calculated from visual ICs or the occipital electrode cluster, therefore was more localised to a specific region. In addition, $1/f$ slope of PSD is computed by measuring the total energy distribution of the signal which is a real-valued quantity and does not contain phase information, whereas ITPC is calculated by averaging phase angles at each time point over trials, therefore is independent of power (Cohen, 2014). Another key difference relates to the signal periodicity; ITPC was calculated from periodic signal, whereas $1/f$ slope captures aperiodic signal properties. Taken together, ITPC constitutes a metric of the temporal synchrony of a set of oscillations locally in the visual cortices, whereas the aperiodic $1/f$ slope indicates excessive noise in the cortex globally.

6.2 Implications

In the present thesis, it was established that increased neural noise in the form of low ITPC occurs in the visual-evoked activity of children with ASC. Although further work is necessary to consolidate this finding, in contrast to children, adults with ASC showed similar patterns of phase-locking to their TD counterparts and adults with ADHD. The above result agrees with previous accounts of low ITPC during visual processing in children with ASC (e.g Milne et al., 2011, also see *Table 2.1* in Chapter 2 for a summary of studies having investigated ITPC in other modalities) and provides further evidence for disrupted patterns of neural noise in ASC. In both children and adults with ASC the strongest phase-alignment was observed in a wide range of frequencies ranging from theta to beta band, whereas for the TD groups maximum ITPC occurred in the theta and alpha band alone. This was a consistent finding replicated across different samples in Chapter 2 and 4.

The exact biological mechanism that gives rise to low ITPC in children with ASC remains unknown, however a few theories have previously been proposed. Rubenstein & Merzenich (2003) previously suggested that some subtypes of ASC are associated with reductions in SNRs in key neural circuits underlying sensory behaviour, likely to be caused by an increased ratio of E/I in those key networks. Difficulties to align phase-angles from trial to trial may be explained by an imbalance in E/I ratio, resulting from disproportionately high excitation (i.e excessive GABA) or weak inhibition (i.e low levels of glutamate) (Rubenstein & Merzenich, 2001). Along those lines, hyperexcitability in the autistic brain has been also suggested to result from sparser, less “sharp” neural representations, further affecting behavioural sensitivity to incoming information (i.e poor discrimination of stimuli) (Uzunova et al., 2016; Ward, 2018). During stimulus presentation, GABA-ergic and glutamatergic neurons are selectively activated. Within the cortical space of minicolumns in the neocortex, GABA-ergic neurons increase the contrast or else “sharpen” the receptive field by mediating activity *between* neighbouring minicolumns through lateral inhibition (Cree, 2014). A breakdown of this “cross-talk” on a synaptic transmission level may be giving rise to irregular and “imprecise” phase-locking during processing of visual stimuli in ASC. Other lines of work suggest that astrocytes and microglia- two types of glial cells known to play a central role in synaptic formation and function- interfere with neural circuit development in ASC, affecting neural synchrony and connectivity (Kanner et al., 2018). It is however important to note that there is currently no direct experimental evidence linking the reductions in ITPC with the above theories.

Although levels of ITPC differed significantly between children with and without ASC at a group level, low ITPC could not differentiate participants with ASC from participants without ASC with adequately high accuracy to be considered a valid endophenotype of ASC. The lack of specificity and sensitivity to a single disorder implies that the neural correlate cannot be used as a diagnostic tool. This is not surprising as behavioural manifestations of ASC are known to arise from multi-factorial gene-environment interactions, leading to great behavioural heterogeneity accompanied by a large number of comorbid conditions (Beauchaine & Constantino, 2017; Masi et al., 2017). As a result, a single pathophysiological route to the range of ASC phenotypic expressions is unlikely to exist (Happé et al., 2006). In addition, emerging evidence suggests that there is not a single neural profile underlying ASC and recent experimental studies point towards the existence of subgroups within ASC with potential neurological differences (Ousley & Cermak, 2014; Milne et al., 2019).

In the present thesis, difficulties to consistently align phase angles from trial-to-trial were prominent in early development but findings were less clear in mid and late adulthood. This result may be explained by a sampling bias or alternatively it could reflect true differences in the strength of phase-locking in adulthood vs childhood. It is plausible that due to the small sample sizes in the adult study, there was lower power to detect any difference in ITPC amongst groups- also explaining the presence of outliers in the data. In addition, the ASC adult sample consisted of participants later diagnosed in adulthood, therefore their cognitive profile differed substantially from the profiles of children with ASC recruited for the child study. However, an intriguing possibility is that the strength of phase-locking changes from one developmental stage to the other in ASC. In a study of cognitive maturation, Marek et al. (2018) showed that theta band phase-locking reduces with development in neurotypical populations, in line with Papenberg et al. (2013). However, it is unclear if a similar pattern characterises ASC and therefore, further work is required to disentangle how network development unfolds in ASC and whether ITPC degrades as part of the neural maturation process and aging.

For the majority of participants, the strongest phase-locking occurred in slow rhythms (i.e theta and alpha band). In a similar study design, Butler et al. (2017) also found the largest ITPC to occur within 3-8Hz in both the ASC and TD samples. Insights into oscillatory network dynamics from other studies investigating ITPC in ASC are limited. For example, studies such

as the one by Milne et al. (2011) measure ITPC in a pre-defined frequency band (i.e. alpha band), whereas other experimental work (see *Table 1.1*) focuses on different types of stimuli (e.g. auditory) and different electrode clusters of interest, therefore there are substantial spatial differences in the analytical approach. On the other hand, a large number of animal studies have previously established that visual stimulation reliably elicits strong phase-locking of theta rhythms locally at the visual cortex, with the hippocampal circuit likely to be driving this neural pattern in an effort to “bind” sensory representations in memory (Fournier et al., 2020). Those have shown that a) naturalistic stimuli i.e a coloured movie modulate the firing rate of multiunit spikes and low-frequency LFP phase at V1 of macaques (Montemurro et al., 2008) and b) with increasing visual stimuli intensity (low, medium, high) there is greater enhancement of theta band spike phase-locking at V1 in mice (Huang et al., 2020). Human studies using a wide variety of metrics to quantify phase coherence have also shown that temporal expectation and attention modulate phase entrainment of slow oscillations in the visual cortex (Cravo et al., 2013; Mazaheri et al., 2010). Considering the studies outlined above and the literature implicating theta oscillations in episodic memory formation, strong phase-alignment of slow oscillations is likely to be directly linked to the active processing of the checkerboard stimulus in the visual cortices during task engagement in an effort to integrate the sensory representation into visual working memory (Herweg et al., 2020). It is also likely that the predictive attentional cue (i.e the cross) presented prior to the checkerboard may have enhanced slow rhythm phase-locking at the time of checkerboard stimulus presentation.

The fact that maximum ITPC was captured in faster oscillating networks for some participants with ASC- high alpha for some adults with ASC and high alpha/low beta for some children with ASC- is striking. Beta oscillations, particularly at the visual cortices, have not been systematically examined in ASC. In the visual domain, some evidence coming from the ASC literature has shown that beta band oscillatory activity is altered across local and distant cortical networks in children with ASC during a visual crowding task (Ronconi et al., 2020) and a long latency flash visual evoked potentials paradigm (Isler et al., 2010). Authors conclude that differences between the ASC and TD groups tap upon underlying E/I imbalances in participants with ASC- which may also be explaining the finding of enhanced ITPC of beta oscillations in some participants in the experimental work summarized here- but without providing further mechanistic insights.

Nevertheless, we propose that this finding is better interpreted in the context of literature suggesting that feedback alpha and beta rhythms mediate feedforward theta and gamma signal projections according to the behavioural context (Bastos et al., 2015). In the present thesis, it is plausible that a high degree of phase consistency trial on trial in the high alpha/low beta band indicates greater attentional top-down influences in an effort to adapt to the visual task demands. In the brain's parallel processing oscillatory architecture, if theta rhythms are responsible for setting the scene by conveying early visual information, alpha and beta rhythms are fundamental for modulating attentional inputs (Fries, 2009; Fries 2015). As Fries (2015) points out, the exact differences between alpha and beta neighbouring frequencies have not yet been precisely determined, however strong beta phase-locking is shown to be associated with top-down gating of contextual information to the early visual cortices (Donner et al., 2007; Spitzer & Haegens, 2017; Richter, Coppola & Bressler, 2018) and alpha phase-locking with the inhibition of task-irrelevant input and the enhancement of task-relevant activity locally (Jensen & Mazaheri, 2010; Klimesch, 2012). It is also possible that the task design employed in the present thesis may have had an influence on this finding. Strong phase-locking of beta oscillations in the visual cortex may reflect contextual gating of information related to visual action feedback (Limanowski, Litvak & Friston, 2020). Therefore, it may be that ITPC was stronger in the beta oscillatory network than other networks due to the fact that those participants with ASC were preparing for the movement execution i.e spacebar presses in anticipation of the deviant spaceship stimulus.

The present thesis was the first to demonstrate that a cluster of visual symptoms can predict levels of ITPC in a group of children with ASC. In the present study, the greater sensitivity to pattern glare a participant demonstrated, the higher their ITPC was in response to the checkerboard stimulus. This was an unexpected finding, which is difficult to explain in the context of existing ASC theories. Rubenstein & Merzenich's (2003) theory postulates that a disruption in E/I balance would lead to increased levels of neural noise and a hyper-excitable cortex, which in turn gives rise to specific aspects of ASC symptomatology (e.g. sensory symptoms). Following Rubenstein & Merzenich's (2003) line of argumentation, it was hypothesized that increased occurrence of visual symptoms would be associated with greater levels of neural noise, taking the form of lower ITPC in the cortex. However, the opposite pattern was observed in Chapter 5 and greater number of visual symptoms were associated with stronger phase coherence. In the pattern glare literature, cortical hyperexcitability is suggested to be the neurobiological mechanism underlying increased sensitivity to pattern glare

(Wilkins, 2021). It has been previously proposed that inhibitory interneurons, which are shared with adjacent columns within V1, may fail to modulate excessive levels of neural excitation in the visual cortex of some individuals, leading to an E/I imbalance locally and causing visual distortions and discomfort at a cognitive level (Meldrum & Wilkins, 1984; Evans & Stevenson, 2008). If this theory is true, one would expect high ITPC to be indicative of a hyperexcitable visual cortex, in contrast to Rubenstein & Merzenich's (2003) proposals. Considering the above, the link between ITPC and neural hyperexcitability remains poorly understood and further experimental work is necessary to shed light on the relationship beyond theory.

Although the link between ITPC and cortical hyperexcitability is yet to be established, the experimental findings presented in the present thesis are promising and indicate that ITPC can provide valuable information on how prone an individual with ASC would be to visual distortions and anomalous visual perceptual experiences. ITPC may not be satisfying the criteria for an ASC endophenotype, however perhaps it can be further utilized for the identification of more cohesive subgroups within a highly heterogeneous psychiatric group. Increased ITPC could be indicative of a subgroup of individuals within ASC, characterised by visuo-perceptual disturbances, unique to or more prevalent in that particular subgroup. On the other hand, low sensitivity to pattern glare and smaller number of anomalous visuo-perceptual experiences is linked to low ITPC, potentially indicating a "less excitable" visual cortex in some children with ASC.

6.3 Limitations

The ability profiles of individuals with ASC vary substantially within the autism spectrum. In the present thesis, the ASC samples recruited consist of individuals characterized by lower ASC symptom severity and higher cognitive ability ($IQ > 70$), therefore findings cannot be generalised to those with more severe forms of ASC. Despite the efforts to eliminate sampling biases by employing innovative recruitment strategies (eg. testing participants at home), individuals with more severe forms of ASC may have had a lower sampling probability to be included in the studies conducted for the present thesis. The opt-in recruitment method employed in the experimental studies summarised in Chapter 2 and 4 is likely to have skewed sampling towards adults and children with ASC who were more able to communicate effectively, and tolerate the experimental procedure. In addition, although a large proportion of those with ASC have a comorbid intellectual impairment, the ASC samples recruited for the two studies were limited to individuals without an intellectual disability, therefore they were not representative of the ASC population at its entirety. For that reason, the question of whether increased neural noise is a feature of the brain of individuals with more severe forms of ASC, remains unanswered.

Another limitation of the present thesis relates to use of clinical questionnaires such as the SRS to ascertain ASC diagnosis, as opposed to the use of direct observational measures such as the ADOS and/or parent focused structural interviews such as the ADI-R. In Chapter 1, SRS was utilised in order to ensure the severity of ASC behaviours is assessed as accurately as possible. Adults with ASC are known to display camouflaging behaviours (Lai et al., 2017), therefore there was a greater chance that some of the ASC behaviours would not surface during a semi-structured observational interaction with the experimenter. Another disadvantage of gold-standard tools such as the ADOS and the ADI-R is the length of administration time, ranging from thirty to sixty minutes for ADOS (Lord et al., 2012) and from one and a half to three hours for ADI-R (Lord et al., 1994). In Chapter 4 and 5, the aim was to utilise a short screening tool which would allow to balance out the speed of data acquisition and the quality of clinical information acquired. This methodological approach allowed to collect data from a large number of children with ASC and meet power requirements to perform regression analysis. Linked to this, in the child studies diagnostic status of comorbid conditions was not confirmed using any clinical tools, but rather, this information was acquired through parent reporting. As

a result, it is still unclear whether specific non-ASC clinical symptoms are linked or have played a role in modulating levels of neural noise in the experimental studies presented in the present thesis. Scatterplots in *Appendix 2* indicated that this is unlikely; a relationship between comorbid conditions and levels of neural noise is not clearly evident in these graphs. Future work however should confirm diagnostic status directly using clinical tools and look at the impact of comorbid clinical symptoms on levels of neural noise in greater detail.

In Chapters 2 and 4, although the confounding effect of age was taken into account when comparing average levels of neural noise between groups, it is possible that age effects were not fully eliminated. This is more relevant for the experimental study outlined in Chapter 4, than Chapter 2, as in the child study, the TD group was younger on average compared to the ASC group. In addition, although a link between ITPC and age was not evident, 1/f noise of PSD and age were significantly correlated in the samples tested. Therefore, the fact that there was an age difference between the ASC and TD groups made it difficult to fully rule out the effect of age in the statistical analyses, particularly when comparing 1/f noise of PSD between groups. In addition, electrode-to-electrode comparisons were not possible due to difficulties to statistically control for these age effects, while also correcting for multiple comparisons.

An important limitation of the present thesis relates to the method by which the ITPC measure was computed. Following the analytical approach implemented by Milne et al. (2019), we extracted maximum ITPC from any independent component at any frequency and at any time point and utilised this value to quantify the amount of neural noise in the cortex for each participant. This approach prioritises the maximum ITPC over similarity in the source across participants and as a result it is difficult to interpret in the context of specific neural processes. In addition, inspection of the topographic scalp maps of the selected ICs revealed that the selected IC was projected at the occipital lobe for the majority of participants but not for all. It is unclear whether in some instances selected ICs reflected mu rhythm, as suggested in Onton et al. (see *Fig 2*, 2006, p.816) or they were true reflection activations of the visual cortex. Source localisation of the specific ICs was not performed, therefore it remains unclear whether the signal captured visual activity.

Another limitation concerns the method by which narrowband oscillatory ‘humps’ were separated from non-oscillatory dynamics i.e 1/f noise in the signal. The present thesis adopted

a regression-based method to parameterise power spectra, originally used in Voytek et al. (2015) and further refined this approach to identify the start and the end of the alpha band peak for each participant individually. Considering that the majority of experimental studies measuring 1/f noise utilise the regression-based method of parameterisation (see Voytek et al., 2015; David et al., 2018), this approach allowed for greater standardisation and comparability of findings across studies. For example, the finding about the relationship between age and 1/f noise of PSD, first reported in Voytek et al. (2015), was replicated in our ASC samples. However, other methods of parameter fitting have also been developed, which were not adopted in the present thesis (i.e see ' $\alpha+1/f$ ', 'FOOF' and 'IRASA' method in Section 1.7.3 of Chapter 1). The FOOF algorithm in particular identifies secondary non-alpha related humps, likely to result in more accurate parameterisation of power spectra. Related to the above, it is still unknown whether this difference in the way periodic activity is calculated and subtracted can impact the direction of group comparison outcomes. First evidence from Ouyang and colleagues (2020) has shown that all methods yield similar results (see *Fig 2* in Ouyang et al., 2020). In addition, in the studies of the present thesis, inspection of the individual channel power spectra figures before and after line fitting and alpha band peak subtraction showed that the gradient does not change between the two stages of processing. Therefore, this provides confidence that the results of group comparisons are robust.

Very few studies have previously examined 1/f slope of PSD and as a result it is still unclear what the optimal analytical method of estimating aperiodic exponents may be. For example, there is currently no consensus on the signal source PSD should be extracted from and consequently the electrode cluster 1/f analysis should be performed on. In the existing literature, this information is often not reported. In the present thesis, two methods of comparing levels of 1/f noise across groups were utilized in order to scrutinize whole-brain dynamics; either the grand average value of the aperiodic exponent was compared across groups and/or single electrode comparisons were performed. It is unclear whether group differences would be evident if a different source of signal had been chosen for analysis. Taken together, the study of aperiodic signal properties is a newly emerging and rapidly evolving field. More refined ways of parameterising PSD are already emerging and as more studies begin to investigate 1/f noise, these will advance scientific thinking regarding best analytical practices.

6.4 Future directions

Another important future direction is to investigate whether low ITPC characterises the brain of individuals with more severe forms of ASC, as well as those with ASC and comorbid intellectual disability. Inadequate representation of those severely affected in studies exploring neural correlates of ASC, leads to a blurry picture of the neural profiles that may exist and their characteristics (Stedman et al., 2018). In order to facilitate participation of this group in EEG studies, it is important to adhere to good autism practice as outlined in the present thesis (i.e data acquisition at home) but also use appropriate strategies to accommodate for the extreme sensory sensitivities participants with more severe forms of ASC may experience. Future work should aim to test the functionality of using a wireless system instead of a wired EEG device and dry electrodes instead of gel-based alternatives. Wireless EEG solutions may be more suitable for children with lower cognitive ability that tend to pull away electrodes or wander during an experiment and dry EEG systems may be more tolerable for those demonstrating extreme sensory reactions to sensory input.

Building upon the finding of reduced ITPC in children with ASC, future studies should also investigate in comparative study designs whether reduced ITPC occurs in children with ASC in response to stimuli targeting different modalities such as somatosensory, auditory and tactile. Studies have previously measured ITPC in all sensory modalities but have not studied these in conjunction and only report group level analysis (for somatosensory modality see Butler et al., 2017, auditory: Edgar et al., 2015; Yu et al., 2018, tactile: Coskun et al., 2009). It is also important to clarify whether ITPC reductions are observed only during low level processing of sensory stimuli or whether these are apparent in more complex task designs which require the engagement of not only the sensory cortices (i.e visual) but also other regions such as the prefrontal cortex.

The literature will also benefit from an in-depth investigation of the relationship between ITPC and visual distortions. Due to the nature of EEG as a neuroscientific method of experimentation, it is not possible to draw definite conclusions with regards to the exact microscopic processes underlying the ITPC-anomalous visual experiences relationship. In follow-up EEG studies, the manipulation of stimulus parameters could shed light on the link between cortical hyperexcitability and ITPC. ITPC should be computed in response to the

standardised Pattern Glare test gratings of 0.5, 3 and 12 cpd to assess whether the strength of phase-locking changes depending on the spatial frequency of the visual stimulus.

In the present thesis, it was established that levels of neural noise as measured by ITPC can be partially predicted by a cluster of visuoperceptual symptoms in a group of children with ASC. An important future direction would be to replicate and consolidate those findings by comparing levels of ITPC in groups susceptible to pattern glare such as individuals with migraine (Palmer et al., 2000; Harle & Evans, 2004), photosensitive epilepsy and/or individuals with a diagnosis of Meares-Irlen Syndrome (Chouinard et al., 2012) against control groups of individuals less prone to pattern glare. In addition, given that visual hallucinations and anomalous visual experiences are more prominent in schizophrenia, it would be informative to measure levels of ITPC, together with the individual's susceptibility to pattern glare and their predisposition to anomalous perceptual experiences, in a group of individuals with ASC and a group of patients with schizophrenia. These future experiments will help disentangle whether individuals experiencing higher occurrence of visual distortions demonstrate a strongly phase-aligned neural response in response to patterns of higher spatial frequency, irrespective of their clinical diagnosis. In that respect, such a study design could shed light on whether ITPC takes the form of a transdiagnostic marker cutting through diagnostic boundaries.

6.5 Conclusion

In the present thesis it was established that increased neural variability in the form of low ITPC occurs only in children with ASC. Adults with ADHD showed similar levels of ITPC to the TD group and adults with ASC. Although levels of ITPC differed significantly between children with and without ASC at a group level, low ITPC could not differentiate participants with ASC from participants without ASC with adequately high accuracy to be considered a biomarker of ASC, as proposed previously in the literature (David et al., 2016). In addition, it was demonstrated that ITPC is not linked to primary phenotypic expressions of ASC but is associated with anomalous visual experiences and visual distortions, a group of visuoperceptual symptoms shown to manifest with varying prevalence in individuals with ASC and other individuals in the general population. Finally, it was established that 1/f noise power spectral dynamics measured during processing of simple visual stimuli and during rest were intact in the ASC and ADHD samples tested, providing evidence against the pathological undercoupling hypothesis proposed by Voytek & Knight (2015).

Appendix 1

Chapter 4

Relationship between neural noise and comorbid conditions

Inspection of the scatterplots of ITPC and 1/f noise of PSD (*Figure 1*) did not reveal any clear relationship between variables indexing neural noise and the number of comorbid conditions (A) and the type of comorbid condition (B) in the ASC group.

Figure 1.1

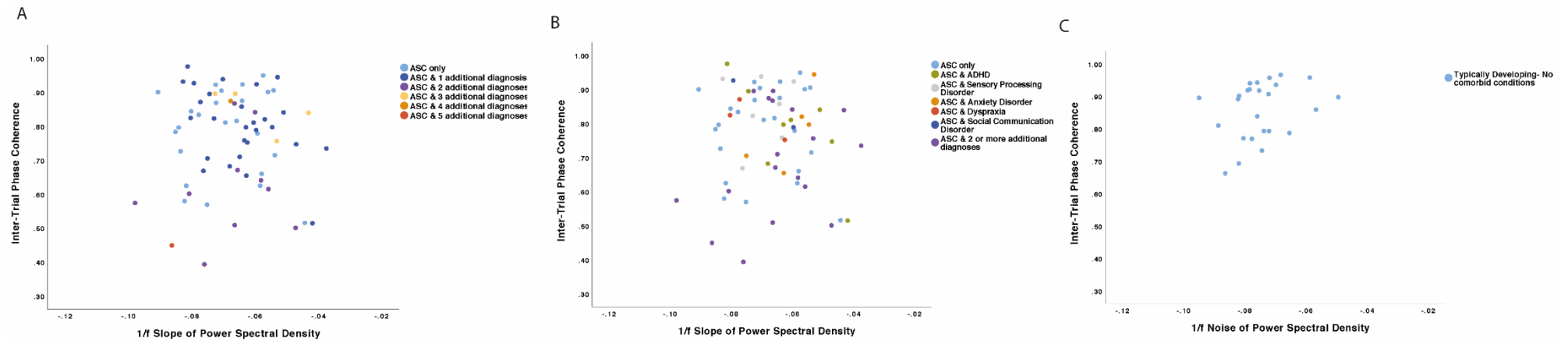


Figure 1.1: Scatterplot of ITPC and 1/f slope of PSD grouped by the number of additional diagnoses and the type of diagnoses for the ASC group (A, B) and the TD group (C).

Annex 1

Chapter 2

Independent Component Analysis

Figure 1.1

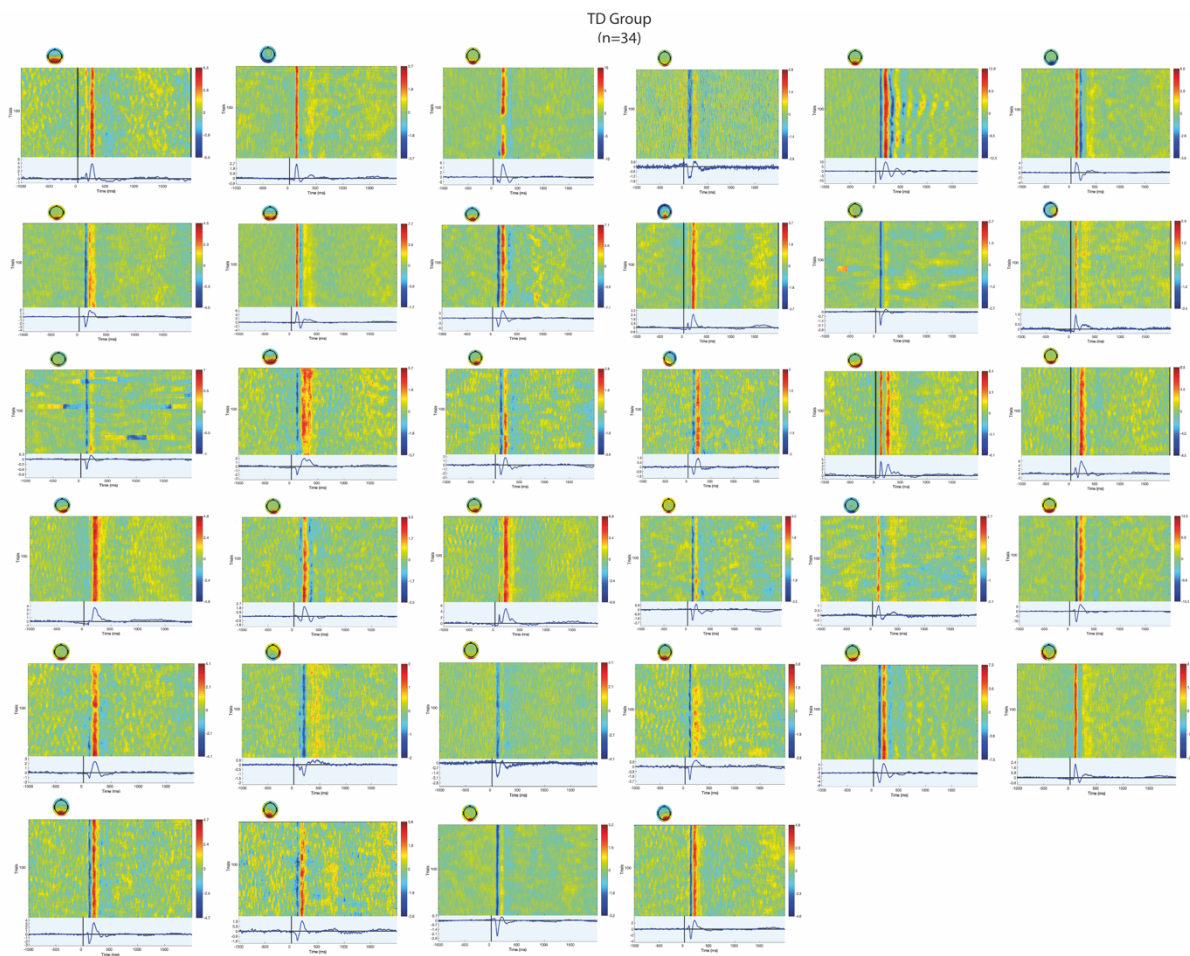


Figure 1.1: ERPs of the selected Independent Components (ICs) included in the group analysis, presented for the TD group ($n=34$)

Figure 1.2

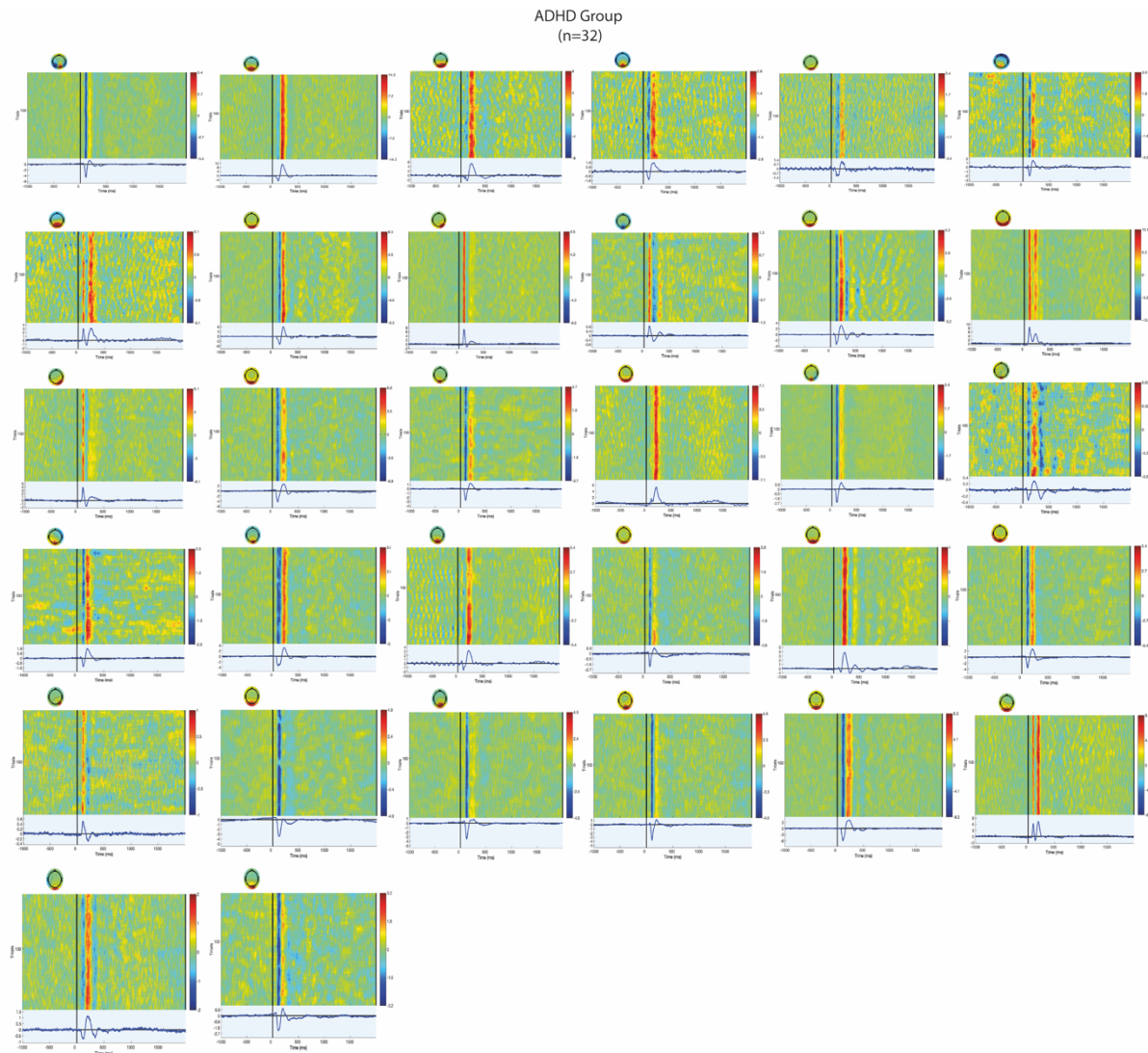


Figure 1.2: ERPs of the selected Independent Components (ICs) included in the group analysis, presented for the ADHD group ($n=32$)

Figure 1.3

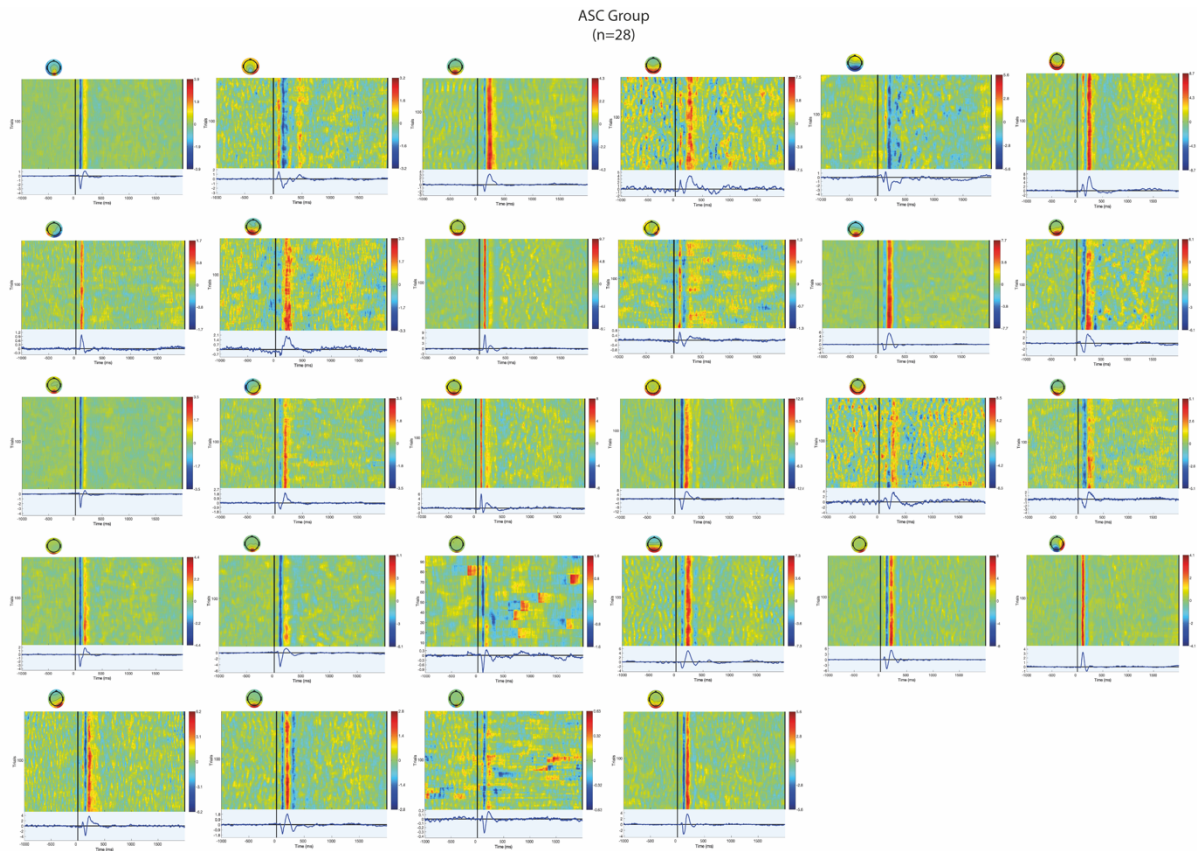


Figure 1.3: ERPs of the selected Independent Components (ICs) included in the group analysis, presented for the ASC group ($n=28$)

Channel Analysis

Figure 1.4

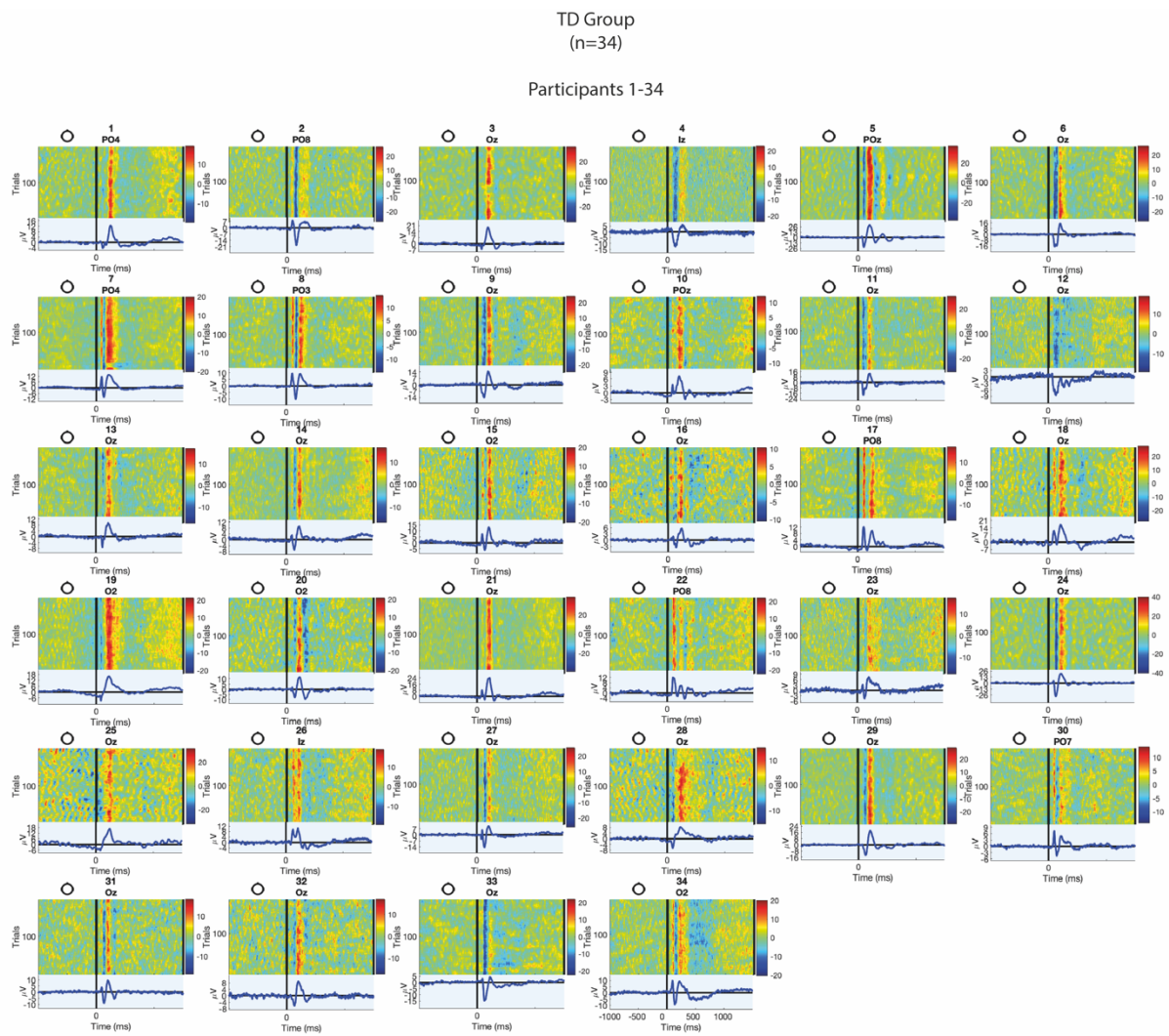


Figure 1.4: ERPs of the selected channels included in the group analysis, presented for the TD group ($n=34$).

Figure 1.5

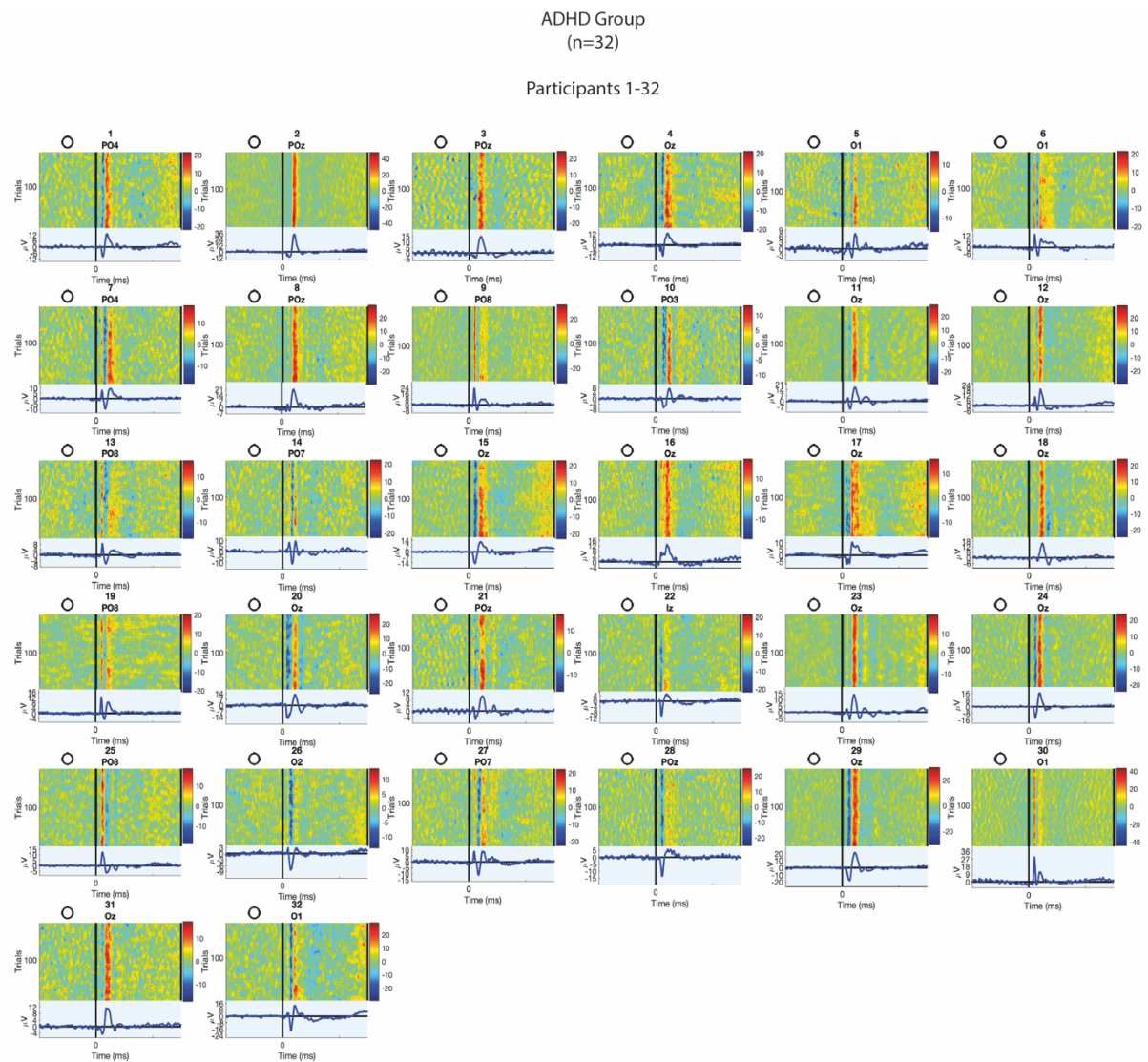


Figure 1.5: ERPs of the selected channels included in the group analysis, presented for the ADHD group ($n=32$).

Figure 1.6

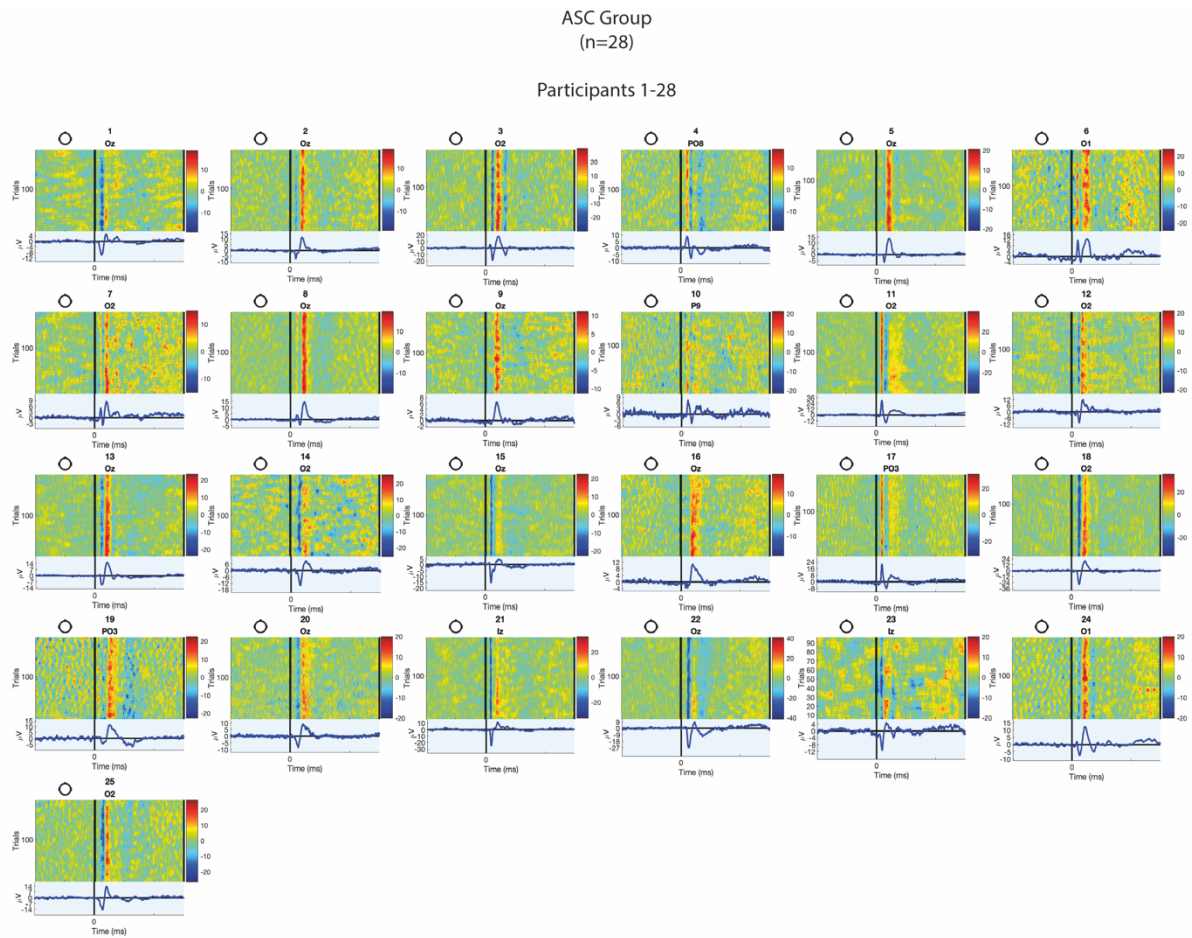


Figure 1.6: ERPs of the selected channels included in the group analysis, presented for the ASC group ($n=28$).

Annex 2

Chapter 2

Figure 2.1

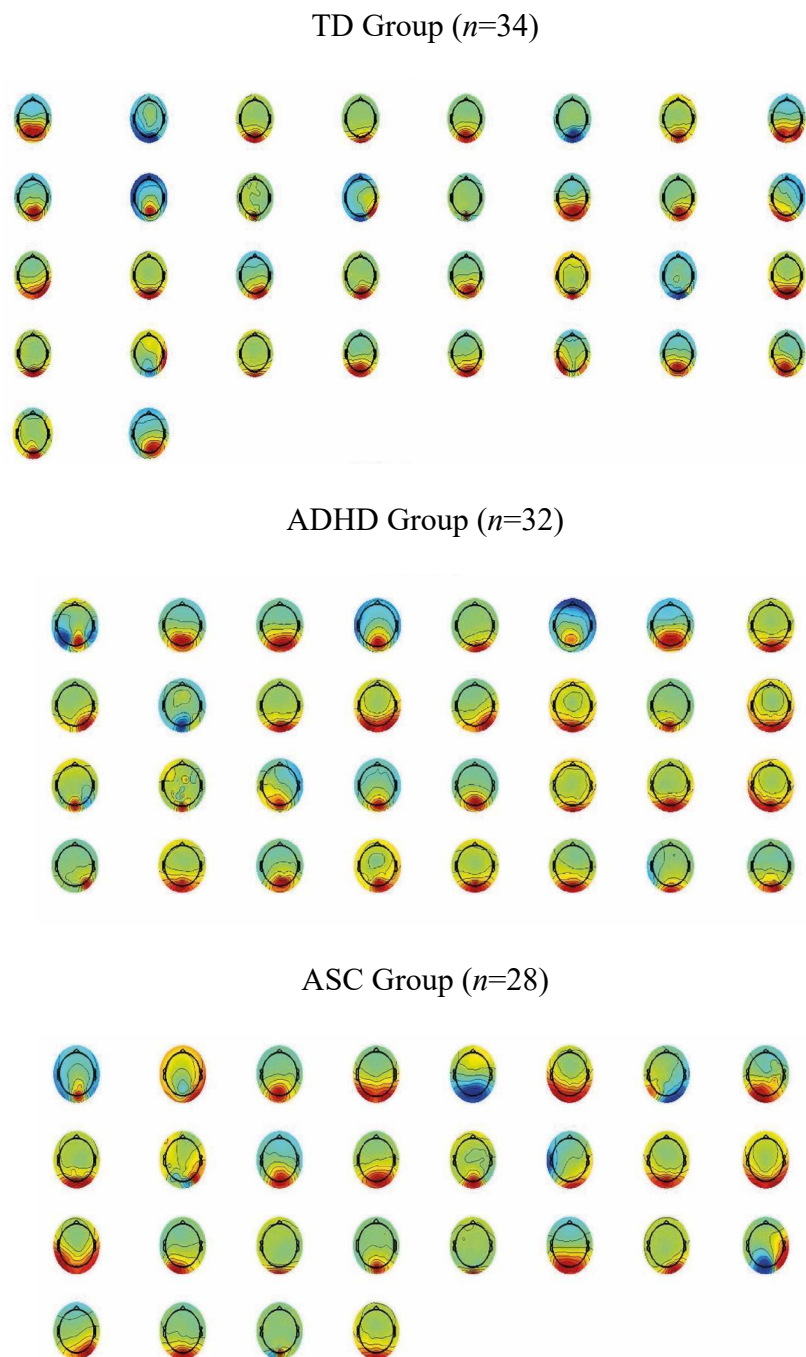


Figure 2.1: Independent Components with maximum ITPC for the TD, ADHD and ASC group.

Annex 3

Chapter 2

Figure 3.1

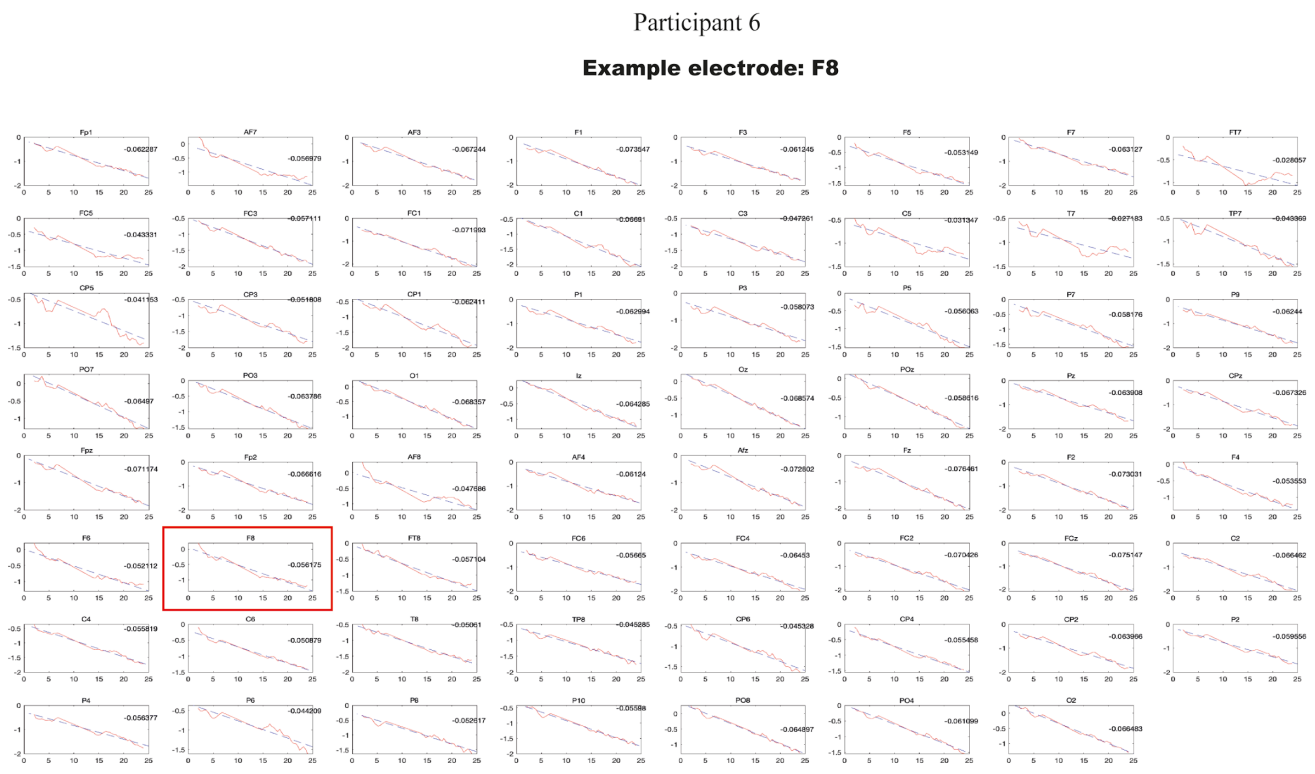


Figure 3.1: 1/f slope of all electrodes computed from Participant 6 in the ASC group.

Annex 4

Chapter 2

Independent Component Analysis

Figure 4.1

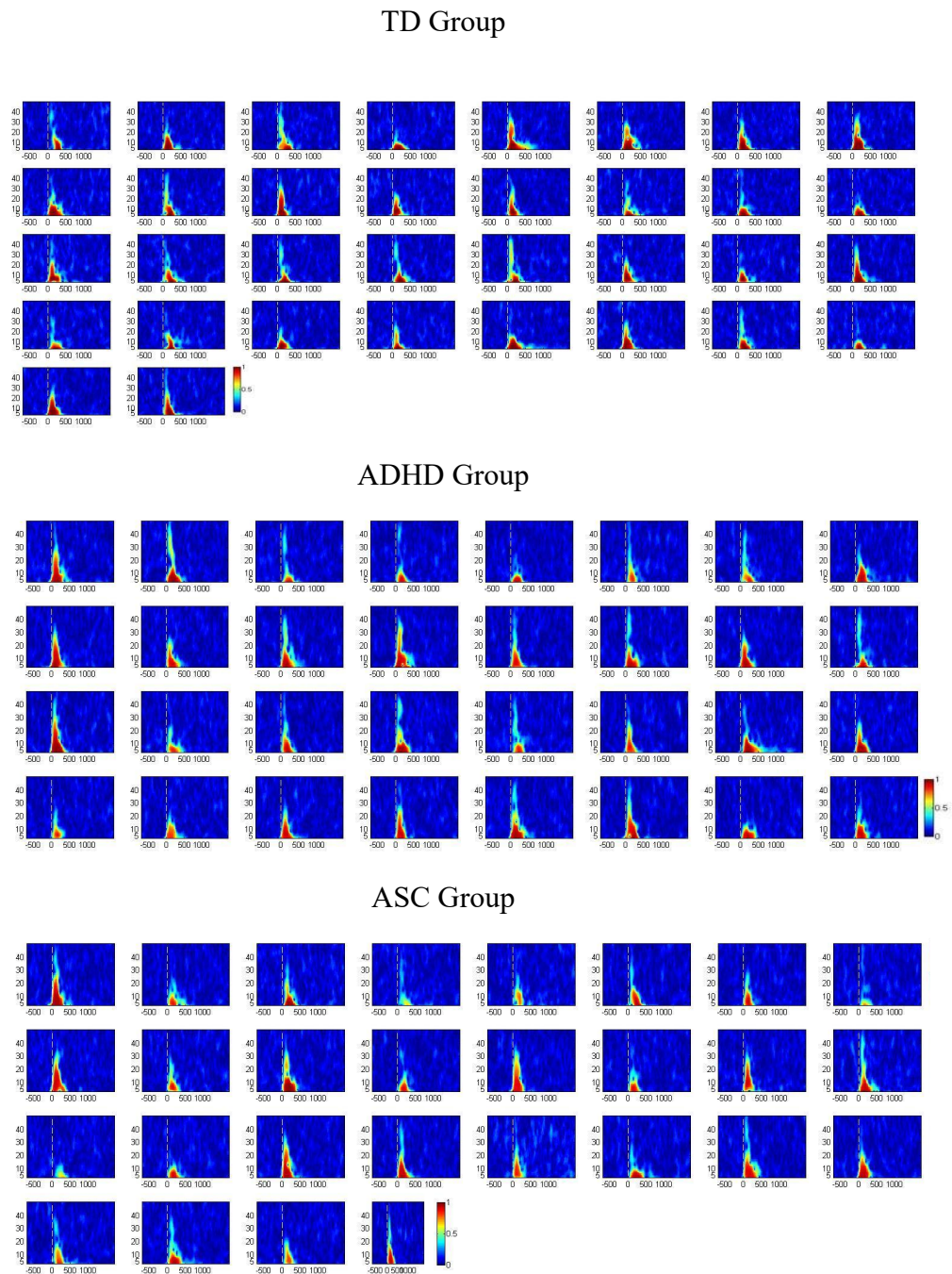


Figure 4.1: Maximum ITPC heat maps for the TD ($n=34$), ADHD ($n=32$) and ASC group ($n=28$)

Annex 5

Chapter 3

Figure 5.1

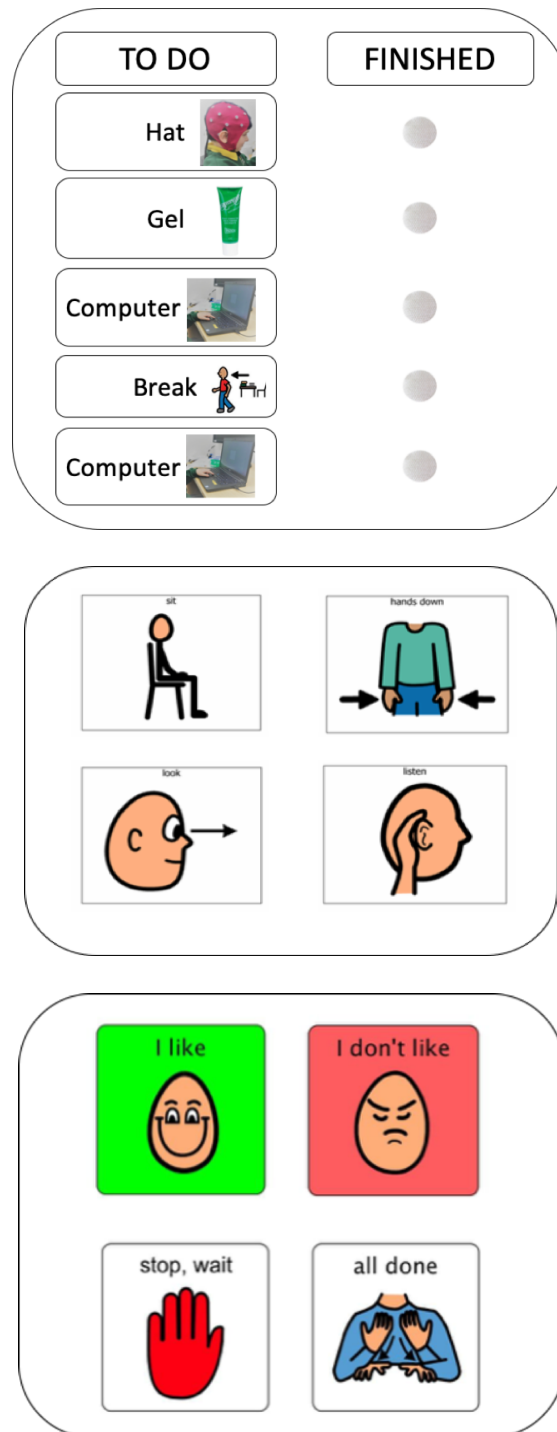


Figure 5.1: Communication cards used during the mobile EEG session

Annex 6

Chapter 3

Figure 6.1



Figure 6.1: Participant and experimenter interactions during the mobile EEG testing session

Annex 7

Chapter 4

Independent Component Analysis

Figure 7.1

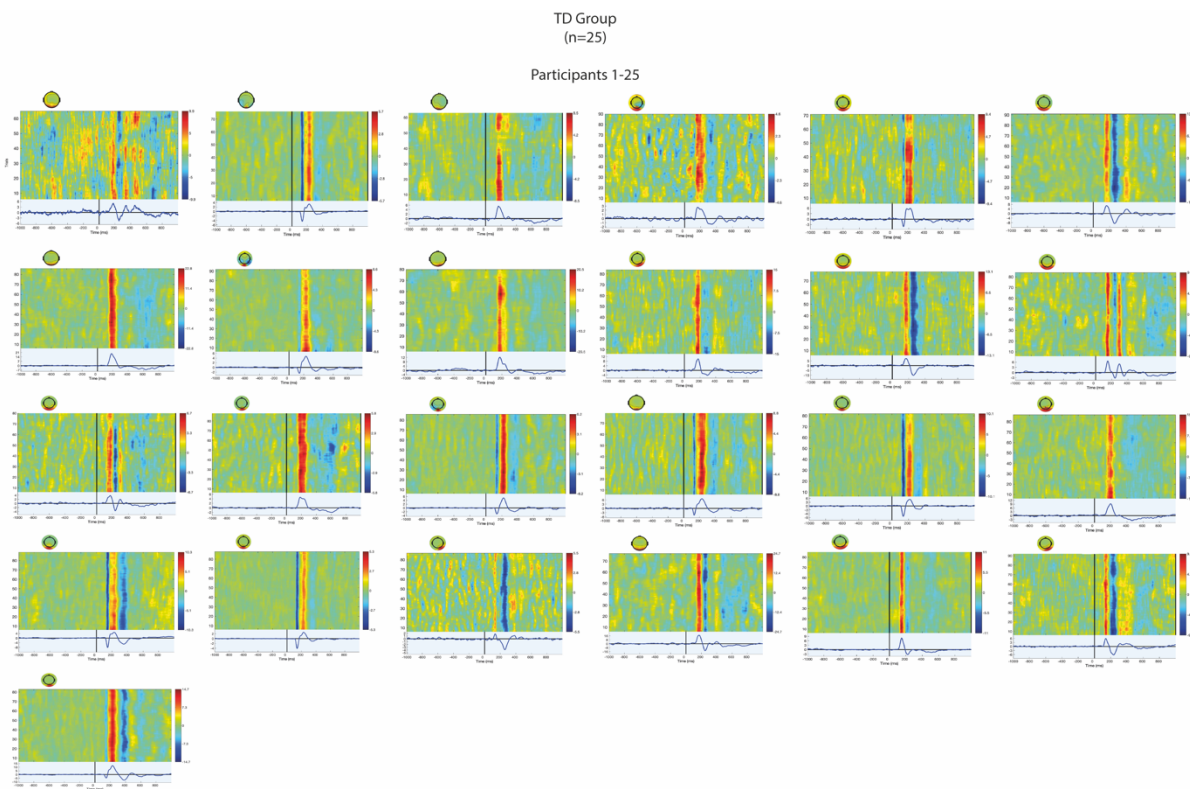


Figure 7.1: ERPs of the selected Independent Components (ICs) included in the group analysis, presented for the TD group ($n=25$).

Figure 7.2

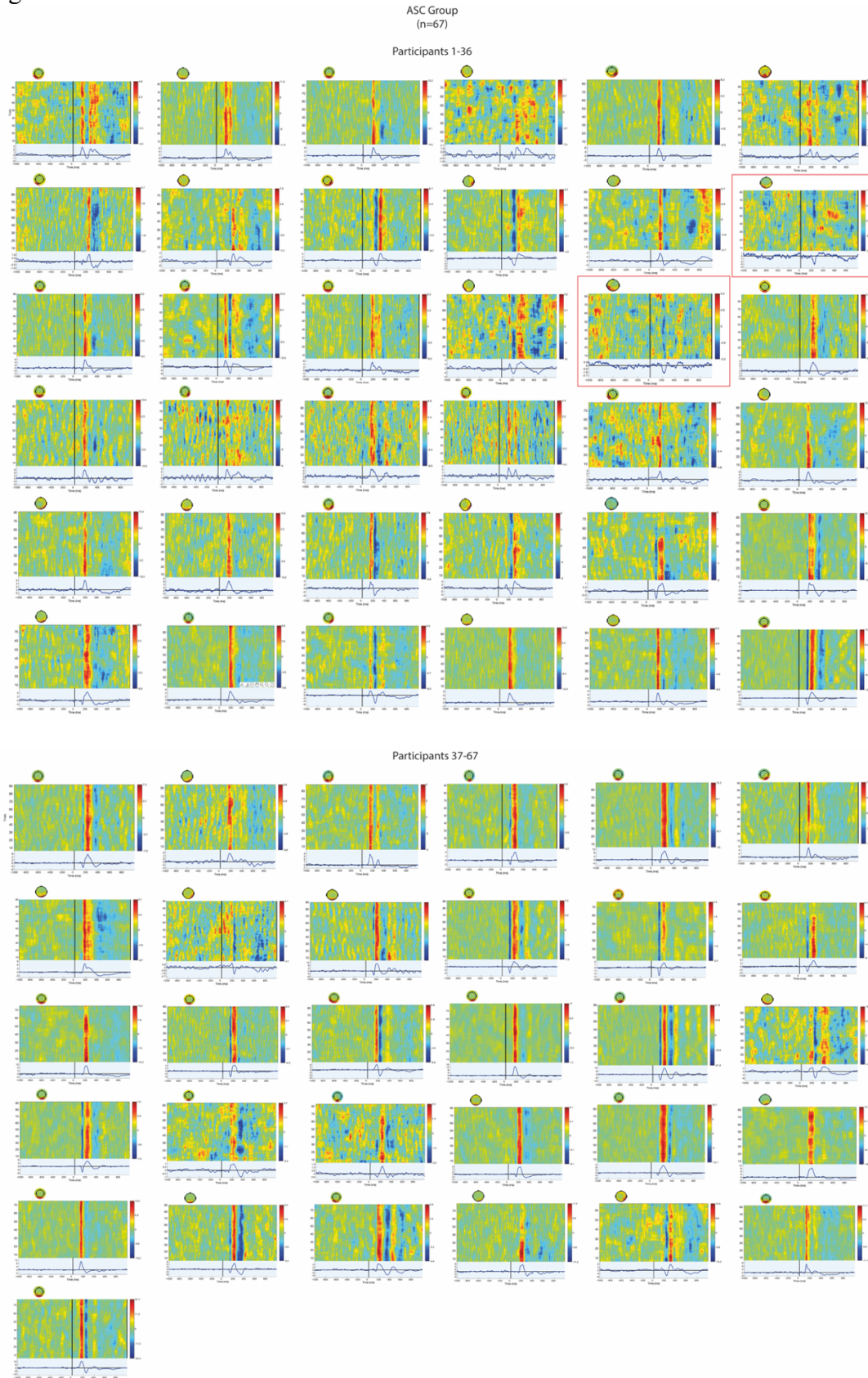


Figure 7.2: ERPs of the selected Independent Components (ICs) included in the group analysis, presented for the ASC group ($n=65$).

Channel Analysis

Figure 7.3

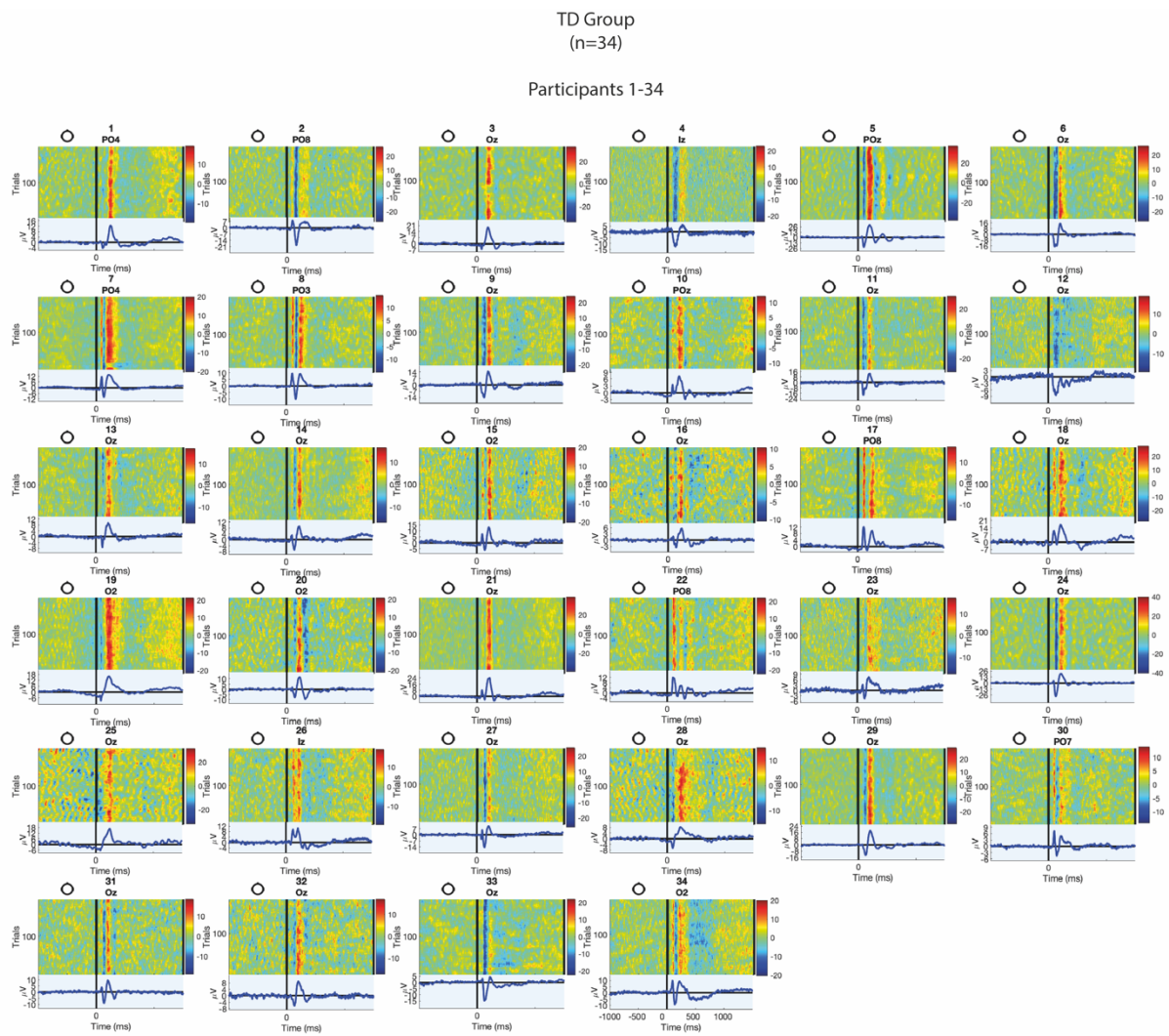
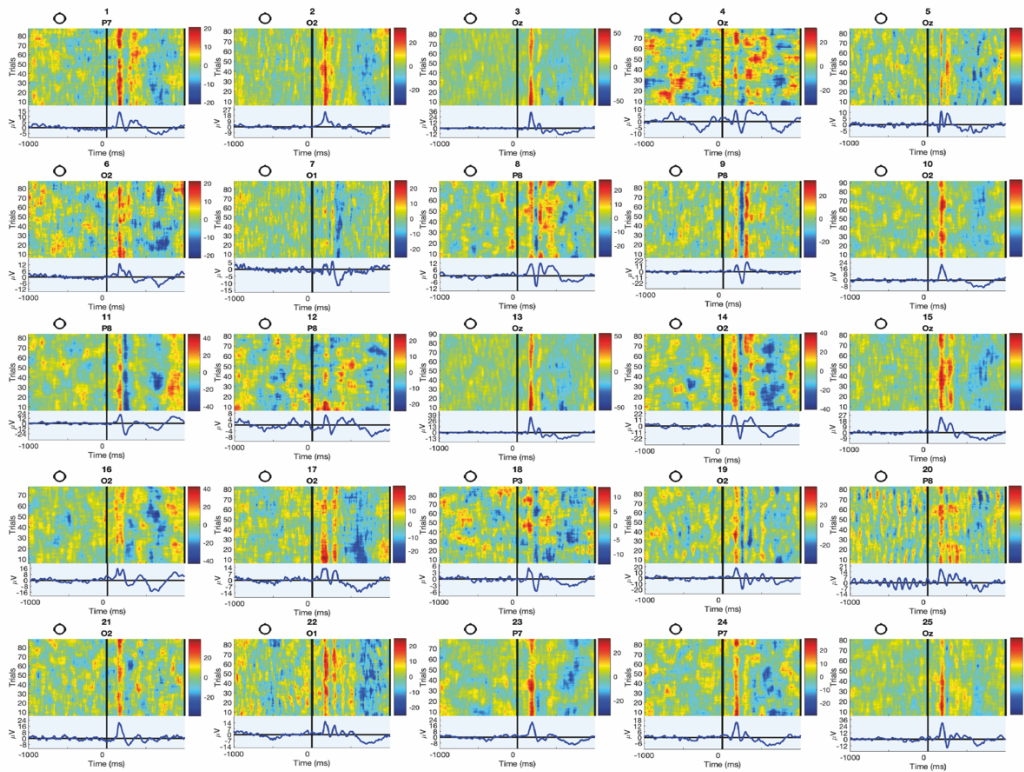


Figure 7.3: ERPs of the selected channels included in the group analysis, presented for the TD group ($n=25$).

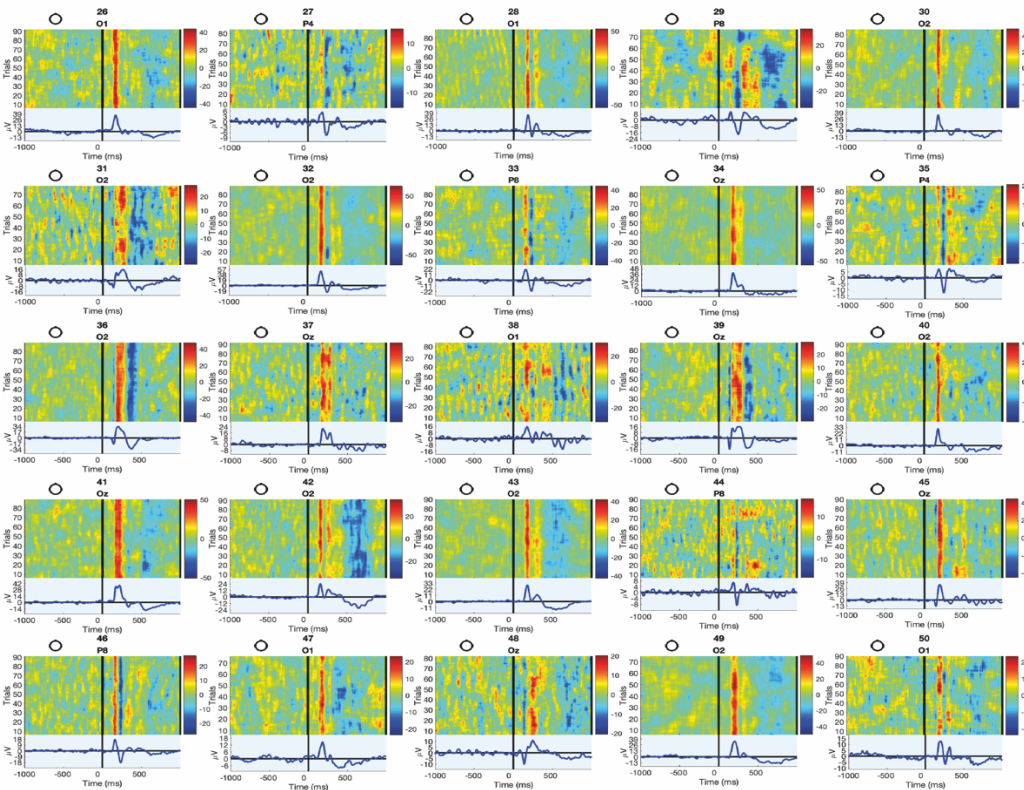
Figure 7.4

ASC Group
(n=67)

Participants 1-25



Participants 26-50



Participants 51-67

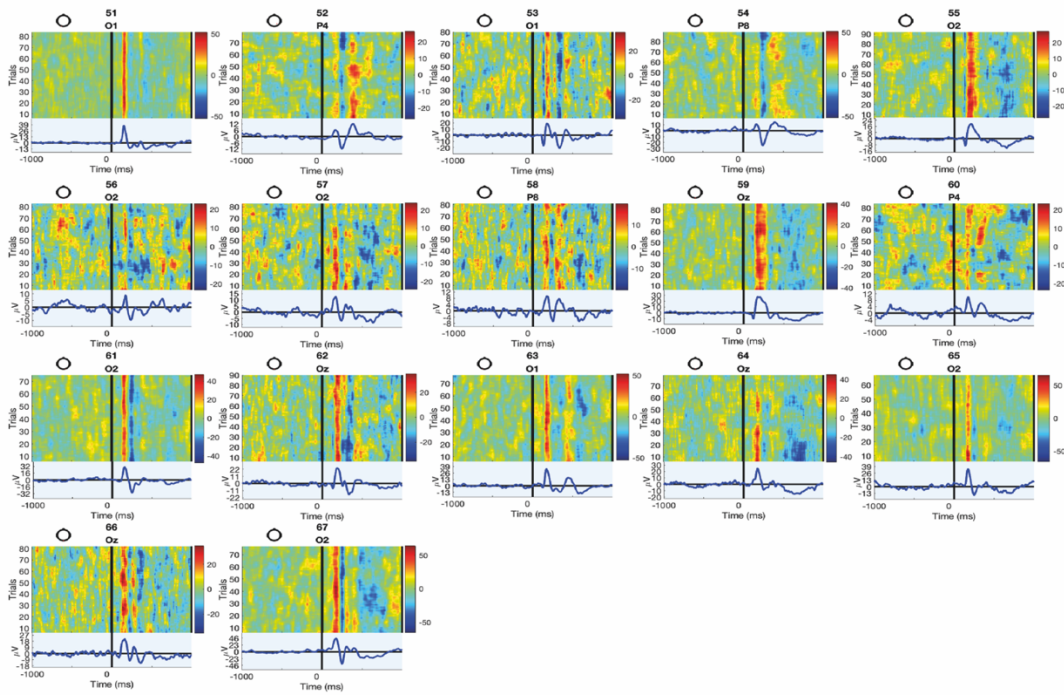


Figure 7.4: ERPs of the selected channels included in the group analysis, presented for the ASC group ($n=67$).

Annex 8

Chapter 4

Figure 8.1

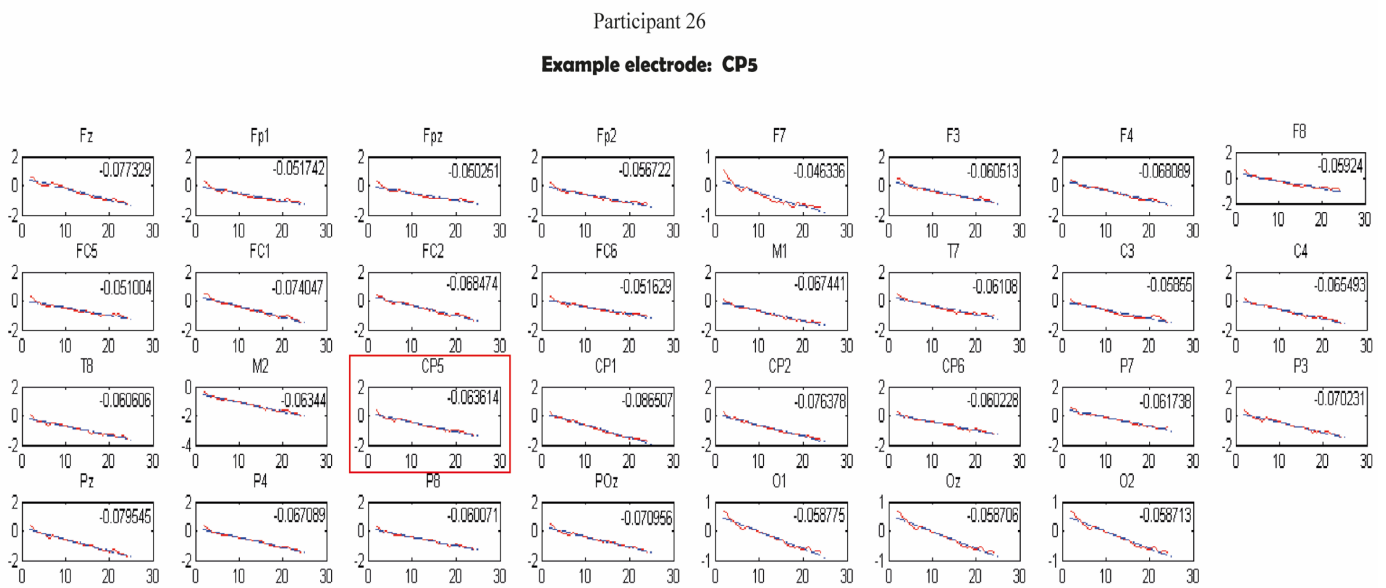


Figure 8.1: 1/f slope of all electrodes computed from Participant 26 in the ASC group.

Annex 9

Chapter 4

Independent Component Analysis

Figure 9.1

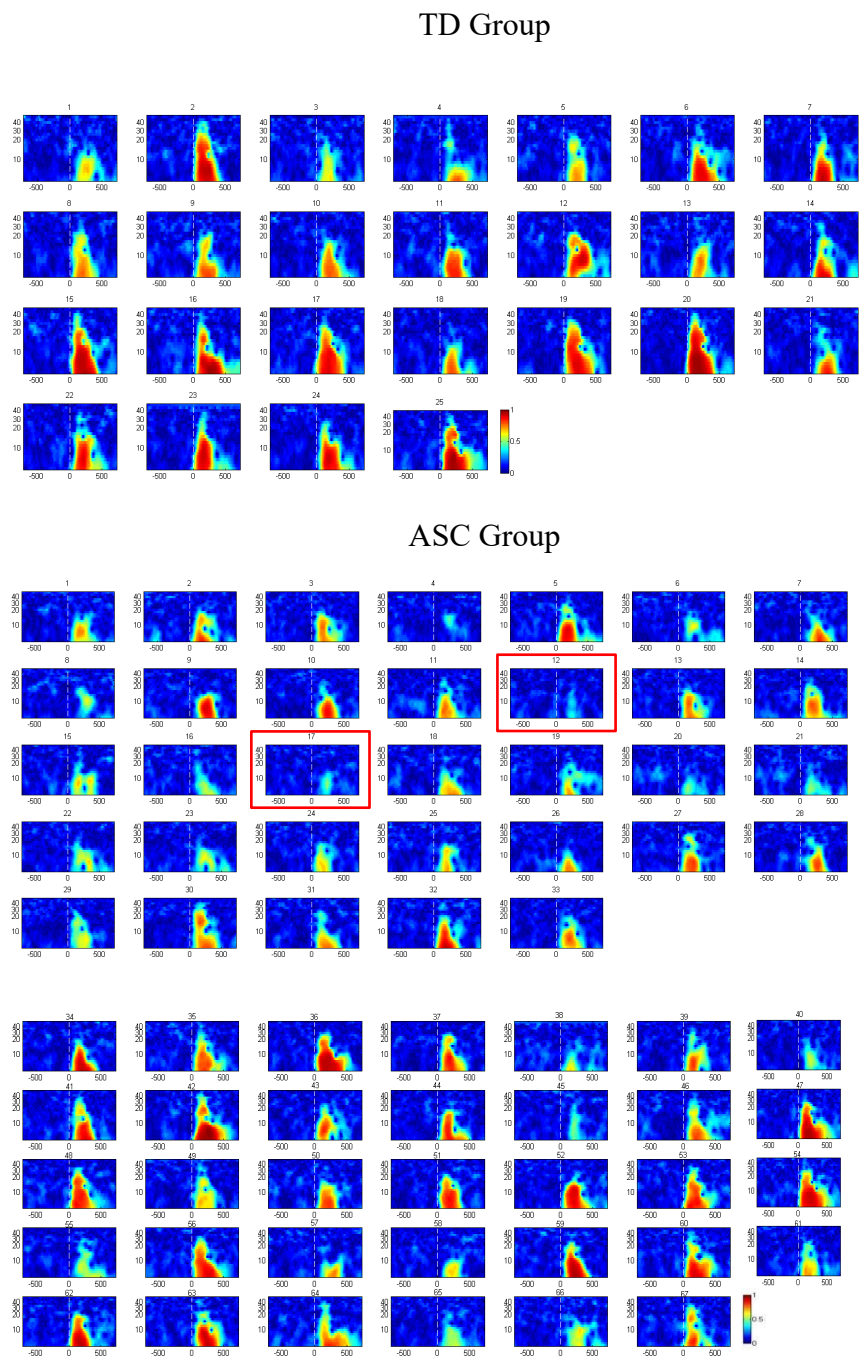


Figure 9.1: Maximum ITPC heat maps for the TD ($n=25$) and ASC group ($n=65$). Participants 12 and 17 in the ASC group were excluded from further analysis.

Annex 10

Chapter 5

Table 10.1

Psychometric tools assessing Sensory Symptoms

Scale	Type	Authors	Subscales	Group	N of items	Comments
Sensory Experiences Questionnaire (SEQ)	caregiver report	Baranek, David, Poe, Stone, & Watson, 2006	<p>PART A: assesses the frequency of occurrence of a child's sensory experience (5-point Likert scale).</p> <p>PART B: asks the caregiver to choose if he/she attempts to change (e.g., intervene with) the child's sensory behaviour, and uses a binary scale –'yes' or 'no'.</p> <p>PART C: requests the caregiver to describe the specific strategies used to change the behaviour (i.e., support, cope, intervene).</p>	Children with ASD 5 months- 6 years (see Brakek et al., 2005; Little et al., 2011)	21 items	<p>Internal consistency: Cronbach's alpha=0.80</p> <p>Test-retest reliability: ICC = .92.</p>
Sensory Perception Quotient (SPQ)	self-report	Tavassoli, Hoekstra & Baron- Cohen, 2014	<p>Sensory modalities assessed: vision (acuity, brightness, colour, motion), hearing (amplitude, frequency, vestibular, complexity), touch (pressure, temperature, pain, vibration), smell (social, danger, food, neutral) and taste (salty, sweet, sour, bitter).</p>	Adults with ASD	92 items or 35 items (short version)	<p>Internal consistency: Cronbach's alpha=0.92 for full 92 item version Cronbach's alpha=0.93 for the reduced 35-item version</p>
Sensory Processing Measure (SPM)	caregiver, teacher or other school personnel report (home form, classroom form, school environments form)	Parham & Ecker, 2007	Social participation, vision, touch, body awareness (proprioception), balance and motion (vestibular function), planning and ideas (praxis), total sensory systems	Standardised in children 5-12 years old but not in ASC	75 items	None
Sensory Over-Responsivity Inventory (SensOR Inventory)	caregiver report	Schoen, Miller & Green, 2008	<p>Sensory modalities assessed: tactile, auditory, gustatory, proprioceptive, vestibular, visual, olfactory</p>	Standardised in TD participants and participants with sensory overresponsivity, aged 3 to 55 but not in ASC	76 items	None
Sensory- Overresponsivity Assessment (SensOR Assessment)	self-report	Schoen, Miller & Green, 2008	<p>Sensory modalities assessed: tactile, auditory, gustatory, proprioceptive, vestibular, visual, olfactory (28 tactile items, 20 auditory items, 9 taste items, 9 movement items, 5 vision items, 5 smell items)</p>	Standardised in TD participants and participants with sensory overresponsivity, ages 3 to 55 but not in ASC	76 items	<p>Internal consistency: Cronbach's alpha=0.93 for the frequency scale Cronbach's alpha=0.94 for the impact scale</p> <p>No significant associations between total SBQ scores and gender ($r = 0.02, p = .90$), age ($r = 0.18, p = .15$) or IQ ($r = 0.05, p = .68$).</p>
Sensory Behavior Questionnaire (SBQ)	caregiver report	Green, 2009; Gringras et al. 2014	<p>Sensory modalities assessed: auditory processing, visual processing, movement (vestibular and proprioceptive) processing, tactile processing, oral motor (including gustatory and olfactory) processing and general reactions and organisation.</p>	66 children with ASD, age range 6-16 years old (see Neil, Green & Pellicano, 2017)	50 items	Initially used with individuals with a moderate-to-severe learning disability or pervasive developmental disorder, with or without a physical disability

Glasgow Sensory Questionnaire (GSQ)	self-report	Robertson & Simmons, 2012	Each item asks how often the respondent performs a particular behaviour ("Never", "Rarely", "Sometimes", "Often" and "Always", scored on a 5-point Likert scale). Example item: "Do you like to spin yourself round and round?". Sensory modalities assessed: vision, hearing, taste, touch, smell, vestibular, proprioception.	Adults with ASD	42 items	Internal consistency: Cronbach's alpha ($r = .935$) <i>Author's report: "During the development of the Sensory Profile 2, children with Autism Spectrum Disorders engaged in behaviours depicted on Child Sensory Profile 2 more often than their peers, with the exception of visual sensory processing items. This is not surprising since visual processing has been reported as a relative strength for children with Autism Spectrum Disorders".</i>
Child Sensory Profile 2	caregiver report	Dunn, 2014	Sensory modalities assessed: Auditory, Visual, Touch, Movement, Body Position, Oral	Children aged 3-14 (used with children with ASD too)	86 items	Internal consistency: Cronbach's alpha=0.70 to 0.90
Short Sensory Profile (SSP)	caregiver report	McIntosh, Miller & Shyu, 1999	Tactile, taste/smell, movement, visual/auditory sensitivity, under-responsive/seeks sensation, auditory filtering, low energy/weak	400 children with ASD between the ages of 3 and 6	38 items	Internal validity: Correlations ranged from 0.25 to 0.76 and were all significant at $p < .01$.
Behaviour and Sensory Interests Questionnaire (BSIQ)	semi- structured interview, self- report	Hanson et al., 2016	6 categories of behaviour assessed: stereotypes behaviours, compulsive and ritualistic behaviours, rigidity, aggression and self-injurious behaviour, language perseveration, perseverative interests	children with ASD	174 items	Assessing RRB not sensory sensitivities per se
Sensory Sensitivity Questionnaire (SSQ)	self- report or parent report (2 versions)	Minshew & Hobson, 2008	Sensory modalities assessed: Low temperature/Pain tolerance (2 items), High temperature/Pain tolerance (2 items), tactile (3 items), overall sensory sensitivities covering questions about light, sounds, odor, covering ears in response to sounds, becoming easily upset (6 items)	tested in 60 individuals with high functioning ASD, 6-54 years old (Minshew & Hobson, 2008)	13 items	Not standardised

References

- Abrahams, B. S., & Geschwind, D. H. (2008). Advances in autism genetics: On the threshold of a new neurobiology. In *Nature Reviews Genetics*. <https://doi.org/10.1038/nrg2346>
- Alba, G., Pereda, E., Mañas, S., Méndez, L. D., Duque, M. R., González, A., & González, J. J. (2016). The variability of EEG functional connectivity of young ADHD subjects in different resting states. *Clinical Neurophysiology*. <https://doi.org/10.1016/j.clinph.2015.09.134>
- Álvarez-Linera Prado, J., Ríos-Lago, M., Martín-Álvarez, H., Hernández-Tamames, J. A., Escribano-Vera, J., & Sánchez Del Río, M. (2007). Functional magnetic resonance imaging of the visual cortex: Relation between stimulus intensity and bold response original. *Revista de Neurologia*. <https://doi.org/10.33588/rn.4503.2006611>
- Amaral, D. G., Li, D., Libero, L., Solomon, M., Van de Water, J., Mastergeorge, A., Naigles, L., Rogers, S., & Wu Nordahl, C. (2017). In pursuit of neurophenotypes: The consequences of having autism and a big brain. In *Autism Research*. <https://doi.org/10.1002/aur.1755>
- American Psychiatric Association. (2013). American Psychiatric Association: Diagnostic and Statistical Manual of Mental Disorders Fifth Edition. In *Arlington*.
- Anguera, J. A., Boccanfuso, J., Rintoul, J. L., Al-Hashimi, O., Faraji, F., Janowich, J., ... & Gazzaley, A. (2013). Video game training enhances cognitive control in older adults. *Nature*, 501(7465), 97-101. <https://doi.org/10.1038/nature12486>
- Arns, M., Conners, C. K., & Kraemer, H. C. (2013). A Decade of EEG Theta/Beta Ratio Research in ADHD: A Meta-Analysis. *Journal of Attention Disorders*, 17(5), 374–383. <https://doi.org/10.1177/1087054712460087>
- Ashburner, J., Bennett, L., Rodger, S., & Ziviani, J. (2013). Understanding the sensory experiences of young people with autism spectrum disorder: A preliminary investigation. *Australian Occupational Therapy Journal*. <https://doi.org/10.1111/1440-1630.12025>

- Atallah BV, Scanziani M. Instantaneous modulation of gamma oscillation frequency by balancing excitation with inhibition. *Neuron*. 2009;62:566–577. <https://doi.org/10.1016/j.neuron.2009.04.027>
- Atkinson, A. J., Colburn, W. A., DeGruttola, V. G., DeMets, D. L., Downing, G. J., Hoth, D. F., Oates, J. A., Peck, C. C., Schooley, R. T., Spilker, B. A., Woodcock, J., & Zeger, S. L. (2001). Biomarkers and surrogate endpoints: Preferred definitions and conceptual framework. In *Clinical Pharmacology and Therapeutics*. <https://doi.org/10.1067/mcp.2001.113989>
- Badcock, N. A., Preece, K. A., deWit, B., Glenn, K., Fieder, N., Thie, J., & Genevieve McArthur. (2015). Validation of the Emotiv EPOC EEG system for research quality auditory event-related potentials in children. *PeerJ*. <https://doi.org/10.7717/peerj.907>
- Bai, D., Yip, B. H. K., Windham, G. C., Sourander, A., Francis, R., Yoffe, R., Glasson, E., Mahjani, B., Suominen, A., Leonard, H., Gissler, M., Buxbaum, J. D., Wong, K., Schendel, D., Kodesh, A., Breshnahan, M., Levine, S. Z., Parner, E. T., Hansen, S. N., ... Sandin, S. (2019). Association of Genetic and Environmental Factors with Autism in a 5-Country Cohort. *JAMA Psychiatry*. <https://doi.org/10.1001/jamapsychiatry.2019.1411>
- Bal, V. H., Kim, S. H., Fok, M., & Lord, C. (2019). Autism spectrum disorder symptoms from ages 2 to 19 years: Implications for diagnosing adolescents and young adults. *Autism Research*. <https://doi.org/10.1002/aur.2004>
- Balogh, L., & Czobor, P. (2016). Post-Error Slowing in Patients With ADHD: A Meta-Analysis. *Journal of Attention Disorders*. <https://doi.org/10.1177/1087054714528043>
- Barbeau, E., Wendling, F., Régis, J., Duncan, R., Poncet, M., Chauvel, P., & Bartolomei, F. (2005). Recollection of vivid memories after perirhinal region stimulations: synchronization in the theta range of spatially distributed brain areas. *Neuropsychologia*, 43(9), 1329-1337. <https://doi.org/10.1016/j.neuropsychologia.2004.11.025>
- Baron-Cohen, S., Leslie, A. M., & Frith, U. (1985). Does the autistic child have a “theory of mind”? *Cognition*. [https://doi.org/10.1016/0010-0277\(85\)90022-8](https://doi.org/10.1016/0010-0277(85)90022-8)

- Barrett, S. L., Uljarević, M., Baker, E. K., Richdale, A. L., Jones, C. R. G., & Leekam, S. R. (2015). The Adult Repetitive Behaviours Questionnaire-2 (RBQ-2A): A Self-Report Measure of Restricted and Repetitive Behaviours. *Journal of Autism and Developmental Disorders*. <https://doi.org/10.1007/s10803-015-2514-6>
- Barry, R. J., Clarke, A. R., McCarthy, R., & Selikowitz, M. (2002). EEG coherence in attention-deficit/hyperactivity disorder: A comparative study of two DSM-IV types. *Clinical Neurophysiology*. [https://doi.org/10.1016/S1388-2457\(02\)00036-6](https://doi.org/10.1016/S1388-2457(02)00036-6)
- Basar-Eroglu, C., Schmiedt-Fehr, C., Marbach, S., Brand, A., & Mathes, B. (2008). Altered oscillatory alpha and theta networks in schizophrenia. *Brain Research*. <https://doi.org/10.1016/j.brainres.2008.06.114>
- Bastos, A. M., Vezoli, J., Bosman, C. A., Schoffelen, J. M., Oostenveld, R., Dowdall, J. R., ... & Fries, P. (2015). Visual areas exert feedforward and feedback influences through distinct frequency channels. *Neuron*, 85(2), 390-401. <https://doi.org/10.1016/j.neuron.2014.12.018>
- Bastiaansen, J. A., Meffert, H., Hein, S., Huizinga, P., Ketelaars, C., Pijnenborg, M., Bartels, A., Minderaa, R., Keyzers, C., & De Bildt, A. (2011). Diagnosing autism spectrum disorders in adults: The use of Autism Diagnostic Observation Schedule (ADOS) module 4. *Journal of Autism and Developmental Disorders*, 41(9), 1256–1266. <https://doi.org/10.1007/s10803-010-1157-x>
- Baudouin, S. J., Gaudias, J., Gerharz, S., Hatstatt, L., Zhou, K., Punnakkal, P., Tanaka, K. F., Spooren, W., Hen, R., De Zeeuw, C. I., Vogt, K., & Scheiffele, P. (2012). Shared synaptic pathophysiology in syndromic and nonsyndromic rodent models of autism. *Science*. <https://doi.org/10.1126/science.1224159>
- Baum, S. H., Stevenson, R. A., & Wallace, M. T. (2015). Behavioral, perceptual, and neural alterations in sensory and multisensory function in autism spectrum disorder. In *Progress in Neurobiology*. <https://doi.org/10.1016/j.pneurobio.2015.09.007>
- Beauchaine, T. P., & Constantino, J. N. (2017). Redefining the endophenotype concept to accommodate transdiagnostic vulnerabilities and etiological complexity. In *Biomarkers in Medicine*. <https://doi.org/10.2217/bmm-2017-0002>

- Beggs, J. M. (2008). The criticality hypothesis: How local cortical networks might optimize information processing. *Philosophical Transactions of the Royal Society A: Mathematical, Physical and Engineering Sciences*. <https://doi.org/10.1098/rsta.2007.2092>
- Beggs, J. M., & Plenz, D. (2003). Neuronal Avalanches in Neocortical Circuits. *Journal of Neuroscience*. <https://doi.org/10.1523/jneurosci.23-35-11167.2003>
- Bell, A. J., & Sejnowski, T. J. (1995). An information-maximization approach to blind separation and blind deconvolution. *Neural Computation*. <https://doi.org/10.1162/neco.1995.7.6.1129>
- Bellato, A., Arora, I., Kochhar, P., Hollis, C., & Groom, M. J. (2020). Atypical electrophysiological indices of eyes-open and eyes-closed resting-state in children and adolescents with ADHD and autism. *Brain Sciences*. <https://doi.org/10.3390/brainsci10050272>
- Belmonte, M. K., Allen, G., Beckel-Mitchener, A., Boulanger, L. M., Carper, R. A., & Webb, S. J. (2004). Autism and abnormal development of brain connectivity. *Journal of Neuroscience*. <https://doi.org/10.1523/JNEUROSCI.3340-04.2004>
- Benayed, R., Gharani, N., Rossman, I., Mancuso, V., Lazar, G., Kamdar, S., Bruse, S. E., Tischfield, S., Smith, B. J., Zimmerman, R. A., DiCicco-Bloom, E., Brzustowicz, L. M., & Millonig, J. H. (2005). Support for the homeobox transcription factor gene ENGRAILED 2 as an autism spectrum disorder susceptibility locus. *American Journal of Human Genetics*. <https://doi.org/10.1086/497705>
- Benjamini, Y., & Hochberg, Y. (1995). Controlling the False Discovery Rate: A Practical and Powerful Approach to Multiple Testing. *Journal of the Royal Statistical Society: Series B (Methodological)*. <https://doi.org/10.1111/j.2517-6161.1995.tb02031.x>
- Berman, J. I., Liu, S., Bloy, L., Blaskey, L., Roberts, T. P. L., & Edgar, J. C. (2015). Alpha-to-gamma phase-amplitude coupling methods and application to autism spectrum disorder. *Brain Connectivity*. <https://doi.org/10.1089/brain.2014.0242>

- Bertelsen, N., Landi, I., Bethlehem, R. A. I., Seidlitz, J., Busuoli, E. M., Mandelli, V., Satta, E., Trakoshis, S., Auyeung, B., Kundu, P., Loth, E., Dumas, G., Baumeister, S., Beckmann, C. F., Bölte, S., Bourgeron, T., Charman, T., Durston, S., Ecker, C., ... Lombardo, M. V. (2021). Imbalanced social-communicative and restricted repetitive behavior subtypes of autism spectrum disorder exhibit different neural circuitry. *Communications Biology*. <https://doi.org/10.1038/s42003-021-02015-2>
- Bertschinger, N., & Natschläger, T. (2004). Real-time computation at the edge of chaos in recurrent neural networks. *Neural Computation*. <https://doi.org/10.1162/089976604323057443>
- Betancur, C. (2011). Etiological heterogeneity in autism spectrum disorders: More than 100 genetic and genomic disorders and still counting. In *Brain Research*. <https://doi.org/10.1016/j.brainres.2010.11.078>
- Bill, B. R., & Geschwind, D. H. (2009). Genetic advances in autism: heterogeneity and convergence on shared pathways. In *Current Opinion in Genetics and Development*. <https://doi.org/10.1016/j.gde.2009.04.004>
- Bink, M., van Boxtel, G. J. M., Popma, A., Bongers, I. L., Denissen, A. J. M., & van Nieuwenhuizen, C. (2015). EEG theta and beta power spectra in adolescents with ADHD versus adolescents with ASD + ADHD. *European Child and Adolescent Psychiatry*. <https://doi.org/10.1007/s00787-014-0632-x>
- Bogdashina, O. (2003). Sensory perceptual issues in autism and Asperger syndrome: Different sensory experiences--different perceptual worlds. In *Sensory perceptual issues in autism and Asperger syndrome: Different sensory experiences--different perceptual worlds*.
- Bonnefond, M., & Jensen, O. (2012). Alpha oscillations serve to protect working memory maintenance against anticipated distracters. *Current biology*, 22(20), 1969-1974. <https://doi.org/10.1016/j.cub.2012.08.029>
- Bosch, S. E., Jehee, J. F., Fernández, G., & Doeller, C. F. (2014). Reinstatement of associative memories in early visual cortex is signaled by the hippocampus. *Journal of Neuroscience*, 34(22), 7493-7500. <https://doi.org/10.1523/JNEUROSCI.0805-14.2014>

- Braithwaite, J. J., Brogna, E., Bagshaw, A. P., & Wilkins, A. J. (2013). Evidence for elevated cortical hyperexcitability and its association with out-of-body experiences in the non-clinical population: New findings from a pattern-glare task. *Cortex*. <https://doi.org/10.1016/j.cortex.2011.11.013>
- Bralten, J., Van Hulzen, K. J., Martens, M. B., Galesloot, T. E., Arias Vasquez, A., Kiemeneij, L. A., Buitelaar, J. K., Muntjewerff, J. W., Franke, B., & Poelmans, G. (2018). Autism spectrum disorders and autistic traits share genetics and biology. *Molecular Psychiatry*. <https://doi.org/10.1038/mp.2017.98>
- Braun, V., Clarke, V., Hayfield, N., & Terry, G. (2019). Thematic analysis. In *Handbook of Research Methods in Health Social Sciences*. https://doi.org/10.1007/978-981-10-5251-4_103
- Bridgemohan, C., Cochran, D. M., Howe, Y. J., Pawlowski, K., Zimmerman, A. W., Anderson, G. M., Choueiri, R., Sices, L., Miller, K. J., Ultmann, M., Helt, J., Forbes, P. W., Farfel, L., Brewster, S. J., Frazier, J. A., & Neumeier, A. M. (2019). Investigating Potential Biomarkers in Autism Spectrum Disorder. *Frontiers in Integrative Neuroscience*, 13(August), 1–11. <https://doi.org/10.3389/fnint.2019.00031>
- Brieber, S., Neufang, S., Bruning, N., Kamp-Becker, I., Remschmidt, H., Herpertz-Dahlmann, B., Fink, G. R., & Konrad, K. (2007). Structural brain abnormalities in adolescents with autism spectrum disorder and patients with attention deficit/hyperactivity disorder. *Journal of Child Psychology and Psychiatry and Allied Disciplines*, 48(12), 1251–1258. <https://doi.org/10.1111/j.1469-7610.2007.01799.x>
- Brovelli, A., Ding, M., Ledberg, A., Chen, Y., Nakamura, R., & Bressler, S. L. (2004). Beta oscillations in a large-scale sensorimotor cortical network: directional influences revealed by Granger causality. *Proceedings of the National Academy of Sciences*, 101(26), 9849–9854. <https://doi.org/10.1073/pnas.0308538101>
- Brock, J., Brown, C. C., Boucher, J., & Rippon, G. (2002). The temporal binding deficit hypothesis of autism. *Development and Psychopathology*. <https://doi.org/10.1017/s0954579402002018>

- Bruining, H., de Sonneville, L., Swaab, H., de Jonge, M., Kas, M., van Engeland, H., & Vorstman, J. (2010). Dissecting the clinical heterogeneity of autism spectrum disorders through defined genotypes. *PLoS ONE*. <https://doi.org/10.1371/journal.pone.0010887>
- Brunel, N., Chance, F. S., Fourcaud, N., & Abbott, L. F. (2001). Effects of synaptic noise and filtering on the frequency response of spiking neurons. *Physical Review Letters*. <https://doi.org/10.1103/PhysRevLett.86.2186>
- Brunsdon, V. E. A., & Happé, F. (2014). Exploring the “fractionation” of autism at the cognitive level. In *Autism*. <https://doi.org/10.1177/1362361313499456>
- Bryson, S. E., Bradley, E. A., Thompson, A., & Wainwright, A. (2008). Prevalence of autism among adolescents with intellectual disabilities. *Canadian Journal of Psychiatry*. <https://doi.org/10.1177/070674370805300710>
- Buard, I., Rogers, S. J., Hepburn, S., Kronberg, E., & Rojas, D. C. (2013). Altered oscillation patterns and connectivity during picture naming in autism. *Frontiers in Human Neuroscience*. <https://doi.org/10.3389/fnhum.2013.00742>
- Butler, J. S., Molholm, S., Andrade, G. N., & Foxe, J. J. (2017). An examination of the neural unreliability thesis of autism. *Cerebral Cortex*. <https://doi.org/10.1093/cercor/bhw375>
- Button, K. S., Ioannidis, J. P. A., Mokrysz, C., Nosek, B. A., Flint, J., Robinson, E. S. J., & Munafò, M. R. (2013). Power failure: Why small sample size undermines the reliability of neuroscience. *Nature Reviews Neuroscience*. <https://doi.org/10.1038/nrn3475>
- Buzsáki, G. (2002). Theta oscillations in the hippocampus. *Neuron*, 33(3), 325-340. [https://doi.org/10.1016/S0896-6273\(02\)00586-X](https://doi.org/10.1016/S0896-6273(02)00586-X)
- Byrne, E. M., Zhu, Z., Qi, T., Skene, N. G., Bryois, J., Pardinas, A. F., Stahl, E., Smoller, J. W., Rietschel, M., Owen, M. J., Walters, J. T. R., O'Donovan, M. C., McGrath, J. G., Hjerling-Leffler, J., Sullivan, P. F., Goddard, M. E., Visscher, P. M., Yang, J., & Wray, N. R. (2020). Conditional GWAS analysis to identify disorder-specific SNPs for psychiatric disorders. *Molecular Psychiatry*. <https://doi.org/10.1038/s41380-020-0705-9>

- Campbell, D. B., Sutcliffe, J. S., Ebert, P. J., Militerni, R., Bravaccio, C., Trillo, S., Elia, M., Schneider, C., Melmed, R., Sacco, R., Persico, A. M., & Levitt, P. (2006). A genetic variant that disrupts MET transcription is associated with autism. *Proceedings of the National Academy of Sciences of the United States of America*. <https://doi.org/10.1073/pnas.0605296103>
- Canolty, R. T., Edwards, E., Dalal, S. S., Soltani, M., Nagarajan, S. S., Kirsch, H. E., Berger, M. S., Barbare, N. M., & Knight, R. T. (2006). High gamma power is phase-locked to theta oscillations in human neocortex. *Science*. <https://doi.org/10.1126/science.1128115>
- Canolty, R. T., & Knight, R. T. (2010). The functional role of cross-frequency coupling. In *Trends in Cognitive Sciences*. <https://doi.org/10.1016/j.tics.2010.09.001>
- Carroll, L., Braeutigam, S., Dawes, J. M., Krsnik, Z., Kostovic, I., Coutinho, E., Dewing, J. M., Horton, C. A., Gomez-Nicola, D., & Menassa, D. A. (2021). Autism Spectrum Disorders: Multiple Routes to, and Multiple Consequences of, Abnormal Synaptic Function and Connectivity. *Neuroscientist*. <https://doi.org/10.1177/1073858420921378>
- Casanova, M. F. (2006). Neuropathological and genetic findings in autism: The significance of a putative minicolumnopathy. In *Neuroscientist*. <https://doi.org/10.1177/1073858406290375>
- Catarino, A., Churches, O., Baron-Cohen, S., Andrade, A., & Ring, H. (2011). Atypical EEG complexity in autism spectrum conditions: A multiscale entropy analysis. *Clinical Neurophysiology*. <https://doi.org/10.1016/j.clinph.2011.05.004>
- Cavanagh, J. F., Cohen, M. X., & Allen, J. J. (2009). Prelude to and resolution of an error: EEG phase synchrony reveals cognitive control dynamics during action monitoring. *Journal of Neuroscience*, 29(1), 98-105. <https://doi.org/10.1523/JNEUROSCI.4137-08.2009>
- Cavanagh, J. F., & Frank, M. J. (2014). Frontal theta as a mechanism for cognitive control. *Trends in cognitive sciences*, 18(8), 414-421. <https://doi.org/10.1016/j.tics.2014.04.012>
- Cheng, C. H., Chan, P. Y. S., Hsieh, Y. W., & Chen, K. F. (2016). A meta-analysis of mismatch negativity in children with attention deficit-hyperactivity disorders. *Neuroscience Letters*, 612, 132–137. <https://doi.org/10.1016/j.neulet.2015.11.033>

- Chouinard, B. D., Zhou, C. I., Hrybouski, S., Kim, E. S., & Cummine, J. (2012). A functional neuroimaging case study of Meares-Irlen syndrome/visual stress (MISViS). *Brain Topography*. <https://doi.org/10.1007/s10548-011-0212-z>
- Cicchetti, D. V. (1994). Guidelines, Criteria, and Rules of Thumb for Evaluating Normed and Standardized Assessment Instruments in Psychology. *Psychological Assessment*. <https://doi.org/10.1037/1040-3590.6.4.284>
- Clayson, P. E., Brush, C. J., & Hajcak, G. (2021). Data quality and reliability metrics for event-related potentials (ERPs): The utility of subject-level reliability. *International Journal of Psychophysiology*. <https://doi.org/10.1016/j.ijpsycho.2021.04.004>
- Coghlan, S., Horder, J., Inkster, B., Mendez, M. A., Murphy, D. G., & Nutt, D. J. (2012). GABA system dysfunction in autism and related disorders: From synapse to symptoms. In *Neuroscience and Biobehavioral Reviews*. <https://doi.org/10.1016/j.neubiorev.2012.07.005>
- Cohen, M. X., & Cavanagh, J. F. (2011). Single-trial regression elucidates the role of prefrontal theta oscillations in response conflict. *Frontiers in psychology*, 2, 30. <https://doi.org/10.3389/fpsyg.2011.00030>
- Cohen, M. X. (2014). Analyzing Neural Time Series Data: Theory and Practice. In *MIT Press*.
- Coleman, M. J., Cestnick, L., Krastoshevsky, O., Krause, V., Huang, Z., Mendell, N. R., & Levy, D. L. (2009). Schizophrenia patients show deficits in shifts of attention to different levels of global-local stimuli: Evidence for magnocellular dysfunction. *Schizophrenia Bulletin*. <https://doi.org/10.1093/schbul/sbp090>
- Colvert, E., Tick, B., McEwen, F., Stewart, C., Curran, S. R., Woodhouse, E., Gillan, N., Hallett, V., Lietz, S., Garnett, T., Ronald, A., Plomin, R., Rijdsdijk, F., Happé, F., & Bolton, P. (2015). Heritability of autism spectrum disorder in a UK population-based twin sample. *JAMA Psychiatry*. <https://doi.org/10.1001/jamapsychiatry.2014.3028>
- Conlon, E., Prideaux, L., & Titchener, K. (2012). Migraine and visual discomfort: The effects of pattern sensitivity on performance. In *Beyond the Lab: Applications of Cognitive Research in Memory and Learning*.

- Constantino, C. P. G. & J. N. (2011). Social Responsiveness Scale (SRS). *Los Angeles, CA: Western Psychological Services.*
- Constantino, J. N., Gruber, C. P., Davis, S., Hayes, S., Passanante, N., & Przybeck, T. (2004). The factor structure of autistic traits. *Journal of Child Psychology and Psychiatry and Allied Disciplines.* <https://doi.org/10.1111/j.1469-7610.2004.00266.x>
- Cooper, P. S., Wong, A. S., McKewen, M., Michie, P. T., & Karayanidis, F. (2017). Frontoparietal theta oscillations during proactive control are associated with goal-updating and reduced behavioral variability. *Biological psychology*, 129, 253-264. <https://doi.org/10.1016/j.biopsycho.2017.09.008>
- Cree, B. A. C. (2014). Sensory System; Overview. In *Encyclopedia of the Neurological Sciences.* <https://doi.org/10.1016/B978-0-12-385157-4.00695-3>
- Croen, L. A., Zerbo, O., Qian, Y., Massolo, M. L., Rich, S., Sidney, S., & Kripke, C. (2015). The health status of adults on the autism spectrum. *Autism.* <https://doi.org/10.1177/1362361315577517>
- Crowley, M. J., van Noordt, S. J., Wu, J., Hommer, R. E., South, M., Fearon, R. M. P., & Mayes, L. C. (2014). Reward feedback processing in children and adolescents: medial frontal theta oscillations. *Brain and cognition*, 89, 79-89. <https://doi.org/10.1016/j.bandc.2013.11.011>
- Dalgleish, T., Black, M., Johnston, D., & Bevan, A. (2020). Transdiagnostic approaches to mental health problems: Current status and future directions. In *Journal of Consulting and Clinical Psychology.* <https://doi.org/10.1037/ccp0000482>
- Dave, S., Brothers, T. A., & Swaab, T. Y. (2018). 1/f neural noise and electrophysiological indices of contextual prediction in aging. *Brain Research.* <https://doi.org/10.1016/j.brainres.2018.04.007>
- David, N., Schneider, T. R., Peiker, I., Al-Jawahiri, R., Engel, A. K., & Milne, E. (2016). Variability of cortical oscillation patterns: A possible endophenotype in autism spectrum disorders? In *Neuroscience and Biobehavioral Reviews.* <https://doi.org/10.1016/j.neubiorev.2016.09.031>

- Davis, G., & Plaisted-Grant, K. (2015). Low endogenous neural noise in autism. *Autism*. <https://doi.org/10.1177/1362361314552198>
- Davis, R. A. O., Bockbrader, M. A., Murphy, R. R., Hetrick, W. P., & O'Donnell, B. F. (2006). Subjective perceptual distortions and visual dysfunction in children with autism. *Journal of Autism and Developmental Disorders*. <https://doi.org/10.1007/s10803-005-0055-0>
- De Bildt, A., Sytema, S., Kraijer, D., & Minderaa, R. (2005). Prevalence of pervasive developmental disorders in children and adolescents with mental retardation. *Journal of Child Psychology and Psychiatry and Allied Disciplines*. <https://doi.org/10.1111/j.1469-7610.2004.00346.x>
- De Geus, E. J. C., & Boomsma, D. I. (2001). A Genetic Neuroscience Approach to Human Cognition. *European Psychologist*. <https://doi.org/10.1027//1016-9040.6.4.241>
- De Munck, J. C., Bijma, F., Gaura, P., Sieluzycycki, C. A., Branco, M. I., & Heethaar, R. M. (2004). A maximum-likelihood estimator for trial-to-trial variations in noisy MEG/EEG data sets. *IEEE Transactions on Biomedical Engineering*. <https://doi.org/10.1109/TBME.2004.836515>
- De Vos, M., Thorne, J. D., Yovel, G., & Debener, S. (2012). Let's face it, from trial to trial: Comparing procedures for N170 single-trial estimation. *NeuroImage*. <https://doi.org/10.1016/j.neuroimage.2012.07.055>
- Deco, G., Jirs, V., McIntosh, A. R., Sporns, O., & Kötter, R. (2009). Key role of coupling, delay, and noise in resting brain fluctuations. *Proceedings of the National Academy of Sciences of the United States of America*. <https://doi.org/10.1073/pnas.0901831106>
- Delorme, A., & Makeig, S. (2003). EEG changes accompanying learned regulation of 12-Hz EEG activity. *IEEE Transactions on Neural Systems and Rehabilitation Engineering*. <https://doi.org/10.1109/TNSRE.2003.814428>
- Delorme, A., & Makeig, S. (2004). EEGLAB: An open source toolbox for analysis of single-trial EEG dynamics including independent component analysis. *Journal of Neuroscience Methods*. <https://doi.org/10.1016/j.jneumeth.2003.10.009>

- Delorme, A., Palmer, J., Onton, J., Oostenveld, R., & Makeig, S. (2012). Independent EEG sources are dipolar. *PLoS ONE*. <https://doi.org/10.1371/journal.pone.0030135>
- Demetriou, E. A., Lampit, A., Quintana, D. S., Naismith, S. L., Song, Y. J. C., Pye, J. E., Hickie, I., & Guastella, A. J. (2018). Autism spectrum disorders: A meta-analysis of executive function. *Molecular Psychiatry*. <https://doi.org/10.1038/mp.2017.75>
- Dickinson, A., DiStefano, C., Lin, Y. Y., Scheffler, A. W., Senturk, D., & Jeste, S. S. (2018). Interhemispheric alpha-band hypoconnectivity in children with autism spectrum disorder. *Behavioural Brain Research*. <https://doi.org/10.1016/j.bbr.2018.04.026>
- Ding, J., Sperling, G., & Srinivasan, R. (2006). Attentional modulation of SSVEP power depends on the network tagged by the flicker frequency. *Cerebral Cortex*. <https://doi.org/10.1093/cercor/bhj044>
- Dinstein, I., Heeger, D. J., Lorenzi, L., Minshew, N. J., Malach, R., & Behrmann, M. (2012). Unreliable Evoked Responses in Autism. *Neuron*. <https://doi.org/10.1016/j.neuron.2012.07.026>
- DiStefano, C., Dickinson, A., Baker, E., & Spurling Jeste, S. (2019). EEG data collection in children with ASD: The role of state in data quality and spectral power. *Research in Autism Spectrum Disorders*. <https://doi.org/10.1016/j.rasd.2018.10.001>
- Doesburg, S. M., Roggeveen, A. B., Kitajo, K., & Ward, L. M. (2008). Large-scale gamma-band phase synchronization and selective attention. *Cerebral cortex*, 18(2), 386-396. <https://doi.org/10.1093/cercor/bhm073>
- Donner, T. H., Siegel, M., Oostenveld, R., Fries, P., Bauer, M., & Engel, A. K. (2007). Population activity in the human dorsal pathway predicts the accuracy of visual motion detection. *Journal of Neurophysiology*, 98(1), 345-359. <https://doi.org/10.1152/jn.01141.2006>
- Donoghue, T., Dominguez, J., & Voytek, B. (2020). Electrophysiological Frequency Band Ratio Measures Conflate Periodic and Aperiodic Neural Activity. *ENeuro*. <https://doi.org/10.1523/ENEURO.0192-20.2020>

- Donoghue, T., Haller, M., Peterson, E. J., Varma, P., Sebastian, P., Gao, R., Noto, T., Lara, A. H., Wallis, J. D., Knight, R. T., Shestyuk, A., & Voytek, B. (2020). Parameterizing neural power spectra into periodic and aperiodic components. *Nature Neuroscience*. <https://doi.org/10.1038/s41593-020-00744-x>
- Durka, P. J., Matysiak, A., Montes, E. M., Sosa, P. V., & Blinowska, K. J. (2005). Multichannel matching pursuit and EEG inverse solutions. *Journal of Neuroscience Methods*. <https://doi.org/10.1016/j.jneumeth.2005.04.001>
- Edgar, J. C., Khan, S. Y., Blaskey, L., Chow, V. Y., Rey, M., Gaetz, W., Cannon, K. M., Monroe, J. F., Cornew, L., Qasmieh, S., Liu, S., Welsh, J. P., Levy, S. E., & Roberts, T. P. L. (2015). Neuromagnetic Oscillations Predict Evoked-Response Latency Delays and Core Language Deficits in Autism Spectrum Disorders. *Journal of Autism and Developmental Disorders*. <https://doi.org/10.1007/s10803-013-1904-x>
- Eidelman-Rothman, M., Ben-Simon, E., Freche, D., Keil, A., Hendler, T., & Levit-Binnun, N. (2019). Sleepless and desynchronized: Impaired inter trial phase coherence of steady-state potentials following sleep deprivation. *NeuroImage*. <https://doi.org/10.1016/j.neuroimage.2019.116055>
- Engel, A. K., & Fries, P. (2010). Beta-band oscillations—signalling the status quo?. *Current opinion in neurobiology*, 20(2), 156-165. <https://doi.org/10.1016/j.conb.2010.02.015>
- Esbensen, A. J., Seltzer, M. M., Lam, K. S. L., & Bodfish, J. W. (2009). Age-related differences in restricted repetitive behaviors in autism spectrum disorders. *Journal of Autism and Developmental Disorders*. <https://doi.org/10.1007/s10803-008-0599-x>
- Evans, B. J. W., Patel, R., & Wilkins, A. J. (2002). Optometric function in visually sensitive migraine before and after treatment with tinted spectacles. *Ophthalmic and Physiological Optics*. <https://doi.org/10.1046/j.1475-1313.2002.00017.x>
- Evans, B. J. W., & Stevenson, S. J. (2008). The Pattern Glare Test: A review and determination of normative values. *Ophthalmic and Physiological Optics*. <https://doi.org/10.1111/j.1475-1313.2008.00578.x>

- Evans, B. J. W., & Allen, P. M. (2016). A systematic review of controlled trials on visual stress using Intuitive Overlays or the Intuitive Colorimeter. *Journal of Optometry*. <https://doi.org/10.1016/j.optom.2016.04.002>
- Faisal, A. A., Selen, L. P. J., & Wolpert, D. M. (2008). Noise in the nervous system. In *Nature Reviews Neuroscience*. <https://doi.org/10.1038/nrn2258>
- Fan, Y. T., & Cheng, Y. (2014). Atypical mismatch negativity in response to emotional voices in people with autism spectrum conditions. *PLoS ONE*, 9(7). <https://doi.org/10.1371/journal.pone.0102471>
- Farzan, F., Atluri, S., Frehlich, M., Dhimi, P., Kleffner, K., Price, R., Lam, R. W., Frey, B. N., Milev, R., Ravindran, A., McAndrews, M. P., Wong, W., Blumberger, D., Daskalakis, Z. J., Vila-Rodriguez, F., Alonso, E., Brenner, C. A., Liotti, M., Dharsee, M., ... Kennedy, S. H. (2017). Standardization of electroencephalography for multi-site, multi-platform and multi-investigator studies: Insights from the canadian biomarker integration network in depression. *Scientific Reports*. <https://doi.org/10.1038/s41598-017-07613-x>
- Fatemi, S. H., Reutiman, T. J., Folsom, T. D., & Thuras, P. D. (2009). GABAA receptor downregulation in brains of subjects with autism. *Journal of Autism and Developmental Disorders*. <https://doi.org/10.1007/s10803-008-0646-7>
- Fell, J., Fernandez, G., Klaver, P., Elger, C. E., & Fries, P. (2003). Is synchronized neuronal gamma activity relevant for selective attention?. *Brain Research Reviews*, 42(3), 265-272. [https://doi.org/10.1016/S0165-0173\(03\)00178-4](https://doi.org/10.1016/S0165-0173(03)00178-4)
- Fell, J., Ludowig, E., Rosburg, T., Axmacher, N., & Elger, C. E. (2008). Phase-locking within human mediotemporal lobe predicts memory formation. *NeuroImage*. <https://doi.org/10.1016/j.neuroimage.2008.07.021>
- Fernandez, D., & Wilkins, A. J. (2008). Uncomfortable images in art and nature. *Perception*. <https://doi.org/10.1068/p5814>
- Fischer, A. G., Endrass, T., Goebel, I., Reuter, M., Montag, C., Kubisch, C., & Ullsperger, M. (2015). Interactive effects of citalopram and serotonin transporter genotype on neural

- correlates of response inhibition and attentional orienting. *NeuroImage*, 116, 59–67. <https://doi.org/10.1016/j.neuroimage.2015.04.064>
- Flint, J., & Munafò, M. R. (2007). The endophenotype concept in psychiatric genetics. In *Psychological Medicine*. <https://doi.org/10.1017/S0033291706008750>
- Folstein, S., & Rutter, M. (1977). INFANTILE AUTISM: A GENETIC STUDY OF 21 TWIN PAIRS. *Journal of Child Psychology and Psychiatry*. <https://doi.org/10.1111/j.1469-7610.1977.tb00443.x>
- Foxe, J. J., & Snyder, A. C. (2011). The role of alpha-band brain oscillations as a sensory suppression mechanism during selective attention. *Frontiers in psychology*, 2, 154. <https://doi.org/10.3389/fpsyg.2011.00154>
- Frazier, T. W., & Hardan, A. Y. (2017). Equivalence of symptom dimensions in females and males with autism. *Autism*. <https://doi.org/10.1177/1362361316660066>
- Freitag, C. M., Luders, E., Hulst, H. E., Narr, K. L., Thompson, P. M., Toga, A. W., Krick, C., & Konrad, C. (2009). Total Brain Volume and Corpus Callosum Size in Medication-Naïve Adolescents and Young Adults with Autism Spectrum Disorder. *Biological Psychiatry*. <https://doi.org/10.1016/j.biopsych.2009.03.011>
- Fries, P. (2005). A mechanism for cognitive dynamics: Neuronal communication through neuronal coherence. *Trends in Cognitive Sciences*. <https://doi.org/10.1016/j.tics.2005.08.011>
- Fries, P. (2009). Neuronal gamma-band synchronization as a fundamental process in cortical computation. *Annual review of neuroscience*, 32, 209-224. <https://doi.org/10.1146/annurev.neuro.051508.135603>
- Fries, P. (2015). Rhythms for Cognition: Communication through Coherence. *Neuron*, 88(1), 220–235. <https://doi.org/10.1016/j.neuron.2015.09.034>
- Frith, U. (2003). Autism: Explaining the Enigma (2nd edition). In *Blackwell; Oxford*.
- Gao, R. (2016). Interpreting the electrophysiological power spectrum. *Journal of Neurophysiology*, 115(2), 628–630. <https://doi.org/10.1152/jn.00722.2015>

- Gao, R., Peterson, E. J., & Voytek, B. (2017). Inferring synaptic excitation/inhibition balance from field potentials. *NeuroImage*, *158*(July 2017), 70–78. <https://doi.org/10.1016/j.neuroimage.2017.06.078>
- Garrett, D. D., Samanez-Larkin, G. R., MacDonald, S. W. S., Lindenberger, U., McIntosh, A. R., & Grady, C. L. (2013). Moment-to-moment brain signal variability: A next frontier in human brain mapping? In *Neuroscience and Biobehavioral Reviews*. <https://doi.org/10.1016/j.neubiorev.2013.02.015>
- Gaugler, T., Klei, L., Sanders, S. J., Bodea, C. A., Goldberg, A. P., Lee, A. B., Mahajan, M., Manaa, D., Pawitan, Y., Reichert, J., Ripke, S., Sandin, S., Sklar, P., Svantesson, O., Reichenberg, A., Hultman, C. M., Devlin, B., Roeder, K., & Buxbaum, J. D. (2014). Most genetic risk for autism resides with common variation. *Nature Genetics*. <https://doi.org/10.1038/ng.3039>
- Geschwind, D. H. (2008). Autism: Many Genes, Common Pathways? In *Cell*. <https://doi.org/10.1016/j.cell.2008.10.016>
- Geschwind, D. H., & State, M. W. (2015). Gene hunting in autism spectrum disorder: On the path to precision medicine. In *The Lancet Neurology*. [https://doi.org/10.1016/S1474-4422\(15\)00044-7](https://doi.org/10.1016/S1474-4422(15)00044-7)
- Giacobini, M. B., Medin, E., Ahnemark, E., Russo, L. J., & Carlqvist, P. (2018). Prevalence, Patient Characteristics, and Pharmacological Treatment of Children, Adolescents, and Adults Diagnosed With ADHD in Sweden. *Journal of Attention Disorders*. <https://doi.org/10.1177/1087054714554617>
- Gillberg, C., & Billstedt, E. (2000). Autism and Asperger syndrome: Coexistence with other clinical disorders. In *Acta Psychiatrica Scandinavica*. <https://doi.org/10.1034/j.1600-0447.2000.102005321.x>
- Gonen-Yaacovi, G., Arazi, A., Shahar, N., Karmon, A., Haar, S., Meiran, N., & Dinstein, I. (2016). Increased ongoing neural variability in ADHD. *Cortex*. <https://doi.org/10.1016/j.cortex.2016.04.010>

- Greent-'t-Jong, T., Gajwani, R., Gross, J., Gumley, A. I., Krishnadas, R., Lawrie, S. M., Schwannauer, M., Schultze-Lutter, F., & Uhlhaas, P. J. (2020). Association of magnetoencephalographically measured high-frequency oscillations in visual cortex with circuit dysfunctions in local and large-scale networks during emerging psychosis. *JAMA Psychiatry*. <https://doi.org/10.1001/jamapsychiatry.2020.0284>
- Greven, C. U., Bralten, J., Mennes, M., O'Dwyer, L., Van Hulzen, K. J. E., Rommelse, N., Schwenen, L. J. S., Hoekstra, P. J., Hartman, C. A., Heslenfeld, D., Oosterlaan, J., Faraone, S. V., Franke, B., Zwiers, M. P., Arias-Vasquez, A., & Buitelaar, J. K. (2015). Developmentally stable whole-brain volume reductions and developmentally sensitive caudate and putamen volume alterations in those with attention-deficit/hyperactivity disorder and their unaffected siblings. *JAMA Psychiatry*, 72(5), 490–499. <https://doi.org/10.1001/jamapsychiatry.2014.3162>
- Griffiths, B. J., Martín-Buro, M. C., Staresina, B. P., Hanslmayr, S., & Staudigl, T. (2021). Alpha/beta power decreases during episodic memory formation predict the magnitude of alpha/beta power decreases during subsequent retrieval. *Neuropsychologia*, 153. <https://doi.org/10.1016/j.neuropsychologia.2021.107755>
- Grion, N., Akrami, A., Zuo, Y., Stella, F., & Diamond, M. E. (2016). Coherence between rat sensorimotor system and hippocampus is enhanced during tactile discrimination. *PLoS Biology*, 14(2). <https://doi.org/10.1371/journal.pbio.1002384>
- Groom, M. J., Cahill, J. D., Bates, A. T., Jackson, G. M., Calton, T. G., Liddle, P. F., & Hollis, C. (2010). Electrophysiological indices of abnormal error-processing in adolescents with attention deficit hyperactivity disorder (ADHD). *Journal of Child Psychology and Psychiatry and Allied Disciplines*. <https://doi.org/10.1111/j.1469-7610.2009.02128.x>
- Grove, J., Ripke, S., Als, T., Mattheisen, M., Walters, R., Won, H., Pallesen, J., Agerbo, E., Andreassen, O., Anney, R., Belliveau, R., Bettella, F., Buxbaum, J., Bybjerg-Grauholm, J., Bækved-Hansen, M., Cerrato, F., Chambert, K., Christensen, J., Churchhouse, C., ... Børglum, A. (2017). Common risk variants identified in autism spectrum disorder. *BioRxiv*. <https://doi.org/10.1101/224774>

- Grzadzinski, R., Huerta, M., & Lord, C. (2013). DSM-5 and autism spectrum disorders (ASDs): An opportunity for identifying ASD subtypes. In *Molecular Autism*. <https://doi.org/10.1186/2040-2392-4-12>
- Güntekin, B., Emek-Savaş, D. D., Kurt, P., Yener, G. G., & Başar, E. (2013). Beta oscillatory responses in healthy subjects and subjects with mild cognitive impairment. *NeuroImage: Clinical*. <https://doi.org/10.1016/j.nicl.2013.07.003>
- Hager, B., Yang, A. C., Brady, R., Meda, S., Clementz, B., Pearlson, G. D., Sweeney, J. A., Tamminga, C., & Keshavan, M. (2017). Neural complexity as a potential translational biomarker for psychosis. *Journal of Affective Disorders*. <https://doi.org/10.1016/j.jad.2016.10.016>
- Haigh, S. M., Cooper, N. R., & Wilkins, A. J. (2015). Cortical excitability and the shape of the haemodynamic response. *NeuroImage*. <https://doi.org/10.1016/j.neuroimage.2015.02.034>
- Haigh, S. M. (2018). Variable sensory perception in autism. *European Journal of Neuroscience*. <https://doi.org/10.1111/ejn.13601>
- Haigh, S. M., Barningham, L., Berntsen, M., Coutts, L. V., Hobbs, E. S. T., Irabor, J., Lever, E. M., Tang, P., & Wilkins, A. J. (2013). Discomfort and the cortical haemodynamic response to coloured gratings. *Vision Research*. <https://doi.org/10.1016/j.visres.2013.07.003>
- Haigh, S. M., Gupta, A., Barb, S. M., Glass, S. A. F., Minshew, N. J., Dinstein, I., Heeger, D. J., Eack, S. M., & Behrmann, M. (2016). Differential sensory fMRI signatures in autism and schizophrenia: Analysis of amplitude and trial-to-trial variability. *Schizophrenia Research*. <https://doi.org/10.1016/j.schres.2016.03.036>
- Haigh, S. M., Heeger, D. J., Dinstein, I., Minshew, N., & Behrmann, M. (2015). Cortical Variability in the Sensory-Evoked Response in Autism. *Journal of Autism and Developmental Disorders*. <https://doi.org/10.1007/s10803-014-2276-6>

- Halgren, M., Ulbert, I., Bastuji, H., Fabó, D., Erőss, L., Rey, M., ... & Cash, S. S. (2019). The generation and propagation of the human alpha rhythm. *Proceedings of the National Academy of Sciences*, 116(47), 23772-23782. <https://doi.org/10.1073/pnas.1913092116>
- Haller, M., Donoghue, T., Peterson, E., Varma, P., Sebastian, P., Gao, R., Noto, T., Knight, R. T., Shestyuk, A., & Voytek, B. (2018). Parameterizing neural power spectra. *BioRxiv*, 299859. <https://doi.org/10.1101/299859>
- Hallmayer, J., Cleveland, S., Torres, A., Phillips, J., Cohen, B., Torigoe, T., Miller, J., Fedele, A., Collins, J., Smith, K., Lotspeich, L., Croen, L. A., Ozonoff, S., Lajonchere, C., Grether, J. K., & Risch, N. (2011). Genetic heritability and shared environmental factors among twin pairs with autism. *Archives of General Psychiatry*. <https://doi.org/10.1001/archgenpsychiatry.2011.76>
- Hanslmayr, S., Klimesch, W., Sauseng, P., Gruber, W., Doppelmayr, M., Freunberger, R., & Pecherstorfer, T. (2005). Visual discrimination performance is related to decreased alpha amplitude but increased phase locking. *Neuroscience Letters*. <https://doi.org/10.1016/j.neulet.2004.10.092>
- Happé, F., & Frith, U. (2020). Annual Research Review: Looking back to look forward – changes in the concept of autism and implications for future research. In *Journal of Child Psychology and Psychiatry and Allied Disciplines*. <https://doi.org/10.1111/jcpp.13176>
- Happé, F., Ronald, A., & Plomin, R. (2006). Time to give up on a single explanation for autism. In *Nature Neuroscience*. <https://doi.org/10.1038/nn1770>
- Harle, D. E., Shepherd, A. J., & Evans, B. J. W. (2006). Visual stimuli are common triggers of migraine and are associated with pattern glare. *Headache*. <https://doi.org/10.1111/j.1526-4610.2006.00585.x>
- Harony, H., Günal, O. B., & Buxbaum, J. D. (2013). SHANK2 and SHANK3 Mutations Implicate Glutamate Signaling Abnormalities in Autism Spectrum Disorders. In *The Neuroscience of Autism Spectrum Disorders*. <https://doi.org/10.1016/B978-0-12-391924-3.00032-6>

- Hartman, C. A., Geurts, H. M., Franke, B., Buitelaar, J. K., & Rommelse, N. N. J. (2016). Changing ASD-ADHD symptom co-occurrence across the lifespan with adolescence as crucial time window: Illustrating the need to go beyond childhood. In *Neuroscience and Biobehavioral Reviews*. <https://doi.org/10.1016/j.neubiorev.2016.09.003>
- Hayne, D. P., & Martin, P. R. (2019). Relating Photophobia, Visual Aura, and Visual Triggers of Headache and Migraine. *Headache*. <https://doi.org/10.1111/head.13486>
- He, H. Y., & Cline, H. T. (2019). What Is Excitation/Inhibition and How Is It Regulated? A Case of the Elephant and the Wisemen. In *Journal of Experimental Neuroscience*. <https://doi.org/10.1177/1179069519859371>
- Heinrich, H., Dickhaus, H., Rothenberger, A., Heinrich, V., & Moll, G. H. (1999). Single-sweep analysis of event-related potentials by wavelet networks-methodological basis and clinical application. *IEEE Transactions on Biomedical Engineering*. <https://doi.org/10.1109/10.771199>
- Henderson, H., Schwartz, C., Mundy, P., Burnette, C., Sutton, S., Zahka, N., & Pradella, A. (2006). Response monitoring, the error-related negativity, and differences in social behavior in autism. *Brain and Cognition*, *61*(1), 96–109. <https://doi.org/10.1016/j.bandc.2005.12.009>
- Herweg, N. A., Apitz, T., Leicht, G., Mulert, C., Fuentemilla, L., & Bunzeck, N. (2016). Theta-alpha oscillations bind the hippocampus, prefrontal cortex, and striatum during recollection: evidence from simultaneous EEG–fMRI. *Journal of Neuroscience*, *36*(12), 3579–3587. <https://doi.org/10.1523/JNEUROSCI.3629-15.2016>
- Herweg, N. A., Solomon, E. A., & Kahana, M. J. (2020). Theta oscillations in human memory. *Trends in cognitive sciences*, *24*(3), 208–227. <https://doi.org/10.1016/j.tics.2019.12.006>
- Hibbard, P. B., & O’Hare, L. (2015). Uncomfortable images produce non-sparse responses in a model of primary visual cortex. *Royal Society Open Science*. <https://doi.org/10.1098/rsos.140535>

- Hickey, P., Merseal, H., Patel, A. D., & Race, E. (2020). Memory in time: Neural tracking of low-frequency rhythm dynamically modulates memory formation. *Neuroimage*, 213, 116693. <https://doi.org/10.1016/j.neuroimage.2020.116693>
- Hill, E., Berthoz, S., & Frith, U. (2004). Brief Report: Cognitive Processing of Own Emotions in Individuals with Auti...: EBSCOhost. *Journal of Autism & Developmental Disorders*, 34(2), 229. <http://web.b.ebscohost.com/ehost/pdfviewer/pdfviewer?sid=d15c4f23-1678-4036-9c4c-3fdf3b312312@sessionmgr115&vid=1&hid=119>
- Hodgson, K., McGuffin, P., & Lewis, C. M. (2017). Advancing psychiatric genetics through dissecting heterogeneity. *Human molecular genetics*, 26(R2), R160-R165.
- Horder, J., Petrinovic, M. M., Mendez, M. A., Bruns, A., Takumi, T., Spooren, W., Barker, G. J., Künnecke, B., & Murphy, D. G. (2018). Glutamate and GABA in autism spectrum disorder-a translational magnetic resonance spectroscopy study in man and rodent models. *Translational Psychiatry*. <https://doi.org/10.1038/s41398-018-0155-1>
- Hossain, M. M., Khan, N., Sultana, A., Ma, P., McKyer, E. L. J., Ahmed, H. U., & Purohit, N. (2020). Prevalence of comorbid psychiatric disorders among people with autism spectrum disorder: An umbrella review of systematic reviews and meta-analyses. In *Psychiatry Research*. <https://doi.org/10.1016/j.psychres.2020.112922>
- Huang, J., Cooper, T. G., Satana, B., Kaufman, D. I., & Cao, Y. (2003). Visual distortion provoked by a stimulus in migraine associated with hyperneuronal activity. *Headache*. <https://doi.org/10.1046/j.1526-4610.2003.03110.x>
- Huang, J., Zong, X., Wilkins, A., Jenkins, B., Bozoki, A., & Cao, Y. (2011). FMRI evidence that precision ophthalmic tints reduce cortical hyperactivation in migraine. *Cephalalgia*. <https://doi.org/10.1177/0333102411409076>
- Huang, P., Xiang, X., Chen, X., & Li, H. (2020). Somatostatin Neurons Govern Theta Oscillations Induced by Salient Visual Signals. *Cell Reports*, 33(8), 108415. <https://doi.org/10.1016/j.celrep.2020.108415>
- Hull, L., Petrides, K. V., Allison, C., Smith, P., Baron-Cohen, S., Lai, M. C., & Mandy, W. (2017). “Putting on My Best Normal”: Social Camouflaging in Adults with Autism

- Spectrum Conditions. *Journal of Autism and Developmental Disorders*, 47(8), 2519–2534. <https://doi.org/10.1007/s10803-017-3166-5>
- Hull, J. V., Dokovna, L. B., Jacokes, Z. J., Torgerson, C. M., Irimia, A., & Van Horn, J. D. (2017). Resting-state functional connectivity in autism spectrum disorders: a review. *Frontiers in psychiatry*, 7, 205. <https://doi.org/10.3389/fpsy.2016.00205>
- Hutchinson, A. D., Mathias, J. L., & Banich, M. T. (2008). Corpus Callosum Morphology in Children and Adolescents With Attention Deficit Hyperactivity Disorder: A Meta-Analytic Review. *Neuropsychology*, 22(3), 341–349. <https://doi.org/10.1037/0894-4105.22.3.341>
- I., D., C., T., K., H., N., M., & M., B. (2009). Is autism caused by mirror system dysfunction or increased neural noise? *Journal of Molecular Neuroscience*.
- Ishii, R., Canuet, L., Aoki, Y., Hata, M., Iwase, M., Ikeda, S., Nishida, K., & Ikeda, M. (2018). Healthy and Pathological Brain Aging: From the Perspective of Oscillations, Functional Connectivity, and Signal Complexity. In *Neuropsychobiology*. <https://doi.org/10.1159/000486870>
- Isler, J. R., Martien, K. M., Grieve, P. G., Stark, R. I., & Herbert, M. R. (2010). Reduced functional connectivity in visual evoked potentials in children with autism spectrum disorder. *Clinical Neurophysiology*, 121(12), 2035-2043. <https://doi.org/10.1016/j.clinph.2010.05.004>
- Janssen, T. W. P., Hillebrand, A., Gouw, A., Geladé, K., Van Mourik, R., Maras, A., & Oosterlaan, J. (2017). Neural network topology in ADHD; evidence for maturational delay and default-mode network alterations. *Clinical Neurophysiology*. <https://doi.org/10.1016/j.clinph.2017.09.004>
- Jarrold, C., & Brock, J. (2004). To Match or Not to Match? Methodological Issues in Autism-Related Research. In *Journal of Autism and Developmental Disorders*. <https://doi.org/10.1023/B:JADD.0000018078.82542.ab>

- Jaskowski, P., & Verleger, R. (1999). Amplitudes and latencies of single-trial ERP's estimated by a maximum-likelihood method. *IEEE Transactions on Biomedical Engineering*. <https://doi.org/10.1109/10.775409>
- Jasmin, K., Gotts, S. J., Xu, Y., Liu, S., Riddell, C. D., Ingeholm, J. E., Kenworthy, L., Wallace, G. L., Braun, A. R., & Martin, A. (2019). Overt social interaction and resting state in young adult males with autism: Core and contextual neural features. *Brain*. <https://doi.org/10.1093/brain/awz003>
- Javitt, D. C., & Freedman, R. (2015). Sensory processing dysfunction in the personal experience and neuronal machinery of schizophrenia. *American Journal of Psychiatry*. <https://doi.org/10.1176/appi.ajp.2014.13121691>
- Jensen, C. M., & Steinhausen, H. C. (2015). Comorbid mental disorders in children and adolescents with attention-deficit/hyperactivity disorder in a large nationwide study. *ADHD Attention Deficit and Hyperactivity Disorders*. <https://doi.org/10.1007/s12402-014-0142-1>
- Jensen, O., & Mazaheri, A. (2010). Shaping functional architecture by oscillatory alpha activity: Gating by inhibition. *Frontiers in Human Neuroscience*. <https://doi.org/10.3389/fnhum.2010.00186>
- Jeste, S. S., & Geschwind, D. H. (2014). Disentangling the heterogeneity of autism spectrum disorder through genetic findings. In *Nature Reviews Neurology*. <https://doi.org/10.1038/nrneurol.2013.278>
- Jokiranta-Olkonemi, E., Cheslack-Postava, K., Sucksdorff, D., Suominen, A., Gyllenberg, D., Chudal, R., Leivonen, S., Gissler, M., Brown, A. S., & Sourander, A. (2016). Risk of psychiatric and neurodevelopmental disorders among siblings of probands with autism spectrum disorders. *JAMA Psychiatry*. <https://doi.org/10.1001/jamapsychiatry.2016.0495>
- Jones, R. S. P., Quigney, C., & Huws, J. C. (2003). First-hand accounts of sensory perceptual experiences in autism: A qualitative analysis. *Journal of Intellectual and Developmental Disability*. <https://doi.org/10.1080/1366825031000147058>

- Jung, T. P., Makeig, S., Westerfield, M., Townsend, J., Courchesne, E., & Sejnowski, T. J. (2001). Analysis and visualization of single-trial event-related potentials. *Human Brain Mapping*. <https://doi.org/10.1002/hbm.1050>
- Just, M. A., Cherkassky, V. L., Keller, T. A., & Minshew, N. J. (2004). Cortical activation and synchronization during sentence comprehension in high-functioning autism: Evidence of underconnectivity. *Brain*. <https://doi.org/10.1093/brain/awh199>
- Jutten, C., & Herault, J. (1991). Blind separation of sources, part I: An adaptive algorithm based on neuromimetic architecture. *Signal Processing*. [https://doi.org/10.1016/0165-1684\(91\)90079-X](https://doi.org/10.1016/0165-1684(91)90079-X)
- K., D., F., H., P., B., & A., R. (2009). Relationship between symptom domains in autism spectrum disorders: A population based twin study. In *Journal of Autism and Developmental Disorders*.
- Kaiser, A., Aggensteiner, P. M., Baumeister, S., Holz, N. E., Banaschewski, T., & Brandeis, D. (2020). Earlier versus later cognitive event-related potentials (ERPs) in attention-deficit/hyperactivity disorder (ADHD): A meta-analysis. In *Neuroscience and Biobehavioral Reviews* (Vol. 112). <https://doi.org/10.1016/j.neubiorev.2020.01.019>
- Kam, J. W. Y., Griffin, S., Shen, A., Patel, S., Hinrichs, H., Heinze, H. J., Deouell, L. Y., & Knight, R. T. (2019). Systematic comparison between a wireless EEG system with dry electrodes and a wired EEG system with wet electrodes. *NeuroImage*. <https://doi.org/10.1016/j.neuroimage.2018.09.012>
- Kanner, S., Goldin, M., Galron, R., Jacob, E. Ben, Bonifazi, P., & Barzilai, A. (2018). Astrocytes restore connectivity and synchronization in dysfunctional cerebellar networks. *Proceedings of the National Academy of Sciences of the United States of America*, 115(31), 8025–8030. <https://doi.org/10.1073/pnas.1718582115>
- Kayser, C., Ince, R. A., & Panzeri, S. (2012). Analysis of slow (theta) oscillations as a potential temporal reference frame for information coding in sensory cortices. *PLoS Computational Biology*, 8 (10). <https://doi.org/10.1371/journal.pcbi.1002717>

- Keitel, C., Thut, G., & Gross, J. (2017). Visual cortex responses reflect temporal structure of continuous quasi-rhythmic sensory stimulation. *Neuroimage*, 146, 58-70. <https://doi.org/10.1016/j.neuroimage.2016.11.043>
- Kessler, R. C., Adler, L., Ames, M., Demler, O., Faraone, S., Hiripi, E., Howes, M. J., Jin, R., Secnik, K., Spencer, T., Ustun, T. B., & Walters, E. E. (2005). The World Health Organization adult ADHD self-report scale (ASRS): A short screening scale for use in the general population. *Psychological Medicine*. <https://doi.org/10.1017/S0033291704002892>
- Khader, P. H., Jost, K., Ranganath, C., & Rösler, F. (2010). Theta and alpha oscillations during working-memory maintenance predict successful long-term memory encoding. *Neuroscience letters*, 468(3), 339-343. <https://doi.org/10.1016/j.neulet.2009.11.028>
- Khan, S., Gramfort, A., Shetty, N. R., Kitzbichler, M. G., Ganesan, S., Moran, J. M., Lee, S. M., Gabrieli, J. D. E., Tager-Flusberg, H. B., Joseph, R. M., Herbert, M. R., Hämäläinen, M. S., & Kenet, T. (2013). Local and long-range functional connectivity is reduced in concert in autism spectrum disorders. *Proceedings of the National Academy of Sciences of the United States of America*. <https://doi.org/10.1073/pnas.1214533110>
- Kienitz, R., Cox, M. A., Dougherty, K., Saunders, R. C., Schmiedt, J. T., Leopold, D. A., ... & Schmid, M. C. (2021). Theta, but not gamma oscillations in area V4 depend on input from primary visual cortex. *Current Biology*, 31(3), 635-642. <https://doi.org/10.1016/j.cub.2020.10.091>
- Kiiski, H., Bennett, M., Rueda-Delgado, L. M., Farina, F. R., Knight, R., Boyle, R., Roddy, D., Grogan, K., Bramham, J., Kelly, C., & Whelan, R. (2020). EEG spectral power, but not theta/beta ratio, is a neuromarker for adult ADHD. *European Journal of Neuroscience*. <https://doi.org/10.1111/ejn.14645>
- Kilavik, B. E., Zaepffel, M., Brovelli, A., MacKay, W. A., & Riehle, A. (2013). The ups and downs of beta oscillations in sensorimotor cortex. *Experimental neurology*, 245, 15-26. <https://doi.org/10.1016/j.expneurol.2012.09.014>
- Kim, M., Lee, T. H., Kim, J. H., Hong, H., Lee, T. Y., Lee, Y., Salisbury, D. F., & Kwon, J. S. (2018). Decomposing P300 into correlates of genetic risk and current symptoms in

- schizophrenia: An inter-trial variability analysis. *Schizophrenia Research*.
<https://doi.org/10.1016/j.schres.2017.04.001>
- Kim, S. H., Macari, S., Koller, J., & Chawarska, K. (2016). Examining the phenotypic heterogeneity of early autism spectrum disorder: Subtypes and short-term outcomes. *Journal of Child Psychology and Psychiatry and Allied Disciplines*.
<https://doi.org/10.1111/jcpp.12448>
- Kim, S., Banaschewski, T., & Tannock, R. (2015). Color vision in attention-deficit/hyperactivity disorder: A pilot visual evoked potential study. *Journal of Optometry*. <https://doi.org/10.1016/j.optom.2014.10.002>
- Kim, Y. S., Choi, J., & Yoon, B. E. (2020). Neuron-Glia Interactions in Neurodevelopmental Disorders. In *Cells*. <https://doi.org/10.3390/cells9102176>
- Kinouchi, O., & Copelli, M. (2006). Optimal dynamical range of excitable networks at criticality. *Nature Physics*. <https://doi.org/10.1038/nphys289>
- Kirihara, K., Rissling, A. J., Swerdlow, N. R., Braff, D. L., & Light, G. A. (2012). Hierarchical organization of gamma and theta oscillatory dynamics in schizophrenia. *Biological Psychiatry*. <https://doi.org/10.1016/j.biopsych.2012.01.016>
- Kirschstein, T., & Köhling, R. (2009). What is the source of the EEG? *Clinical EEG and Neuroscience*. <https://doi.org/10.1177/155005940904000305>
- Kitsune, G. L., Cheung, C. H. M., Brandeis, D., Banaschewski, T., Asherson, P., McLoughlin, G., & Kuntsi, J. (2015). A Matter of Time: The Influence of Recording Context on EEG Spectral Power in Adolescents and Young Adults with ADHD. *Brain Topography*.
<https://doi.org/10.1007/s10548-014-0395-1>
- Kloosterman, N. A., Meindertsma, T., Hillebrand, A., van Dijk, B. W., Lamme, V. A., & Donner, T. H. (2015). Top-down modulation in human visual cortex predicts the stability of a perceptual illusion. *Journal of neurophysiology*, 113(4), 1063-1076.
<https://doi.org/10.1152/jn.00338.2014>

- Klimesch, W. (1999). EEG alpha and theta oscillations reflect cognitive and memory performance: a review and analysis. *Brain research reviews*, 29(2-3), 169-195. [https://doi.org/10.1016/S0165-0173\(98\)00056-3](https://doi.org/10.1016/S0165-0173(98)00056-3)
- Klimesch, W., Schack, B., Schabus, M., Doppelmayr, M., Gruber, W., & Sauseng, P. (2004). Phase-locked alpha and theta oscillations generate the P1–N1 complex and are related to memory performance. *Cognitive Brain Research*, 19(3), 302-316. <https://doi.org/10.1016/j.cogbrainres.2003.11.016>
- Klimesch, W., Sauseng, P., & Hanslmayr, S. (2007). EEG alpha oscillations: the inhibition–timing hypothesis. *Brain research reviews*, 53(1), 63-88. <https://doi.org/10.1016/j.brainresrev.2006.06.003>
- Klimesch, W. (2012). Alpha-band oscillations, attention, and controlled access to stored information. *Trends in cognitive sciences*, 16(12), 606-617. <https://doi.org/10.1016/j.tics.2012.10.007>
- Koerner, T. K., & Zhang, Y. (2015). Effects of background noise on inter-trial phase coherence and auditory N1–P2 responses to speech stimuli. *Hearing Research*, 328, 113-119. <https://doi.org/10.1016/j.heares.2015.08.002>
- Koh, Y., Shin, K. S., Kim, J. S., Choi, J. S., Kang, D. H., Jang, J. H., Cho, K. H., O'Donnell, B. F., Chung, C. K., & Kwon, J. S. (2011). An MEG study of alpha modulation in patients with schizophrenia and in subjects at high risk of developing psychosis. *Schizophrenia Research*. <https://doi.org/10.1016/j.schres.2010.10.001>
- Kondo, H. M., Van Loon, A. M., Kawahara, J. I., & Moore, B. C. J. (2017). Auditory and visual scene analysis: An overview. *Philosophical Transactions of the Royal Society B: Biological Sciences*. <https://doi.org/10.1098/rstb.2016.0099>
- Kothe, C. (2014). Lab streaming layer (LSL). <https://github.com/Scn/Labstreaminglayer>. Accessed on October 2020.
- Kovarski, K., Malvy, J., Khanna, R. K., Arsène, S., Batty, M., & Latinus, M. (2019). Reduced visual evoked potential amplitude in autism spectrum disorder, a variability effect? *Translational Psychiatry*. <https://doi.org/10.1038/s41398-019-0672-6>

- Kowalczyk, O. S., Mehta, M. A., O'Daly, O. G., & Criaud, M. (2021). Task-based functional connectivity in attention-deficit/hyperactivity disorder: A systematic review. *Biological Psychiatry Global Open Science*. <https://doi.org/10.1016/j.bpsgos.2021.10.006>
- Koychev, I., El-Deredy, W., & William Deakin, J. F. (2011). New visual information processing abnormality biomarkers for the diagnosis of schizophrenia. In *Expert Opinion on Medical Diagnostics*. <https://doi.org/10.1517/17530059.2011.586029>
- Kulashekhar, S., Pekkola, J., Palva, J. M., & Palva, S. (2016). The role of cortical beta oscillations in time estimation. *Human brain mapping*, 37(9), 3262-3281. <https://doi.org/10.1002/hbm.23239>
- Kylliäinen, A., Jones, E. J. H., Gomot, M., Warreyn, P., & Falck-Ytter, T. (2014). Practical Guidelines for Studying Young Children With Autism Spectrum Disorder in Psychophysiological Experiments. *Review Journal of Autism and Developmental Disorders*. <https://doi.org/10.1007/s40489-014-0034-5>
- Lai, M. C., Lombardo, M. V., Ruigrok, A. N. V., Chakrabarti, B., Auyeung, B., Szatmari, P., Happé, F., & Baron-Cohen, S. (2017). Quantifying and exploring camouflaging in men and women with autism. *Autism*. <https://doi.org/10.1177/1362361316671012>
- Lai, M. C., Lombardo, M. V., Ruigrok, A. N. V., Chakrabarti, B., Wheelwright, S. J., Auyeung, B., Allison, C., Bailey, A. J., Baron-Cohen, S., Bolton, P. F., Bullmore, E. T., Carrington, S., Catani, M., Craig, M. C., Daly, E. M., Deoni, S. C., Ecker, C., Happé, F., Henty, J., ... Williams, S. C. (2012). Cognition in Males and Females with Autism: Similarities and Differences. *PLoS ONE*. <https://doi.org/10.1371/journal.pone.0047198>
- Lakatos, P., Karmos, G., Mehta, A. D., Ulbert, I., & Schroeder, C. E. (2008). Entrainment of neuronal oscillations as a mechanism of attentional selection. *Science*. <https://doi.org/10.1126/science.1154735>
- Lau-Zhu, A., Fritz, A., & McLoughlin, G. (2019). Overlaps and distinctions between attention deficit/hyperactivity disorder and autism spectrum disorder in young adulthood: Systematic review and guiding framework for EEG-imaging research. In *Neuroscience and Biobehavioral Reviews*. <https://doi.org/10.1016/j.neubiorev.2018.10.009>

- Leekam, S., Tandos, J., McConachie, H., Meins, E., Parkinson, K., Wright, C., Turner, M., Arnott, B., Vittorini, L., & Couteur, A. Le. (2007). Repetitive behaviours in typically developing 2-year-olds. *Journal of Child Psychology and Psychiatry and Allied Disciplines*. <https://doi.org/10.1111/j.1469-7610.2007.01778.x>
- Lemi, L., Gwilliams, L., Samaha, J., Auksztulewicz, R., Cycowicz, Y. M., King, J. R., ... & Haegens, S. (2021). Ongoing neural oscillations influence behavior and sensory representations by suppressing neuronal excitability. *NeuroImage*, 247. <https://doi.org/10.1016/j.neuroimage.2021.118746>
- Lenartowicz, A., & Loo, S. K. (2014). Use of EEG to Diagnose ADHD. In *Current Psychiatry Reports*. <https://doi.org/10.1007/s11920-014-0498-0>
- Light, G. A., Hsu, J. L., Hsieh, M. H., Meyer-Gomes, K., Sprock, J., Swerdlow, N. R., & Braff, D. L. (2006). Gamma Band Oscillations Reveal Neural Network Cortical Coherence Dysfunction in Schizophrenia Patients. *Biological Psychiatry*. <https://doi.org/10.1016/j.biopsych.2006.03.055>
- Limanowski, J., Litvak, V., & Friston, K. (2020). Cortical beta oscillations reflect the contextual gating of visual action feedback. *NeuroImage*, 222. <https://doi.org/10.1016/j.neuroimage.2020.117267>
- Lionel, A. C., Tammimies, K., Vaags, A. K., Rosenfeld, J. A., Ahn, J. W., Merico, D., Noor, A., Runke, C. K., Pillalamarri, V. K., Carter, M. T., Gazzellone, M. J., Thiruvahindrapuram, B., Fagerberg, C., Laulund, L. W., Pellecchia, G., Lamoureux, S., Deshpande, C., Clayton-Smith, J., White, A. C., ... Scherer, S. W. (2014). Disruption of the ASTN2/TRIM32 locus at 9q33.1 is a risk factor in males for autism spectrum disorders, ADHD and other neurodevelopmental phenotypes. *Human Molecular Genetics*. <https://doi.org/10.1093/hmg/ddt669>
- Little, J. A. (2018). Vision in children with autism spectrum disorder: a critical review. In *Clinical and Experimental Optometry*. <https://doi.org/10.1111/cxo.12651>
- Lo, Y. C., Chen, Y. J., Hsu, Y. C., Chien, Y. L., Gau, S. S. F., & Tseng, W. Y. I. (2019). Altered frontal aslant tracts as a heritable neural basis of social communication deficits in autism

- spectrum disorder: A sibling study using tract-based automatic analysis. *Autism Research*. <https://doi.org/10.1002/aur.2044>
- Lodato, M. A., & Walsh, C. A. (2019). Genome aging: somatic mutation in the brain links age-related decline with disease and nominates pathogenic mechanisms. In *Human Molecular Genetics*. <https://doi.org/10.1093/hmg/ddz191>
- Lombardi, F., Herrmann, H. J., & de Arcangelis, L. (2017). Balance of excitation and inhibition determines 1/f power spectrum in neuronal networks. *Chaos*. <https://doi.org/10.1063/1.4979043>
- Lord, C., Rutter, M., DiLavore, P., Risi, S., Gotham, K., & Bishop, S. (2012). Autism Diagnostic Observation Schedule, (ADOS-2) Modules 1-4. In *Los Angeles, California*:
- Lord, C., Rutter, M., & Le Couteur, A. (1994). Autism Diagnostic Interview-Revised: A revised version of a diagnostic interview for caregivers of individuals with possible pervasive developmental disorders. *Journal of Autism and Developmental Disorders*. <https://doi.org/10.1007/BF02172145>
- Loth, E., & Evans, D. W. (2019). Converting tests of fundamental social, cognitive, and affective processes into clinically useful bio-behavioral markers for neurodevelopmental conditions. In *Wiley Interdisciplinary Reviews: Cognitive Science*. <https://doi.org/10.1002/wcs.1499>
- Lubar, J. F. (1991). Discourse on the development of EEG diagnostics and biofeedback for attention-deficit/hyperactivity disorders. *Biofeedback and Self-Regulation*. <https://doi.org/10.1007/BF01000016>
- Luck, S. J., Stewart, A. X., Simmons, A. M., & Rhemtulla, M. (2021). Standardized measurement error: A universal metric of data quality for averaged event-related potentials. *Psychophysiology*. <https://doi.org/10.1111/psyp.13793>
- Ludlow, A. K., Giannadou, A., Franklin, A., Allen, P. M., Simmons, D. R., & Wilkins, A. J. (2020). The possible use of precision tinted lenses to improve social cognition in children with autism spectrum disorders. *Vision Research*. <https://doi.org/10.1016/j.visres.2020.03.007>

- Ludlow, A. K., & Wilkins, A. J. (2016). Atypical Sensory behaviours in children with Tourette's Syndrome and in children with Autism Spectrum Disorders. *Research in Developmental Disabilities*. <https://doi.org/10.1016/j.ridd.2016.05.019>
- Ludlow, A. K., Wilkins, A. J., & Heaton, P. (2006). The effect of coloured overlays on reading ability in children with autism. *Journal of Autism and Developmental Disorders*. <https://doi.org/10.1007/s10803-006-0090-5>
- Lukmanji, S., Manji, S. A., Kadhim, S., Sauro, K. M., Wirrell, E. C., Kwon, C. S., & Jetté, N. (2019). The co-occurrence of epilepsy and autism: A systematic review. In *Epilepsy and Behavior*. <https://doi.org/10.1016/j.yebeh.2019.07.037>
- Machado, C., Estévez, M., Leisman, G., Melillo, R., Rodríguez, R., DeFina, P., Hernández, A., Pérez-Nellar, J., Naranjo, R., Chinchilla, M., Garófalo, N., Vargas, J., & Beltrán, C. (2015). QEEG Spectral and Coherence Assessment of Autistic Children in Three Different Experimental Conditions. *Journal of Autism and Developmental Disorders*. <https://doi.org/10.1007/s10803-013-1909-5>
- Makeig, S., Westerfield, M., Jung, T. P., Enghoff, S., Townsend, J., Courchesne, E., & Sejnowski, T. J. (2002). Dynamic brain sources of visual evoked responses. *Science*. <https://doi.org/10.1126/science.1066168>
- Makeig, S., Bell, A. J., Jung, T., & Sejnowski, T. J. (1996). Independent Component Analysis of Electroencephalographic Data. In *Advances in Neural Information Processing Systems* 8.
- Mallat, S. G., & Zhang, Z. (1993). Matching Pursuits With Time-Frequency Dictionaries. *IEEE Transactions on Signal Processing*. <https://doi.org/10.1109/78.258082>
- Mandy, W., & Lai, M. C. (2016). Annual Research Review: The role of the environment in the developmental psychopathology of autism spectrum condition. In *Journal of Child Psychology and Psychiatry and Allied Disciplines*. <https://doi.org/10.1111/jcpp.12501>
- Mandy, W., Murin, M., & Skuse, D. (2015). The cognitive profile in autism spectrum disorders. *Key Issues in Mental Health*. <https://doi.org/10.1159/000363565>

- Marek, S., Tervo-Clemmens, B., Klein, N., Foran, W., Ghuman, A. S., & Luna, B. (2018). Adolescent development of cortical oscillations: Power, phase, and support of cognitive maturation. *PLoS biology*, 16(11). <https://doi.org/10.1371/journal.pbio.2004188>
- Marini, F., Lee, C., Wagner, J., Makeig, S., & Gola, M. (2019). A comparative evaluation of signal quality between a research-grade and a wireless dry-electrode mobile EEG system. *Journal of Neural Engineering*. <https://doi.org/10.1088/1741-2552/ab21f2>
- Marković, D., & Gros, C. (2014). Power laws and self-organized criticality in theory and nature. In *Physics Reports*. <https://doi.org/10.1016/j.physrep.2013.11.002>
- Markovska-Simoska, S., & Pop-Jordanova, N. (2017). Quantitative EEG in Children and Adults with Attention Deficit Hyperactivity Disorder: Comparison of Absolute and Relative Power Spectra and Theta/Beta Ratio. *Clinical EEG and Neuroscience*.
- Masi, A., DeMayo, M. M., Glozier, N., & Guastella, A. J. (2017). An Overview of Autism Spectrum Disorder, Heterogeneity and Treatment Options. In *Neuroscience Bulletin*. <https://doi.org/10.1007/s12264-017-0100-y>
- Masquelier, T. (2013). Neural variability, or lack thereof. *Frontiers in Computational Neuroscience*. <https://doi.org/10.3389/fncom.2013.00007>
- Mathewson, K. E., Harrison, T. J. L., & Kizuk, S. A. D. (2017). High and dry? Comparing active dry EEG electrodes to active and passive wet electrodes. *Psychophysiology*. <https://doi.org/10.1111/psyp.12536>
- Mazaheri, A., Coffey-Corina, S., Mangun, G. R., Bekker, E. M., Berry, A. S., & Corbett, B. A. (2010). Functional disconnection of frontal cortex and visual cortex in attention-deficit/hyperactivity disorder. *Biological psychiatry*, 67(7), 617-623. <https://doi.org/10.1016/j.biopsych.2009.11.022>
- Mazaheri, A., Fassbender, C., Coffey-Corina, S., Hartanto, T. A., Schweitzer, J. B., & Mangun, G. R. (2014). Differential oscillatory electroencephalogram between attention-deficit/hyperactivity disorder subtypes and typically developing adolescents. *Biological Psychiatry*. <https://doi.org/10.1016/j.biopsych.2013.08.023>

- Mazefsky, C. A., Kao, J., & Oswald, D. P. (2011). Preliminary evidence suggesting caution in the use of psychiatric self-report measures with adolescents with high-functioning autism spectrum disorders. *Research in Autism Spectrum Disorders*. <https://doi.org/10.1016/j.rasd.2010.03.006>
- McCarthy, S. E., Gillis, J., Kramer, M., Lihm, J., Yoon, S., Berstein, Y., Mistry, M., Pavlidis, P., Solomon, R., Ghiban, E., Antoniou, E., Kelleher, E., O'Brien, C., Donohoe, G., Gill, M., Morris, D. W., McCombie, W. R., & Corvin, A. (2014). De novo mutations in schizophrenia implicate chromatin remodeling and support a genetic overlap with autism and intellectual disability. *Molecular Psychiatry*. <https://doi.org/10.1038/mp.2014.29>
- McDonnell, M. D., & Abbott, D. (2009). What is stochastic resonance? Definitions, misconceptions, debates, and its relevance to biology. In *PLoS Computational Biology*. <https://doi.org/10.1371/journal.pcbi.1000348>
- McKinnon, C. J., Eggebrecht, A. T., Todorov, A., Wolff, J. J., Elison, J. T., Adams, C. M., Snyder, A. Z., Estes, A. M., Zwaigenbaum, L., Botteron, K. N., McKinstry, R. C., Marrus, N., Evans, A., Hazlett, H. C., Dager, S. R., Paterson, S. J., Pandey, J., Schultz, R. T., Styner, M. A., ... Pruett, J. R. (2019). Restricted and Repetitive Behavior and Brain Functional Connectivity in Infants at Risk for Developing Autism Spectrum Disorder. *Biological Psychiatry: Cognitive Neuroscience and Neuroimaging*. <https://doi.org/10.1016/j.bpsc.2018.09.008>
- McLoughlin, G., Albrecht, B., Banaschewski, T., Rothenberger, A., Brandeis, D., Asherson, P., & Kuntsi, J. (2009). Performance monitoring is altered in adult ADHD: A familial event-related potential investigation. *Neuropsychologia*. <https://doi.org/10.1016/j.neuropsychologia.2009.07.013>
- McLoughlin, G., Makeig, S., & Tsuang, M. T. (2014). In search of biomarkers in psychiatry: EEG-based measures of brain function. *American Journal of Medical Genetics, Part B: Neuropsychiatric Genetics*. <https://doi.org/10.1002/ajmg.b.32208>
- McLoughlin, G., Gyurkovics, M., Palmer, J., & Makeig, S. (2021). Midfrontal Theta Activity in Psychiatric Illness: An Index of Cognitive Vulnerabilities Across Disorders. *Biological psychiatry*, 91(2), 173-182. <https://doi.org/10.1016/j.biopsych.2021.08.020>

- McMahon, C. M., & Henderson, H. A. (2015). Error-monitoring in response to social stimuli in individuals with higher-functioning Autism Spectrum Disorder. *Developmental Science*. <https://doi.org/10.1111/desc.12220>
- Meisel, C., Storch, A., Hallmeyer-Elgner, S., Bullmore, E., & Gross, T. (2012). Failure of adaptive self-organized criticality during epileptic seizure attacks. *PLoS Computational Biology*. <https://doi.org/10.1371/journal.pcbi.1002312>
- Meldrum, B. S., & Wilkins, A. J. (1984). Photosensitive epilepsy: integration of pharmacological and psychophysical evidence. In *Electrophysiology and Epilepsy* (pp. 51–77). Academic Press.
- Metting van Rijn, A. C., Peper, A., & Grimbergen, C. A. (1990). High-quality recording of bioelectric events. *Medical & Biological Engineering & Computing*. <https://doi.org/10.1007/bf02441961>
- Meyer, L., & Schaadt, G. (2020). Aberrant Prestimulus Oscillations in Developmental Dyslexia Support an Underlying Attention Shifting Deficit. *Cerebral Cortex Communications*. <https://doi.org/10.1093/texcom/tgaa006>
- Meziane, N., Webster, J. G., Attari, M., & Nimunkar, A. J. (2013). Dry electrodes for electrocardiography. *Physiological Measurement*. <https://doi.org/10.1088/0967-3334/34/9/R47>
- Miller, K. J., Sorensen, L. B., Ojemann, J. G., & Den Nijs, M. (2009). Power-law scaling in the brain surface electric potential. *PLoS Computational Biology*. <https://doi.org/10.1371/journal.pcbi.1000609>
- Millichap, J. G. (2005). Pattern-Sensitive Epilepsy. *Pediatric Neurology Briefs*. <https://doi.org/10.15844/pedneurbriefs-19-2-1>
- Milne, E. (2011). Increased intra-participant variability in children with autistic spectrum disorders: Evidence from single-trial analysis of evoked EEG. *Frontiers in Psychology*. <https://doi.org/10.3389/fpsyg.2011.00051>

- Milne, E., Dickinson, A., & Smith, R. (2017). Adults with autism spectrum conditions experience increased levels of anomalous perception. *PLoS ONE*. <https://doi.org/10.1371/journal.pone.0177804>
- Milne, E., Gomez, R., Giannadou, A., & Jones, M. (2019). Atypical EEG in autism spectrum disorder: Comparing a dimensional and a categorical approach. *Journal of Abnormal Psychology*. <https://doi.org/10.1037/abn0000436>
- Milne, E., Scope, A., Pascalis, O., Buckley, D., & Makeig, S. (2009). Independent Component Analysis Reveals Atypical Electroencephalographic Activity During Visual Perception in Individuals with Autism. *Biological Psychiatry*. <https://doi.org/10.1016/j.biopsych.2008.07.017>
- Monastra, V. J., Lubar, J. F., Linden, M., VanDeusen, P., Green, G., Wing, W., Phillips, A., & Fenger, N. T. (1999). Assessing attention deficit hyperactivity disorder via quantitative electroencephalography: An initial validation study. *Neuropsychology*. <https://doi.org/10.1037/0894-4105.13.3.424>
- Monk, C. S., Peltier, S. J., Wiggins, J. L., Weng, S. J., Carrasco, M., Risi, S., & Lord, C. (2009). Abnormalities of intrinsic functional connectivity in autism spectrum disorders. *NeuroImage*. <https://doi.org/10.1016/j.neuroimage.2009.04.069>
- Montemurro, M. A., Rasch, M. J., Murayama, Y., Logothetis, N. K., & Panzeri, S. (2008). Phase-of-firing coding of natural visual stimuli in primary visual cortex. *Current biology*, 18(5), 375-380. <https://doi.org/10.1016/j.cub.2008.02.023>
- Morton, J. (2008). Understanding Developmental Disorders: A Causal Modelling Approach. In *Understanding Developmental Disorders: A Causal Modelling Approach*. <https://doi.org/10.1002/9780470773307>
- Müller, R. A., Shih, P., Keehn, B., Deyoe, J. R., Leyden, K. M., & Shukla, D. K. (2011). Underconnected, but how? A survey of functional connectivity MRI studies in autism spectrum disorders. In *Cerebral Cortex*. <https://doi.org/10.1093/cercor/bhq296>

- Murias, M., Webb, S. J., Greenson, J., & Dawson, G. (2007). Resting State Cortical Connectivity Reflected in EEG Coherence in Individuals With Autism. *Biological Psychiatry*. <https://doi.org/10.1016/j.biopsych.2006.11.012>
- Murphy, C. M., Christakou, A., Daly, E. M., Ecker, C., Giampietro, V., Brammer, M., Smith, A. B., Johnston, P., Robertson, D. M., Murphy, D. G., Rubia, K., Bailey, A. J., Baron-Cohen, S., Bolton, P. F., Bullmore, E. T., Carrington, S., Chakrabarti, B., Deoni, S. C., Happe, F., ... Williams, S. C. (2014). Abnormal functional activation and maturation of fronto-striato-temporal and cerebellar regions during sustained attention in autism spectrum disorder. *American Journal of Psychiatry*, *171*(10), 1107–1116. <https://doi.org/10.1176/appi.ajp.2014.12030352>
- Murphy, M., Stickgold, R., & Öngür, D. (2020). Electroencephalogram Microstate Abnormalities in Early-Course Psychosis. *Biological Psychiatry: Cognitive Neuroscience and Neuroimaging*. <https://doi.org/10.1016/j.bpsc.2019.07.006>
- Murray, M. M., & Wallace, M. T. (Eds.). (2011). *The neural bases of multisensory processes*. CRC Press.
- Musser, E. D., Hawkey, E., Kachan-Liu, S. S., Lees, P., Rouillet, J. B., Goddard, K., Steiner, R. D., & Nigg, J. T. (2014). Shared familial transmission of autism spectrum and attention-deficit/ hyperactivity disorders. *Journal of Child Psychology and Psychiatry and Allied Disciplines*, *55*(7), 819–827. <https://doi.org/10.1111/jcpp.12201>
- Nazhvani, A. D., Boostani, R., Afrasiabi, S., & Sadatnezhad, K. (2013). Classification of ADHD and BMD patients using visual evoked potential. *Clinical Neurology and Neurosurgery*. <https://doi.org/10.1016/j.clineuro.2013.08.009>
- Neil, L., Green, D., & Pellicano, E. (2017). The Psychometric Properties of a New Measure of Sensory Behaviors in Autistic Children. *Journal of Autism and Developmental Disorders*. <https://doi.org/10.1007/s10803-016-3018-8>
- Nigbur, R., Cohen, M. X., Ridderinkhof, K. R., & Stürmer, B. (2012). Theta dynamics reveal domain-specific control over stimulus and response conflict. *Journal of Cognitive Neuroscience*, *24*(5), 1264–1274. https://doi.org/10.1162/jocn_a_00128

- Nunez, P. L., Silberstein, R. B., Cadusch, P. J., Wijesinghe, R. S., Westdorp, A. F., & Srinivasan, R. (1994). A theoretical and experimental study of high resolution EEG based on surface Laplacians and cortical imaging. *Electroencephalography and Clinical Neurophysiology*. [https://doi.org/10.1016/0013-4694\(94\)90112-0](https://doi.org/10.1016/0013-4694(94)90112-0)
- O'Hare, L., & Hibbard, P. B. (2016). Visual processing in migraine. In *Cephalalgia*. <https://doi.org/10.1177/0333102415618952>
- O'Hare, L., & Hibbard, P. B. (2011). Spatial frequency and visual discomfort. *Vision Research*, 51(15), 1767–1777. <https://doi.org/10.1016/j.visres.2011.06.002>
- O'Reilly, C., Lewis, J. D., & Elsabbagh, M. (2017). Is functional brain connectivity atypical in autism? A systematic review of EEG and MEG studies. *PLoS ONE*. <https://doi.org/10.1371/journal.pone.0175870>
- Onton, J., & Makeig, S. (2009). High-frequency broadband modulations of electroencephalographic spectra. *Frontiers in Human Neuroscience*. <https://doi.org/10.3389/neuro.09.061.2009>
- Oostenveld, R., & Oostendorp, T. F. (2002). Validating the boundary element method for forward and inverse EEG computations in the presence of a hole in the skull. *Human Brain Mapping*. <https://doi.org/10.1002/hbm.10061>
- Orchard, E., & van Boxtel, J. J. A. (2019). Divergent correlations between autism traits and multiplicative noise in fine and coarse motion discrimination tasks. In *bioRxiv*. <https://doi.org/10.1101/561548>
- Ostlund, B. D., Alperin, B. R., Drew, T., & Karalunas, S. L. (2021). Behavioral and cognitive correlates of the aperiodic (1/f-like) exponent of the EEG power spectrum in adolescents with and without ADHD. *Developmental Cognitive Neuroscience*. <https://doi.org/10.1016/j.dcn.2021.100931>
- Ousley, O., & Cermak, T. (2014). Autism Spectrum Disorder: Defining Dimensions and Subgroups. *Current Developmental Disorders Reports*. <https://doi.org/10.1007/s40474-013-0003-1>

- Ouyang, G., Hildebrandt, A., Schmitz, F., & Herrmann, C. S. (2020). Decomposing alpha and 1/f brain activities reveals their differential associations with cognitive processing speed. *NeuroImage*. <https://doi.org/10.1016/j.neuroimage.2019.116304>
- Palmer, J. E., Chronicle, E. P., Rolan, P., & Mulleners, W. M. (2000). Cortical hyperexcitability is cortical under-inhibition: Evidence from a novel functional test of migraine patients. *Cephalalgia*. <https://doi.org/10.1046/j.1468-2982.2000.00075.x>
- Palva, S., & Palva, J. M. (2011). Functional roles of alpha-band phase synchronization in local and large-scale cortical networks. *Frontiers in psychology*, 2, 204. <https://doi.org/10.3389/fpsyg.2011.00204>
- Palva, J. M., Palva, S., & Kaila, K. (2005). Phase synchrony among neuronal oscillations in the human cortex. *Journal of Neuroscience*, 25(15), 3962-3972. <https://doi.org/10.1523/JNEUROSCI.4250-04.2005>
- Palva, J. M., Wang, S. H., Palva, S., Zhigalov, A., Monto, S., Brookes, M. J., Schoffelen, J. M., & Jerbi, K. (2018). Ghost interactions in MEG/EEG source space: A note of caution on inter-areal coupling measures. *NeuroImage*. <https://doi.org/10.1016/j.neuroimage.2018.02.032>
- Papenberg, G., Hämmerer, D., Müller, V., Lindenberger, U., & Li, S. C. (2013). Lower theta inter-trial phase coherence during performance monitoring is related to higher reaction time variability: a lifespan study. *NeuroImage*, 83, 912-920. <https://doi.org/10.1016/j.neuroimage.2013.07.032>
- Parish-Morris, J., Liberman, M. Y., Cieri, C., Herrington, J. D., Yerys, B. E., Bateman, L., Donaher, J., Ferguson, E., Pandey, J., & Schultz, R. T. (2017). Linguistic camouflage in girls with autism spectrum disorder. *Molecular Autism*. <https://doi.org/10.1186/s13229-017-0164-6>
- Park, W. J., Schauder, K. B., Zhang, R., Bennetto, L., & Tadin, D. (2017). High internal noise and poor external noise filtering characterize perception in autism spectrum disorder. *Scientific Reports*. <https://doi.org/10.1038/s41598-017-17676-5>

- Pearl, A. M., & Mayes, S. D. (2015). Methods and procedures for measuring comorbid disorders: Psychological. In *Comorbid Conditions Among Children with Autism Spectrum Disorders*. https://doi.org/10.1007/978-3-319-19183-6_3
- Pellicano, E., & Burr, D. (2012). When the world becomes “too real”: A Bayesian explanation of autistic perception. In *Trends in Cognitive Sciences*. <https://doi.org/10.1016/j.tics.2012.08.009>
- Penacchio, O., & Wilkins, A. J. (2015). Visual discomfort and the spatial distribution of Fourier energy. *Vision Research*. <https://doi.org/10.1016/j.visres.2014.12.013>
- Pennington, B. F., & Ozonoff, S. (1996). Executive functions and developmental psychopathology. In *Journal of Child Psychology and Psychiatry and Allied Disciplines*. <https://doi.org/10.1111/j.1469-7610.1996.tb01380.x>
- Perez Velazquez, J. L., Barcelo, F., Hung, Y., Leshchenko, Y., Nenadovic, V., Belkas, J., Raghavan, V., Brian, J., & Garcia Dominguez, L. (2009). Decreased brain coordinated activity in autism spectrum disorders during executive tasks: Reduced long-range synchronization in the fronto-parietal networks. *International Journal of Psychophysiology*. <https://doi.org/10.1016/j.ijpsycho.2009.05.009>
- Pérez-Cervera, A., Seara, T. M., & Huguet, G. (2020). Phase-locked states in oscillating neural networks and their role in neural communication. *Communications in Nonlinear Science and Numerical Simulation*. <https://doi.org/10.1016/j.cnsns.2019.104992>
- Pernet, C. R., Chauveau, N., Gaspar, C., & Rousselet, G. A. (2011). LIMO EEG: A toolbox for hierarchical linear modeling of electroencephalographic data. *Computational Intelligence and Neuroscience*. <https://doi.org/10.1155/2011/831409>
- Pertermann, M., Bluschke, A., Roessner, V., & Beste, C. (2019). The Modulation of Neural Noise Underlies the Effectiveness of Methylphenidate Treatment in Attention-Deficit/Hyperactivity Disorder. *Biological Psychiatry: Cognitive Neuroscience and Neuroimaging*. <https://doi.org/10.1016/j.bpsc.2019.03.011>
- Peters, J. M., Taquet, M., Vega, C., Jeste, S. S., Fernández, I. S., Tan, J., Nelson, C. A., Sahin, M., & Warfield, S. K. (2013). Brain functional networks in syndromic and non-syndromic

- autism: A graph theoretical study of EEG connectivity. *BMC Medicine*.
<https://doi.org/10.1186/1741-7015-11-54>
- Peterson, E. J., Rosen, B. Q., Campbell, A. M., Belger, A., & Voytek, B. (2017). 1/F Neural Noise Is a Better Predictor of Schizophrenia Than Neural Oscillations. *Doi.Org*, 113449.
<https://doi.org/10.1101/113449>
- Pfurtscheller, G., Stancak, A. Jr., and Neuper, C. (1996). Event-related synchronization (ERS) in the alpha band—an electrophysiological correlate of cortical idling: a review. *Int. J. Psychophysiol.* 24, 39–46. [https://doi.org/10.1016/S0167-8760\(96\)00066-9](https://doi.org/10.1016/S0167-8760(96)00066-9)
- Picci, G., Gotts, S. J., & Scherf, K. S. (2016). A theoretical rut: revisiting and critically evaluating the generalized under/over-connectivity hypothesis of autism. *Developmental Science*. <https://doi.org/10.1111/desc.12467>
- Piven, J., Bailey, J., Ranson, B. J., & Arndt, S. (1997). An MRI study of the corpus callosum in autism. *American Journal of Psychiatry*. <https://doi.org/10.1176/ajp.154.8.1051>
- Poil, S. S., Hardstone, R., Mansvelder, H. D., & Linkenkaer-Hansen, K. (2012). Critical-state dynamics of avalanches and oscillations jointly emerge from balanced excitation/inhibition in neuronal networks. *Journal of Neuroscience*. <https://doi.org/10.1523/JNEUROSCI.5990-11.2012>
- Ponjavic-Conte, K. D., Hambrook, D. A., Pavlovic, S., & Tata, M. S. (2013). Dynamics of distraction: competition among auditory streams modulates gain and disrupts inter-trial phase coherence in the human electroencephalogram. *PloS one*, 8(1). <https://doi.org/10.1371/annotation/631b811c-5665-4b9d-9b3a-d5e41284f2b2>
- Port, R. G., Dipiero, M. A., Ku, M., Liu, S., Blaskey, L., Kuschner, E. S., Edgar, J. C., Roberts, T. P. L., & Berman, J. I. (2019). Children with Autism Spectrum Disorder Demonstrate Regionally Specific Altered Resting-State Phase-Amplitude Coupling. *Brain Connectivity*. <https://doi.org/10.1089/brain.2018.0653>
- Pritchard, W. S. (1996). The EEG data indicate stochastic nonlinearity . *Behavioral and Brain Sciences*. <https://doi.org/10.1017/s0140525x00042837>

- Quirk, C. R., Zutshi, I., Srikanth, S., Fu, M. L., Devico Marciano, N., Wright, M. K., ... & Leutgeb, S. (2021). Precisely timed theta oscillations are selectively required during the encoding phase of memory. *Nature Neuroscience*, 24(11), 1614-1627. <https://doi.org/10.1038/s41593-021-00919-0>
- Radhakrishnan, K., St. Louis, E. K., Johnson, J. A., McClelland, R. L., Westmoreland, B. F., & Klass, D. W. (2005). Pattern-sensitive epilepsy: Electroclinical characteristics, natural history, and delineation of the epileptic syndrome. In *Epilepsia*. <https://doi.org/10.1111/j.0013-9580.2005.26604.x>
- Radüntz, T. (2018). Signal quality evaluation of emerging EEG devices. *Frontiers in Physiology*. <https://doi.org/10.3389/fphys.2018.00098>
- Rane, P., Cochran, D., Hodge, S. M., Haselgrove, C., Kennedy, D. N., & Frazier, J. A. (2015). Connectivity in Autism: A Review of MRI Connectivity Studies. In *Harvard Review of Psychiatry*. <https://doi.org/10.1097/HRP.0000000000000072>
- Ratti, E., Waninger, S., Berka, C., Ruffini, G., & Verma, A. (2017). Comparison of medical and consumer wireless EEG systems for use in clinical trials. *Frontiers in Human Neuroscience*. <https://doi.org/10.3389/fnhum.2017.00398>
- Ravassard, P., Kees, A., Willers, B., Ho, D., Aharoni, D., Cushman, J., ... & Mehta, M. R. (2013). Multisensory control of hippocampal spatiotemporal selectivity. *Science*, 340(6138), 1342-1346. <https://doi.org/10.1126/science.1232655>
- Reiersen, A. M., Constantino, J. N., Grimmer, M., Martin, N. G., & Todd, R. D. (2008). Evidence for shared genetic influences on self-reported ADHD and autistic symptoms in young adult Australian twins. *Twin Research and Human Genetics*. <https://doi.org/10.1375/twin.11.6.579>
- Renart, A., & Machens, C. K. (2014). Variability in neural activity and behavior. In *Current Opinion in Neurobiology*. <https://doi.org/10.1016/j.conb.2014.02.013>
- Richter, C. G., Coppola, R., & Bressler, S. L. (2018). Top-down beta oscillatory signaling conveys behavioral context in early visual cortex. *Scientific reports*, 8(1), 1-12. <https://doi.org/10.1038/s41598-018-25267-1>

- Rippon, G., Brock, J., Brown, C., & Boucher, J. (2007). Disordered connectivity in the autistic brain: Challenges for the “new psychophysiology.” *International Journal of Psychophysiology*. <https://doi.org/10.1016/j.ijpsycho.2006.03.012>
- Robbie, J. C., Clarke, A. R., Barry, R. J., Dupuy, F. E., McCarthy, R., & Selikowitz, M. (2016). Coherence in children with AD/HD and excess alpha power in their EEG. *Clinical Neurophysiology*. <https://doi.org/10.1016/j.clinph.2016.02.008>
- Roberts, K., Dowell, A., & Nie, J. B. (2019). Attempting rigour and replicability in thematic analysis of qualitative research data; A case study of codebook development. *BMC Medical Research Methodology*. <https://doi.org/10.1186/s12874-019-0707-y>
- Rohrer-Baumgartner, N., Zeiner, P., Eadie, P., Egeland, J., Gustavson, K., Reichborn-Kjennerud, T., & Aase, H. (2016). Language Delay in 3-Year-Old Children With ADHD Symptoms. *Journal of Attention Disorders*. <https://doi.org/10.1177/1087054713497253>
- Rojas, D. C., Maharajh, K., Teale, P., & Rogers, S. J. (2008). Reduced neural synchronization of gamma-band MEG oscillations in first-degree relatives of children with autism. *BMC Psychiatry*. <https://doi.org/10.1186/1471-244X-8-66>
- Rommelse, N. N. J., Franke, B., Geurts, H. M., Hartman, C. A., & Buitelaar, J. K. (2010). Shared heritability of attention-deficit/hyperactivity disorder and autism spectrum disorder. In *European Child and Adolescent Psychiatry*. <https://doi.org/10.1007/s00787-010-0092-x>
- Ronald, A., Happé, F., Bolton, P., Butcher, L. M., Price, T. S., Wheelwright, S., Baron-Cohen, S., & Plomin, R. (2006). Genetic heterogeneity between the three components of the autism spectrum: A twin study. *Journal of the American Academy of Child and Adolescent Psychiatry*. <https://doi.org/10.1097/01.chi.0000215325.13058.9d>
- Ronald, A., Larsson, H., Anckarsäter, H., & Lichtenstein, P. (2014). Symptoms of autism and ADHD: A Swedish twin study examining their overlap. *Journal of Abnormal Psychology*. <https://doi.org/10.1037/a0036088>
- Ronald, A., Sieradzka, D., Cardno, A. G., Haworth, C. M. A., McGuire, P., & Freeman, D. (2014). Characterization of psychotic experiences in adolescence using the specific

psychotic experiences questionnaire: Findings from a study of 5000 16-Year-Old Twins. *Schizophrenia Bulletin*. <https://doi.org/10.1093/schbul/sbt106>

Ronald, A., Simonoff, E., Kuntsi, J., Asherson, P., & Plomin, R. (2008). Evidence for overlapping genetic influences on autistic and ADHD behaviours in a community twin sample. *Journal of Child Psychology and Psychiatry and Allied Disciplines*. <https://doi.org/10.1111/j.1469-7610.2007.01857.x>

Ronconi, L., Vitale, A., Federici, A., Pini, E., Molteni, M., & Casartelli, L. (2020). Altered neural oscillations and connectivity in the beta band underlie detail-oriented visual processing in autism. *NeuroImage Clin*, 28. <https://doi.org/10.1016/j.nicl.2020.102484>

Rosen, T. E., Mazefsky, C. A., Vasa, R. A., & Lerner, M. D. (2018). Co-occurring psychiatric conditions in autism spectrum disorder. In *International Review of Psychiatry*. <https://doi.org/10.1080/09540261.2018.1450229>

Rosenberg, R. E., Law, J. K., Yenokyan, G., McGready, J., Kaufmann, W. E., & Law, P. A. (2009). Characteristics and concordance of autism spectrum disorders among 277 twin pairs. *Archives of Pediatrics and Adolescent Medicine*. <https://doi.org/10.1001/archpediatrics.2009.98>

Rubenstein, J. L. R., & Merzenich, M. M. (2003). Model of autism: Increased ratio of excitation/inhibition in key neural systems. In *Genes, Brain and Behavior*. <https://doi.org/10.1034/j.1601-183X.2003.00037.x>

Russell, G., Mandy, W., Elliott, D., White, R., Pittwood, T., & Ford, T. (2019). Selection bias on intellectual ability in autism research: A cross-sectional review and meta-analysis. In *Molecular Autism*. <https://doi.org/10.1186/s13229-019-0260-x>

Russo, F. B., Freitas, B. C., Pignatari, G. C., Fernandes, I. R., Sebat, J., Muotri, A. R., & Beltrão-Braga, P. C. B. (2018). Modeling the Interplay Between Neurons and Astrocytes in Autism Using Human Induced Pluripotent Stem Cells. *Biological Psychiatry*. <https://doi.org/10.1016/j.biopsych.2017.09.021>

Rutter, M. (2000). Genetic studies of autism: From the 1970s into the millennium. In *Journal of Abnormal Child Psychology*. <https://doi.org/10.1023/A:1005113900068>

- Rutter, M. L. (2011). Progress in understanding autism: 2007-2010. *Journal of Autism and Developmental Disorders*. <https://doi.org/10.1007/s10803-011-1184-2>
- Ruzich, E., Allison, C., Smith, P., Watson, P., Auyeung, B., Ring, H., & Baron-Cohen, S. (2015). Measuring autistic traits in the general population: A systematic review of the Autism-Spectrum Quotient (AQ) in a nonclinical population sample of 6,900 typical adult males and females. *Molecular Autism*. <https://doi.org/10.1186/2040-2392-6-2>
- S.-I. Amari, A. Cichocki, & Yang, H. H. (1996). A new learning algorithm for blind source separation. *In Advances in Neural Information Processing System*.
- Salajegheh, A., Link, A., Elster, C., Burghoff, M., Sander, T., Trahms, L., & Poeppel, D. (2004). Systematic latency variation of the auditory evoked M100: From average to single-trial data. *NeuroImage*. <https://doi.org/10.1016/j.neuroimage.2004.05.022>
- Samaha, J., Bauer, P., Cimaroli, S., & Postle, B. R. (2015). Top-down control of the phase of alpha-band oscillations as a mechanism for temporal prediction. *Proceedings of the National Academy of Sciences of the United States of America*. <https://doi.org/10.1073/pnas.1503686112>
- Sanders, S. J., Ercan-Sencicek, A. G., Hus, V., Luo, R., Murtha, M. T., Moreno-De-Luca, D., Chu, S. H., Moreau, M. P., Gupta, A. R., Thomson, S. A., Mason, C. E., Bilguvar, K., Celestino-Soper, P. B. S., Choi, M., Crawford, E. L., Davis, L., Davis Wright, N. R., Dhodapkar, R. M., DiCola, M., ... State, M. W. (2011). Multiple Recurrent De Novo CNVs, Including Duplications of the 7q11.23 Williams Syndrome Region, Are Strongly Associated with Autism. *Neuron*. <https://doi.org/10.1016/j.neuron.2011.05.002>
- Satterstrom, F. K., Walters, R. K., Singh, T., Wigdor, E. M., Lescai, F., Demontis, D., Kosmicki, J. A., Grove, J., Stevens, C., Bybjerg-Grauholm, J., Bækvad-Hansen, M., Palmer, D. S., Maller, J. B., Nordentoft, M., Mors, O., Robinson, E. B., Hougaard, D. M., Werge, T. M., Bo Mortensen, P., ... Daly, M. J. (2019). Autism spectrum disorder and attention deficit hyperactivity disorder have a similar burden of rare protein-truncating variants. *Nature Neuroscience*. <https://doi.org/10.1038/s41593-019-0527-8>

- Saunders, A., Kirk, I. J., & Waldie, K. E. (2016). Hemispheric Coherence in ASD with and without Comorbid ADHD and Anxiety. *BioMed Research International*. <https://doi.org/10.1155/2016/4267842>
- Sauseng, P., & Klimesch, W. (2008). What does phase information of oscillatory brain activity tell us about cognitive processes? In *Neuroscience and Biobehavioral Reviews*. <https://doi.org/10.1016/j.neubiorev.2008.03.014>
- Saville, C. W. N., Feige, B., Kluckert, C., Bender, S., Biscaldi, M., Berger, A., Fleischhaker, C., Henighausen, K., & Klein, C. (2015). Increased reaction time variability in attention-deficit hyperactivity disorder as a response-related phenomenon: Evidence from single-trial event-related potentials. *Journal of Child Psychology and Psychiatry and Allied Disciplines*. <https://doi.org/10.1111/jcpp.12348>
- Scarr, E., Millan, M. J., Bahn, S., Bertolino, A., Turck, C. W., Kapur, S., Möller, H. J., & Dean, B. (2015). Biomarkers for psychiatry: The journey from fantasy to fact, a report of the 2013 CINP think tank. In *International Journal of Neuropsychopharmacology*. <https://doi.org/10.1093/ijnp/pyv042>
- Schaaf, C. P., Betancur, C., Yuen, R. K. C., Parr, J. R., Skuse, D. H., Gallagher, L., Bernier, R. A., Buchanan, J. A., Buxbaum, J. D., Chen, C. A., Dies, K. A., Elsabbagh, M., Firth, H. V., Frazier, T., Hoang, N., Howe, J., Marshall, C. R., Michaud, J. L., Rennie, O., ... Vorstman, J. A. S. (2020). A framework for an evidence-based gene list relevant to autism spectrum disorder. In *Nature Reviews Genetics*. <https://doi.org/10.1038/s41576-020-0231-2>
- Schwartz, S., Kessler, R., Gaughan, T., & Buckley, A. W. (2017). Electroencephalogram Coherence Patterns in Autism: An Updated Review. In *Pediatric Neurology*. <https://doi.org/10.1016/j.pediatrneurol.2016.10.018>
- Seymour, R. A., Rippon, G., Gooding-Williams, G., Schoffelen, J. M., & Kessler, K. (2019). Dysregulated oscillatory connectivity in the visual system in autism spectrum disorder. *Brain*. <https://doi.org/10.1093/brain/awz214>
- Shattuck, P. T., Seltzer, M. M., Greenberg, J. S., Orsmond, G. I., Bolt, D., Kring, S., Lounds, J., & Lord, C. (2007). Change in autism symptoms and maladaptive behaviors in

- adolescents and adults with an autism spectrum disorder. *Journal of Autism and Developmental Disorders*. <https://doi.org/10.1007/s10803-006-0307-7>
- Shephard, E., Tye, C., Ashwood, K. L., Azadi, B., Asherson, P., Bolton, P. F., & McLoughlin, G. (2018). Resting-State Neurophysiological Activity Patterns in Young People with ASD, ADHD, and ASD + ADHD. *Journal of Autism and Developmental Disorders*. <https://doi.org/10.1007/s10803-017-3300-4>
- Shephard, E., Tye, C., Ashwood, K. L., Azadi, B., Johnson, M. H., Charman, T., Asherson, P., McLoughlin, G., & Bolton, P. F. (2019). Oscillatory neural networks underlying resting-state, attentional control and social cognition task conditions in children with ASD, ADHD and ASD+ADHD. *Cortex*. <https://doi.org/10.1016/j.cortex.2019.03.005>
- Shepherd, A. J., Hine, T. J., & Beaumont, H. M. (2013). Color and spatial frequency are related to visual pattern sensitivity in migraine. *Headache*. <https://doi.org/10.1111/head.12062>
- Shin, K. S., Kim, J. S., Kim, S. N., Hong, K. S., O'Donnell, B. F., Chung, C. K., & Kwon, J. S. (2015). Intraindividual neurophysiological variability in ultra-highrisk for psychosis and schizophrenia patients: Single-trial analysis. *Npj Schizophrenia*. <https://doi.org/10.1038/npjrschz.2015.31>
- Shu, Y., Hasenstaub, A., Badoual, M., Bal, T., & McCormick, D. A. (2003). Barrages of Synaptic Activity Control the Gain and Sensitivity of Cortical Neurons. *Journal of Neuroscience*. <https://doi.org/10.1523/jneurosci.23-32-10388.2003>
- Siapas, A. G., Lubenov, E. V., & Wilson, M. A. (2005). Prefrontal phase locking to hippocampal theta oscillations. *Neuron*, 46(1), 141-151. <https://doi.org/10.1016/j.neuron.2005.02.028>
- Siegel, M., Warden, M. R., & Miller, E. K. (2009). Phase-dependent neuronal coding of objects in short-term memory. *Proceedings of the National Academy of Sciences*, 106(50), 21341-21346. <https://doi.org/10.1073/pnas.0908193106>
- Sieluzycski, C., König, R., Matysiak, A., Kuś, R., Ircha, D., & Durka, P. J. (2009). Single-trial evoked brain responses modeled by multivariate matching pursuit. *IEEE Transactions on Biomedical Engineering*. <https://doi.org/10.1109/TBME.2008.2002151>

- Simmons, D. R., McKay, L., McAleer, P., Toal, E., Robertson, A., & Pollick, F. E. (2007). Neural noise and autism spectrum disorders. *Perception*.
- Simmons, D. R., Robertson, A. E., McKay, L. S., Toal, E., McAleer, P., & Pollick, F. E. (2009). Vision in autism spectrum disorders. In *Vision Research*.
<https://doi.org/10.1016/j.visres.2009.08.005>
- Simmons, D. R., Toal, E., McKay, L. S., Robertson, A. E., McAleer, P., & Pollick, F. E. (2008). The Role of Chronic Neural Noise in Autism Spectrum Disorders. *International Meeting for Autism Research*.
- Simmons, D., & Milne, E. (2015). Response to Davis and Plaisted-Grant: Low or high endogenous neural noise in autism spectrum disorder? In *Autism*.
<https://doi.org/10.1177/1362361314557683>
- Simonoff, E., Pickles, A., Charman, T., Chandler, S., Loucas, T., & Baird, G. (2008). Psychiatric disorders in children with autism spectrum disorders: Prevalence, comorbidity, and associated factors in a population-derived sample. *Journal of the American Academy of Child and Adolescent Psychiatry*, 47(8), 921–929.
<https://doi.org/10.1097/CHI.0b013e318179964f>
- Singer, W., & Gray, C. M. (1995). Visual feature integration and the temporal correlation hypothesis. In *Annual Review of Neuroscience*.
<https://doi.org/10.1146/annurev.ne.18.030195.003011>
- Sohal, V. S., & Rubenstein, J. L. R. (2019). Excitation-inhibition balance as a framework for investigating mechanisms in neuropsychiatric disorders. *Molecular Psychiatry*.
<https://doi.org/10.1038/s41380-019-0426-0>
- Sokhadze, E. M., Baruth, J. M., Sears, L., Sokhadze, G. E., El-Baz, A. S., Williams, E. L., Klapheke, R., & Casanova, M. F. (2012). Event-Related Potential Study of Attention Regulation During Illusory Figure Categorization Task in ADHD, Autism Spectrum Disorder, and Typical Children. *Journal of Neurotherapy*.
<https://doi.org/10.1080/10874208.2012.650119>

- Soltész, F., Szucs, D., Leong, V., White, S., & Goswami, U. (2013). Differential Entrainment of Neuroelectric Delta Oscillations in Developmental Dyslexia. *PLoS ONE*. <https://doi.org/10.1371/journal.pone.0076608>
- Somerville, L. H. (2016). Searching for Signatures of Brain Maturity: What Are We Searching For? In *Neuron*. <https://doi.org/10.1016/j.neuron.2016.10.059>
- Sorati, M., & Behne, D. M. (2019). Musical expertise affects audiovisual speech perception: Findings from event-related potentials and inter-trial phase coherence. *Frontiers in psychology*, 10, 2562. <https://doi.org/10.3389/fpsyg.2019.02562>
- Soso, M. J., Lettich, E., & Belug, J. H. (1980). Pattern-Sensitive Epilepsy. I: A Demonstration of a Spatial Frequency Selective Epileptic Response to Gratings. *Epilepsia*. <https://doi.org/10.1111/j.1528-1157.1980.tb04075.x>
- Spitzer, B., & Haegens, S. (2017). Beyond the status quo: a role for beta oscillations in endogenous content (re) activation. *Eneuro*, 4(4). <https://doi.org/10.1523/ENEURO.0170-17.2017>
- Spyropoulos, G., Bosman, C. A., & Fries, P. (2018). A theta rhythm in macaque visual cortex and its attentional modulation. *Proceedings of the National Academy of Sciences*, 115(24). <https://doi.org/10.1073/pnas.1719433115>
- Stedman, A., Taylor, B., Erard, M., Peura, C., & Siegel, M. (2019). Are Children Severely Affected by Autism Spectrum Disorder Underrepresented in Treatment Studies? An Analysis of the Literature. *Journal of Autism and Developmental Disorders*, 49(4), 1378–1390. <https://doi.org/10.1007/s10803-018-3844-y>
- Stone, J. V. (2002). Independent component analysis: An introduction. In *Trends in Cognitive Sciences*. [https://doi.org/10.1016/S1364-6613\(00\)01813-1](https://doi.org/10.1016/S1364-6613(00)01813-1)
- Stoodley, C. J. (2014). Distinct regions of the cerebellum show gray matter decreases in autism, ADHD, and developmental dyslexia. *Frontiers in Systems Neuroscience*, 8(MAY). <https://doi.org/10.3389/fnsys.2014.00092>

- Tada, M., Nagai, T., Kirihara, K., Koike, S., Suga, M., Araki, T., Kobayashi, T., & Kasai, K. (2016). Differential Alterations of Auditory Gamma Oscillatory Responses between Pre-Onset High-Risk Individuals and First-Episode Schizophrenia. *Cerebral Cortex*. <https://doi.org/10.1093/cercor/bhu278>
- Takarae, Y., & Sweeney, J. (2017). Neural hyperexcitability in autism spectrum disorders. *Brain Sciences*, 7(10). <https://doi.org/10.3390/brainsci7100129>
- Tallon-Baudry, C., Bertrand, O., Delpuech, C., & Pernier, J. (1996). Stimulus specificity of phase-locked and non-phase-locked 40 Hz visual responses in human. *Journal of Neuroscience*. <https://doi.org/10.1523/jneurosci.16-13-04240.1996>
- Tallon-Baudry, C., Bertrand, O., Peronnet, F., & Pernier, J. (1998). Induced γ -band activity during the delay of a visual short-term memory task in humans. *Journal of Neuroscience*, 18(11), 4244-4254. <https://doi.org/10.1523/JNEUROSCI.18-11-04244.1998>
- Tallon-Baudry, C. (2009). The roles of gamma-band oscillatory synchrony in human visual cognition. *Front Biosci*, 14(321-332), 26. <https://doi.org/10.2741/3246>
- Taylor, M., Charman, T., & Ronald, A. (2011). Overlapping genetic influences on traits of autism and ADHD: Evidence from a 12-year-old communitybased twin sample. *Behavior Genetics*.
- Terhune, D. B., Murray, E., Near, J., Stagg, C. J., Cowey, A., & Kadosh, R. C. (2015). Phosphene perception relates to visual cortex glutamate levels and covaries with atypical visuospatial awareness. *Cerebral Cortex*. <https://doi.org/10.1093/cercor/bhv015>
- Thapar, A., & Rutter, M. (2020). Genetic Advances in Autism. In *Journal of Autism and Developmental Disorders*. <https://doi.org/10.1007/s10803-020-04685-z>
- Thomas, D. R. (2006). A General Inductive Approach for Analyzing Qualitative Evaluation Data. *American Journal of Evaluation*. <https://doi.org/10.1177/1098214005283748>
- Thut, G., Nietzel, A., Brandt, S. A., and Pascual-Leone, A. (2006). Alpha-band electroencephalographic activity over occipital cortex indexes visuospatial attention bias

- and predicts visual target detection. *J. Neurosci.* 26, 9494–9502.
<https://doi.org/10.1523/JNEUROSCI.0875-06.2006>
- Tick, B., Bolton, P., Happé, F., Rutter, M., & Rijdsdijk, F. (2016). Heritability of autism spectrum disorders: A meta-analysis of twin studies. *Journal of Child Psychology and Psychiatry and Allied Disciplines*. <https://doi.org/10.1111/jcpp.12499>
- Tinker, J., & Velazquez, J. L. P. (2014). Power law scaling in synchronization of brain signals depends on cognitive load. *Frontiers in Systems Neuroscience*. <https://doi.org/10.3389/fnsys.2014.00073>
- Treder, M., Charest, I., Michelmann, S., Martín-Buro, M. C., Roux, F., Carceller-Benito, F., ... & Staesina, B. P. (2021). The hippocampus as the switchboard between perception and memory. *Proceedings of the National Academy of Sciences*. 118(50). <https://doi.org/10.1073/pnas.2114171118>
- Trembath, D., & Vivanti, G. (2014). Problematic but predictive: Individual differences in children with autism spectrum disorders. *International Journal of Speech-Language Pathology*. <https://doi.org/10.3109/17549507.2013.859300>
- Turner-Brown, L. M., Baranek, G. T., Reznick, J. S., Watson, L. R., & Crais, E. R. (2013). The first year inventory: A longitudinal follow-up of 12-month-old to 3-year-old children. *Autism*. <https://doi.org/10.1177/1362361312439633>
- Tye, C., Asherson, P., Ashwood, K. L., Azadi, B., Bolton, P., & McLoughlin, G. (2014). Attention and inhibition in children with ASD, ADHD and co-morbid ASD + ADHD: An event-related potential study. *Psychological Medicine*. <https://doi.org/10.1017/S0033291713001049>
- Tye, C., Battaglia, M., Bertolotti, E., Ashwood, K. L., Azadi, B., Asherson, P., Bolton, P., & McLoughlin, G. (2014). Altered neurophysiological responses to emotional faces discriminate children with ASD, ADHD and ASD + ADHD. *Biological Psychology*. <https://doi.org/10.1016/j.biopsycho.2014.08.013>
- Tye, C., Mercure, E., Ashwood, K. L., Azadi, B., Asherson, P., Johnson, M. H., Bolton, P., & McLoughlin, G. (2013). Neurophysiological responses to faces and gaze direction

- differentiate children with ASD, ADHD and ASD + ADHD. *Developmental Cognitive Neuroscience*. <https://doi.org/10.1016/j.dcn.2013.01.001>
- Uhlhaas, P. J., Pipa, G., Lima, B., Melloni, L., Neuenschwander, S., Nikolić, D., & Singer, W. (2009). Neural synchrony in cortical networks: History, concept and current status. *Frontiers in Integrative Neuroscience*. <https://doi.org/10.3389/neuro.07.017.2009>
- Uhlhaas, P. J., & Singer, W. (2007). What Do Disturbances in Neural Synchrony Tell Us About Autism? In *Biological Psychiatry*. <https://doi.org/10.1016/j.biopsych.2007.05.023>
- Uljarević, M., Cooper, M. N., Bebbington, K., Glasson, E. J., Maybery, M. T., Varcin, K., Alvares, G. A., Wray, J., Leekam, S. R., & Whitehouse, A. J. O. (2020). Deconstructing the repetitive behaviour phenotype in autism spectrum disorder through a large population-based analysis. *Journal of Child Psychology and Psychiatry and Allied Disciplines*. <https://doi.org/10.1111/jcpp.13203>
- Uzunova, G., Pallanti, S., & Hollander, E. (2016). Excitatory/inhibitory imbalance in autism spectrum disorders: Implications for interventions and therapeutics. In *World Journal of Biological Psychiatry*. <https://doi.org/10.3109/15622975.2015.1085597>
- Uzunova, G., Pallanti, S., & Hollander, E. (2016). Excitatory/inhibitory imbalance in autism spectrum disorders: Implications for interventions and therapeutics. In *World Journal of Biological Psychiatry*. <https://doi.org/10.3109/15622975.2015.1085597>
- Van der Groen, O., & Wenderoth, N. (2016). Transcranial random noise stimulation of visual cortex: Stochastic resonance enhances central mechanisms of perception. *Journal of Neuroscience*. <https://doi.org/10.1523/JNEUROSCI.4519-15.2016>
- Van der Hallen, R., Evers, K., Boets, B., Steyaert, J., Noens, I., & Wagemans, J. (2016). Visual Search in ASD: Instructed Versus Spontaneous Local and Global Processing. *Journal of Autism and Developmental Disorders*. <https://doi.org/10.1007/s10803-016-2826-1>
- Van der Meer, J. M., Oerlemans, A. M., Van Steijn, D. J., Lappenschaar, M. G., De Sonnevile, L. M., Buitelaar, J. K., & Rommelse, N. N. (2012). Are autism spectrum disorder and attention-deficit/hyperactivity disorder different manifestations of one overarching

- disorder? Cognitive and symptom evidence from a clinical and population-based sample. *Journal of the American Academy of Child & Adolescent Psychiatry*, 51(11), 1160-1172.
- Van Diepen, R. M., Cohen, M. X., Denys, D., & Mazaheri, A. (2015). Attention and temporal expectations modulate power, not phase, of ongoing alpha oscillations. *Journal of Cognitive Neuroscience*. https://doi.org/10.1162/jocn_a_00803
- Van Doorn, J., van den Bergh, D., Böhm, U., Dablander, F., Derks, K., Draws, T., ... & Wagenmakers, E. J. (2020). The JASP guidelines for conducting and reporting a Bayesian analysis. *Psychonomic Bulletin & Review*. 1-14. <https://doi.org/10.3758/s13423-020-01798-5>
- Van Kerkoerle, T., Self, M. W., Dagnino, B., Gariel-Mathis, M. A., Poort, J., Van Der Togt, C., & Roelfsema, P. R. (2014). Alpha and gamma oscillations characterize feedback and feedforward processing in monkey visual cortex. *Proceedings of the National Academy of Sciences*, 111(40), 14332-14341. <https://doi.org/10.1073/pnas.1402773111>
- Van Naarden Braun, K., Christensen, D., Doernberg, N., Schieve, L., Rice, C., Wiggins, L., Schendel, D., & Yeargin-Allsopp, M. (2015). Trends in the prevalence of autism spectrum disorder, cerebral palsy, hearing loss, intellectual disability, and vision impairment, metropolitan Atlanta, 1991-2010. *PLoS ONE*. <https://doi.org/10.1371/journal.pone.0124120>
- Van Noordt, S., Wu, J., Venkataraman, A., Larson, M. J., South, M., & Crowley, M. J. (2017). Inter-trial coherence of medial frontal theta oscillations linked to differential feedback processing in youth and young adults with autism. *Research in Autism Spectrum Disorders*. <https://doi.org/10.1016/j.rasd.2017.01.011>
- Viding, E., & Blakemore, S. J. (2007). Endophenotype approach to developmental psychopathology: Implications for autism research. In *Behavior Genetics*. <https://doi.org/10.1007/s10519-006-9105-4>
- Vilidaite, G., Yu, M., & Baker, D. H. (2017). Internal noise estimates correlate with autistic traits. *Autism Research*. <https://doi.org/10.1002/aur.1781>

- Vlamings, P. H. J. M., Jonkman, L. M., Hoeksma, M. R., Van Engeland, H., & Kemner, C. (2008). Reduced error monitoring in children with autism spectrum disorder: An ERP study. *European Journal of Neuroscience*. <https://doi.org/10.1111/j.1460-9568.2008.06336.x>
- Von Spreckelsen, M., von Spreckelsen, M., & Bromm, B. (1988). Estimation of Single-Evoked Cerebral Potentials by Means of Parametric Modeling and Kalman Filtering. *IEEE Transactions on Biomedical Engineering*. <https://doi.org/10.1109/10.7270>
- Von Stein, A., & Sarnthein, J. (2000). Different frequencies for different scales of cortical integration: from local gamma to long range alpha/theta synchronization. *International journal of psychophysiology*, 38(3), 301-313. [https://doi.org/10.1016/s0167-8760\(00\)00172-0](https://doi.org/10.1016/s0167-8760(00)00172-0)
- Voytek, B., & Knight, R. T. (2015). Dynamic network communication as a unifying neural basis for cognition, development, aging, and disease. In *Biological Psychiatry*. <https://doi.org/10.1016/j.biopsych.2015.04.016>
- Voytek, B., Kramer, M. A., Case, J., Lepage, K. Q., Tempesta, Z. R., Knight, R. T., & Gazzaley, A. (2015). Age-related changes in 1/f neural electrophysiological noise. *Journal of Neuroscience*, 35(38), 13257–13265. <https://doi.org/10.1523/JNEUROSCI.2332-14.2015>
- Wang, D., Clouter, A., Chen, Q., Shapiro, K. L., & Hanslmayr, S. (2018). Single-trial phase entrainment of theta oscillations in sensory regions predicts human associative memory performance. *Journal of Neuroscience*, 38(28), 6299-6309. <https://doi.org/10.1523/JNEUROSCI.0349-18.2018>
- Ward, J. (2018). Individual differences in sensory sensitivity: A synthesizing framework and evidence from normal variation and developmental conditions. *Cognitive Neuroscience*. <https://doi.org/10.1080/17588928.2018.1557131>
- Warrier, V., Toro, R., Won, H., Leblond, C. S., Cliquet, F., Delorme, R., De Witte, W., Bralten, J., Chakrabarti, B., Børglum, A. D., Grove, J., Poelmans, G., Hinds, D. A., Bourgeron, T., & Baron-Cohen, S. (2019). Social and non-social autism symptoms and trait domains are

genetically dissociable. *Communications Biology*. <https://doi.org/10.1038/s42003-019-0558-4>

Waters, F., Collerton, D., Ffytche, D. H., Jardri, R., Pins, D., Dudley, R., Blom, J. D., Mosimann, U. P., Eperjesi, F., Ford, S., & Laroi, F. (2014). Visual hallucinations in the psychosis spectrum and comparative information from neurodegenerative disorders and eye disease. *Schizophrenia Bulletin*. <https://doi.org/10.1093/schbul/sbu036>

Webb, S. J. an., Bernier, R., Henderson, H. A., Johnson, M. H., Jones, E. J. H., Lerner, M. D., McPartland, J. C., Nelson, C. A., Rojas, D. C., Townsend, J., & Westerfield, M. (2015). Guidelines and best practices for electrophysiological data collection, analysis and reporting in autism. *Journal of Autism and Developmental Disorders*, 45(2), 425–443. <https://doi.org/10.1007/s10803-013-1916-6>

Wechsler, D. (1999). Manual for the Wechsler abbreviated intelligence scale (WASI). In *WASI*.

Weinger, P. M., Zemon, V., Soorya, L., & Gordon, J. (2014). Low-contrast response deficits and increased neural noise in children with autism spectrum disorder. *Neuropsychologia*. <https://doi.org/10.1016/j.neuropsychologia.2014.07.031>

Welch, P. D. (1967). The Use of Fast Fourier Transform for the Estimation of Power Spectra: A Method Based on Time Averaging Over Short, Modified Periodograms. *IEEE Transactions on Audio and Electroacoustics*. <https://doi.org/10.1109/TAU.1967.1161901>

Wheless, J. W., Simos, P. G., & Butler, I. J. (2002). Language dysfunction in epileptic conditions. *Seminars in Pediatric Neurology*. <https://doi.org/10.1053/spen.2002.35504>

White, J. A., Klink, R., Alonso, A., & Kay, A. R. (1998). Noise from voltage-gated ion channels may influence neuronal dynamics in the entorhinal cortex. *Journal of Neurophysiology*. <https://doi.org/10.1152/jn.1998.80.1.262>

Wilkins, A. (1995). *Visual stress*. Oxford University Press.

Wilkins, A. (2021). Visual stress: origins and treatment. *CNS*, 6, 74–86.

- Wilkins, A. J., Andermann, F., & Ives, J. (1975). Stripes, complex cells and seizures: An attempt to determine the locus and nature of the trigger mechanism in pattern-sensitive epilepsy. *Brain*. <https://doi.org/10.1093/brain/98.3.365>
- Wilkins, A. J., Smith, J., Willison, C. K., Beare, T., Boyd, A., Hardy, G., Mell, L., Peach, C., & Harper, S. (2007). Stripes within words affect reading. *Perception*. <https://doi.org/10.1068/p5651>
- Wilkins, A. J., & Evans, B. J. W. (2010). Visual stress, its treatment with spectral filters, and its relationship to visually induced motion sickness. *Applied Ergonomics*. <https://doi.org/10.1016/j.apergo.2009.01.011>
- Wilkins, A., Emmett, J., & Harding, G. (2005). Characterizing the patterned images that precipitate seizures and optimizing guidelines to prevent them. In *Epilepsia*. <https://doi.org/10.1111/j.1528-1167.2005.01405.x>
- Wilkins, A., Nimmo-smith, I., Tait, A., Mcmanus, C., Sala, S. Della, Tilley, A., Arnold, K., Barrie, M., & Scott, S. (1984). A neurological basis for visual discomfort. *Brain*, *107*(4), 989–1017. <https://doi.org/10.1093/brain/107.4.989>
- Wilkins, A., & Evans, B. J. W. (2001). Pattern glare test instructions. *IOO Sales Ltd, London*.
- Wing, L., & Potter, D. (2002). The epidemiology of autistic spectrum disorders: Is the prevalence rising? In *Mental Retardation and Developmental Disabilities Research Reviews*. <https://doi.org/10.1002/mrdd.10029>
- Winter, W. R., Nunez, P. L., Ding, J., & Srinivasan, R. (2007). Comparison of the effect of volume conduction on EEG coherence with the effect of field spread on MEG coherence. *Statistics in Medicine*. <https://doi.org/10.1002/sim.2978>
- Wong, Y. T., Fabiszak, M. M., Novikov, Y., Daw, N. D., & Pesaran, B. (2016). Coherent neuronal ensembles are rapidly recruited when making a look-reach decision. *Nature neuroscience*, *19*(2), 327-334. <https://doi.org/10.1038/nn.4210>

- Wood, K. C., Blackwell, J. M., & Geffen, M. N. (2017). Cortical inhibitory interneurons control sensory processing. In *Current Opinion in Neurobiology*. <https://doi.org/10.1016/j.conb.2017.08.018>
- Wright, J. J., & Liley, D. T. J. (1996). Dynamics of the brain at global and microscopic scales: Neural networks and the EEG. In *Behavioral and Brain Sciences*. <https://doi.org/10.1017/s0140525x00042679>
- Yener, G. G., Fide, E., Özbek, Y., Emek-Savaş, D. D., Aktürk, T., Çakmur, R., & Güntekin, B. (2019). The difference of mild cognitive impairment in Parkinson's disease from amnesic mild cognitive impairment: Deeper power decrement and no phase-locking in visual event-related responses. *International Journal of Psychophysiology*. <https://doi.org/10.1016/j.ijpsycho.2019.03.002>
- Yordanova, J., Banaschewski, T., Kolev, V., Woerner, W., & Rothenberger, A. (2001). Abnormal early stages of task stimulus processing in children with attention-deficit hyperactivity disorder - Evidence from event-related gamma oscillations. *Clinical Neurophysiology*. [https://doi.org/10.1016/S1388-2457\(01\)00524-7](https://doi.org/10.1016/S1388-2457(01)00524-7)
- Yu, L., Wang, S., Huang, D., Wu, X., & Zhang, Y. (2018). Role of inter-trial phase coherence in atypical auditory evoked potentials to speech and nonspeech stimuli in children with autism. *Clinical Neurophysiology*. <https://doi.org/10.1016/j.clinph.2018.04.599>
- Zareian, B., Maboudi, K., Daliri, M. R., Abrishami Moghaddam, H., Treue, S., & Esghaei, M. (2020). Attention strengthens across-trial pre-stimulus phase coherence in visual cortex, enhancing stimulus processing. *Scientific Reports*. <https://doi.org/10.1038/s41598-020-61359-7>
- Zavala, B., Tan, H., Ashkan, K., Foltynie, T., Limousin, P., Zrinzo, L., ... & Brown, P. (2016). Human subthalamic nucleus–medial frontal cortex theta phase coherence is involved in conflict and error related cortical monitoring. *Neuroimage*, 137, 178-187. <https://doi.org/10.1016/j.neuroimage.2016.05.031>
- Zeljic, K., Xiang, Q., Wang, Z., Pan, Y., Shi, Y., Zhou, Z., Wang, Z., & Liu, D. (2021). Heightened perception of illusory motion is associated with symptom severity in

schizophrenia patients. *Progress in Neuro-Psychopharmacology and Biological Psychiatry*. <https://doi.org/10.1016/j.pnpbp.2020.110055>

Zeng, K., Kang, J., Ouyang, G., Li, J., Han, J., Wang, Y., Sokhadze, E. M., Casanova, M. F., & Li, X. (2017). Disrupted brain network in children with autism spectrum disorder. *Scientific Reports*. <https://doi.org/10.1038/s41598-017-16440-z>

Zhang, L., Huang, C. C., Dai, Y., Luo, Q., Ji, Y., Wang, K., Deng, S., Yu, J., Xu, M., Du, X., Tang, Y., Shen, C., Feng, J., Sahakian, B. J., Lin, C. P., & Li, F. (2020). Symptom improvement in children with autism spectrum disorder following bumetanide administration is associated with decreased GABA/glutamate ratios. *Translational Psychiatry*. <https://doi.org/10.1038/s41398-020-0692-2>

Zhaoping, L. (2006). Theoretical understanding of the early visual processes by data compression and data selection. In *Network (Bristol, England)*. <https://doi.org/10.1080/09548980600931995>

Zheng, S., Hume, K. A., Able, H., Bishop, S. L., & Boyd, B. A. (2020). Exploring Developmental and Behavioral Heterogeneity among Preschoolers with ASD: A Cluster Analysis on Principal Components. *Autism Research*. <https://doi.org/10.1002/aur.2263>